Gauge/Gravity Duality
with Backreacting Background

Dissertation zur Erlangung des
naturwissenschaftlichen Doktorgrades
der Julius-Maximilians-Universität Würzburg

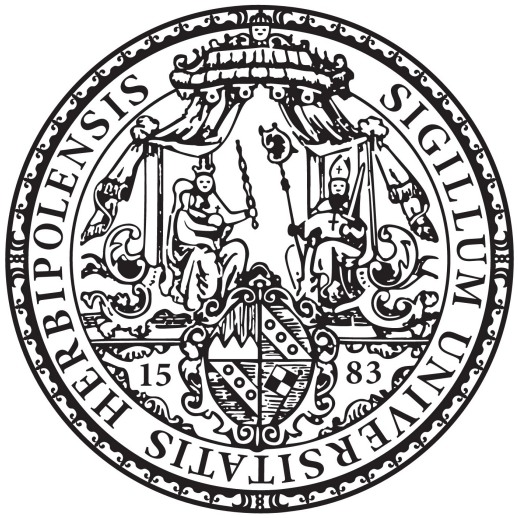

vorgelegt von
Yiqiang Du
aus der Provinz Shandong (Volksrepublik China)

Würzburg, 2019

Eingereicht am: 22.07.2019
bei der Fakultät für Physik und Astronomie

1. Gutachter: Prof. Dr. Johanna Erdmenger
2. Gutachter: Prof. Dr. Thorsten Ohl
3. Gutachter: .....
der Dissertation

Vorsitzende(r): .....
1. Prüfer: Prof. Dr. Johanna Erdmenger
2. Prüfer: Prof. Dr. Thorsten Ohl
3. Prüfer: Prof. Dr. Raimund Ströhmer
im Promotionkolloquiums

Tag des Promotionskolloquiums: 16.09.2019

Doktorurkunde ausgehändigt am: .....

To Xiaotong

Abstract

The topic of this thesis is generalizations of the Anti de Sitter/Conformal Field Theory (AdS/CFT) correspondence, often referred to as holography, and their application to models relevant for condensed matter physics. A particular virtue of AdS/CFT is to map strongly coupled quantum field theories, for which calculations are inherently difficult, to more tractable classical gravity theories. I use this approach to study the crossover between Bose-Einstein condensation (BEC) and the Bardeen-Cooper-Schrieffer (BCS) superconductivity mechanism. I also study the phase transitions between the AdS black hole and AdS soliton spacetime in the presence of disorder. Moreover, I consider a holographic model of a spin impurity interacting with a strongly correlated electron gas, similar to the Kondo model.

In AdS/CFT, the BEC/BCS crossover is modeled by a soliton configuration in the dual geometry and we study the BEC and BCS limits. The backreaction of the matter field on the background geometry is considered, which provides a new approach to study the BEC/BCS crossover. The behaviors of some physical quantities such as depletion of charge density under different strength of backreaction are presented and discussed. Moreover, the backreaction enables us to obtain the effective energy density of the soliton configurations, which together with the surface tension of the solitons leads to an argument for the occurrence of so called snake instability for dark solitons, i.e. for the solitons to form a vortex-like structures.

Disordering strongly coupled and correlated quantum states of matter may lead to new insights into the physics of many body localized (MBL) strongly correlated states, which may occur in the presence of strong disorder. We are interested in potential insulator-metal transitions induced by disorder, and how disorder affects the Hawking-Page phase transition in AdS gravity in general. We introduce a metric ansatz and numerically construct the corresponding disordered AdS soliton and AdS black hole solutions, and discuss the calculation of the free energy in these states.

In the Kondo effect, the rise in resistivity in metals with scarce magnetic impurities at low temperatures can be explained by the RG flow of the antiferromagnetic coupling between the impurity and conduction electrons in CFT. The generalizations to $SU(N)$ in the large N limit make the treatment amenable to the holographic approach. We add a Maxwell term to a previously existing holographic model to study the conductivity of the itinerant electrons. Our goal is to find the $log(T)$ behavior in the DC resistivity. In the probe limit, we introduce junction conditions to connect fields crossing the defect. We then consider backreactions, which give us a new metric ansatz and new junction conditions for the gauge fields.

Zusammenfassung

Das Thema dieser Arbeit sind Verallgemeinerungen der Korrespondenz Anti-de-Sitter/Conformal Field Theory (AdS/CFT), oft als Holographie bezeichnet, und deren Anwendung auf Modelle, die für die Physik der kondensierten Materie relevant sind. Ein besonderer Vorteil von AdS/CFT ist die Abbildung starker gekoppelter Quantenfeldtheorien, für die Berechnungen durchgeführt werden sind von Natur aus schwierige, leichter zu fassende klassische Gravitationstheorien. In dieser Arbeit untersuche ich anhand dieses Ansatzes den Übergang zwischen der Bose-Einstein-Kondensation (BEC) und dem Bardeen-Cooper-Schrieffer (BCS) Supraleitungsmechanismus. Ich untersuche auch die Phasenübergänge zwischen AdS Black Hole und AdS Soliton Spacetime. Darüber hinaus betrachte ich ein holographisches Modell einer Spin-Verunreinigung, die mit einem stark korrelierten Elektronengas wechselwirkt, ähnlich wie das Kondo-Modell.

Die BEC/BCS-Frequenzweiche wird durch eine Solitonenkonfiguration in der Doppelgeometrie modelliert, und wir untersuchen die BEC-Grenze und die BCS-Grenze der BEC/BCS-Frequenzweiche. Die Rückreaktion wird auf das System übertragen, das einen neuen Ansatz zur Untersuchung der BEC/BCS-Frequenzweiche bietet. Das Verhalten einiger physikalischer Größen, wie z. B. die Abnahme der Ladungsdichte bei unterschiedlicher Stärke der Rückreaktion, wird vorgestellt und diskutiert. Darüber hinaus ermöglicht die Rückreaktion, die effektive Energiedichte von Solitonen-Konfigurationen zu erhalten, was zusammen mit der Oberflächenspannung zu einem Argument für das Auftreten einer Schlangeninstabilität für dunkle Solitonen führt, d. H. Für die Solitonen, um wirbelartige Strukturen zu bilden.

Die Unordnung stark gekoppelter und korrelierter Quantenzustände der Materie kann zu neuen Erkenntnissen über die Physik vieler körperlokalisierter (MBL) stark korrelierter Zustände führen, die bei Vorhandensein einer starken Störung auftreten können. Wir interessieren uns für potenzielle Isolator-Metall-Übergänge, die durch Störung induziert werden, und wie sich Störung der Hawking-Page-Phasenübergang in der AdS-Schwerkraft im Allgemeinen auswirkt. Wir führen einen metrischen Ansatz ein und konstruieren numerisch die entsprechenden ungeordneten AdS-Solitonen- und AdS-Black-Hole-Lösungen.

Beim Kondo-Effekt kann der Anstieg des spezifischen Widerstands bei niedrigen Temperaturen durch den RG-Fluss der antiferromagnetischen Kopplung zwischen den Störstellen- und Leitungselektronen in der CFT erklärt werden. Die Verallgemeinerungen zu SU (N) in der großen N-Grenze machen die Behandlung für den holographischen Ansatz zugänglich. Wir fügen einem zuvor existierenden holografischen Modell einen Maxwell - Term hinzu, um die Ausbreitung der

Umgebungselektronen zu untersuchen. Unser Ziel ist es, das log(T)-Verhalten im UV-Widerstand zu untersuchen. In der Sondengrenze führen wir Übergangsbedingungen ein, um Felder zu verbinden, die den Defekt kreuzen. Dann betrachten wir eine Rückreaktion, die uns einen neuen metrischen Ansatz und neue Verknüpfungsbedingungen zum Messen von Feldern gibt.

Contents

1 Introduction and Overview

In the twentieth century, two great progress was made in physics: general gravity and quantum theory. These helped us to have a much deeper understanding of how our real world works. There are four fundamental forces known today: electromagnetic, weak, strong interactions as well as gravitational force.

Except for gravity, the Standard Model of particle physics is essentially defined by the local $SU(3)\times SU(2)\times U(1)$ internal gauge symmetry, and describes the first three forces. It classifies all known elementary particles into matters and interaction/force carriers in the mathematical framework of quantum field theory.

Electromagnetic and weak interactions, even though they appear very different at low energies, can be unified into the electroweak interaction above the unification energy of 246 GeV, which is described by the $SU(2)\times U(1)$ gauge group. The Higgs mechanism, caused by interactions with a spin zero gauge boson called Higgs boson, results in spontaneous symmetry breaking of the symmetry from $SU(2)\times U(1)_Y$ to $U(1)_{em}$, producing the massless photon, γ, of the electromagnetic force and the massive $W^{\pm}$ and Z bosons of the weak force.

The strong force is described by quantum chromodynamics (QCD) in the standard model and based on the local gauge symmetry group $SU(3)$. QCD is a non-abelian gauge theory which describes the strong interactions between quarks (matter particles) and gluons (interaction carriers) as well as gluons themselves. In the QCD Lagrangian, quark fields are in the fundamental representation of $SU(3)$ symmetry while spin 1/2 and gluons are massless and in the adjoint representation with spin 1. Unlike other elementary particles, quarks and gluons carry non-vanishing color charge which makes the strong interaction only occur between them. Color confinement and asymptotic freedom are two main properties of QCD. The former property forbids us from creating isolate color charges. The latter makes perturbation theory of QCD accurate at very high energy (For example, 13 TeV-14 TeV of proton-proton collision energy that can be reached at the Large Hadron Collider (LHC)) but not good enough in the energy of high-energy heavy-ion collisions (for example, the approximately 175 Mev transition energy for the quark-gluon plasma (QGP)). Non-perturbative approaches to QCD are necessary for the exploration of phases of quark matter and quark-gluon plasma, and lattice QCD is the most well established one.

The incompatibility of special relativity and quantum mechanics led to the development of quantum field theory. After that we faced a new incompatibility: general

relativity can not be quantized straightforward because the resulting theory is non-renormalizable. String theory is one of the most remarkable theories trying to unify general relativity and quantum field theory. String theory abandons the concept that the elementary particles are mathematical points. Instead, it develops a quantum field theory of one-dimensional objects, called strings. The goal of the string theory is to be a unified quantum theory that describes all the fundamental forces including gravity which would give us a new standard model and a deeper understanding of cosmology.

There are realistic string theories of elementary particles that include the standard model, and string theory has shown some features that are generic and important. The first is that general relativity arises naturally from the theory and gets modified at short distances/high energies while it is exactly the classic form proposed by Einstein at ordinary distances and energies. The second is that the Yang-Mills gauge theories which comprise the standard model arise naturally in string theory. The third is that string theory predicts the existence of supersymmetry which is crucial for it to be mathematical consistent.

Gerard 't Hooft proposed a principle called the holographic principle[1] inspired by black hole thermodynamics (see [2] for a review) which states that a system coupled to gravity in spacetime can be described by a quantum system on the lower-dimensional boundary of that spacetime. The most successful and concrete realization of the holographic principle is the Anti-de Sitter/Conformal Field Theory (AdS/CFT) correspondence proposed by Juan Maldacena [3]. The AdS/CFT correspondence (AdS/CFT duality) connects two kinds of physical theories, where the CFT lives on the boundary of AdS spacetimes. The AdS spacetimes are solutions of Einstein equations, while the conformal field theories (CFTs) are quantum field theories.

The generalized case of AdS/CFT correspondence is usually called gauge/gravity duality. The duality provides a non-perturbative formulation of string theory which can help us have a deeper understanding of string theory and gravity. Because the gravity side is a weakly interacting system and is thus easier for mathematical calculation, the duality provides a powerful toolkit for studying strongly coupled quantum field theories if they have gravitational correspondences. This strong-weak property has been widely used to study many aspects of elementary particles, nuclear physics and condensed matter physics by translating strongly coupled problems into mathematically solvable string theory problems.

Many features associated with strongly coupled condensed matter physics that are hard to study by perturbation theory such as Bose-Einstein condensation/Bardeen-Cooper-Schrieffer (BEC/BCS) crossover in superfluid, are tractable in corresponding holographic models. Studying superfluidity in ultracold Fermi gases has been of great interest in recent years. Superfluidity can be achieved by cooling a fermionic

[1] A precise interpretation of the holographic principle from string theory was then given by Leonard Susskind [1].

atoms to ultra-low temperature and tuning the interactions in the fermionic gas with a controllable external magnetic field in the laboratory. One side of interacting limit of this system is BCS[2]-like phase described by condensed loosely bound Cooper pairs of fermions. The other side of interacting limit is BEC[3]-like phase where the fermions become very strongly bound and the system is effectively characterized as a condensate of bosonic degree of freedom. For such a system of two different "species" Fermi particles equally populated with attractive interspecies interaction, it is thought that there may be a state between the BEC and BCS states, where the interaction strength may decrease continuously from a Bose-Einstein condensation of tightly bound di-fermionic molecules to weakly attracting independent fermions of Cooper-pairing form. This process is referred to as "BEC-BCS crossover" (see [4] for a review). Theoretical study of the BEC-BCS crossover started from [**?**] where Schafrot, Butler and Blatt used a variant of BEC to understand superconductivity. Later, [5] studied superconductivity in doped semiconductors which led to the first mean-field treatment of the BEC-BCS crossover. All of the early works are theoretical in nature, until the BEC-BCS crossover was realized experimentally in ultracold Fermi gas near a Feshbach resonance [6–12]. The unitary Fermi gas which lies in the middles of the BEC/BCS crossover is another example of intrinsically scale invariant strongly coupled system (see [13] for a review).

As such, we must find a suitable probe to study the BEC/BCS crossover. As mentioned in [14], solitons in a superfluid provide nice probes for the short distance structure even at the mean field level [15, 16]. When there exist solitons, the superfluid interpolates from the symmetry broken phase to symmetry restored phase across the soliton's core, then the features of the cores may characterize the short distance features of the system.

The first dark solitons[4] in holographic relativistic superfluids were constructed in [19], where the length scales associated with the condensate and the charge density depletion are studied and two scales differ by a non-trivial function of the chemical potential. [20] extended the study of the dark solitons for two possible condensing operators in the probe limit, and found that both of them share common features with their standard superfluid counterparts. The relative charge depletion factor was also investigated in the two different condensates. By comparing with [16], where it is shown that the density depletion fraction is directly related to whether the system is BEC-like (large depletion of nearly 100%) or BCS-like (small depletion of less than 60%) at zero temperature for nonrelativistic systems, [20] argued that

[2]The BCS theory describes superconductivity by a condensation of electron pairs called Cooper pairs into a boson-like state.

[3]The Bose-Einstein condensate (BEC) is a state of matter formed by dilute bosonic gas at ultra-low temperatures. In this state, a large fraction of bosons occupy the ground state and quantum phenomena become macroscopical.

[4]There are dark and bright solitons which are defined by the interfaces of reduced or increased charge density between two superfluid phases (see e.g. [17, 18] for a review). The solitons here are dark solitons.

the condensation in "standard case"[5] is BCS-like and condensation in "alternative case" is BEC-like. The real BEC-BCS systems in experiment are non-relativistic. However, as [21] points out, many features in non-relativistic condensates are expected to have relativistic analogs, because both are motivated from the same nature of bound states.

We study the BEC/BCS crossover by a soliton configuration in the dual geometry as well. In particular, we study the BEC limit and BCS limit of the BEC/BCS crossover. We considered backreaction on the holographic superfluid systems, which provides another dimension to study BEC/BCS crossover. The dark soliton configurations are achieved by solving Einstein's Field Equations for coupled matter field numerically. We use the Einstein-de Turck method for finding the stationary solutions. The Einstein-de Turck method is first introduced in [22] and further developed in [23–26]. This method can reformulate the Einstein equation into a manifestly elliptic form by adding a covariant gauge-fixing de Turck term to the Einstein equation and then gives a well-posed boundary value problem. The Einstein-de Turck method requires a choice of reference metric with the same asymptotics and symmetries as the metric we are trying to solve for.

The work on the BEC/BCS crossover [27] was performed in collaboration with Zhongshan Xu, Johanna Erdmenger, Yu Tian, Jie Ren and Zhuoyu Xian. From our calculation, we find that the healing length[6] of soliton increases with the strength of backreaction. Correspondingly, the charge density depletion deceases, which means the backreaction leads to effective attraction towards boundary physical system. The charge density depletion results are unexpected: in the probe limit [20], the density depletion does not show the tendency of reaching 100% when temperature approach zero in BEC-like case, and this may be caused by not working at exactly zero temperature and not considering backreaction; at first we believed this tendency could be better when backreaction is included, but the results show the opposite behavior. Moreover, the backreaction enables us to obtain the effective energy density of soliton configurations, which together with the surface tension implies an explanation for the so called *snake instability* of dark solitons.

The work on phase transition with disorder [28] was performed in collaboration with Johanna Erdmenger, Florian Goth, René Meyer, Jackson Wu and Zhongshan Xu. Disordering strongly coupled and correlated quantum states of matter may lead to new insights into the physics of many body localized strongly correlated states, possibly in the presence of strong disorder. In AdS/CFT, the probe limit is not suitable for strong disorder, and the backreacted solution needs to be constructed. We are interested in potential insulator-metal transitions induced by disorder, and how disorder affects the Hawking-Page phase transition [29, 30] in AdS gravity in general.

[5] We will explain "standard case" and "alternative case" in detail in 3.2 of chapter 3.

[6] The condensate density grows from the lowest value for dark solitons (it will be highest value for bright solitons) to value in equilibrium over a distance called the healing length.

To be specific, when there is no matter field, we have two spacetime geometries–AdS black hole and AdS soltion spacetimes–which are connected by "double Wick rotation". Both them are solutions of Einstein's equation with negative cosmological constant. There is a dimensionless parameter Tl in the theory, where T is the temperature of the AdS black hole and l is the periodicity of the S^1-compactified coordinate. A first-order phase transition occurs at $Tl = 1$, where the AdS black hole geometry and the AdS soliton geometry has the same free energy. By adding disorder to the system around this phase transition point, we injecting kinetic energy to the system. Because there is energy dissipation in the AdS black hole geometry, we predict the free energy of the AdS black hole geometry may smaller than that of the AdS soliton geometry, such that a phase transition would happen. We introduce a metric ansatz from an adaption of the black hole geometry [31]. We numerically construct the corresponding disordered AdS soliton and AdS black hole solutions. The free energy of the system is proportional to the on-shell Euclidean action. Counter terms are added to the action in order to get a finite result.

The work on defect embeddings in holographic background with propagating matter fields [32] was performed in collaboration with Johanna Erdmenger, René Meyer and Dilyn Fullerton. In the presence of magnetic impurities in conductors, the electrical resistivity of the system increases logarithmically at low temperatures [33], which is called the Kondo effect. The rise in resistivity can be explained by the RG flow of the antiferromagnetic coupling between impurities and conduction electrons in CFT. This is a strongly coupled problem in nature, similar to the RG running of QCD. The generalizations to $SU(N)$ in the large N limit make the treatment amendable to the holographic approach [34]. Many aspects of the holographic Kondo model are still unexplored: the conductivity has not been calculated; the backreaction to the background geometry may be necessary to consider at the point of the impurity; and higher dimensional generalization to Kondo lattices need to be investigated. We add a Maxwell term to the holographic model [34] and our goal is to study the $log(T)$ behavior in the DC resistivity. In the probe limit, we introduce first and second junction conditions to connect fields crossing the defect. We then consider backreaction, which gives us a new metric ansatz and new junction conditions to gauge fields.

This thesis applies the AdS/CFT correspondence to strongly coupled systems, specifically to models relevant for condensed matter physics. I use this approach to study the crossover between Bose-Einstein condensation and the Bardeen-Cooper-Schrieffer superconductivity mechanism. A phase transitions between the AdS black hole and the AdS soliton spacetime induced by disorder is also an interesting topic for me. Moreover, a holographic model of a spin impurity interacting with a strongly correlated electron gas which is similar to the Kondo model is also studied. The results of this thesis will enter the forthcoming publications [27, 28, 32].

2 The Foundation of AdS/CFT Correspondence

As mentioned in introduction, the original formulation of AdS/CFT correspondence [3, 35, 36] started with a solution of low energy string theory containing D3-brane charges, and the near-horizon limit of this D3-brane metric [37] corresponds to the direct product of AdS_5 in a Poincaré chart and a compact S^5 space, i.e., $AdS_5 \times S^5$. String theory in this ten-dimensional space is dual to a four-dimensional conformal field theory, and we denote this as AdS_5/CFT_4 (or AdS/CFT for short) correspondence. In this chapter, we will review the AdS spacetime and string theory, which are the foundations to this correspondence.

2.1 AdS Spacetime

2.1.1 AdS_2 Spacetime

The AdS spacetime has constant negative curvature, and can be embedded into higher dimensional flat spacetime. Let us first take sphere S^2 space as an example for the embedding. The three dimensional Euclidean space can be written as

$$ds^2 = dx^2 + dy^2 + dz^2, \tag{2.1}$$

where the sphere is a hypersurface of the Euclidean space defined by the constraint

$$x^2 + y^2 + z^2 = R^2. \tag{2.2}$$

The metric of the two-dimensional sphere have two intrinsic parameters and becomes

$$ds^2 = R^2(d\theta^2 + \sin^2\theta d\phi^2), \tag{2.3}$$

with coordinates transformation

$$x = R\sin\theta\cos\phi, \qquad y = R\sin\theta\sin\phi, \quad z = R\cos\theta. \tag{2.4}$$

Because the constraint (2.2) satisfies $SO(3)$ invariance of the Euclidean space, the S^2 also preserves the symmetry, which therefore can map any point on the map to the other points.

Like S^2, the AdS_2 spacetime[1] can be embedded into a flat spacetime

$$ds^2 = -dz^2 - dy^2 + dx^2, \tag{2.5}$$

with constraint

$$-z^2 - y^2 + x^2 = -L^2, \tag{2.6}$$

where L is called the AdS radius. Under the transformation

$$z = L\cosh\rho\cos t, \quad y = L\cosh\rho\sin t, \quad x = L\sinh\rho, \tag{2.7}$$

we can rewrite the metric with intrinsic coordinates ρ and t (they are called global coordinates) as

$$ds^2 = L^2(-\cosh^2\rho dt^2 + d\rho^2). \tag{2.8}$$

The curvature of AdS_2 spacetime is $R = -2/L^2$, which is negative. As (2.2) shows, the coordinate t has periodicity of 2π, so we usually unwrap this timelike direction and expanding the coordinate to $-\infty < t < \infty$ to cover the AdS_2 spacetime (Fig. 2.1).

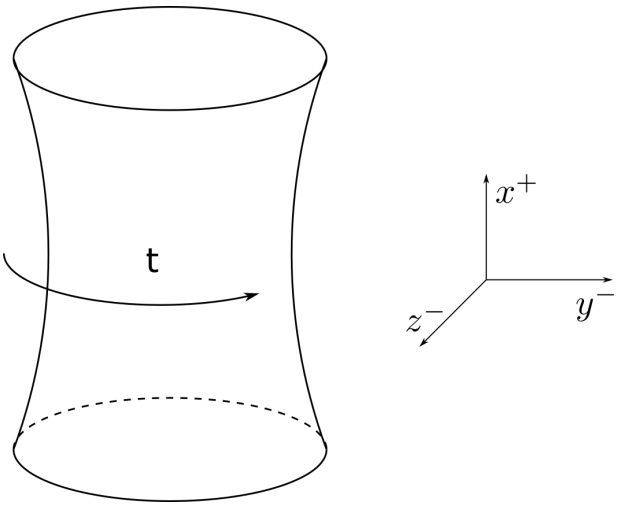

Figure 2.1: The embedding of AdS_2 into $\mathbb{R}^{2,1}$. Note that the timelike direction t is periodic.

AdS_2 in Conformal Coordinates and Poincaré Coordinates

If we define a new coordinate, θ, by $\tan\theta := \sinh\rho$ with $\theta : -\pi/2 \to \pi/2$, then the AdS_2 metric (2.8) changes to

$$ds^2 = \frac{L^2}{\cos^2\theta}\left(-dt^2 + d\theta^2\right). \tag{2.9}$$

[1]In this thesis we adopt the convention that the metric in a timelike direction is negative, i.e. the default signature of spacetime is $(-,+,+,\cdots,+)$. The form of Reimann tensor we use is $R^a{}_{bcd}$, and the Ricci tensor is $R_{ab} = R^c{}_{acb}$.

Note that the coordinate t here is the unwraped with $-\infty < t < \infty$. The expression has a conformal factor and is conformal flat with spacial boundary $\theta = \pm\pi/2$, which is called AdS boundary.

If we define the following coordinate transformation in (2.7)

$$\begin{aligned} z &= \frac{Lr}{2}\left(1 - t^2 + \frac{1}{r^2}\right), \\ y &= Lrt, \\ x &= \frac{Lr}{2}\left(-1 - t^2 + \frac{1}{r^2}\right), \end{aligned} \tag{2.10}$$

where $r > 0$ and $t : -\infty \to \infty$, the metric becomes

$$ds^2 = L^2(-r^2 dt^2 + \frac{dr^2}{r^2}). \tag{2.11}$$

This coordinate system will be generalized to Fefferman-Graham form [38–40] and is very useful for getting the standard AdS/CFT correspondence dictionary. In fact, we usually compactify the r direction for the convenience of numerical calculation with

$$z := \frac{1}{r}, \tag{2.12}$$

such that the metric becomes

$$ds^2 = \frac{L^2}{z^2}\left(-dt^2 + dz^2\right). \tag{2.13}$$

2.1.2 AdS_{d+1} in Global Coordinates and Poincaré Coordintates

As reviewed in [41], the AdS spacetime in $d+1$ dimensions can be obtained by embedding a hyperboloid of radius L,

$$-X_0^2 - X_{d+1}^2 + \sum_{i=1}^{d} X_i^2 = -L^2, \tag{2.14}$$

into a $d+2$ dimensional flat spacetime with metric

$$ds^2 = -dX_0^2 - dX_{d+1}^2 + \sum_{i=1}^{d} dX_i^2. \tag{2.15}$$

Introducing the following coordinates transformation into (2.14)

$$\begin{aligned} X_0 &= L\sec\rho\cos t, \\ X_{d+1} &= L\sec\rho\sin t, \\ X_i &= L\tan\rho\Omega_i, \quad i = 1, \cdots, d, \end{aligned} \tag{2.16}$$

where $0 \leq \rho < \pi/2, -\pi < t < \pi, -1 \leq \Omega_i \leq 1$ and $\sum_{i=1}^{d} \Omega_i^2 = 1$. Because the range of the parameters describes all the hyperboloid, they are called global coordinates. Then the AdS_{d+1} metric in the new coordinates is

$$ds^2 = \frac{L^2}{\cos^2 \rho} \left(-dt^2 + d\rho^2 + \sin^2 \rho \sum_{i=1}^{d} d\Omega_i^2 \right). \tag{2.17}$$

We can see the AdS spacetime has a boundary at $\rho = \pi/2$. Combined with this boundary, the AdS spacetime is now compactified with $0 \leq \rho \leq \pi/2$.

In order to get the metric in Poincaré coordinate, we introduce the light-cone coordinates

$$\begin{aligned} u &:= \frac{X_0 - X_d}{L^2}, \\ v &:= \frac{X_0 + X_d}{L^2}, \end{aligned} \tag{2.18}$$

and transform the other coordinates as

$$\begin{aligned} x_i &:= \frac{X_i}{Lu}, \\ t &:= \frac{X_{d+1}}{Lu}, \end{aligned} \tag{2.19}$$

then the constrain (2.14) becomes

$$uv + u^2 \left(t^2 - \overrightarrow{x}^2 \right) = 1, \tag{2.20}$$

with $\overrightarrow{x}^2 := \sum_{i=1}^{n} x_i^2$. Also for analytical and numerical convenience, we define

$$z := \frac{1}{u}, \tag{2.21}$$

and we can rewrite the old coordinates in terms of the new ones as

$$\begin{aligned} X_0 &= \frac{-t^2 + z^2 + \overrightarrow{x}^2 + L^2}{2z}, \\ X_i &= \frac{L x_i}{z}, \\ X_d &= \frac{-t^2 + z^2 + \overrightarrow{x}^2 - L^2}{2z}, \\ X_{d+1} &= \frac{Lt}{z}. \end{aligned} \tag{2.22}$$

Now we get the AdS metric in Poincaré coordinates

$$ds^2 = \frac{L^2}{z^2}\left(-dt^2 + dz^2 + d\overrightarrow{x}^2\right), \tag{2.23}$$

where we construct coordinate z such that it behaves as radial coordinate and $z = 0$ locates the boundary. The usual case we use is $z > 0$, which is just the half of entire AdS spacetime described in global coordinates. The region covered by Poincaré coordinates is called Poincaré patch. This metric preserves the scale invariance

$$(t, \overrightarrow{x}) \to \lambda\,(t, \overrightarrow{x}), \qquad z \to \lambda z. \tag{2.24}$$

Symmetries of AdS_{d+1} Spacetime

Like in the S^2 case, AdS_{d+1} spacetime has a larger symmetry $SO\,(2, d)$. First we count the number of symmetry generators for $SO\,(1, d)$ which is obviously obeyed by the metric of AdS_{d+1}, and it is $d\,(d+1)\,/2$. Adding the $d+1$ translation generators we have $(d+1)\,(d+2)\,/2$ in total, which is the number of symmetry generators of $SO\,(2, d)$ and also the maximum number of symmetry generators in AdS_{d+1}. For maximally symmetric sapcetimes, the Reimann tensor can be written as

$$R_{abcd} = \pm\frac{1}{L^2}\left(g_{ac}g_{bd} - g_{ad}g_{bc}\right), \tag{2.25}$$

where $\pm$ corresponds to positive (dS spacetime) or negative curvature (AdS spacetime). The Ricci tensor and Ricci scalar curvature are similarly

$$R_{ab} = \pm\frac{d}{L^2}g_{ab}, \qquad R = \pm\frac{d\,(d+1)}{L^2}. \tag{2.26}$$

One can then find the Einstein tensor $G_{ab} = R_{ab} - \frac{1}{2}Rg_{ab}$ to be

$$G_{ab} = \mp\frac{d\,(d-1)}{2L^2}g_{ab}. \tag{2.27}$$

The theory of Einstein gravity with cosmological constant Λ, is described by the following Lagrangian density

$$\mathcal{L} = \frac{1}{16\pi G_{d+1}}\left(R - 2\Lambda\right), \tag{2.28}$$

where G_{d+1} is the gravitational constant in d+1 dimensional spacetime. The Einstein equation is

$$G_{\mu\nu} + \Lambda g_{\mu\nu} = 0. \tag{2.29}$$

So, comparing with (2.27), we can see AdS_{d+1} spacetime has negative cosmological constant

$$\Lambda = -\frac{d\,(d-1)}{2L^2}. \tag{2.30}$$

2.2 Introduction to String Theory

As mentioned before, the AdS/CFT correspondence was originally proposed in the context of string theory. In this chapter we will review some basic elements of string theory, which is the necessary prerequisite for understanding the AdS/CFT conjecture. We will first have a short review of the bosonic string theory which is an unrealistic theory because there is only bosons, but it involves many of the issues that arise for superstrings. The detailed of this review can be found in [42–48]

2.2.1 Bosonic String

The Relativistic Point Particles

In special relativity, we can write down the action for relativistic point particle as

$$S = \int \mathcal{L} dt = -m \int dt \sqrt{1 - \dot{\vec{x}} \cdot \dot{\vec{x}}}, \tag{2.31}$$

with fixed coordinates $(t, \vec{x})$. We can easily get the conjugate momentum of $\vec{x}$

$$\vec{p} := \frac{\partial \mathcal{L}}{\partial \dot{\vec{x}}} = \frac{m \dot{\vec{x}}}{\sqrt{1 - \dot{\vec{x}} \cdot \dot{\vec{x}}}}, \tag{2.32}$$

and the energy of the particle which is equal to the Hamiltonian

$$E = H = \vec{p} \cdot \dot{\vec{x}} - \mathcal{L} = \sqrt{m^2 + \vec{p}^{\,2}}. \tag{2.33}$$

Both momentum and energy are the results we learned in special relativity. But there is a flaw in action (2.31): the space coordinates $(\vec{x})$ and time coordinate (t) play different roles. The space coordinates $\vec{x}$ is dynamical and the time t is just a label even though Lorentz transformations are supposed to mix them up.

In order to write down an action with manifest Lorentz symmetry, we have two options. One is to treat both space and time as labels which is the case in Quantum Field Theory (QFT). The other one is to promote time to a dynamical degree of freedom. Following the later, we obtain the action for point particle

$$S = -m \int d\tau \sqrt{-\dot{X}^\mu \dot{X}^\nu \eta_{\mu\nu}}, \tag{2.34}$$

with $\eta_{u\nu} = \text{diag}\,(-1, +1, +1, \cdots, +1)$, $\mu = 0, \cdots, d$ and $X^\mu = \dot{d}X^\mu/d\tau$. Here the introduced parameter τ is affine parameter which labels the position along the worldline of the particle (Fig. 2.2). Now we have an action with manifest Poincaré symmetry

$$X^\mu \to \Lambda^\mu_{\ \nu} X^\nu + c^\mu, \tag{2.35}$$

where c^μ is constant translation and $\Lambda^\mu_{\ \nu}$ is the Lorentz transformation with $\Lambda^\mu_{\ \rho}\eta^{\rho\sigma}\Lambda^\nu_{\ \sigma} = \eta^{\mu\nu}$. In fact, in (2.34) the element

$$\int d\tau\sqrt{-\dot{X}^\mu\dot{X}^\nu\eta_{\mu\nu}} = \int\sqrt{-X^\mu X_\mu} = \int\sqrt{-ds^2} \tag{2.36}$$

is just the proper time of the particle along the worldline.

It seems that now we have one more degrees of freedom than (2.31), because the time t is now a dynamical variable

$$X^0 = X^0(\tau) := t. \tag{2.37}$$

In fact, this is an illusion because action 2.34 has reparameterization invariance. If we pick a different affine parameter $\tilde{\tau}$ on the worldline with relation

$$\tilde{\tau} = \tilde{\tau}\,(\tau)\,, \tag{2.38}$$

the integration measure will change as $d\tau = d\tilde{\tau}(\frac{d\tau}{d\tilde{\tau}})$ and the velocities will change as

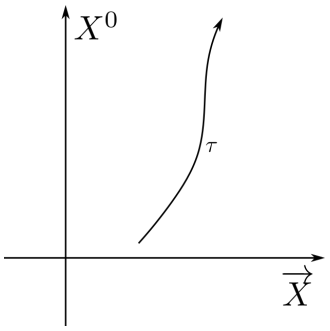

Figure 2.2: The worldline of point particle.

$$\frac{dX^\mu}{d\tau} = \frac{dX^\mu}{d\tilde{\tau}}\frac{d\tilde{\tau}}{d\tau}. \tag{2.39}$$

Substituting these into (2.34), we get the action in new parameterization

$$S = -m\int d\tilde{\tau}\sqrt{-\frac{dX^\mu}{d\tilde{\tau}}\frac{dX^\nu}{d\tilde{\tau}}\eta_{\mu\nu}}. \tag{2.40}$$

Thus we conclude that not all X^μ are physical, and the reparameterization invariance which is non-physical is the gauge symmetry of the system (i.e. this symmetry will not affect or give a constraint to our physical process). This is the price we pay to manifest Poincaré symmetry into action. Moreover, taking use of the gauge symmetry we can choose τ to be

$$\tau = X^0(\tau) = t, \tag{2.41}$$

and the original action (2.31) will be recovered from (2.34). The other way to see the existence of redundant symmetry in new action is through the conjugate momentum of X^μ

$$P_\mu := \frac{\partial\mathcal{L}}{\partial\dot{X}^\mu} = \frac{m\dot{X}^\nu\eta_{\mu\nu}}{\sqrt{-\dot{X}^\rho\dot{X}^\sigma\eta_{\rho\sigma}}}. \tag{2.42}$$

We have

$$P^\mu P_\mu + m^2 = 0, \tag{2.43}$$

which show the dependence between the momentums.

Nambu-Goto Action

In Minkowski space, just like a point particle sweeps out a worldline, a string sweeps out a two-dimensional worldsheet. We can choose two intrinsic parameters to describe the worldsheet: the timelike coordinate τ and the spacelike coordinate σ. If we compact σ to range like

$$0 \leq \sigma < 2\pi, \tag{2.44}$$

we get closed strings, otherwise we get open strings (Fig. 2.3).

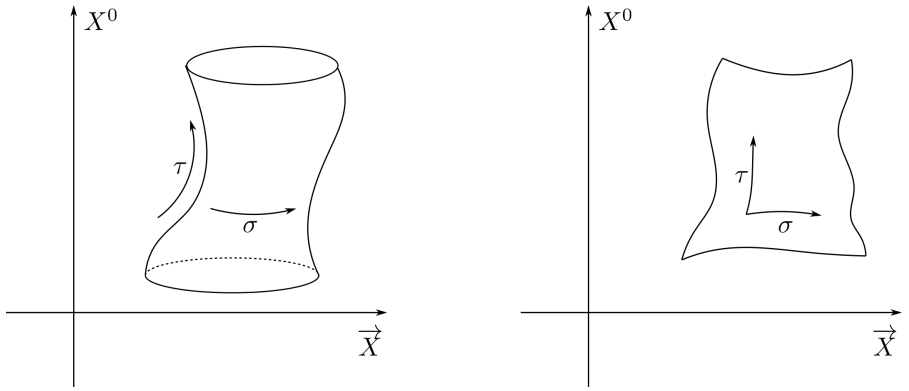

Figure 2.3: The worldsheet of strings from being embedded into Minkowski target spacetime. The left one is a closed string with periodic spacelike intrinsic parameter σ that looks like a cylinder. The right one is an open string that looks like a strip.

In the following we take the closed string to illustrate some basic properties of string theory. We package the two worldsheet coordinates together for convenience as $\sigma^\alpha = (\tau, \sigma), \quad \alpha = 0, 1$. The cylinder that the closed string worldsheet sweeps out lives in Minkowski spacetime with coordinates $X^\mu(\tau)$ which is sometimes referred to as the target space to distinguish it from string worldsheet. For the closed string, we have

$$X^\mu(\tau, \sigma) = X^\mu(\tau, \sigma + 2\pi). \tag{2.45}$$

Now we need to write down the action that describes the dynamics of this string. Motivated by the relativistic point particle case, where the action is proportional to the length of worldline, we may obtain the action for strings from its area of worldsheet. The worldsheet is a curved two-dimensional surface after being embedded in flat space and the induced metric on worldsheet ($\gamma_{\alpha\beta}$) is the pull-back of the flat metric on Minkowski space ($\eta_{\mu\nu}$),

$$\gamma_{\alpha\beta} = \frac{\partial X^\mu}{\partial \sigma^\alpha} \frac{\partial X^\nu}{\partial \sigma^\beta} \eta_{\mu\nu} = \begin{pmatrix} \dot{X}^2 & \dot{X} \cdot X' \\ \dot{X} \cdot X' & X'^2 \end{pmatrix}, \tag{2.46}$$

where we introduce the notation $\dot{X}^\mu = \partial X^\mu/\partial\tau$ and $\dot{X}^{\mu\prime} = \partial X^\mu/\partial\sigma$. Then the action is given by

$$S = -T\int d^2\sigma\sqrt{-\det\gamma} = -T\int d^2\sigma\sqrt{-\dot{X}^2X'^2 + \left(\dot{X}\cdot X'\right)^2}, \tag{2.47}$$

where the proportionality constant T is called the tension of string, which means the mass per unit length. The tension is usually written by

$$T = \frac{1}{2\pi\alpha'}. \tag{2.48}$$

Varying the action with respect to X^μ ,we get the equation of motion for X^μ

$$\partial_\alpha\left(\sqrt{-\gamma}\gamma^{\alpha\beta}\partial_\beta X^\mu\right) = 0. \tag{2.49}$$

Because we take the unit that length has dimension $[X^\mu] = -1$, the dimension of tension is $[T] = 2$. We can introduce string scale l_s which has dimension $[l_s] = -1$, such that

$$\alpha' = l_s^2. \tag{2.50}$$

The Polyakov Action

Due to the square root in Nambu-Goto action, it is difficult to quantize it using path integral techniques. We usually use another form of action for string, and it is the Polyakov action

$$S = -\frac{1}{4\pi\alpha'}\int d^2\sigma\sqrt{-g}g^{\alpha\beta}\partial_\alpha X^\mu\partial_\beta X^\nu\eta_{\mu\nu}. \tag{2.51}$$

Comparing with Nambu-Goto action, we introduce new field $g_{\alpha\beta}$, which has its own dynamics. Take variance of the action with respect to $g_{\alpha\beta}$ (recall that $\delta\sqrt{-g} = \frac{1}{2}\sqrt{-g}g^{\alpha\beta}\delta g_{\alpha\beta} = -\frac{1}{2}\sqrt{-g}g_{\alpha\beta}\delta g^{\alpha\beta}$), we get the equation of motion for $g_{\alpha\beta}$

$$g_{\alpha\beta} = 2f\left(\tau,\sigma\right)\partial_\alpha X\cdot\partial_\beta X = 2f\left(\tau,\sigma\right)\gamma_{\alpha\beta}, \tag{2.52}$$

with

$$f\left(\tau,\sigma\right) = \left(g^{\alpha\beta}\partial_\alpha X\cdot\partial_\beta X\right)^{-1}. \tag{2.53}$$

Compared with $\gamma_{\alpha\beta}$, $\sqrt{-g}$ scales as $2f\left(\tau,\sigma\right)$ in the action (2.51) and $g^{\alpha\beta}$ scales as $\frac{1}{2}f^{-1}\left(\tau,\sigma\right)$, so substituting (2.52) back into action (2.51), the conformal factor f will be canceled away and we recover the Nambu-Goto action. Thus the equation of motion for X^μ are the same

$$\partial_\alpha\left(\sqrt{-g}g^{\alpha\beta}\partial_\beta X^\mu\right) = 0. \tag{2.54}$$

Symmetries and Stress-energy Tensor

The Polyakov action still has the two symmetries that the Nambu-Goto action has:

- Global Poincaré invariance $X^\mu \to \Lambda^\mu_\nu X^\nu + c^\mu$.
- Reparameterization invariance on the worldsheet $\sigma^\alpha \to \tilde{\sigma}^\alpha(\sigma)$[2], under which the fields X^μ transform as scalars on worldsheet while $g_{\alpha\beta}$ transforms as tensor:

$$\begin{aligned} X^\mu(\sigma) &\to \tilde{X}^\mu(\tilde{\sigma}) = X^\mu(\sigma), \\ g_{\alpha\beta}(\sigma) &\to \tilde{g_{\alpha\beta}}(\tilde{\sigma}) = \frac{\partial\sigma^\gamma}{\partial\tilde{\sigma}^\alpha}\frac{\partial\sigma^\delta}{\partial\tilde{\sigma}^\beta} g_{\gamma\delta}(\sigma). \end{aligned} \tag{2.55}$$

Besides these two symmetries, there is also a new and novel symmetry for Polyakov action called

- Weyl invariance

$$g_{\alpha\beta}(\sigma) \to \Omega^2(\sigma)\, g_{\alpha\beta}(\sigma), \tag{2.56}$$

while the fields X^μ transform as $X^\mu(\sigma) \to \tilde{X}^\mu(\sigma)$. Weyl invariance is the symmetry of the theory under a local change of scale which changes the length between two points but preserves the angles between lines. Just like the scale factor f in (2.52), the parameter Ω only depends on worldsheet coordinates σ, and will be canceled in action and EoMs.

The worldsheet metric $g_{\alpha\beta}(\sigma)$ has three independent components. The two reparameterization can make the metric locally conformally flat which is called conformal gauge

$$g_{\alpha\beta} = e^{2\omega(\sigma)}\eta_{\alpha\beta}, \tag{2.57}$$

and Weyl symmetry can let us set $\omega = 0$, so the worldsheet metric can be safely chosen to be

$$g_{\alpha\beta} = \eta_{\alpha\beta}. \tag{2.58}$$

Interestingly and excitingly, we end up with flat metric on the embedded worldsheet in Minkowski coordinates.

With the choice of above flat metric, the Polyakov action becomes the theory of $d+1$ free scalar fields

$$S = -\frac{1}{4\pi\alpha'}\int d^2\sigma \partial_\alpha X \cdot \partial^\alpha X, \tag{2.59}$$

and the equation of motion for scalar fields X^μ is just the free wave equation

$$\partial_\alpha\partial^\alpha X^\mu = 0. \tag{2.60}$$

[2]From here on, we package coordinates (τ, σ) into σ when (τ, σ) shows as function variable or all referred worldsheet coordinates. For instance, $\tilde{\sigma}^\alpha(\sigma)$ is short-hand for $\tilde{\sigma}^\alpha(\tau, \sigma)$.

Be careful that the results (2.59) and (2.60) are obtained with the prerequisite that the EoM for $g_{\alpha\beta}$ is satisfied, which equals to

$$\frac{\delta S}{\delta g^{\alpha\beta}} = 0. \tag{2.61}$$

This variation with respect to action is proportional to stress-energy tensor, $T_{\alpha\beta}$, which has the definition

$$T_{\alpha\beta} := -\frac{2}{T}\frac{1}{\sqrt{-g}}\frac{\partial S}{\partial g^{\alpha\beta}}. \tag{2.62}$$

$$= \partial_\alpha X \cdot \partial_\beta X - \frac{1}{2}\eta_{\alpha\beta}\partial_\rho X \cdot \partial^\rho X. \tag{2.63}$$

The EoM associated to metric $g_{\alpha\beta}$ is $T_{\alpha\beta} = 0$ which is known as Virasoro constraints, and in detail,

$$\begin{aligned} T_{01} &= \dot{X} \cdot X' = 0, \\ T_{00} = T_{11} &= \frac{1}{2}\left(\dot{X}^2 + X'^2\right) = 0. \end{aligned} \tag{2.64}$$

Therefore, we learn that the EoM of the string is the wave equation (2.60) subject to the two constrains (2.64). The first constraint means the motion of string is perpendicular to the string itself, or the physical modes of the string are transverse oscillations. For the second constraint, one can see it relates the length of the string to the instantaneous velocity of the string by taking use of the residual gauge symmetry to choose so called static gauge (see [46] for more details)

$$X^0 := t. \tag{2.65}$$

We introduce lightcone coordinates on the worldsheet

$$\sigma^\pm = \tau \pm \sigma, \tag{2.66}$$

and the Virasoro constraints becomes

$$T_{++} = \partial_+ X^\mu \partial_+ X_\mu = 0,\ T_{--} = \partial_- X^\mu \partial_- X_\mu = 0, \quad T_{+-} = T_{-+} = 0, \tag{2.67}$$

where $\partial_\pm = \partial/\partial\sigma^\pm$.

String Spectrum and Mode Expansions

In the lightcone coordinates, the equation of motion for string simply read

$$\partial_+ \partial_- X^\mu = 0, \tag{2.68}$$

and it is straightforward to decompose the solution of X^μ into a left-moving mode $X_L^\mu(\sigma^+)$ and a right-moving mode $X_R^\mu(\sigma^-)$

$$X^\mu(\tau,\sigma) = X_L^\mu\left(\sigma^+\right) + X_R^\mu\left(\sigma^-\right). \tag{2.69}$$

The general periodic solution for closed string can be expanded in Fourier modes

$$\begin{aligned} X_L^\mu\left(\sigma^+\right) &= \frac{1}{2}x^\mu + \frac{1}{2}\alpha' p^\mu \sigma^+ + i\sqrt{\frac{\alpha'}{2}}\sum_{n\neq 0}\frac{1}{n}\tilde{\alpha}_n^\mu e^{-in\sigma^+}, \\ X_R^\mu\left(\sigma^-\right) &= \frac{1}{2}x^\mu + \frac{1}{2}\alpha' p^\mu \sigma^- + i\sqrt{\frac{\alpha'}{2}}\sum_{n\neq 0}\frac{1}{n}\alpha_n^\mu e^{-in\sigma^-}. \end{aligned} \tag{2.70}$$

The variable x^μ is the position of the center of mass of the string, while p^μ is the conserved charge from Noether currents that induced by translation symmetry $X^\mu \to X^\mu + c^\mu$, so p^μ is the momentum of the center of mass of the string. The sum of X_L^μ and X_R^μ satisfies the periodic conditiion $\sigma \to \sigma + 2\pi$ required for the closed string. X^μ has to be real therefore the coefficients of the Fourier modes obey

$$\alpha_n^\mu = (\alpha_{-n}^\mu)^\star, \qquad \tilde{\alpha}_n^\mu = (\tilde{\alpha}_{-n}^\mu)^\star. \tag{2.71}$$

Now we need to impose the mode expansion back into Virasoro constrains (2.67). First let us calculate

$$\partial_+ X^\mu = \partial_+ X_L^\mu = \frac{\alpha'}{2}p^\mu + \sqrt{\frac{\alpha'}{2}}\sum_{n\neq 0}\tilde{\alpha}_n^\mu e^{-in\sigma^+} = \sqrt{\frac{\alpha'}{2}}\sum_{n\in\mathbf{Z}}\tilde{\alpha}_n^\mu e^{-in\sigma^+}, \tag{2.72}$$

where we have defined zero mode $\tilde{\alpha}_0^\mu$ to be

$$\tilde{\alpha}_0^\mu := \sqrt{\frac{\alpha'}{2}}p^\mu. \tag{2.73}$$

Thus the constraint $T_{++} = 0$ can be written as

$$(\partial_+ X)^2 = \frac{\alpha'}{2}\sum_{m,p\in\mathbf{Z}}\tilde{\alpha}_m \cdot \tilde{\alpha}_p e^{-i(m+p)\sigma^+} \tag{2.74}$$

$$= \frac{\alpha'}{2}\sum_{m,n}\tilde{\alpha}_m \cdot \tilde{\alpha}_{n-m} e^{-in\sigma^+} \tag{2.75}$$

$$:= \alpha'\sum_n \tilde{L}_n e^{-in\sigma^+} = 0, \tag{2.76}$$

where we have defined

$$\tilde{L}_n = \frac{1}{2}\sum_m \tilde{\alpha}_m \cdot \tilde{\alpha}_{n-m}. \tag{2.77}$$

Similarly, from the constraint $T_{--} = 0$ we can define

$$L_n = \frac{1}{2}\sum_m \alpha_m \cdot \alpha_{n-m}. \tag{2.78}$$

with corresponding zero mode to be

$$\alpha_0^\mu := \sqrt{\frac{\alpha'}{2}} p^\mu, \tag{2.79}$$

and as such we have $\tilde{\alpha}_0^\mu = \alpha_0^\mu$.

Now we end up with solution of string (2.70) as well as constraints

$$\tilde{L}_n = L_n = 0, \qquad n \in \boldsymbol{Z}. \tag{2.80}$$

Among these infinity number of constraints, the

$$L_0 = \tilde{L}_0 = 0 \tag{2.81}$$

constraints are special, because they involve the square of the momentum p^μ which relates the rest of mass of a particle in Minkowski space:

$$p^\mu p_\mu = -m^2. \tag{2.82}$$

Therefore (2.81) implies

$$M^2 = \frac{4}{\alpha'}\sum_{n>0} \alpha_n \cdot \alpha_{-n} = \frac{4}{\alpha'}\sum_{n>0} \tilde{\alpha}_n \cdot \tilde{\alpha}_{-n}. \tag{2.83}$$

This expression tells us that the mass can be expressed in terms right-moving excited oscillators α_n^μ or in terms of left-moving excited oscillators $\tilde{\alpha}_n^\mu$, and both terms are equal to each other which is called *level matching*.

Covariant Quantization

All of the discussions above are classic part of the string theory. We will now move forward to the quantization of the string theory. Following the standard quantization procedure, we first prompt X^μ and their conjugate momentum

$$\Pi_\mu = \frac{\partial \mathcal{L}}{\partial \dot{X}^\mu} = \frac{1}{2\pi\alpha'}\dot{X}^\mu \tag{2.84}$$

to operator valued fields, which obey the canonical equal-time commutation relations

$$\begin{aligned} \left[X^\mu(\tau,\sigma), \Pi_\nu(\tau,\sigma')\right] &= i\delta(\sigma-\sigma')\,\delta^\mu_\nu, \\ \left[X^\mu(\tau,\sigma), X^\nu(\tau,\sigma')\right] &= \left[\Pi_\mu(\tau,\sigma), \Pi_\nu(\tau,\sigma')\right] = 0. \end{aligned} \tag{2.85}$$

Substituting the mode expansion (2.70) into the above commutation relations we obtain

$$[x^\mu, p_\nu] = i\delta^\mu_\nu, \quad [\alpha^\mu_n, \alpha^\nu_m] = [\tilde{\alpha}^\mu_n, \tilde{\alpha}^\nu_m] = n\eta^{\mu\nu}\delta_{n+m,0}, \tag{2.86}$$

and all others zero. Defining the annihilation operators and creation operators as

$$a^\mu_n = \frac{\alpha^\mu_n}{\sqrt{n}}, \quad a^{\mu\dagger}_n = \frac{\alpha^\mu_{-n}}{\sqrt{n}}, \qquad n > 0, \tag{2.87}$$

then we can rewrite commutation relations (2.86) in the form

$$\left[a^\mu_n, a^{\nu\dagger}_m\right] = \eta^{\mu\nu}\delta_{nm}, \quad [a^\mu_n, a^\nu_m] = \left[a^{\mu\dagger}_n, a^{\nu\dagger}_m\right] = 0. \tag{2.88}$$

Next step we may build the Fock space with above commutation relations, but there is a problem with (2.88). The timelike oscillators would have negative norm states because $\left[a^0_n, a^{0\dagger}_n\right] = -1$, which means we have *ghosts* in our theory. In order to have a sensible quantum theory we have to make sure that these negative norm states will decouple from any physical processes. The ghost problem may be solved by next imposing constraints equations on the states. But now we will take another way. We first solve the constraints in order to find a parameterization of all classical solutions of the string system, i.e., the classical phase space of the theory with only physical degrees of freedom.

Lightcone Quantization

Even though we have used reparameterizations and Weyl symmetry to fix the world-sheet metric $g_{\alpha\beta}$ into $\eta_{\alpha\beta}$ in (2.58), we still have a residue gauge symmetry in world-sheet lightcone coordinates:

$$\sigma^+ \to \tilde{\sigma}^+\left(\sigma^+\right), \quad \sigma^- \to \tilde{\sigma}^-\left(\sigma^-\right), \tag{2.89}$$

which will result in an overall factor

$$\eta_{\alpha\beta} \to \Omega^2(\sigma)\,\eta_{\alpha\beta}, \tag{2.90}$$

and can be undone by the compensating Weyl transformation. Now we introduce the spacetime lightcone coordinates to remove this remaining reparameterization (2.89)

$$X^\pm = \sqrt{\frac{1}{2}}\left(X^0 \pm X^{D-1}\right). \tag{2.91}$$

Now the target Minkowski spacetime reads

$$ds^2 = -2dX^+dX^- + \sum_{i=1}^{D-2} dX^i dX^i. \tag{2.92}$$

Recall the equation of motion for string (2.68), we have

$$X^+ = X_L^+\left(\sigma^+\right) + X_R^+\left(\sigma^-\right). \tag{2.93}$$

Using the remaining reparameterization (2.89), we choose the following coordinates such that

$$X_L^+ = \frac{1}{2}x^+ + \frac{1}{2}\alpha' p^+\sigma^+, \quad X_R^+ = \frac{1}{2}x^+ + \frac{1}{2}\alpha' p^+\sigma^-, \tag{2.94}$$

and in this gauge choice we have X^+ in *lightcone gauge*:

$$X^+ = x^+ + \alpha' p^+\tau. \tag{2.95}$$

The same equation of motion for X^- make us again expand it as

$$X^- = X_L^-\left(\sigma^+\right) + X_R^-\left(\sigma^-\right). \tag{2.96}$$

We don not need to solve the equation of motion for X^-, because it is completely determined by the constraints (2.67). For example, $T_{++} = 0$ gives $\left(\partial_+ X\right)^2 = 0$, which means

$$2\partial_+ X^- \partial_- X^+ = \sum_{i=1}^{D-2} \partial_+ X^i \partial_+ X^i. \tag{2.97}$$

Substituting (2.95) into above equation we obtain

$$\partial_+ X_L^- = \frac{1}{\alpha' p^+}\sum_{i=1}^{D-2} \partial_+ X^i \partial_+ X^i. \tag{2.98}$$

Similarly, from the constraints $T_{--} = 0$ we get

$$\partial_- X_R^- = \frac{1}{\alpha' p^+}\sum_{i=1}^{D-2} \partial_- X^i \partial_- X^i. \tag{2.99}$$

Thus we find that function $X^-\left(\sigma^+, \sigma^-\right)$ is completely determined (up to an integration constant x^-) in terms of $X^i\left(\sigma^+, \sigma^-\right), \quad i \in [1, d-2]$. Writing down the usual mode expansion for X^-

$$X_L^-\left(\sigma^+\right) = \frac{1}{2}x^- + \frac{1}{2}\alpha' p^- \sigma^+ + i\sqrt{\frac{\alpha'}{2}}\sum_{n\neq 0}\frac{1}{n}\tilde{\alpha}_n^- e^{-in\sigma^+}, \tag{2.100}$$

$$X_L^-\left(\sigma^+\right) = \frac{1}{2}x^- + \frac{1}{2}\alpha' p^- \sigma^- + i\sqrt{\frac{\alpha'}{2}}\sum_{n\neq 0}\frac{1}{n}\alpha_n^- e^{-in\sigma^-}, \tag{2.101}$$

we can see that p^-, $\tilde{\alpha}_n^-$ and α_n^- are all fixed by constraints. Specifically, we have

$$\alpha_n^- = \sqrt{\frac{1}{2\alpha'}}\frac{1}{p^+}\sum_{m=-\infty}^{+\infty}\sum_{i=1}^{D-2}\alpha_{n-m}^i\alpha_m^i = \sqrt{\frac{1}{2\alpha'}}\frac{1}{p^+}\sum_{m=-\infty}^{+\infty}\sum_{i=1}^{D-2}\tilde{\alpha}_{n-m}^i\tilde{\alpha}_m^i, \tag{2.102}$$

with $\alpha_0^- = \sqrt{\alpha'/2}p^-$. If α_n^i are specified then all the other oscillator modes are determined. On α_0^-, we have

$$\frac{\alpha' p^-}{2} = \frac{1}{2p^+}\sum_{i=1}^{D-2}\left(\frac{1}{2}\alpha' p^i p^i + \sum_{n\neq 0}\alpha_n^i\alpha_{-n}^i\right) = \frac{1}{2p^+}\sum_{i=1}^{D-2}\left(\frac{1}{2}\alpha' p^i p^i + \sum_{n\neq 0}\tilde{\alpha}_n^i\tilde{\alpha}_{-n}^i\right). \tag{2.103}$$

Now we can reconstruct the level matching condition (2.83) in the lightcone coordinates

$$M^2 = -p^\mu p_\mu = 2p^+p^- - \sum_{i=1}^{D-2} p^i p^i = \frac{4}{\alpha'}\sum_{i=1}^{D-2}\sum_{n>0}\alpha_n^i\alpha_{-n}^i = \frac{4}{\alpha'}\sum_{i=1}^{D-2}\sum_{n>0}\tilde{\alpha}_n^i\tilde{\alpha}_{-n}^i. \tag{2.104}$$

Comparing with (2.83) we can see now the m^2 is expressed in terms of α^i and $\tilde{\alpha}^i$ only, with $i = 1, 2, \cdots D-2$. The physical degrees of freedom are therefore $x^i,\ p,^i\ x,^-\ p^+$ and α_n^i with $n \neq 0$. Now we can define the vacuum state $|0;p\rangle$ of the Hilbert space such that

$$\hat{p}^\mu|0;p\rangle = p^\mu|0;p\rangle, \qquad \alpha_n^i|0;p\rangle = \tilde{\alpha}_n^i|0;p\rangle = 0, \quad \text{with } n > 0. \tag{2.105}$$

The indexes in the commutation relation (2.88) also change to be $\mu \to i, \nu \to j$, and as such there is no ghost now.

In the above quantization, there is an ordering ambiguity in the sum on the right-hand side of (2.104). Considering our new commutation relation, there should be an overall constant, a, if we choose all operators to be normal ordered

$$M^2 = \frac{4}{\alpha'}(\sum_{i=1}^{D-2}\sum_{n>0}\alpha_n^i\alpha_{-n}^i - a) = \frac{4}{\alpha'}(\sum_{i=1}^{D-2}\sum_{n>0}\tilde{\alpha}_n^i\tilde{\alpha}_{-n}^i - a), \tag{2.106}$$

where

$$a = \frac{D-2}{2}\sum_{n>0} n = -\frac{D-2}{24}, \tag{2.107}$$

and we have used the Zeta-function to get the last equal sign. In the following we will use the definition $N := \sum_{i=1}^{D-2}\sum_{n>0}\alpha_n^i\alpha_{-n}^i$ and $\tilde{N} := \sum\sum_{n>0}\tilde{\alpha}_n^i\tilde{\alpha}_{-n}^i$ for simplification.

String spectrum

The vacuum state has no excited oscillators with mass

$$M^2 = -\frac{1}{\alpha'}\frac{D-2}{6}. \tag{2.108}$$

When $D > 2$ the mass square of the ground state is negative and thus the particles are tachyons[3]. The string theory is unstable and no one knows whether there is a

[3]Note that in superstring theory, there is no tachyon

minimum potential for it elsewhere. Though this is a problem for bosonic string, it will not appear in superstring theory where we introduce fermions on the worldsheet. Let us ignore the problem and continue to see the first excited states. Considering the level matching condition (2.104), the first excited states should look like

$$\tilde{\alpha}^i_{-1}\alpha^j_{-1}\left|0;p\right\rangle, \tag{2.109}$$

where there are $(D-2)^2$ particle states and each of which has mass

$$M^2 = \frac{4}{\alpha'}\left(1-\frac{D-2}{24}\right). \tag{2.110}$$

Now we hope to see the $(D-2)^2$ states satisfy the Lorentz invariance $SO(1,D-1)$. If the particle is massive in $\mathbb{R}^{1,D-1}$, we can always choose frame to stay in the rest frame of the particle and have $p^\mu = (p,0,\cdots,0)$. Then any massive particle must form a representation of little group $SO(D-1)$ of $ISO(1,D-1)$ which is impossible for our independent $(D-2)^2$ states. If the particle is massless, we can always choose the momentum of the particle with form $p^\mu = (p,0,\cdots,0,p)$, and each of such particles should be the representation of little group $SO(D-2)$, which is the case for our $(D-2)^2$ first excited states. Now we learn that, in order to keep the Lorenz symmetry in the first excited state and avoid anomalies, the dimension of the spacetime is

$$D = 26. \tag{2.111}$$

The excited states (2.109) transform in the $24\otimes 24$ representation of group $SO(24)$, and can be decomposed into three irreducible representations with associated massless fields:

$$\text{traceless symmetric } G_{\mu\nu}(X) \oplus \text{anti-symmetric } B_{\mu\nu}(X) \oplus \text{singlet (trace) } \Phi(X). \tag{2.112}$$

The massless spin 2 $G_{\mu\nu}(X)$ is thought to be equivalent to graviton by the argument from Feynman and Weinberg. The anti-symmetric tensor field $B_{\mu\nu}(X)$ is also called the "Kalb-Ramond field" and the scalar field is called the *dilaton*.

Lorentz Symmetry and Critical Dimension

In the lightcone gauge (2.95), it is not obvious whether the spacetime Lorentz symmetry is preserved. We would like to preserve the Lorentz symmetry during quantization to avoid anormaly. Consider an infinitesimal linear transformation of the form $X^\mu \to X^\mu + \delta X^\mu$, where

$$\delta X^\mu = \epsilon^{\mu\nu}X_\nu. \tag{2.113}$$

We require this transformation to preserve the Lorentz symmetry, such that

$$\delta\left(\eta_{\mu\nu}X^\mu X^\nu\right) = 2\eta_{\mu\nu}\left(\delta X^\mu\right)X^\nu = 2\eta_{\mu\nu}\left(\epsilon^{\mu\rho}X_\rho\right)X^\nu = 2\epsilon^{\mu\rho}X_\rho X_\mu = 0. \tag{2.114}$$

The vanishing of (2.114) for all values of X_μ implies that the symmetric part of $\epsilon^{\mu\nu}$ is zero, and therefore $\epsilon^{\mu\nu}$ is antisymmetric

$$\epsilon^{\mu\nu} = -\epsilon^{\nu\mu}. \tag{2.115}$$

The Polyakov action (2.59) is invariant under Lorentz symmetry, so we have the corresponding conserved Noether current $j^\alpha_{\mu\nu}$:

$$\epsilon^{\mu\nu} j^\alpha_{\mu\nu} = \frac{\partial \mathcal{L}}{\partial\left(\partial_\alpha X^\mu\right)} \delta X^\mu = \mathcal{P}^\alpha_\mu \epsilon^{\mu\nu} X^\nu = \left(-\frac{1}{2}\epsilon^{\mu\nu}\right)\left(X_\mu \mathcal{P}^\alpha_\mu - X_\nu \mathcal{P}^\alpha_\mu\right). \tag{2.116}$$

We define the current

$$\mathcal{M}^\alpha_{\mu\nu} = X_\mu \mathcal{P}^\alpha_\nu - X_\nu \mathcal{P}^\alpha_\mu, \tag{2.117}$$

with the equation of current conservation

$$\frac{\partial \mathcal{M}^\tau_{\mu\nu}}{\partial\tau} + \frac{\partial \mathcal{M}^\sigma_{\mu\nu}}{\partial\sigma} = 0. \tag{2.118}$$

The Lorentz charges $M_{\mu\nu}$ can be obtained by using constant τ lines as

$$M_{\mu\nu} = \int \mathcal{M}^\tau_{\mu\nu}(\tau,\sigma)\, d\sigma = \int \left(X_\mu \mathcal{P}^\tau_\mu - X_\nu \mathcal{P}^\tau_\mu\right) d\sigma. \tag{2.119}$$

Recalling that the lightcone coordinates (2.91) are formed by two special coordinates, we are not sure whether the consistent Lorentz generators exist to obey the commutation relations of the Lorentz Lie algebra, namely

$$[M^{\mu\nu}, M^{\rho\sigma}] = i\eta^{\mu\rho} M^{\nu\sigma} - i\eta^{\nu\rho} M^{\mu\sigma} + i\eta^{\mu\sigma} M^{\rho\nu} - i\eta^{\nu\sigma} M^{\rho\mu}. \tag{2.120}$$

The generator M^{i-} in lightcone gauge is rather complicated functions of transversal oscillators

$$M^{i-} = x^i p^- - x^- p^i - i\sum_{n=1}^{\infty} \frac{1}{n}\left(\alpha^i_{-n}\alpha^-_n - \alpha^-_{-n}\alpha^i_n\right) - i\sum_{n=1}^{\infty} \frac{1}{n}\left(\tilde{\alpha}^i_{-n}\tilde{\alpha}^-_n - \tilde{\alpha}^-_{-n}\tilde{\alpha}^i_n\right). \tag{2.121}$$

In order to realize a unitary representation of the Poincaré group in the quantum theory, we require the Lorentz generators to be Hermitian, i.e. $(M^{\mu\nu})^\dagger = M^{\mu\nu}$ and normal-ordered. Therefore, we rewrite (2.121) as

$$M^{i-} = \frac{1}{2}(x^i p^- + p^- x^i) - x^- p^i - i\sum_{n=1}^{\infty} \frac{1}{n}\left(\alpha^i_{-n}\alpha^-_n - \alpha^-_{-n}\alpha^i_n\right) - i\sum_{n=1}^{\infty} \frac{1}{n}\left(\tilde{\alpha}^i_{-n}\tilde{\alpha}^-_n - \tilde{\alpha}^-_{-n}\tilde{\alpha}^i_n\right) \tag{2.122}$$

to be the candidates of the Lorentz algebra symmetry (2.120), i.e.

$$\left[M^{i-}, M^{j-}\right] = 0. \tag{2.123}$$

After tedious calculation (see [43] for example for detailed calculation), we have

$$\left[M^{i-}, M^{j-}\right] = \frac{2}{\alpha' \left(p^+\right)^2} \sum_{n>0} \left(\left[\frac{D-2}{24} - 1 \right] n + \frac{1}{n} \left[a - \frac{D-2}{24} \right] \right) \left(\alpha^i_{-n} \alpha^j_n - \alpha^j_{-n} \alpha^i_n \right) + (\alpha \leftrightarrow \tilde{\alpha}) \,. \tag{2.124}$$

Thus we find that for general values of a and d the theory is not Lorentz invariant, and the right-hand side of (2.124) is anomalous which means the Lorentz invariance is destroyed during the quantization. However, for special values

$$D = 26, \qquad a = 1, \tag{2.125}$$

the anomaly vanishes and the Lorentz invariance is restored.

2.2.2 Open Strings and D-Branes

We are going to discuss open strings in this section. Open strings have two end points and we can parameterize the spatial coordinates of the string by

$$\sigma \in [0, \pi] \,. \tag{2.126}$$

The action for an open string is still the Polyakov action

$$S = -\frac{1}{4\pi\alpha'} \int d^2\sigma \partial_\alpha X \cdot \partial^\alpha X, \tag{2.127}$$

which is in conformal gauge. As the case with the closed string, we obtain the equation of motion by finding the extrema of the action supplemented by adding suitable boundary conditions to determine how the end points move:

$$\begin{aligned} \delta S &= -\frac{1}{2\pi\alpha'} \int_{\tau_i}^{\tau_f} d\tau \int_0^\pi \partial_\alpha X \cdot \partial^\alpha \delta X \\ &= -\frac{1}{2\pi\alpha'} \int_{\tau_i}^{\tau_f} d\tau \int_0^\pi [\partial_\alpha (\partial^\alpha X \cdot \delta X) - (\partial_\alpha \partial^\alpha X) \cdot \delta X]. \end{aligned} \tag{2.128}$$

The second term of (2.128) gives us the equation of motion if the first total derivative term vanishes. Expanding the total derivative term

$$-\frac{1}{2\pi\alpha'} \int_{\tau_i}^{\tau_f} d\tau \int_0^\pi [\partial_\alpha (\partial^\alpha X \cdot \delta X)] \tag{2.129}$$

$$= \frac{1}{2\pi\alpha'} [\int_0^\pi d\sigma \dot{X} \cdot \delta X]_{\tau=\tau_i}^{\tau=\tau_f} - \frac{1}{2\pi\alpha'} [\int_{\tau_i}^{\tau_f} d\tau X' \cdot \delta X]_{\sigma=0}^{\sigma=\pi}, \tag{2.130}$$

we know that the first term of (2.130) vanishes because $\delta X^\mu = 0$ is required at the time slices $\tau = \tau_i$ and $\tau = \tau_f$ in order to obtain the equation of motion. However, in order to vanish the second term, we need

$$\partial_\sigma X^\mu \delta X_\mu = 0 \qquad \text{at } \sigma = 0, \pi. \tag{2.131}$$

This means we can impose two different types of boundary conditions:

- Neumann boundary conditions.

$$\partial_\sigma X^\mu = 0 \qquad \text{at } \sigma = 0,\ \pi. \tag{2.132}$$

As with the closed string, in the static gauge we find that the free end-point of the string moves at the speed of light [46].

- Dirichlet boundary conditions.

$$\delta X^\mu = 0 \qquad \text{at } \sigma = 0,\ \pi. \tag{2.133}$$

This means that the end points of the string lie at some fixed position in space, $X^\mu = c^\mu$. This may seem to be odd that the strings are fixed at some point c^μ.

In order to understand what the Dirichlet boundary conditions mean to strings, we consider Neumann boundary conditions for some coordinates of the string and Dirichlet boundary conditions for the others, so at both end points of the string we have

$$\partial_\sigma X^a = 0 \qquad \text{for } a = 0, \cdots p, \tag{2.134}$$

$$X^I = c^I \qquad \text{for } I = p+1, \cdots D-1. \tag{2.135}$$

Now we fix the end points of the string to a $(p+1)$-dimensional hypersurface which is called *D-brane* or *Dp*-brane, and the Lorentz group of the theory is broken to

$$SO(1, D-1) \to SO(1, p) \times SO(D-p-1). \tag{2.136}$$

In *Dp*-brane where D means Dirichlet and p is the number of the spatial dimensions of the brane, we can see a $D0$-brane is a particle; a $D1$-brane is a string; a $D2$-brane is a membrane and so on. The *Dp*-brane sits at fixed position c^I and also has its own dynamics.

We take the usual mode expansion for open string, $X^\mu = X_L^\mu(\sigma^+) + X_R^\mu(\sigma^-)$, and

$$\begin{aligned} X_L^\mu\left(\sigma^+\right) &= \frac{1}{2}x^\mu + \alpha' p^\mu \sigma^+ + i\sqrt{\frac{\alpha'}{2}} \sum_{n\neq 0} \frac{1}{n} \tilde{\alpha}_n^\mu e^{-in\sigma^+} \\ X_R^\mu\left(\sigma^-\right) &= \frac{1}{2}x^\mu + \alpha' p^\mu \sigma^- + i\sqrt{\frac{\alpha'}{2}} \sum_{n\neq 0} \frac{1}{n} \alpha_n^\mu e^{-in\sigma^-}. \end{aligned} \tag{2.137}$$

The modes of the string are related because of the boundary conditions. For the Neumann boundary conditions $\partial_\sigma X^a = 0$ we have

$$\alpha_n^a = \tilde{\alpha}_n^a. \tag{2.138}$$

For the Dirichlet boundary conditions $X^I = c^I$ we have

$$x^I = c^I, \qquad p^I = 0, \qquad \alpha_n^I = -\tilde{\alpha}_n^I. \tag{2.139}$$

So we only have one independent set of oscillators, say α_n, and the other modes can be determined by the boundary conditions.

Quantization

We quantize the open string by promoting the fields x^a, p^a and α_n^μ to operators, and the other elements in the mode expansion are fixed by the boundary conditions, so the states we get after quantization are restricted to lie on the Dp-brane. As the case in closed string, we choose spacetime lightcone coordinate which lie within the brane,

$$X^\pm = \sqrt{\frac{1}{2}}\left(X^0 \pm X^p\right). \tag{2.140}$$

Following the procedure of closed string, we can get the mass formula for states which is the sum over the transverse modes of the string,

$$M^2 = \frac{1}{\alpha'}\left(\sum_{i=1}^{p-1}\sum_{n>0}\alpha_{-n}^i\alpha_n^i + \sum_{i=p+1}^{D-1}\sum_{n>0}\alpha_{-n}^i\alpha_n^i - a\right), \tag{2.141}$$

where a is the ordering constant. As in the closed string case, requiring the Lorentz symmetry $SO(1,p)\times SO(D-p-1)$ of the quantum theory, we are forced to choose

$$D = 26, \qquad a = 1. \tag{2.142}$$

It is worth pointing out that there is a factor of 2 difference in the p^μ term in the mode expansion between the open string (2.137) and the closed string (2.70). This is because in the open string $\sigma \in (0,\pi)$, not $\sigma \in (0,2\pi)$ as in the closed string, which is to make sure the conserved charge in open string is still p^μ. The factor 2 difference also contribute to an overall factor of 4 difference in the mass formula. The other difference is that the sum in mass formula here is only over α modes, and the $\tilde{\alpha}$ modes are not independent because of the boundary conditions.

The ground state of the quantum theory is defined by

$$\alpha_n^i\left|0;p\right\rangle = 0 \qquad n > 0, \tag{2.143}$$

where the spatial index runs over $i-1,\cdots,p-1,p+1,\cdots,D-1$. The mass of the ground state is

$$M^2 = -\frac{1}{\alpha'}, \tag{2.144}$$

and it is a tachyon. Here the tachyon is confined to the brane, which means the brane is unstable. The brane will decay with the open string dissolving into closed string modes.

The first excited states are massless and fall into two classes:

- Oscillators longitudinal to the brane,

$$\alpha_{-1}^a\left|0;p\right\rangle \qquad a = 1,\cdots p-1. \tag{2.145}$$

These states lie within the brane and transform under the $SO(1,p)$ Lorentz group. The particles have spin-1 and are photons.

- Oscillators transverse to the brane,

$$\alpha_{-1}^{I}\left|0;p\right\rangle \qquad I=p+1,\cdots D-1. \tag{2.146}$$

These states are vectors under the $SO\left(D-p-1\right)$ rotation group and are transverse to the brane. They are scalars under the $SO\left(1,p\right)$ Lorentz group of the brane and are regarded as fluctuations of the brane in the transverse directions, which implies that the D-brane is a dynamical object.

In higher excited states, say at level N, the mass of the string is

$$M^2=\frac{1}{\alpha'}\left(N-1\right). \tag{2.147}$$

The maximal spin angular momentum (without orbital angular momentum) J is then

$$J=N=\alpha' M^2+1. \tag{2.148}$$

This linear relation between angular momentum and mass square are usually called *Regge trajectories* (or Chew-Fraschuti trajectories). The Regge trajectories are seen in the spectrum of both mesons and baryons. Figure 2.4 shows the ρ-meson case.

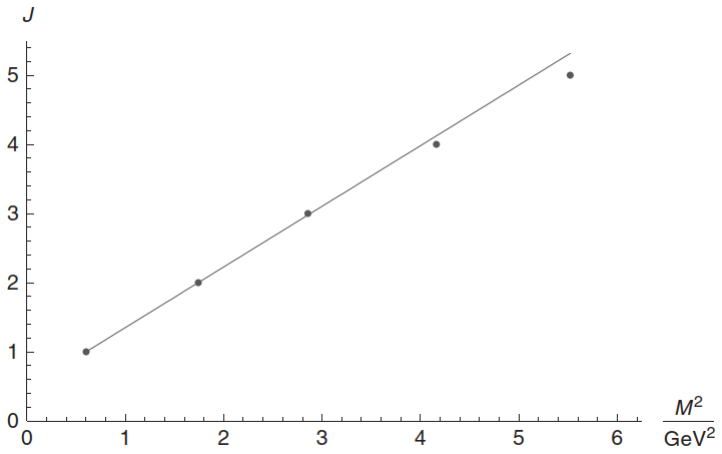

Figure 2.4: Regge trajectory for the ρ-mesons $\rho\left(776\right)$, $a_2\left(1320\right)$, $\rho_3\left(1690\right)$, $a_4\left(2040\right)$, and $\rho_5\left(2350\right)$. The line is fit to go through the $\rho\left(776\right)$ and $a_2\left(1320\right)$.

String theory seemed to be a reasonable candidate for strong interactions because of the natural emergence of this relationship between J and M^2 and the parameter α' has its name "Regge slope" from here. Even though QCD instead of string theory[4] adopted as the strong interaction theory, a meson in QCD that is a pair of quarks can be approximately described in the string picture as held at the ends of an open string forming a confining flux tube.

[4]There are unwanted massless vectors and massless tensors in the string description.

String perturbation theory

In quantum field theory with a fixed background, the basic objects we compute are the correlation functions

$$\langle \phi(x_1) \cdots \phi(x_n) \rangle . \tag{2.149}$$

However in gravity (we will discuss the emergency of gravity in string theory soon), there are gauge symmetries, i.e. diffeomorphisms, which can map points x_i to another point. This means correlation functions are not physical because only gauge invariant observables make sense in gauge theory. Instead, the object that we can compute in string theory is the S-matrix, where we take the points in the correlation function to infinity: $x_i \to \infty$. Moreover, a conformal transformation is imposed to bring each of these infinite external legs to a finite distance, and the S-matrix is now equivalent to a worldsheet with the topology of sphere, dotted with vertex operators where the legs used to be (see Fig. 2.5 for closed string case).

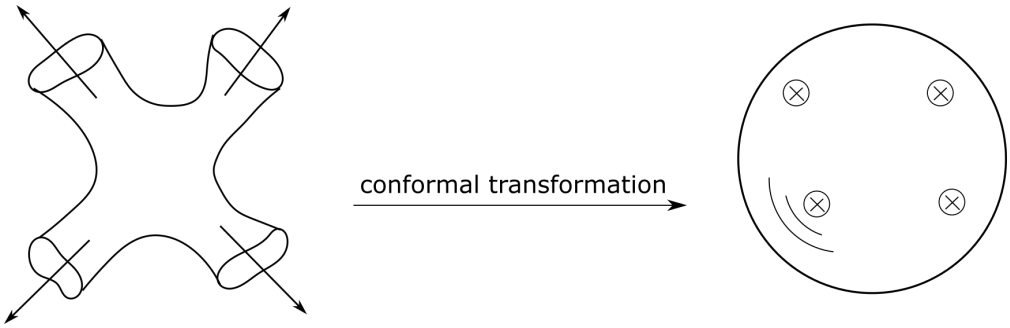

Figure 2.5

In the Polyakov path integral, we need to sum over all different worldsheet topologies which connect initial and final string configurations. The action for perturbed string theory is the augmented Ployakov action

$$S_{string} = S_{Poly} + \lambda\chi, \tag{2.150}$$

where λ is just a real number and χ is given by an integral in Euclidean signature over the worldsheet

$$\chi = \frac{1}{4\pi} \int d^2\sigma \sqrt{g} R. \tag{2.151}$$

Here R is the Ricci scalar of the worldsheet metric and is invariant under the reparameterizations and Weyl transformations. In two dimensions which is the dimension of our worldsheet, Gauss-Bonnet theorem says that the integral of the Ricci scalar over the worldsheet gives an integer, χ, called the Euler number of the worldsheet. The Euler number is related to the genus of the worldsheet by $\chi = 2(1-g)$, where g is called the *genus* of the surface which naively can be regarded as the handles of the worldsheet (see Fig. 2.6).

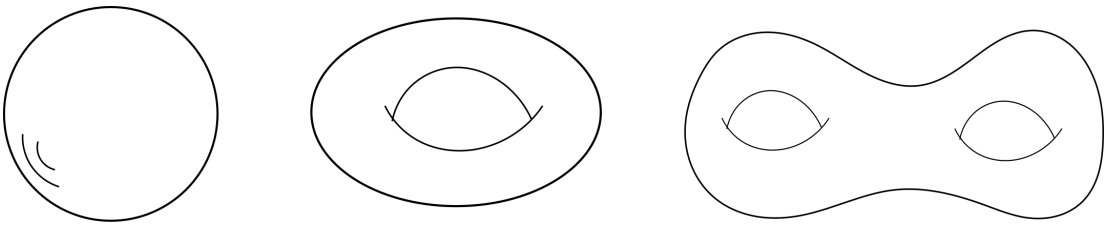

Figure 2.6: Genus of orientable surfaces.

Then the integral over the worldsheet Σ decomposes into a sum over all genus g and an integral over the corresponding worldsheets Σ_g

$$Z = \int_{\Sigma} \mathcal{D}X\mathcal{D}g_{\alpha\beta}e^{-S_{string}} = \sum_{g=0}^{\infty} e^{-2\lambda(1-g)} \int_{\Sigma_g} \mathcal{D}X\mathcal{D}g_{\alpha\beta}e^{-S_{Poly}}. \tag{2.152}$$

The $e^{-2\lambda(1-g)}$ gives different weighted factors to different worldsheet topologies. For closed strings, adding a handle or increasing genus by one corresponds to emitting and reabsorbing a closed string, so the closed string coupling constant g_{closed} may thus be identified with

$$g_s = g_{closed} = e^{\lambda}. \tag{2.153}$$

An analogous argument for open strings shows that $g_{open}^2 = e^{\lambda}$. After a conformal map, the tree level scattering for closed string corresponds to a worldsheet with topology of a sphere, with vertex operators inserted for the initial and final states. One-loop scattering corresponds to a toroidal worldsheet with vertex operators. Therefore the sum over worldsheets in (2.152) becomes a sum over Riemann surfaces of increasing genus with vertex operators inserted, each of which is weighted by

$$\left(g_s^2\right)^{g-1}. \tag{2.154}$$

The low-energy effective action: emergency of gravity

Up to now, we have only discussed strings propagating in the flat spacetime. In this section we will consider strings propagating in curved spacetime which is equivalent to having different CFTs on the worldsheet of string. As discussed in the string spectrum section, the first excited states $\tilde{\alpha}_{-1}^{i}\alpha_{-1}^{j}\left|0;p\right\rangle$ can be decomposed into three irreducible representations with associated massless fields: the symmetric tensor field $G_{\mu\nu}\left(X\right)$ which is thought to be equivalent to graviton, the anti-symmetric Kalb-Ramond field $B_{\mu\nu}\left(X\right)$ and the scalar field $\Phi\left(X\right)$ which is called dilaton.

The generalization of the Polyakov action describing a string moving in curved spacetime is

$$S = \frac{1}{4\pi\alpha'} \int d^2\sigma\sqrt{g}g^{\alpha\beta}\partial_{\alpha}X^{\mu}\partial_{\beta}X^{\nu}G_{\mu\nu}\left(X\right), \tag{2.155}$$

which is in Euclidean signature. Actions of this form are known as *non-linear sigma models*. In addition to the anti-symmetric Kalb-Ramond field $B_{\mu\nu}$ and dilaton $\Phi(X)$, the action of a string moving in these background is given by

$$S = \frac{1}{4\pi\alpha'}\int d^2\sigma\sqrt{g}(g^{\alpha\beta}\partial_\alpha X^\mu \partial_\beta X^\nu G_{\mu\nu}(X) + i\epsilon^{\alpha\beta}\partial_\alpha X^\mu \partial_\beta X^\nu B_{\mu\nu}(X) + \alpha'\Phi(X) R^{(2)}), \tag{2.156}$$

where $R^{(2)}$ is the two-dimensional Ricci scalar of the worldsheet. Generally, the last term (dilaton coupling term) in this action does not respect Weyl invariance. An exception is the constant dilation $\Phi(X) = \lambda$, such that the dilaton coupling term reduces to what we have seen before:

$$S_{dilaton} \equiv S = \frac{1}{4\pi\alpha'}\int d^2\sigma\sqrt{g}(\alpha'\Phi(X) R^{(2)}) = \lambda\chi. \tag{2.157}$$

This means that the constant mode of the dilaton $\langle\Phi\rangle$, which is usually taken to be the asymptotic value of the dilaton

$$\Phi_0 = \lim_{X\to\infty}\Phi(X), \tag{2.158}$$

determines the string coupling constant by

$$g_s = e^{\Phi_0}, \tag{2.159}$$

which means the string coupling is not an independent parameter of string theory and is just the expectation value of a field that can be determined dynamically. To ensure Weyl invariance of the theory with dilaton $\Phi(X)$, we have to impose the tracelessness of the worldsheet energy-momentum tensor. The trace of the stress-energy momentum tensor is

$$\langle T^\alpha{}_\alpha\rangle = -\frac{1}{2\alpha'}\beta_{\mu\nu}(G)\, g^{\alpha\beta}\partial_\alpha X^\mu \partial_\beta X^\nu - \frac{i}{2\alpha'}\beta_{\mu\nu}(B)\,\epsilon^{\alpha\beta}\partial_\alpha X^\mu \partial_\beta X^\nu - \frac{1}{2}\beta(\Phi) R^{(2)}, \tag{2.160}$$

where the three β functions of order α' are given by

$$\beta_{\mu\nu}(G) = \alpha' R_{\mu\nu} + 2\alpha'\nabla_\mu\nabla_\nu\Phi - \frac{\alpha'}{4}H_{\mu\lambda\kappa}H_\nu{}^{\lambda\kappa}, \tag{2.161}$$

$$\beta_{\mu\nu}(B) = -\frac{\alpha'}{2}\nabla^\lambda H_{\lambda\mu\nu} + \alpha'\nabla^\lambda\Phi H_{\lambda\mu\nu}, \tag{2.162}$$

$$\beta(\Phi) = -\frac{\alpha'}{2}\nabla^2\Phi + \alpha'\nabla_\mu\Phi\nabla^\mu\Phi - \frac{\alpha'}{24}H_{\mu\nu\lambda}H^{\mu\nu\lambda}, \tag{2.163}$$

where the filed strength H is defined for Kalb-Ramond field by $H = dB$, or

$$H_{\mu\nu\rho} = \partial_\mu B_{\nu\rho} + \partial_\nu B_{\rho\mu} + \partial_\rho B_{\mu\nu}. \tag{2.164}$$

The 3-form H provides an anti-symmetric component to the affine connection sometimes known as torsion. In order to keep the Weyl invariance of the string theory,

the energy-momentum tensor should be traceless, $\langle T^{\alpha}_{\alpha} \rangle = 0$ and thus $\beta_{u\nu}(G) = \beta_{\mu\nu}(B) = \beta(\Phi) = 0$.

From another perspective, we can view the equations $\beta_{u\nu}(G) = \beta_{\mu\nu}(B) = \beta(\Phi) = 0$ as equations of motion for the background where the string propagates. Remarkably, theses equations may be derived as equations of motion from the target spacetime action

$$S = \frac{1}{2\kappa_0^2} \int d^D X \sqrt{-G} e^{-2\Phi} \left(R - \frac{1}{12} H_{\mu\nu\rho} H^{\mu\nu\rho} + 4\nabla_\mu \Phi \nabla^\mu \Phi - \frac{2(D-26)}{3\alpha'} + \mathcal{O}(\alpha') \right), \tag{2.165}$$

where we have done a Wick rotation back to Minkowski space for this expression, and R and ∇_μ are respectively the Ricci scalar and the covariant derivatives associated with the target spacetime metric $G_{\mu\nu}$. This forms the low-energy effective action of the bosonic string for the massless closed string states $G_{\mu\nu}$, $B_{\mu\nu}$ and Φ.

It is also worth pointing out that the kinetic term for Φ in (2.165) seems to be opposite to the usual convention. In fact this is not a problem. The kinetic term is not canonically normalized because of the factor $e^{-2\Phi}$. Before we normalize the action, we define the varying part of the dilaton as

$$\tilde{\Phi} = \Phi - \Phi_0. \tag{2.166}$$

Then we define a new metric $\tilde{G_{\mu\nu}}$ for $D > 2$ as

$$\tilde{G}_{\mu\nu}(X) = e^{-4\tilde{\Phi}/(D-2)} G_{\mu\nu}, \tag{2.167}$$

and the Einstein-Hilbert term of the action (2.165) is also normalized canonically and prefactor of the kinetic term for Φ turns negative

$$\begin{aligned} S = \frac{1}{2\kappa^2} \int d^D X \sqrt{-\tilde{G}} (\tilde{R} - \frac{1}{12} e^{-\frac{8}{D-2}\tilde{\Phi}} H_{\mu\nu\rho} H^{\mu\nu\rho} - \frac{4}{D-2} \nabla_\mu \tilde{\Phi} \nabla^\mu \tilde{\Phi} \\ - \frac{2(D-26)}{3\alpha'} e^{\frac{4}{D-2}\tilde{\Phi}} + \mathcal{O}(\alpha')). \end{aligned} \tag{2.168}$$

The Einstein-Hilbert term now takes the standard form and the gravitational coupling is given by

$$\kappa^2 = \kappa_0^2 e^{2\Phi_0}. \tag{2.169}$$

The relation of κ and Newton's constant usually is $\kappa^2 = 8\pi G_D$, where G_D is the Newton's constant in D dimensions. Considering the consistency of quantum string theory we now take $D = 26$ dimensions and have

$$\kappa^2 = \kappa_0^2 e^{2\Phi_0} \sim l_s^{24} g_s^2. \tag{2.170}$$

If we define the Planck length from the Newton's constant, $8\pi G_D = l_p^{24}$, we see that the weak string coupling condition on which we understand string theory best, $g_s \ll 1$, is equivalent to

$$l_s \gg l_p. \tag{2.171}$$

The original action (2.165) with original metric $G_{\mu\nu}$ is usually called *string-frame action* and the action with $\tilde{G}_{\mu\nu}$ is called *Einstein-frame action*.

2.3 The Anti-de Sitter/Conformal Field Theory Correspondence

The AdS/CFT correspondence in the weak form, as explained in the next subsection, is a map between strongly coupled quantum field theory and weakly coupled gravity, which was motivated by D3-branes in open string and closed string pictures. The statement is that both pictures should describe the same physics and in the low energy limit, the correspondence is achieved. The AdS/CFT correspondence is a concrete realization of the holographic principle [49,50], which states that a quantum field theory in d dimensions is mapped to gravity theory in $d+1$ dimensions. The quantum field theory lives on the boundary of the gravity theory and both theories have the same amount of degrees of freedom. According to the correspondence, any operator in the quantum field theory is mapped to fields in the gravity side.

2.3.1 Simple Road to AdS_5/CFT_4

The holographic principle was inspired by the thermodynamics of black holes [51–53]. By comparing with the law of thermodynamics, one can obtain the entropy of the Schwarzschild black hole as

$$S = \frac{A}{4l_P^2} k_B, \tag{2.172}$$

where A is the area of the black hole horizon, l_P is the Planck length where the quantum gravity effects are not negligible, and k_B is the Boltzmann constant. Usually, entropy measures the degrees of freedom or the amount of the microscopic states of a statistical system. The area law of (2.172) indicates that a black hole corresponds to a usual statistical system with spatial dimension lower than the corresponding gravitational theory by one.

In order to approach the AdS/CFT correspondence further, we first introduce the large-N_c gauge theory [54] which was proposed by 't Hooft as an approximation method to solve QCD. There are two parameters in the theory: the number of colors N_c and the gauge theory coupling constant g_{YM}, and the effective coupling constant for the theory is called 't Hooft coupling $\lambda := g_{YM}^2 N_c$. The large$-N_c$ limit is $N_c \to \infty$ while keeping λ fixed and large.

The large$-N_c$ gauge theory has a Poincré symmetry $ISO(1,3)$. If we impose scale invariance on the theory and require the new theory keeping the invariance quantum mechanically, which means the 1-loop $\beta(g_{YM})$ function for the $SU(N_c)$ vanishes, a theory called $\mathcal{N}=4$ super-Yang-Mills theory (SYM) emerges which has the largest symmetries among such theories. This super-Yang-Mills theory has the maximum number of supercharges ($\mathcal{N}=4$) in four dimensions, and contains a gauge field A_μ, 4 Weyl fermions and 6 scalar fields. The corresponding spacetime metric with the

same symmetry is the AdS_5 spacetime given by

$$ds^2_{AdS_5} = L^2\frac{dr^2}{r^2} + (\frac{r}{L})^2(-dt^2 + d\vec{x}_3^2), \tag{2.173}$$

which is the solution of Einstein equation with the negative cosmological constant

$$S_5 = \frac{1}{16\pi G_5}\int d^5x\sqrt{-g}(R - 2\Lambda), \tag{2.174}$$

where $\Lambda = -6/L^2$.

The partition function of the large-N_c gauge theory is given by a summation over two-dimensional surfaces of different topology, which is the same for a perturbative expansion of string theory where the summation is over the topologies of two-dimensional world-sheet surfaces. In particular, the summation of two-dimensional closed surfaces with different genus corresponds to the gravitational perturbative expansion. Now we have

$$Z_{CFT_4} = Z_{AdS_5}, \tag{2.175}$$

where the right-hand side is the partition function of string theory on the AdS_5 spacetime. (2.175) is known as the GKP-Witten relation. The parameters between these two theories have the relation

$$N_c^2 = \frac{\pi}{2}\frac{L^3}{G_5}, \qquad \lambda = (\frac{L}{l_s})^4. \tag{2.176}$$

2.3.2 Field-operator map

In the AdS/CFT correspondence, we are interested the strong/weak duality. In order to achieve this, we take $N_c \to \infty$ and $\lambda \to \infty$ on the conformal field theory side. We can see from (2.176) that this means: 1) the string length is very small compared to the radius of curvature L, and we obtain the point-particle limit of the type IIB string theory which is type IIB supergravity on $AdS_5 \times S^5$; 2) $G_5 \to 0$ on the gravity side which is weakly coupled. This special limit is referred as the weak form of the AdS/CFT correspondence.

In Euclidean signature, the AdS/CFT correspondence is given by

$$Z[\phi_{(0)}] = \left\langle exp\left(\int d^dx\phi_{(0)}\mathcal{O}(x)\right)\right\rangle_{CFT} = Z_{string}|_{\lim\limits_{z\to 0}(\phi(z,x)z^{\Delta-d})=\phi_{(0)}(x)} \tag{2.177}$$

$$\approx e^{-S_{supergravity}}|_{\lim\limits_{z\to 0}(\tilde{\phi}(z,x)z^{\Delta-d})=\phi_{(0)}(x)}, \tag{2.178}$$

where Z_{string} is the partition function of superstring theory which is not known explicitly, ϕ is a general field propagating in the bulk which dual to an operator of dimension Δ, and near the boundary at $z \to 0$, ϕ takes the asymptotic leading behavior $\phi(z,x) \sim z^{d-\Delta}\phi_{(0)}(x)$. In the weak form of the correspondence, the

superstring partition function Z_{string} at one saddle point (or on-shell) is approximately given by the type IIB supergravity with $\tilde{\phi}$ denoting the solution of the type IIB supergravity. Now the on-shell bulk action $S_{supergravtiy}$ acts as the generating functional for the connected correlation functions involving the operator $\mathcal{O}$ on the boundary.

We list some of the basic dictionary for the AdS/CFT correspondence that we will use later.

Boundary: field theory	Bulk: gravity theory
Scalar operator/order parameter $\mathcal{O}$	Scalar field ϕ
Vacuum expectation value of the operator	Leading (sub-leading) coefficient of the normalisable (non-normalisable) solution
Energy-momentum tensor $T^{\mu\nu}$	Metric field g_{ab}
Global internal symmetry current J^{μ}	Maxwell field A_a
Chemical potential/charge density	Boundary value of the electrostatic potential A_t
Free energy	On-shell value of the action
Finite temperature	Hawking temperature of the black hole

3 Dark Solitons in Holographic Superfluids

3.1 Introduction and Summary

As discussed before, the gauge/gravity duality provides us a powerful tool to calculate correlation functions in strongly coupled systems where the perturbative theory is no longer reliable [35,36]. Holographic method has been applied to various strongly interacting condensed matter systems (for example, [55, 56]) including superfluids (see [57, 58] for early works). In particular, there are some characteristic structures that can be created in superfluids such as vortex[1] and soliton. The holographic solitonic configurations were first established in [19]. The soliton, a solitary wave behaving like a particle, widely exists in the field of nonlinear science. Formally, it is a physical configuration of the differential equations possessing a profound mathematical structure which interpolate between two phases.

The traditional dark soliton solution can be obtained from the time independent Gross-Pitaevskii (GP) equation for the superfluid order parameter Φ

$$-\frac{1}{2m_B}\partial_x^2\Phi+\left(2V-\mu\right)\Phi+g\Phi|\Phi|^2=0, \tag{3.1}$$

where all coefficients depend on chemical potential and temperature. This equation may also be obtained from the microscopic Bogoliubov-de Gennes equation in a strong coupling limit as a mean field description for fermionic systems [62].The solution for (3.1) is

$$\Phi\left(x\right)=\sqrt{\frac{\mu-2V}{2g}}\tanh\left(\frac{x}{\xi}\right),\rho\left(x\right)=q|\Phi|^2, \tag{3.2}$$

where ρ is the charge density and q is the unit of $U\left(1\right)$ charge. ξ is the coherence length

$$\xi=\frac{1}{\sqrt{2\left(\mu-2V\right)m_B}}. \tag{3.3}$$

[1]Vortex solutions in the holographic superfluids were established by different groups [59,60] based on the work [61].

The dark soliton solution is a configuration interpolating between the phases

$$\Phi(\infty) = \sqrt{\frac{\mu - 2V}{2g}}, \Phi(-\infty) = -\sqrt{\frac{\mu - 2V}{2g}}. \tag{3.4}$$

The above solution and the relation between the chemical potential and coherence length are just guides for [19] to create solitonic solutions in holographic superfluid system [61].

The solitons we focus on are localized and long-lived defects in the condensate superfluid. Following [19,20] (see [14] for a brief review), we study the behavior of dark solitons with backreaction in holographic superfluid system. The previous discussions was in the probe limit that ignored backreaction to the metric. A shortcoming of this approximation is that condensate diverges near zero temperature in some cases. This is actually an artefact of the probe limit [63]. In other words, the backreaction will be significant at low temperature.

The superfluidity is a quantum phenomenon occurring in both bosonic and fermionic systems at low temperature. Particularly, the latter can display BCS-like as well as BEC-like superfluidity and even a smooth transition known as BCS-BEC crossover, which can be experimentally realized in ultracold gases of fermionic atoms (see [13] for a review). It describes a system of elementary fermions with tunable attractive interaction. When fermions pair into bosonic diatomic molecules, the energy scale associated with pairing is the binding energy which corresponds to an onset temperature T^*. Below this temperature, the pairs start to form. They then can occupy both the ground state and excited states. As the temperature keeps lowering, the paired bosons tend to populate more lower energy states. Eventually at some critical temperature T_c, the Bose–Einstein condensation of the Cooper pairs takes place and the ground state is macroscopically occupied. One limiting case is $T^* = T_c$ which is the BCS limit, where the pairs condense as soon as they form. The other one is $T^* \gg T_c$ which is the BEC limit, where the pairs have already formed even at room temperature which make it looks like starting with bosons. Between these two limit, there is a large regime where the two temperatures are comparable but not equal. This is the region of unconventional superconductivity and superfluidity for which the BCS-BEC crossover scenario is proposed. Figure 3.1 sketches out qualitative phase diagram based on theoretical studies.

In [14, 19], the solitons serve as a probe to study the behavior of holographic superfluid. Comparisons with superfluid experiments about the amount of central density depletion of soliton indicates that the condensation under standard (alternative) quantization is likely to be BCS (BEC) type mentioned in Fig. 3.1. Furthermore, the authors conjectured that one may achive BCS-BEC crossover in the holographic superfluid systems via varying the scaling dimension of the condensing operator, i.e. changing the scaling dimension might be interpreted as a family of conformal field theories corresponding to different kinds of superfluids.

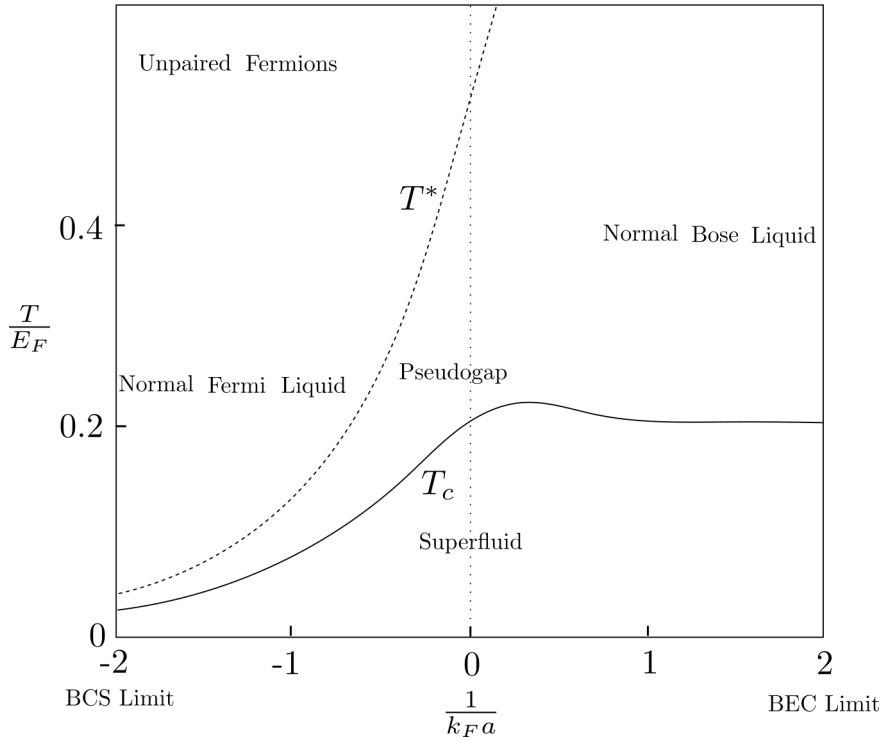

Figure 3.1: Qualitative phase diagram reproduced from [13] of the BCS-BEC crossover as a function of temperature T/E_F and coupling $1/k_F a$, where k_F is the Fermi momentum and a the scattering length. T^* is the pairing onset temperature, while T_c is the critical temperature for the superfluidity.

In [64], it was argued that one could introduce double trace deformations of charged scalar as modeling the interaction between fermionic constituents of the boundary system towards capturing the physics of the BCS-BEC crossover. In fact, the two independent works are related by double trace deformation theory. According to [65–67], perturbing the large N boundary theory by a relevant double trace deformation corresponds in the bulk to imposing "mixed" boundary conditions for the field dual to $\mathcal{O}$. The coupling constant $\kappa = 0$ ($\kappa = -\infty$) is nothing other than boundary condition $\psi_+ = 0$ ($\psi_- = 0$) of alternative (standard) quantization. Adding the perturbation will trigger a RG flow from the original CFT in the UV to another conformal fixed point in the IR. Under this flow, the conformal dimension of $\mathcal{O}$ varies between Δ_- in the UV and Δ_+in the IR. i.e. the two inequivalent boundary CFTs $\Delta = \Delta_\pm$ can be recovered as two limits of the same deformed theory.

By solving Einstein Field Equations coupled matter field numerically, we constructed the dark soliton configuration with backreaction in holographic superfluid systems. We found that the healing length of soliton increases with the strength of backreaction, and correspondingly, the charge density depletion deceases. This means the backreaction leads to effective attraction towards boundary physical system. In addition, we check the conjecture of modeling the BCS-BEC crossover via holography

in several aspects and connect the proposal with another double trace deformation approach to the same extent. Moreover, the backreaction enables us to obtain the effective energy density of soliton configuration, which together with the surface tension leads to an argument for the snake instability of dark solitons.

This chapter is organized as follows. In next section, we briefly introduce holographic superfluid model and analyze the ansatzs and boundary conditions for solving the equation of motion. In section 3.3, the numerical scheme and main results are discussed. Section 3.4 is devoted to ascertaining the mechanism of insability of the soliton. The summary and outlook are included in section 3.5.

3.2 Setup

We work with the simplest holographic superfluid model which requires gravity coupled to a Maxwell field A_μ and charged scalar field Ψ with the change q and mass $m^2L^2=-2$. The bulk action reads

$$S=\int d^4x\sqrt{-g}\left[\frac{1}{2\kappa_4^2}\left(R-2\Lambda\right)-\frac{1}{q^2}\left(\frac{1}{4}F_{\mu\nu}F^{\mu\nu}+\left|D\Psi\right|^2+m^2\left|\Psi\right|^2\right)\right], \tag{3.5}$$

where we have rescaled A_μ,Ψ as $\frac{A_\mu}{q},\frac{\Psi}{q}$ instead of their original forms [61, 68]. L is the AdS radius related to the cosmological constant as $\Lambda=-\frac{3}{L^2}$. In our units, $L=1$. $D=\nabla-iA$ and $F=dA$. The equations of motion derived from the action take the following form:

$$\begin{aligned}0=&R_{\mu\nu}-\Lambda g_{\mu\nu}-\frac{2\kappa_4^2}{q^2}\{\frac{1}{2}\left[D_\mu\Psi\left(D_\nu\Psi\right)^\dagger+D_\nu\Psi\left(D_\mu\Psi\right)^\dagger+g_{\mu\nu}m^2\left|\Psi\right|^2\right]\\&+\left(\frac{1}{2}F_{\mu\sigma}F_\nu{}^\sigma-\frac{1}{8}F_{\sigma\rho}F^{\sigma\rho}g_{\mu\nu}\right)\},\end{aligned} \tag{3.6}$$

$$0=D^\mu D_\mu\Psi-m^2\Psi, \tag{3.7}$$

$$0=\nabla_\mu F^{\mu\nu}-ig^{\mu\nu}\left[\Psi^\dagger\left(D_\mu\Psi\right)-\Psi\left(D_\mu\Psi\right)^\dagger\right]. \tag{3.8}$$

The limit $\frac{2\kappa_4^2}{q^2}\to 0$ is so-called probe limit. Since we are interested in the effect of the backreaction which implies $\frac{2\kappa_4^2}{q^2}$ is finite, we set $q=1$ and take $\epsilon\equiv 2\kappa_4^2$ as a with which parameter to measure the strength of backreaction.

In the absence of charged scalars in action (3.5), the solution of Einstein equations is the well-known Reissner-Nordstrom-AdS (RN-AdS) black brane with metric

$$ds^2 = \frac{L^2}{z^2}\left[-f(z)\,dt^2 + \frac{dz^2}{f(z)} + dz^2 + dy^2\right], \tag{3.9}$$

$$f(z) = 1 - \left(1 + \frac{\epsilon\mu^2 z_+^2}{4}\right)\left(\frac{z}{z_+}\right)^3 + \frac{\epsilon\mu^2 z_+^2}{4}\left(\frac{z}{z_+}\right)^4, \tag{3.10}$$

$$A = \mu\left[1 - \left(\frac{z}{z_+}\right)\right]dt, \tag{3.11}$$

wherein μ is the chemical potential and z_+ parametrizes the black brane temperature as

$$T = \frac{1}{4\pi z_+}\left(3 - \frac{\epsilon\mu^2 z_+^2}{4}\right). \tag{3.12}$$

For numerical convenience, we take following radial coordinate transformation with $z_h \equiv \frac{1}{z_+}$

$$z = \frac{1 - r^2}{z_h}. \tag{3.13}$$

We adopt the following ansatz compatible with the symmetries for hairy black brane geometry in low temperature

$$ds^2 = \frac{L^2 z_h^2}{(1-r)^2}\left[-Q_1 f(r)\,dt^2 + \frac{4r^2 Q_2 dr^2}{z_h^2 f(r)} + Q_4\left(dx - \frac{2r}{z_h}Q_3 dr\right)^2 + Q_5 dy^2\right], \tag{3.14}$$

$$\Psi = \left(\frac{1 - r^2}{z_h}\right)Q_6, \tag{3.15}$$

$$A = \mu r^2 Q_7 dt, \tag{3.16}$$

where $\{Q_i | i = 1, 2, \cdots, 7\}$ are unknown functions of r and x, to be determined by our numerical scheme. The conformal boundary is located at $r = 1$ and $r = 0$ denotes the horizon. At the horizon, regularity of Q_i must be imposed. Expanding the equations of motion near the horizon as a power series in r and requiring the leading order to vanish

$$Q_1|_{r=0} = Q_2|_{r=0}; (\partial_r Q_j)|_{r=0} = 0, j = 2, 3, \cdots 7. \tag{3.17}$$

Because of the first Dirichlet boundary condition in (3.17), the temperature of the black brane is still given by (3.12). At the conformal boundary, we demand the metric approaches AdS_4 by setting

$$Q_1|_{r=1} = Q_2|_{r=1} = Q_4|_{r=1} = Q_5|_{r=1} = 1; Q_3|_{r=1} = 0. \tag{3.18}$$

The boundary CFT operators are related to the behavior of bulk fields in the asymptotically AdS regime, in which scalar field Ψ and A_t admits the following expansion in Fefferman-Graham coordinate with $\Delta_\pm = 3/2 \pm \sqrt{9/4 + m^2}$

$$\Psi = \psi_- z^{\Delta_-} + \psi_+ z^{\Delta_+} + \ldots, \tag{3.19}$$

$$A_t = \mu - \rho z + \ldots. \tag{3.20}$$

According to AdS/CFT correspondences [69, 70], in standard quantization, one can identify ψ_- as the source of the operator $\mathcal{O}_2$ that dual to ψ with scaling dimension $\Delta_+ = 2$, while ψ_+ is regarded as the expectation value. Alternatively, one can exchange the role of ψ_- and ψ_+ in the dual-field theory, i.e. ψ is dual to the scaling dimension $\Delta_- = 1$ operator $\mathcal{O}_1$ with source ψ_+ and expectation value ψ_-. Since we want the condensation without being sourced, we will set $\psi_- = 0$ (standard case) or $\psi_+ = 0$ (alternative case). Generally, the fixed boundary condition $\psi_+ = \kappa\psi_-$ can also be imposed, which is known as double trace boundary condition since it corresponds to a deformation of the dual theory by adding the term $\sim \int d^3x \mathcal{O}^\dagger\mathcal{O}$ to its boundary action S_{bdry}. μ is interpreted as a chemical potential, and ρ is the charge (or particle number) density.

In order to compute the holographic stress energy tensor, following the process of [**?**], we need to know the asymptotic expansion of the metric at the conformal boundary, which is obtained by solving Einstein-de Turck equation (3.36) (see the detailed discussion in the next section) with boundary conditions order by order in $(1 - r)$ and additionally imposing the de Turck vector $\xi^\mu = 0$.

$$Q_i(r, x) = 1 - \frac{\epsilon Q_6^{(0)}(x)}{z_h^2}(1 - r)^2 + q_i(x)(1 - r)^3 + O\left[(1 - r)^4\right], i = 1, 4, 5, \tag{3.21}$$

$$Q_2(r, x) = 1 + \frac{8\epsilon Q_6^{(0)}(x) Q_6^{(1)}(x)}{3z_h^2}(1 - r)^3 + O\left[(1 - r)^4\right], \tag{3.22}$$

$$Q_3(r, x) = \frac{2\epsilon Q_6^{(0)}(x)\partial_x Q_6^{(0)}(x)}{z_h^3}(1 - r)^3 + O\left[(1 - r)^4\right], \tag{3.23}$$

$$Q_6(r, x) = Q_6^{(0)}(x) + Q_6^{(1)}(x)(1 - r) + \cdots, \tag{3.24}$$

$$Q_7(r, x) = Q_7^{(0)}(x) + Q_7^{(1)}(x)(1 - r) + \cdots, \tag{3.25}$$

where $q_1(x), q_4(x), q_5(x)$ satisfy (3.26) related with the trace and covariant derivative of boundary stress energy tensor.

$$q_1(x) + q_4(x) + q_5(x) = -\frac{\epsilon Q_6^{(0)}(x)\left(-3Q_6^{(0)}(x) + 8Q_6^{(1)}(x)\right)}{z_h^2}, \tag{3.26}$$

$$\partial_x q_4(r,x) = -\frac{2\epsilon\left[\left(-3Q_6^{(0)}(x)+8Q_6^{(1)}(x)\right)\partial_x Q_6^{(0)}(x)+2Q_6^{(0)}(x)\,\partial_x Q_6^{(1)}(x)\right]}{3z_h^2}. \tag{3.27}$$

By now we have obtained the asymptotic behavior of metric. As explained in [38], it is good to use Fefferman-Graham coordinates (z,v) in an expansion of series (3.28) and demand $g_{zz}=\frac{1}{z}$ and $g_{zv}=0$ to determine the two function $\{a_k(v),b_k(v)\}$ order by order about z. We provide the first few terms for the latter computation of holographic stress energy tensor.

$$\begin{cases} r = 1-\frac{z_h}{2}z+\sum_{k=2}^{\infty}a_k(v)\,z^k, \\ x = v+\sum_{k=1}^{\infty}b_k(v)\,z^k, \end{cases} \tag{3.28}$$

$$a_2(v) = -\frac{z_h^2}{8},\quad a_3(v) = -\frac{z_h^3}{16}, \tag{3.29}$$

$$a_4(v) = \frac{z_h^2\left(24\epsilon\mu^2+51z_h^2+32\epsilon Q_6^{(0)}(v)\,Q_6^{(1)}(v)\right)}{1152}, \tag{3.30}$$

$$b_1(v) = b_2(v) = b_3(v) = 0, \tag{3.31}$$

$$b_4(v) = -\frac{\epsilon Q_6^{(0)}(v)\,\partial_v Q_6^{(0)}(v)}{16}. \tag{3.32}$$

Finally, the holographic stress energy tensor is computed by (3.33) for the standard case and (3.34) for the alternative case [71, 72]. $K_{\mu\nu}$ is the extrinsic curvature associated with an inward unit vector n^σ of the constant $z=\epsilon$ surface nearby the boundary. $\gamma_{\mu\nu}$ is the induced metric on the cut-off surface. The last term in (3.33) and (3.34) cancels the divergences due to the presence of scalar field [73],

$$T_{\mu\nu} = \frac{1}{\kappa_4^2}\lim_{z\to 0}\frac{1}{z}\left(K_{\mu\nu}-\gamma_{\mu\nu}K-2\gamma_{\mu\nu}-\frac{\epsilon}{2}|\Psi|^2\gamma_{\mu\nu}\right), \tag{3.33}$$

$$T_{\mu\nu} = \frac{1}{\kappa_4^2}\lim_{z\to 0}\frac{1}{z}\left[K_{\mu\nu}-\gamma_{\mu\nu}K-2\gamma_{\mu\nu}+\frac{\epsilon}{2}\left(-\Psi^\dagger n^\sigma D_\sigma\Psi-C.C.+|\Psi|^2\right)\gamma_{\mu\nu}\right]. \tag{3.34}$$

Using the relation (3.26), one can explicitly check that the stress energy tensor is traceless and conserved when the source is turned off:

$$T_i^i = 0,\quad \partial_i T^{ij} = 0. \tag{3.35}$$

3.3 Numerical schemes and results

We employ the de Turck method which has been reviewed in [74], to solve Einstein equations. The essence of the trick is to add the $\frac{1}{2}\left(\mathcal{L}_\xi g\right)_{\mu\nu} = \nabla_{(\mu}\xi_{\nu)}$ term into

(3.6), which renders the Einstein equations elliptic. Essentially, rather than solve the Einstein equations, we instead solve the Einstein-De Turck equation,

$$R_{\mu\nu} - \Lambda g_{\mu\nu} - \epsilon \left\{ \frac{1}{2} \left[D_\mu \Psi \left(D_\nu \Psi \right)^\dagger + D_\nu \Psi \left(D_\mu \Psi \right)^\dagger + g_{\mu\nu} m^2 \left| \Psi \right|^2 \right] + \left(\frac{1}{2} F_{\mu\sigma} F_\nu{}^\sigma - \frac{1}{8} F_{\mu\nu} F^{\mu\nu} \right) \right\} - \nabla_{(\mu} \xi_{\nu)} = 0. \tag{3.36}$$

where the de Turck vector ξ^ν is built from the difference of two Christoffel symbols (Levi-Civita connections) as $\xi^\nu \equiv g^{\rho\sigma} \left[\Gamma^\nu_{\rho\sigma}(g) - \overline{\Gamma}^\nu_{\rho\sigma}(\bar{g}) \right]$. $\overline{\Gamma}\left(\bar{g}\right)$ is Christoffel symbol associated with reference metric $\bar{g}$. Since the difference of two connections is a tensor, although the connections themselves are not, ξ^ν transforms as a space-time vector. The reference metric is arbitrary except it should have the same asymptotic behavior and horizon structure as the g we seek. This produces non-degenerate kinetic terms for all of the metric components and automatically fixes the gauge [75]. In practice, the reference metric serves as an initial "guess", and so it pays to choose a reference which is reasonably close to the expected solution. In our scheme, we take standard RN-AdS metric which corresponds to $Q_1 = Q_2 = Q_4 = Q_5 = 1$ and $Q_3 = 0$ in (3.14). Solutions of the Einstein-De Turck equation will only coincide with solutions of the Einstein equations if $\xi = 0$.

The nonlinear PDEs (3.36), (3.7), (3.8), together with boundary conditions (3.17), (3.18) are solved via Newton-Kantorovich method. To be specific, we firstly linearize the PDEs and then discretize the linear partial differential equations into algebraic equations via the standard pseodospectral procedure, where we represent unknown functions as a linear combination of Chebyshev polynomials for z coordinate and Fourier series for x coordinate[2]. Throughout the paper, we take the fixed $\mu = 5.6$. Our integration domains lives on a rectangular grid, $(r, x) \in (0, 1) \otimes \left(-\frac{L_x}{2}, \frac{L_x}{2} \right)$.The resulting linear systems is solved by LU decomposition or other iterative techniques.

The instability of black brane occurring at $T = T_c$ corresponds to a continuous phase transition in boundary systems. Now we need to find the critical temperature for given ϵ, where the solutions become unstable and start to form scalar hair. As described in [70] and [77], one can perturb the RN background by the scalar field $\psi = \phi\left(r\right) e^{-i\omega_p t}$, at the onset of the instability, such that the unstable mode becomes a zero mode. The critical temperature T_c itself is therefore found by looking for a static normalizable solution to the scalar equation of motion with $\omega_p = 0$. We equivalently solve the quadratic eigenvalue problem about $\phi\left(r\right)$ and z_h in this paper. Finally, the z_h of the critical temperature corresponds to the maximum eigenvalue. The results are shown in Fig. 3.2 (Zhongshan Xu draws this picture and the following pictures in this chapter). As is predicted in previous analysis, the

[2]Since a single soliton has no periodicity in the x direction, for simplicity in spatial boundary conditions and efficiency in numerics, we instead construct the double soliton (kink–anti-kink) configuration that has been achieved in [76], and then show the outcome of a single soliton.

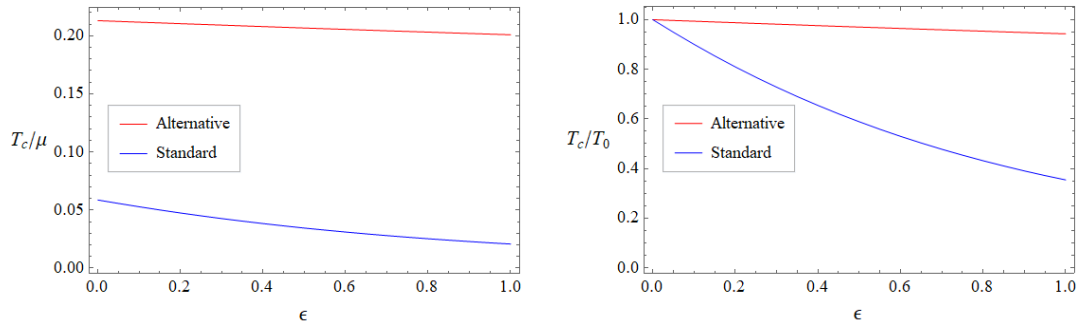

(a) Critical temperature **(b)** Normalized critical temperature

Figure 3.2: Critical temperature for varying ϵ, T_0 is the critical temperature at $\epsilon = 0$.

critical temperature drops when increasing the strength of backreaction in standard case, i.e. the backreaction can hinder the generation of condensation and make the critical temperature lower. However, in the alternative case, we notice that the critical temperature is almost invariant and T_c/μ approaches constant 0.2, which coincides with BEC-like condensation in Fig. 3.1.

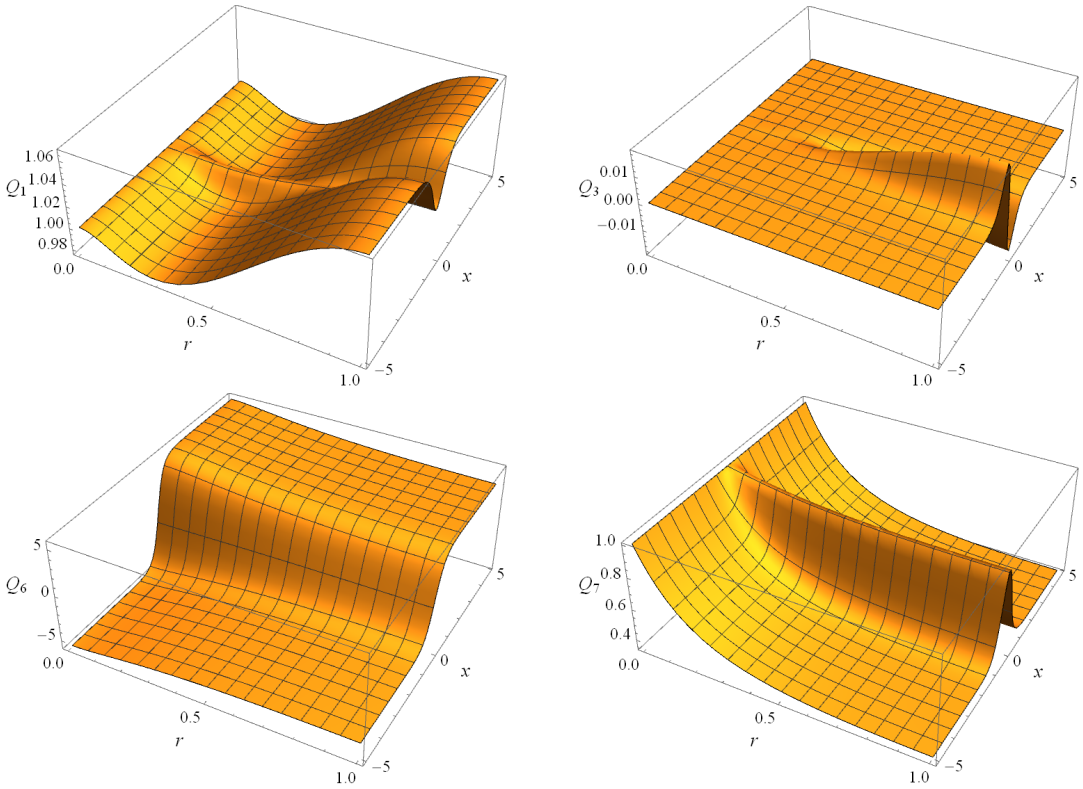

Figure 3.4: The profile of metric components and the configuration of matter fields at $\epsilon = 0.25, T/T_c = 0.5$ in the alternative case.

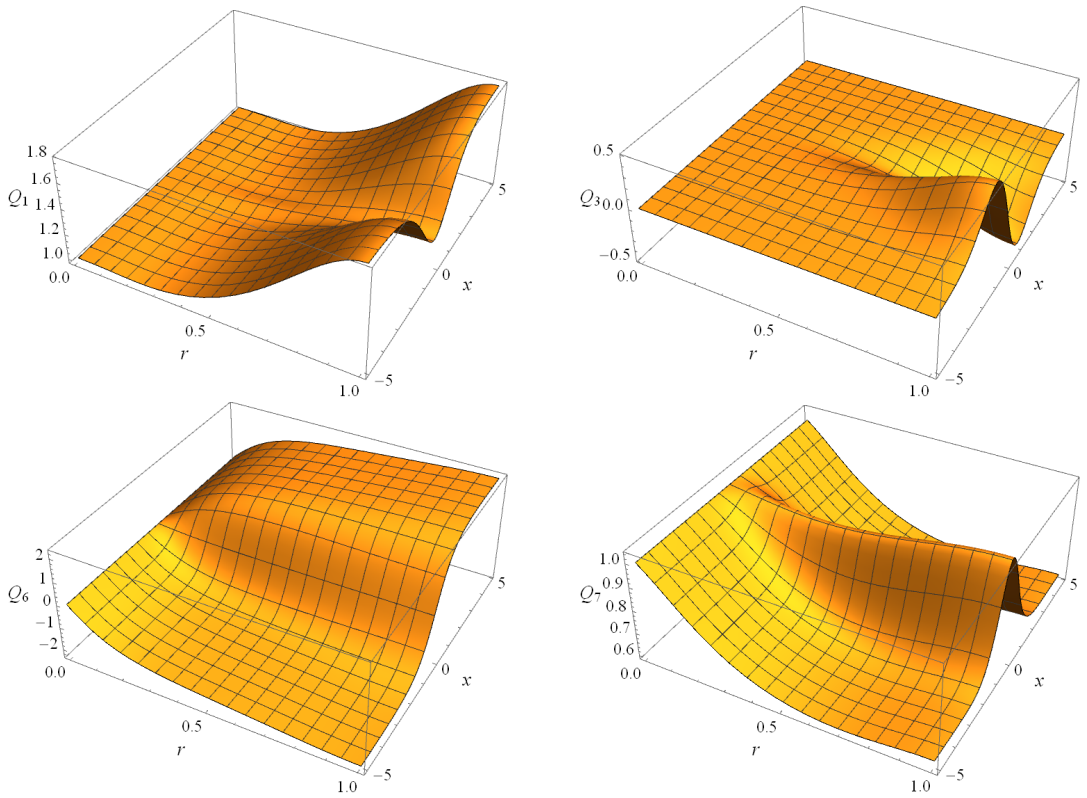

Figure 3.3: The profile of metric components and the configuration of matter fields at $\epsilon = 0.25, T/T_c = 0.5$ in the standard case.

Having found the critical temperature, we can next find the solutions for $T < T_c$. That is the hairy charged black hole dual to superfluid phase. The part components of metric and the configuration of matter fields are indicated in Fig. 3.3 and Fig. 3.4. We can see that larger fluctuations of spacetime appear only near the core of the soliton.

From the asymptotic form of the matter fields, one can read off the expectation value of the charged condensation and particle number density in the dual fields respectively, which are demonstrated in Fig. 3.5. As has been discussed in probe limit, the soliton in a BEC-like superfluid has larger depletion.

The Fig. 3.6 shows that depletion decays as the backreaction grows larger. In particular, the healing length of the soliton increases in the BCS-like superfluid. This means the soliton becomes "shallower" and "wider". Since repulsive interactions leads to the generation of the dark soliton, we may argue that the bulk backreaction brings about an effective attraction interaction to boundary physical systems and balances out part repulsion giving rise to dark soliton. So the "deformed" soliton compared to the probe limit has lower depletion.

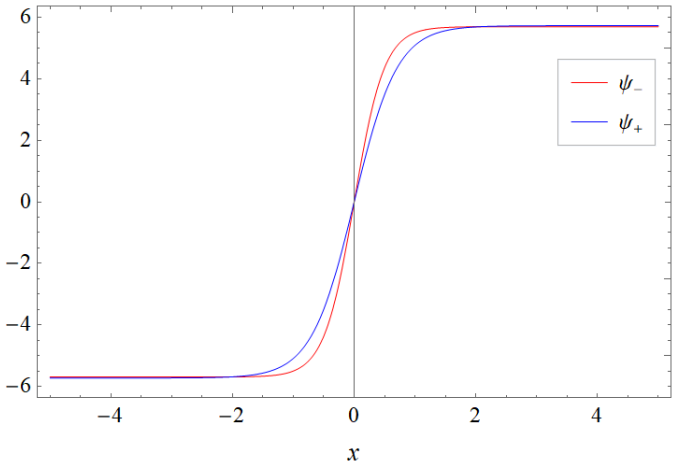

(a) Condensation (order parameter)

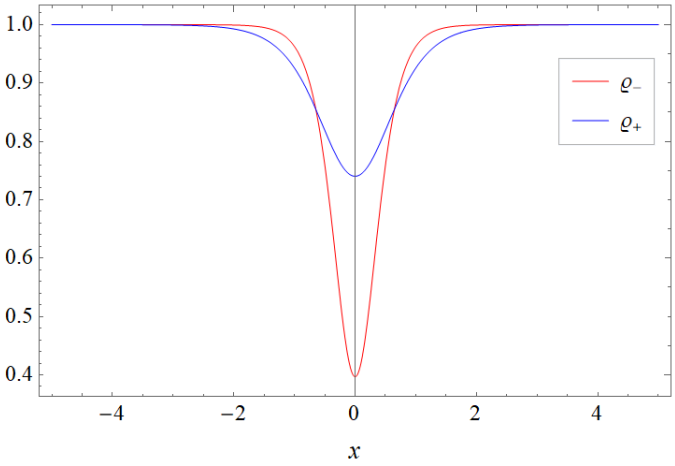

(b) Particle number density

Figure 3.5: The condensation and the particle number density as a function of x at $\epsilon = 0.25, T/T_c = 0.5$. ϱ_+ (ϱ_-) is the normalized particle number density.

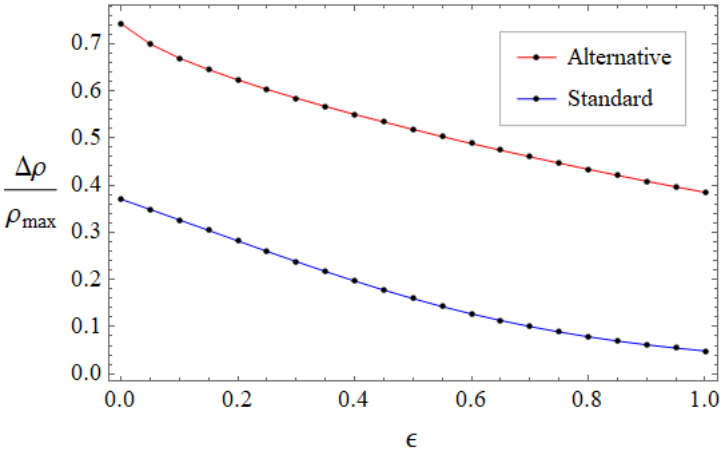

Figure 3.6: The depletion of particle number density as a function of ϵ at $T/T_c = 0.5$

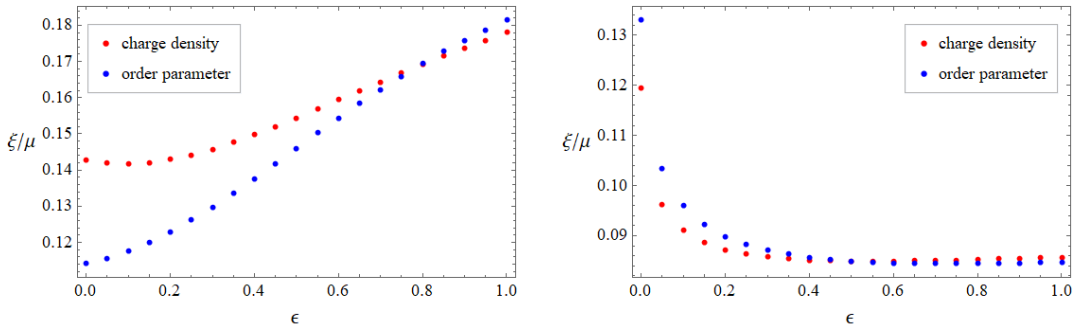

(a) Standard case **(b)** Alternative case

Figure 3.7: The change of healing length with ϵ at $T/T_c = 0.5$

The relationship between depletion of particle number density and temperature for different ϵ is plotted in Fig. 3.8. Differing from the expectation in [20] for the BEC-like soliton, the depeletion in the core is considerably away from 100% and even lower than in the probe limit at low temperature.[3] That is because backreaction itself results in the reduction of depletion discussed above.

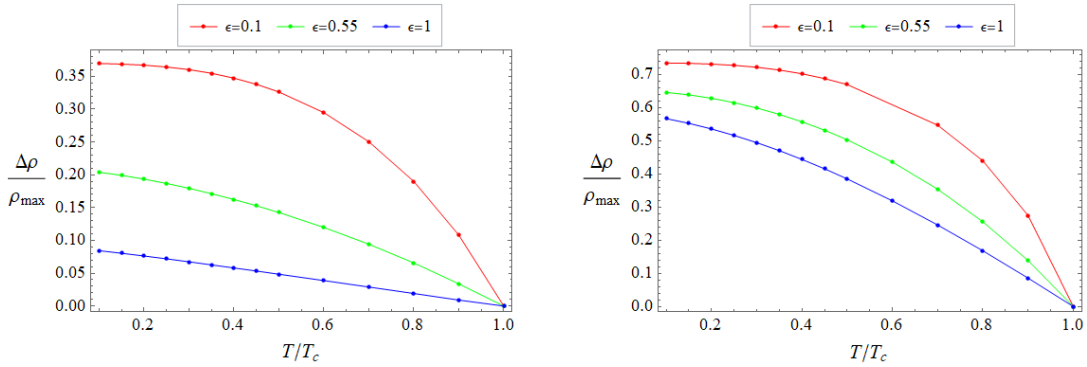

(a) Standard case **(b)** Alternative case

Figure 3.8: The depletion of particle number density as a function of T/T_c for different ϵ.

3.4 Thermodynamics in grand canonical ensemble

We are interested in the instability of dark solitons, so now we turn to the discussion of thermodynamics. Since the boundary chemical potential and temperature are fixed, our system lives in the grand canonical ensemble characterized by the grand potential

[3] One possible reason is that the temperature here is not low enough. In fact, the solution with backreaction at lower temperature is still difficult to obtain in numerics.

$$\Omega = E - TS - \mu N, \tag{3.37}$$

where N is the total particle number obtained by integrating ρ; E is internal energy

$$E = \int_{\Sigma_t} d^2x\sqrt{\eta}\left[T_{\mu\nu}\left(\partial_t\right)^{\mu}\right]t^{\nu}. \tag{3.38}$$

The energy E is defined above in which $\eta_{\mu\nu}$ is the induced metric on the surface Σ_t of $z = 0$ and $t = const$ with unit normal t^{ν}, and entropy S given by

$$S = \frac{A_h}{4G} = \frac{4\pi z_h^2}{\epsilon}\int\sqrt{Q_4\left(0,x\right)Q_5\left(0,x\right)}dxdy. \tag{3.39}$$

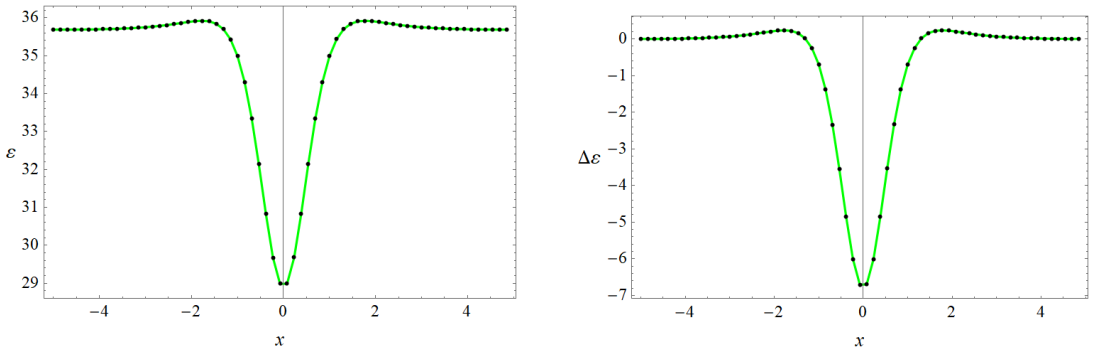

(a) Total energy density **(b)** Subtracted energy density

Figure 3.9: Energy density at $\epsilon = 0.25$, $T = 0.5T_c$

Without integration in the above thermodynamic quantities, we can have the following local thermodynamic relation:

$$\omega = \varepsilon - Ts - \mu\rho, \tag{3.40}$$

with ω the grand potential density and s the entropy density.[4] Far away from the soliton center, these local quantities will approach their (homogeneous) equilibrium values. Therefore, what really matter are the values relative to their (homogeneous) equilibrium backgrounds. For the energy density, the subtracted distribution is plotted in Fig. 3.9b, where we can see obvious energy depletion around the soliton centers.[5] Upon integration along x, this depletion gives a negative effective energy

[4] Actually, due to the absence of local equilibrium in the vicinity of solitons, the above relation does not hold, or even the quantities themselves are not well defined, in the usual thermodynamic sense. However, that will not be an essential problem in our following discussion of the effective mass (energy) and surface tension of solitons, as will be made clear shortly.

[5] In this section, we only show the result for the soliton in the BCS-like superfluid, while that for the BEC-like case is similar.

-47.6629 (and is also the effective mass in our relativistic setting) of the soliton. For the grand potential density, the subtracted distribution is plotted in Fig. 3.10b, where we can see that there is a grand potential cost for the soliton with respect to the homogeneous background.

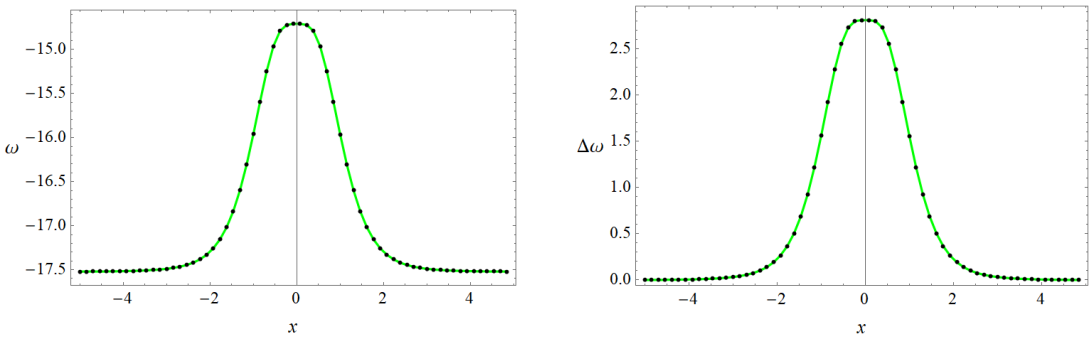

(a) Total grand potential density **(b)** Subtracted grand potential density

Figure 3.10: Grand potential density at $\epsilon = 0.25$, $T = 0.5T_c$

It is easy to argue that in our case the grand potential cost (upon integration along x) of the soliton is just the surface tension coefficient of it. The surface tension coefficient σ of a surface structure (i.e. a soliton in higher dimensions) is defined as the external work W done (under certain conditions) to enlarge the surface by a unit area. The certain conditions for our static configurations here are fixed temperature and fixed chemical potential. Under those conditions, the external work is just the increase of the grand potential due to the appearance of the surface:

$$W = \Omega - \Omega_0, \tag{3.41}$$

with Ω_0 the grand potential of the corresponding homogeneous system (without the surface). So in our 1D setting, the surface tension coefficient σ of the soliton is its grand potential cost (upon integration along x) discussed above. Numerically, σ is calculated to be 42.6598 in the case of Fig. 3.10b. We also plot the pressure anisotropy $B \equiv p_x - p$ in Fig. 3.11a and check the thermodynamic relation $\omega = -p$, with p the average pressure, which should hold far away from the soliton center.

With these thermodynamic variables, we can make further analysis about the instability of solitons. As the soliton has a negative effective mass, the energy of the soliton decreases with increasing velocity. This means that if there is dissipation, then the soliton will show the so-called "instability of self-acceleration" [78]. On the other hand, the soliton can be viewed as a surface in the superfluid with the surface tension coefficient σ. When transverse perturbations are added to bend the depeletion plane of the dark soliton a little, the positive surface tension reacts against the surface deformation caused by the perturbation. However, since the effective mass of the soliton is negative, the acceleration tends to enhance the bending caused by

the perturbation. So the actual effect is that the bending of the dark soliton will be magnified and it will eventually break up into vortex–anti-vortex pairs, which is known as the snake instability [79]. The two decay mechanism of dark solitons are both found in non-equilibrium dynamics of superfluids. There exists a critical temperature T_d that separates the decay of a dark soliton into two distinct regimes, by the snake instability below T_d and by the self-acceleration above T_d [80].

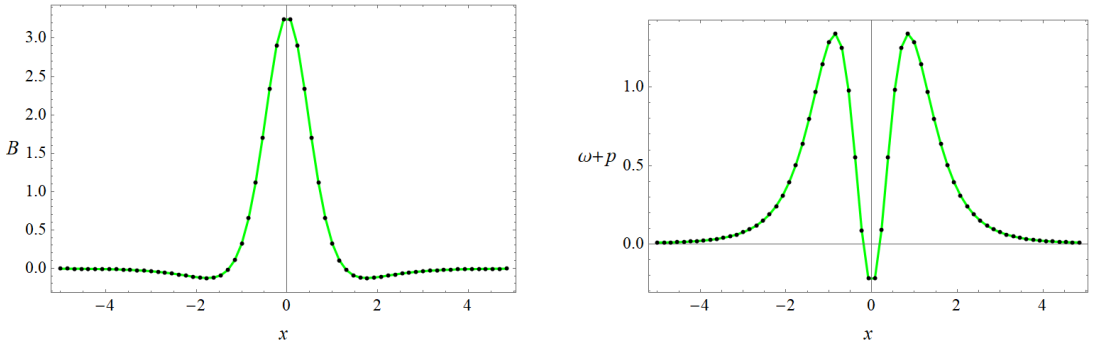

(a) Pressure anisotropy

(b) Validity of the thermodynamic relation $\omega = -p$

Figure 3.11: Pressure anisotropy and thermodynamical relation at $\epsilon = 0.25$, $T = 0.5T_c$

3.5 Discussion

Motivated by the effect of backreaction on the behavior of dark soliton, we investigated the features of solitons beyond the probe limit in holographic superfluid systems, which are obtained by solving the Einstein equations coupled with matter fields numerically. In agreement with the analysis in the probe limit, the depletion of particle number density under backreaction still shares smilar characteristics with the actual BCS-BES experiment. We also observe that the depletion decreases with increasing backreaction at fixed chemical potential and temperature, which may imply that the backreaction leads to an effective attraction towards the boundary physical system. We may expect this could provide the feasibility for bright soliton construction in holography. Moreover, we connect the conjecture of modeling the BCS-BEC crossover via holography with double trace deformation approach. Finally, we computed the holographic stress energy tensor of systems and discussed the instability of the dark soliton.

4 Gravity Dual Phase Transitions

4.1 Introduction and Summary

In previous chapter we studied the properties of dark solitons with backreaction. In this chapter we introduce the study of phase transitions between AdS soliton spacetime and AdS black hole spacetime. Disordering strongly coupled and correlated quantum states of matter may lead to new insights into the physics of many body localized strongly correlated states, possibly in the presence of strong disorder. In condensed matter physics, Anderson proposed that electrons may be localized in a lattice potential or in a disordered medium, where the waves (such as electromagnetic waves, spin waves and so on) do not diffuse. The phenomenon is known as Anderson localization [81].

In AdS/CFT, introducing strong disorder strongly changes the geometry of the spacetime. The probe limit is not suitable for this case , and the backreacted solution needs to be constructed. We are interested in the potential metal-insulator transitions in holographic conductors with disorder. By using the De Turck method to change the Einstein equations into a set of elliptic PDEs, we are solving the backreacted equations with different strength of disorder. We present results for the backreacted disordered AdS black hole and AdS soliton solutions, which respectively describes a disordered strongly interacting metal and insulator. We also calculate the free energy of the system.

4.2 Set-up

We consider a real scalar coupled to gravity in $d+1$ dimensions. The action is the same as used in [31, 82]:

$$S = \frac{1}{2\kappa_N^2}\int d^{d+1}x\sqrt{-g}\left[R - \Lambda - 2|\nabla\Phi|^2 - 4V(\Phi)\right] , \tag{4.1}$$

where $\kappa_N^2 = 8\pi G_N$ and $\Lambda = -\frac{d(d-1)}{L^2}$ is the usual AdS_{d+1} cosmological constant. The equations of motion (EOMs) are

$$\Box\Phi - V'(\Phi) = 0\,, \quad R_{AB} = 2\nabla_A\Phi\nabla_B\Phi + \frac{g_{AB}}{d-1}\left[4V(\Phi) + \Lambda\right] . \tag{4.2}$$

For the scalar potential, we take

$$V(\Phi) = -\frac{\mu}{2L^2}\Phi^2 \,. \tag{4.3}$$

By the holographic dictionary, Φ is dual to an operator $\mathcal{O}$ with dimensions

$$\Delta = \frac{d}{2} + \sqrt{(\frac{d}{2})^2 - \mu} \,. \tag{4.4}$$

Near the AdS_{d+1} boundary, the metric in the Poincaré patch approaches

$$ds^2 = \frac{L^2}{r^2}\left(dr^2 + \eta_{ab}dx^a dx^b\right) \tag{4.5}$$

as $r \to \infty$, and the scalar behaves as

$$\Phi|_{r\to\infty} = r^{d-\Delta}\Phi_1(x^a) + r^{\Delta}\Phi_2(x^a) + \cdots \,. \tag{4.6}$$

Φ_1 is then identified as the source for $\mathcal{O}$, while Φ_2 the response.

Here, we consider a short-ranged, quenched, and Gaussian disorder ensemble with the source ensemble determined by

$$\overline{\Phi_1(x^i)} = 0 \,, \quad \overline{\Phi_1(x^i)\Phi_1(y^i)} = \bar{V}^2\delta^{(d-1)}(x^i - y^i) \,. \tag{4.7}$$

All other moments of the distribution are fixed by Wick contraction.

From dimensional analysis, $[\Phi_1] = d - \Lambda$. Eq.(4.7) then suggests

$$2[\Phi_1] = 2[\bar{V}] + d - 1 \Rightarrow [\bar{V}] = \frac{d+1}{2} - \Lambda \,. \tag{4.8}$$

For "marginal" disorder such that the distribution saturates the Harris criterion, $[\bar{V}] = 0$, which also fixes the scalar mass parameter to be

$$\mu = \frac{d^2 - 1}{4} \,. \tag{4.9}$$

We realize the disorder using the spectral representation:

$$\Phi_1(x^i) = \bar{V}\sum_{\{n_i\}=1}^{N-1} C_{\{n_i\}} \prod_{i=1}^{d-1} \cos(k_{i,n_i}x^i + \gamma_{n_i}) \,, \tag{4.10}$$

where γ_{n_i} are random phases uniformly distributed over $(0,\, 2\pi)$, while constans $C_{\{n_i\}}$ and the selection of k_{i,n_i} determines the distribution. To capture the disorder strictly in the thermodynamic limit, $N \to \infty$ has to be taken. The disorder average of a quantity f is then given by

$$\bar{f} = \lim_{N\to\infty}\int\left[\prod_{i=1}^{d-1}\prod_{n_i=1}^{N-1}\frac{d\gamma_{i,n_i}}{2\pi}\right] f. \tag{4.11}$$

For the simplest case of a short range, Gaussian, and isotropic disorder distribution we have

$$C_{\{n_i\}} = C = (2\sqrt{\Delta k})^{d-1} \,, \quad k_{i,n_i} = n_i\Delta k \,, \quad \Delta k = \frac{k_0}{N} \,. \tag{4.12}$$

4.3 Perturbative Geometry

We take the background without disorder ($\bar{V} \to 0$) to be the AdS_{d+1} soliton (we set $L = 1$ from now on):

$$ds^2 = \frac{1}{r^2}\left[f_{sl}(r)d\chi^2 + \frac{dr^2}{f_{sl}(r)} - dt^2 + \sum_{i=1}^{d-2}(dx^i)^2\right], \tag{4.13}$$

where $f_{sl}(r) = 1 - (r/r_0)^d$, with r_0 is an IR cutoff of the soliton. In order to have a smooth geometry, we must make the identification

$$\chi \sim \chi + \frac{4\pi}{d}r_0\,. \tag{4.14}$$

4.3.1 Scalar Solution at $\mathcal{O}(\bar{V})$

Turning on the disorder of strength $\bar{V}$ turns on the scalar. Expanding the scalar perturbatively in $\bar{V}$:

$$\Phi(r, x^i) = \sum_{l=0}^{\infty} \bar{V}^{2l+1}\Phi^{(2l+1)}(r, x^i)\,, \tag{4.15}$$

where its solution at $\mathcal{O}(\bar{V})$ is determined by the wave equation in the background of Eq. (4.13):

$$r^{d+1}\partial_r\left(r^{-(d-1)}f_{sl}\partial_r\Phi^{(1)}\right) + r^2\partial_i^2\Phi^{(1)} + \mu\Phi^{(1)} = 0\,. \tag{4.16}$$

Decomposing the bulk scalar into harmonics as

$$\Phi^{(1)}(r, x^i) = \bar{V}C\sum_{\{n_i\}}\phi_k(r)\prod_i \cos(k_{i,n_i}x^i + \gamma_i)\,, \tag{4.17}$$

where each ϕ_k now solves the ODE

$$r^{d+1}\partial_r\left(r^{-(d-1)}f_{sl}\partial_r\phi_k\right) + (k^2r^2 - \mu)\phi_k = 0\,, \quad k^2 = \sum_i k_{i,n_i}\,, \tag{4.18}$$

such that it is regular at $r = r_0$ and $\phi_k \sim r^{d-\Lambda}$ as $r \to 0$. There does not appear to be a closed form solution for $d > 2$.

4.3.2 Geometry at $\mathcal{O}(\bar{V}^2)$

Once the bulk scalar is turned on, they source the Einstein equations at $\mathcal{O}(\bar{V}^2)$. Consider first the geometry induced by the averaged stress tensor at this order:

$$\kappa_N^2\bar{V}^2\Theta_{AB} \equiv 2\overline{\nabla_A\Phi^{(1)}\nabla_B\Phi^{(1)}} - g_{AB}\frac{2\mu}{d-1}\overline{(\Phi^{(1)})^2}\,. \tag{4.19}$$

Using the spectral decomposition (4.17), the sources are

$$\kappa_N^2 \Theta_{tt} = \frac{C^2 \mu}{2^{d-3}(d-1)} \sum_{\{n_i\}} \frac{\phi_k^2}{r^2} \,, \tag{4.20}$$

$$\kappa_N^2 \Theta_{\chi\chi} f_{sl}^{-1} = -\frac{C^2 \mu}{2^{d-3}(d-1)} \sum_{\{n_i\}} \frac{\phi_k^2}{r^2} \,, \tag{4.21}$$

$$\kappa_N^2 \Theta_{rr} f_{sl} = \frac{C^2}{2^{d-3}} \sum_{\{n_i\}} \left[f_{sl} (\phi_k')^2 - \frac{\mu}{d-1} \frac{\phi_k^2}{r^2} \right] \,, \tag{4.22}$$

$$\kappa_N^2 \Theta_{ii} = \frac{C^2}{2^{d-3}} \sum_{\{n_i\}} \left(k_{i,n_i}^2 r^2 - \frac{\mu}{d-1} \right) \frac{\phi_k^2}{r^2} \,. \tag{4.23}$$

Note since the distribution is taken to be isotropic, Θ_{ii} are equal for all spatial index i.

Given the form of the scalar sources, we make the following ansatz for the perturbative geometry at $\mathcal{O}(\bar{V}^2)$:

$$\begin{aligned} ds^2 = \frac{1}{r^2} \Bigg[& f_{sl}(r) \Big(1 + \bar{V}^2 A(r) \Big) d\chi^2 + \frac{dr^2}{f_{sl}(r)} \,, \\ & - \Big(1 + \bar{V}^2 B_t(r) \Big) dt^2 + \Big(1 + \bar{V}^2 B(r) \Big) \sum_{i=1}^{d-2} (dx^i)^2 \Bigg] \,. \end{aligned} \tag{4.24}$$

The resulting equations for the metric functions can be arranged into a first order constraint equation and three decoupled second-order equations:

$$\begin{aligned} 0 = {} & 2(d-1) f_{sl} \frac{\partial_r A}{r} + \left[d + (d-2) f_{sl} \right] \frac{\partial_r B_t}{r} + (d-2) \left[d + (d-2) f_{sl} \right] \frac{\partial_r B}{r} \\ & + 2\kappa_N^2 \left(-\Theta_{\chi\chi} f_{sl}^{-1} + \Theta_{rr} f_{sl} + \Theta_{tt} - \sum_i \Theta_{ii} \right) \,, \end{aligned} \tag{4.25}$$

$$0 = 2 \frac{\left[d + (d-2) f_{sl} \right]^2}{r^{1-d} f_{sl}^{1/2}} \partial_r \left[\frac{r^{1-d} f_{sl}^{3/2}}{d + (d-2) f_{sl}} \partial_r A \right] + j_A(r) \,, \tag{4.26}$$

$$0 = 2 r^{d-1} f_{sl}^{1/2} \, \partial_r \left(\frac{f_{sl}^{1/2}}{r^{d-1}} \partial_r B_+ \right) + j_{B_+}(r) \,, \tag{4.27}$$

$$0 = r^{d-1} \, \partial_r \left(\frac{f_{sl}}{r^{d-1}} \partial_r B_- \right) + j_{B_-}(r) \,, \tag{4.28}$$

where $B_+ \equiv \sum_i B + B_t$, $B_- \equiv B - B_t$, with scalar sources

$$j_A = \frac{2\kappa_N^2}{d+(d-2)f_{sl}} \Bigg\{ \left[d+3(d-2)f_{sl}\right] f_{sl}^{-1} \Theta_{\chi\chi} + \left[d-(d-2)f_{sl}\right] \left(\Theta_{rr} f_{sl} + \Theta_{tt} - \sum_i \Theta_{ii} \right) \Bigg\} , \tag{4.29}$$

$$j_{B_+} = 2\kappa_N^2 \left(-\Theta_{\chi\chi} f_{sl}^{-1} + \Theta_{rr} f_{sl} - \Theta_{tt} + \sum_i \Theta_{ii} \right) , \tag{4.30}$$

$$j_{B_-} = 2\kappa_N^2 (\Theta_{tt} + \Theta_{ii}) . \tag{4.31}$$

It is convenient to work in the rescaled coordinate $\rho \equiv r/r_0$. Scaling also the sources $r_0^2 j_{A,B_\pm} \to j_{A,B_\pm}$, the solution can be written as

$$A(\rho) = \alpha_1 + \alpha_2 \left[(d-2)f_{sl} - 2\right] f_{sl}^{-1/2} + \frac{1}{d} \int_\rho^1 \frac{du}{u^{d-1}} \left[\frac{d-(d-2)f_{sl}}{f_{sl}} \right]_\rho^u \frac{f_{sl}^{1/2}(u) j_A(u)}{\left[d+(d-2)f_{sl}(u)\right]^2} , \tag{4.32}$$

$$B_+(\rho) = \beta_{1,+} + \beta_{2,+} \left[f_{sl}^{1/2}(\rho) - 1 \right] + \frac{1}{d} \int_\rho^1 \frac{du}{u^{d-1}} \left[1 - \frac{f_{sl}^{1/2}(\rho)}{f_{sl}^{1/2}(u)} \right] j_{B_+}(u) , \tag{4.33}$$

$$B_-(\rho) = \beta_{1,-} + \beta_{2,-} \log f_{sl} + \frac{1}{d} \int_\rho^1 \frac{du}{u^{d-1}} \log \left(\frac{f_{sl}(u)}{f_{sl}(\rho)} \right) j_{B_+}(u) , \tag{4.34}$$

where integration by parts has been used to arrive at the form above.

The constants of integration are fixed by the boundary conditions, i.e. horizon regularity and having an asymptotically AdS_{d+1} geometry. Horizon regularity requires that $\alpha_2 = \beta_{2,-} = 0$, the constraint then sets $\beta_{2,+} = 0$ also. At the conformal boundary, we require $A(0) = B(0) = B_t(0)$, which means $B_-(0) = 0$. Since their actual value can be scaled away by a coordinate redefinition, we set $A(0) = B_\pm(0) = 0$, which then fixes α_1 and $\beta_{1,\pm}$.

4.4 Numerics

Since we want to investigate the influence of disorder on the phase transition between gapped low temperature AdS soliton phase and ungapped high temperature AdS black hole phase, we need ansatz suitable for the numerical solution of Einstein's equations in both phases. The proper ansatz in the high temperature black hole phase is an adaption of the black hole geometry used in [82],

$$ds^2 = \frac{1}{y^2} \left[-(1-y^3) y_+^2 A_T dt^2 + \frac{B_T}{1-y^3} dy^2 + y_+^2 S_T \left(dx + F_T dy\right)^2 + y_+^2 H_T d\chi^2 \right] , \tag{4.35}$$

with y_+ being the position of the black hole horizon in the holographic y direction, y_0 being the gap scale of the compactified χ direction ($\chi \sim \chi + 2\pi$), and the free functions A_T, B_T, S_T, F_T all being functions of (y, x), where x is the disordered direction. For the scalar we take

$$\Phi(y, x) = \frac{y}{y_+}\tilde{\Phi}(y, x)\,. \tag{4.36}$$

For the low temperature solitonic phase, we double Wick rotate (4.45) as $(t, \chi, y_+, y+0) \mapsto (i\chi, it, y_0, y_+)$, such that

$$ds^2 = \frac{1}{y^2}\left[(1-y^3)y_+^2 A_0 d\chi^2 + \frac{B_0}{1-y^3}dy^2 + y_0^2 S_0\left(dx + F_0 dy\right)^2 - y_+^2 H_0 dt^2\right]\,, \tag{4.37}$$

together with the same ansatz for the scalar (4.36). The two metric ansatz are static, with a Killing vector ∂_t, and have a U(1) symmetry in χ direction with Killing vector ∂_χ. A_0, B_0, S_0, F_0 are all functions of (y, x).

As described in (3.3), we will use de Turck method to solve Einstein's equations. The de Turk equations for the action (4.1) are

$$0 = R_{\mu\nu} - \frac{1}{2}g_{\mu\nu}(R - \Lambda) - T_{\mu\nu} - \nabla_{(\mu}\xi_{\nu)}\,, \tag{4.38}$$

$$\xi^\alpha = g^{\mu\nu}\left(\Gamma^\alpha_{\mu\nu}[g] - \bar{\Gamma}^\alpha_{\mu\nu}[\bar{g}]\right)\,, \quad \Gamma^\alpha_{\mu\nu} = \frac{1}{2}g^{\alpha\beta}\left(\partial_\mu g_{\beta\nu} + \partial_\nu g_{\beta\mu} - \partial_\beta g_{\mu\nu}\right)\,, \tag{4.39}$$

where the de Turck vector ξ^α is built from the difference of two Christoffel symbols (see section (3.3) for the detail of the de Turck method). ∇ in (4.38) is the covariant derivative with respect to $\Gamma[g]$, and $T_{\mu\nu}$ is the matter energy momentum tensor

$$T_{\mu\nu} = \frac{1}{\sqrt{-g}}\frac{\delta S_{matter}[\Phi]}{\delta g^{\mu\nu}} = 2\nabla_\mu\Phi\nabla_\nu\Phi - |\nabla\Phi|^2 g_{\mu\nu} - 2V(\Phi)g_{\mu\nu}. \tag{4.40}$$

Rewriting (4.38), we get

$$0 = R_{\mu\nu} - 2\nabla_\mu\Phi\nabla_\nu\Phi - \frac{1}{d-1}g_{\mu\nu}(4V(\Phi) + \Lambda) - \nabla_{(\mu}\xi_{\nu)}\,. \tag{4.41}$$

The Einstein-DeTurk equations (4.38) still have to be supplemented by the wave equation for the scalar Φ. Since we work with a real scalar, no additional gauge symmetry needs to be fixed in our system. We choose the AdS-Schwarzschild black brane or the AdS-Soliton geometry, as long as the disorder is weak. Once the disorder gets larger, the sought-for metric g will deviate more and more from the background metric, and the time it takes for the code to converge to $\xi^\alpha\xi_\alpha = 0 \Leftrightarrow \xi^\alpha = 0$ (ξ^α is space-like for a static metric) will take longer and longer. In this case we update the reference solution $\bar{g}$ to a already obtained physical solution.

The form we will take is

$$\Phi_1(x) = \bar{V}\sum_{n=1}^{N-1} C_n \cos(k_n x + \gamma_n)\,, \tag{4.42}$$

with $\bar{V} = 0.1, 0.2, ..., 1.0, N = 50$.

$$C_n = C = (2\sqrt{\Delta k})^{d-1}\,, \quad k_n = n\Delta k\,, \quad \Delta k = \frac{k_0}{N}\,, \tag{4.43}$$

and

$$\frac{k_0}{N} << T = \frac{3y_+}{4\pi} << k_0\,. \tag{4.44}$$

In the following we take $k_0 = 1$ and vary temperature. Note: we may need 500 points at the periodic direction.

4.5 Free Energy

Now we look at the free energy of the two spacetime geometries. For the black hole solution,

$$ds^2 = \frac{1}{y^2}\left[-(1-y^3)y_+^2 A dt^2 + \frac{B}{1-y^3}dy^2 + y_+^2 S\left(dx + Fdy\right)^2 + y_+^2 H d\chi^2\right]\,, \tag{4.45}$$

$$0 < \chi \leq l.$$

For the soliton solution,

$$ds^2 = \frac{1}{y^2}\left[(1-y^3)y_+^2 A d\chi'^2 + \frac{B}{1-y^3}dy^2 + y_+^2 S\left(dx + Fdy\right)^2 - y_+^2 H dt'^2\right]\,, \tag{4.46}$$

$$l = 12\pi y_+ \sqrt{\frac{B}{A}},$$

which is obtained from the black hole solution by the "double Wick rotation" $\chi' = it, \chi = it'$.

According to the AdS/CFT duality, the free energy of the corresponding boundary system is proportional to the on-shell Euclidean action. We first write down the finite Euclidean action:

$$\begin{aligned} 2\kappa_N^2 S = &\lim_{y_c \to 0}\{-\int_{y>y_c}^{1} d^{d+1}x\sqrt{-g}[R - \Lambda - 2|\nabla\Phi|^2 - 4V(\Phi)] \\ &+ \int_{y=y_c} d^d x\sqrt{-\gamma}[-2K + \frac{2(d-1)}{L} + 2\frac{d-\Delta}{L}|\Phi|^2]\}. \end{aligned} \tag{4.47}$$

The unit normal covector of y equaling constant is

$$n_\mu = (0, -\frac{1}{\sqrt{g^{yy}}}, 0, 0).$$

The minus sign in n_y component is because we want the normal vector point to the infinity direction ($y = 0$). Thus, K is given by

$$\begin{aligned} K &= \gamma^{\mu\nu}\nabla_\mu n_\nu \\ &= \gamma^{\mu\nu}(-\Gamma^y_{\mu\nu} n_y). \end{aligned} \tag{4.48}$$

Making a change of coordinate to $r = \sqrt{1-y}$, we have

$$\begin{aligned} 2\kappa_N^2 S =& \lim_{\epsilon\to 0}\{-\int_{r=0}^{1-\epsilon} d^{d+1}x\sqrt{-\hat{g}}[R - \Lambda - 2|\nabla\Phi|^2 - 4V(\Phi)] \\ &+ \int_{r=1-\epsilon} d^d x\sqrt{-\hat{\gamma}}[-2K + \frac{2(d-1)}{L} - 2\frac{d-\Delta}{L}|\Phi|^2]\}. \end{aligned} \tag{4.49}$$

Substituting EOM (4.2) into (4.49) and taking $L = 1, d = 3$, we have

$$\begin{aligned} 2\kappa_N^2 S =& \lim_{\epsilon\to 0}\{-\int_{r=0}^{1-\epsilon} d^{d+1}x\sqrt{-\hat{g}}[\Lambda - 2\partial_\mu\Phi\partial^\mu\Phi] \\ &+ \int_{r=1-\epsilon} d^d x\sqrt{-\hat{\gamma}}[-2K + \frac{2(d-1)}{L} - 2\frac{d-\Delta}{L}|\Phi|^2]\} \\ =& \lim_{\epsilon\to 0}\{-\int_{r=0}^{1-\epsilon} d^{3+1}x\sqrt{-\hat{g}}[-6 - 2\partial_\mu\Phi\partial^\mu\Phi] \\ &+ \int_{r=1-\epsilon} d^3 x\sqrt{-\hat{\gamma}}[-2K + 4 - 2|\Phi|^2]\}. \end{aligned} \tag{4.50}$$

The unit normal covector is

$$n_\mu = (0, \frac{1}{\sqrt{g^{rr}}}, 0, 0).$$

By now, we only get the backreacted solutions (Fig. 4.1 and 4.2). We then need to calculate the free energy numerically to investigate the potential phase transition induced by disorder.

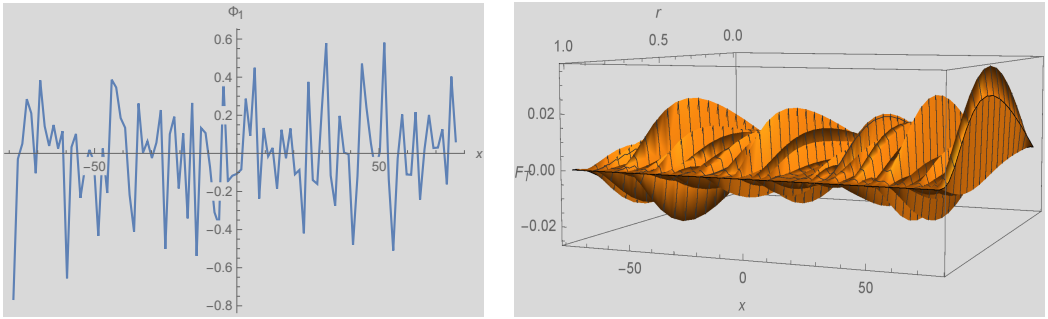

Figure 4.1: Black hole case: $r = 1$ is the boundary. We take 25 disordered modes here and 100 grids at x direction. The left one shows a scalar source Φ_1 as a function of kx at the boundary with $\bar{V} = 0.5$, $\frac{T}{k_0} = 0.1$. The right one for metric funtion F_T.

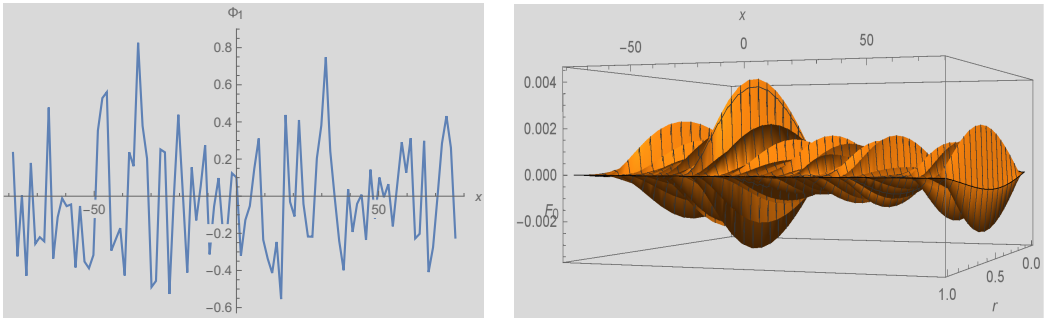

Figure 4.2: Soliton case: The left one shows a scalar source Φ_1 as a function of kx at the boundary with $\bar{V} = 0.5$, $\frac{y_+}{k_0} = \frac{0.4\pi}{3}$. The right one for metric funtion F_T.

4.6 Discussion

Following [82], where the planar black hole solutions in AdS_3 and AdS_4 were constructed with marginally relevant disorder, we analytically constructed the AdS_{d+1} soliton geometry in which the boundary was perturbed with marginally relevant quenched disorder. In order to investigate the Hawking-Page phase transition induced by disorder, we resorted to numerical calculation to obtain the precise geometry solutions of AdS soliton and AdS black hole. The free energy expression is presented, and the next step is to calculate it numerically for solutions with different strength of disorder.

5 Holographic Kondo Model

5.1 Introduction and Summary

The electrical resistivity in metals mainly contributed from the scattering of the conduction electrons by the vibrating nuclei. The resistivity increases rapidly and monotonically with temperature as the lattice vibrating energy grows, which is the case for most metals. At the very low temperature, where the lattice vibrations are almost dead, there is still residual resistivity since the electrons still scatters with impurities, defects and vacancies. However, in 1934 a resistance minimum was observed in the low temperature range in gold (see Fig. 5.1) and the resistivity increases as $T \to 0$. This phenomenon is called *Kondo effect*. The existence of a resistance minimum at low temperature were later similarly observed in other examples of metals. An additional scattering mechanism is needed to describe this new phenomenon. In the early 1960s, magnetic impurities, which provide local magnetic moment in the metal, were recognized as the reason for resistance minimum. Finally in 1964 Kondo proposed a model [33] using perturbation theory to describe the interactions of a localized magnetic spin impurity with a free electron gas which gave rise to a $log\,(T)$ term in the resistivity expression. The Kondo model provides a satisfactory explanation for the resistance minimum and is in agreement with experiment.

There is a critical temperature in the Kondo model called *Kondo temperature* (T_K) approaching which the perturbed results become invalid. The Kondo model then is developed further beyond its origin. [83] developed a Fermi-liquid description for the Kondo model. It was also solved by the "Bethe ansatz" and yields the specific heat and magnetization [84, 85]. The Kondo model plays significant role in the development of the renormalization group (RG) (see Wilson's numerical RG method [86]). The beta function of the impurity coupling is negative and is therefore a strongly coupled problem in its nature at low energies that is similar to the RG running of QCD. Moreover, the Kondo model corresponds to a boundary RG flow of the antiferromagnetic coupling between the impurity and conduction electrons. The RG flow connects two RG fixed points corresponding to a UV and IR CFT. The Kondo model can be studied by using CFT techniques as well, which can be applied to the multi-channel Kondo problem (see [87–92] for a review).

The generalizations of the impurity spin to $SU(N)$ with large N provide a new approach to the Kondo problem [93–95] and the large-N limit makes the treatment amenable to the holographic approach [34]. In this holographic bottom-up model, the ambient electrons are strongly coupled which differs from the free electron gas in

the original Kondo model. The impurity and ambient electrons degrees of freedom are dual to an AdS_2 subspace and a gravity theory in an AdS_3 bulk geometry at finite temperature. Several characteristic features of the Kondo model are exhibited in this model, such as a dynamically generated scale, power-law scalings at low temperature (without $ln\,(T/T_K)$ behavior due to the large-N limit), screening of the impurity and so on.

However, many aspects in the holographic model are sitll unexplored, such as the conductivity of the electrons and higher dimensional generalization to Kondo lattices. Another problem is the backreaction to the background geometry may be necessary to consider at the point of the impurity. We add a Maxwell term to the holographic model [34] instead of the Chern-Simons term to investigate the DC resistivity of the electrons. In the probe limit, we introduce junction conditions to connect fields crossing the defect. Then we consider backreaction which gives us a new metric ansatz and new junction conditions to gauge fields. Some of the new results reported below were obtained in collaboration with exchange student Dilyn Fullerton [96].

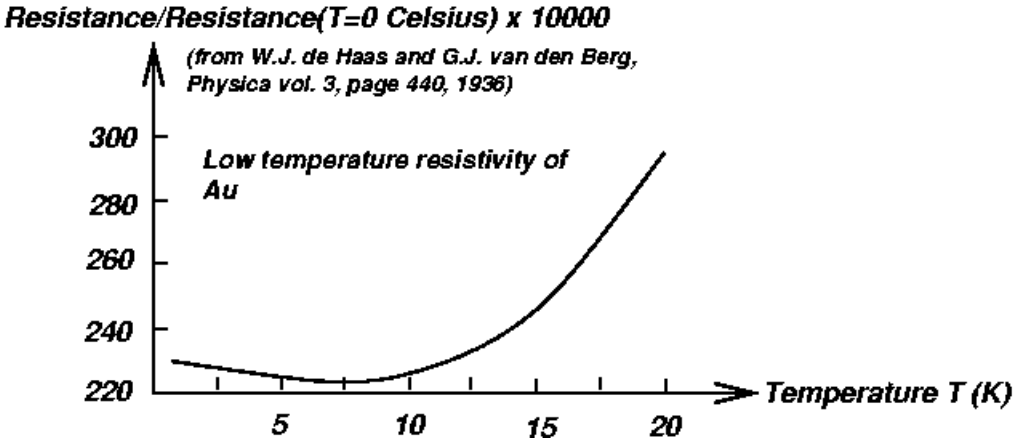

Figure 5.1: A resistance minimum is observed in gold with a small amount of what were likely iron impurities at low temperature.

5.1.1 Original Kondo Model in Quantum Field Theory

As T $\to$ 0, the electrical resistivity $\rho(T)$ of metals either decreases to zero (phonons or electron-electron interactions), or reaches a constant (with non-magnetic impurities). However, the resistivity of metals containing magnetic impurities increases as $T \to 0$ and form a resistance minimum at very low temperature.

The Kondo effect describes the scattering of conduction electrons in a metal due to magnetic impurities, resulting in a characteristic change in electrical resistivity with temperature because of the screening of a magnetic impurity by conduction electrons

at low temperature. The original Kondo model [33] introduces the interaction of a free electron gas with a $SU(2)$ spin impurity in the Hamiltonian

$$H = \sum_{\vec{k},\alpha} \frac{v_F}{2\pi} i\psi^{\dagger\alpha}_{\vec{k}} \partial_x \psi_{\vec{k}\alpha} + \frac{v_F}{2} \lambda_K \delta(x) \overrightarrow{J} \cdot \overrightarrow{S}, \tag{5.1}$$

where the $\psi_{\vec{k}\alpha}$'s are conduction electron annihilation operators (of momentum $\vec{k}$, spin α), v_F is the Fermi velocity, $\vec{S}$ represents the spin of the magnetic impurity located at $\vec{x} = 0$ with

$$[S^a, S^b] = i\epsilon^{abc} S^c, \tag{5.2}$$

and $\overrightarrow{J}$ is the electron current

$$J^a = \psi^\dagger \sigma^a \psi, \tag{5.3}$$

with σ^a the Pauli matrices. The resistivity can be calculated in perturbation theory to finite order:

$$\rho(T) \sim \rho_0 [\lambda_K + \nu \lambda_K^2 \ln \frac{D}{T} + \dots]^2 \tag{5.4}$$

where D is the band-width, ν the density of states. The rise of resistivity due to logarithmic term is satisfactorily in agreement with experimental results at very low temperature (see Fig. 5.2).

However, the results which comes from perturbation theory breaks down near or at Kondo temperature $T_K = De^{-\frac{1}{\nu\lambda}}$, where the $O(\lambda^2)$ term is as big as the $O(\lambda)$ term. The results also do not contain higher order information.

5.1.1.1 1+1 Dimensional CFT Approach

Now we are going to study Kondo model in field theory following Affleck and Ludwig. The Kondo Hamiltonian density is

$$H_K = \psi^\dagger_\alpha \frac{-\nabla^2}{2m} \psi_{\vec{k}\alpha} + \lambda_K \delta(\vec{x}) \vec{S} \cdot \psi^\dagger_{\alpha'} \frac{1}{2} \vec{\tau}_{\alpha'\alpha} \psi_{\vec{k}\alpha}. \tag{5.5}$$

Performing a partial wave decomposition of electrons $\psi_{\vec{k}\alpha}\alpha$, only the s-wave is left. Linearizing the dispersion relation around Fermi momentum k_F, one gets the effective theory defined on the positive real axis, representing the radial distance to the impurity with in- and out-going appearing as left- and right moving fermions. Extending the axis to negative values (see Fig.(5.3)) we will have left-movers alone moving on the entire real axis and interact with the impurity at the origin,

$$H = \frac{v_F}{2\pi} \psi^\dagger_L i\partial_x \psi_L + v_F \delta(x) \vec{S} \cdot \psi^\dagger_L i \frac{1}{2} \vec{\tau} \psi_L, \tag{5.6}$$

where $v_F = k_F/m$ is the Fermi velocity.

In the UV, $\lambda_K \to 0$, so H reduces to a kinetic term which is trivially a (1+1)-dimensional CFT. Defining $z \equiv \tau + ix$ with τ the Euclidean time, we can see ψ_L

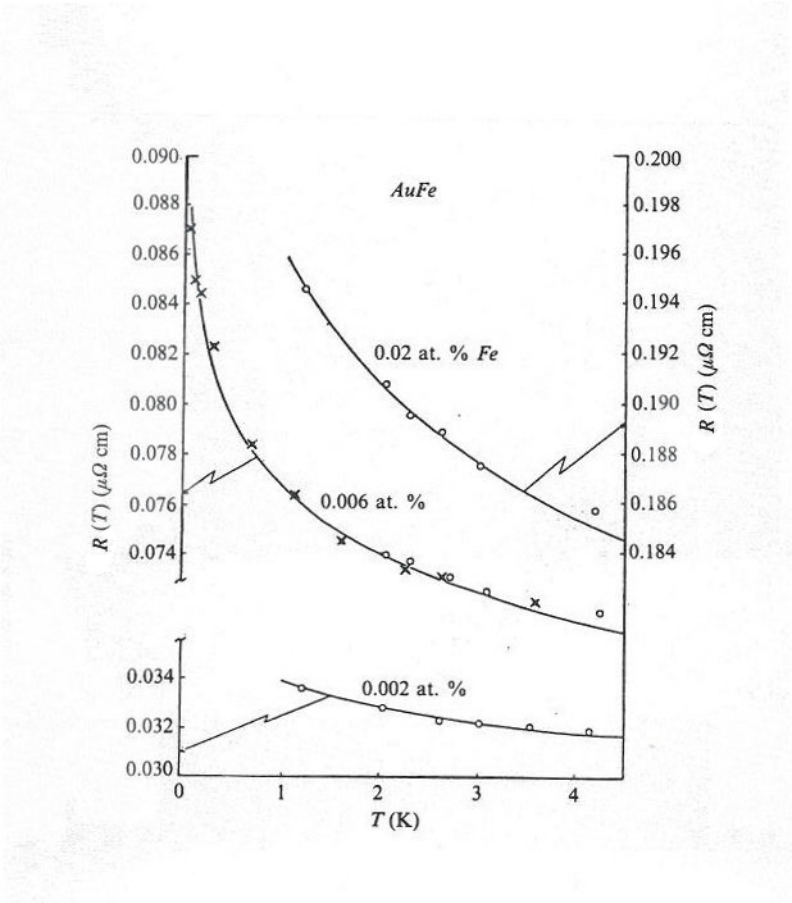

Figure 5.2: Figure taken from [33]. The points are experimental results for the resistivity of gold with iron impurities at very low temperature. The solid lines are the predictions that includes a logarithmic term due to the Kondo effect.

and the spin, channel, and charge currents are all holomorphic in z, and moreover each of the currents obeys a Kac-Moody algebra.

$$[J_n^a, J_m^b] = if^{abc}J_{n+m}^c + k\frac{n}{2}\delta^{ab}\delta_{n,-m} \tag{5.7}$$

which is the $SU(N)$ level k Kac-Moody algebra. In the IR, they get the IR fixed point of H and λ_K by rewriting the Hamiltonian in Sugawara form. Due to the anomaly matching, the IR fixed point has the same symmetry $SU(N)_k \times SU(k)_N \times U(1)$ as the UV fixed point. The Kondo problem reduces to finding how the representations re-arrange in going from the UV to the IR.

5.1.1.2 Large N Kondo model

[97, 98] find that the Kondo model simplifies considerably when the rank N of the spin group is taken to infinity. The spin-electron interaction term $\overrightarrow{J} \cdot \overrightarrow{S}$ reduces to a

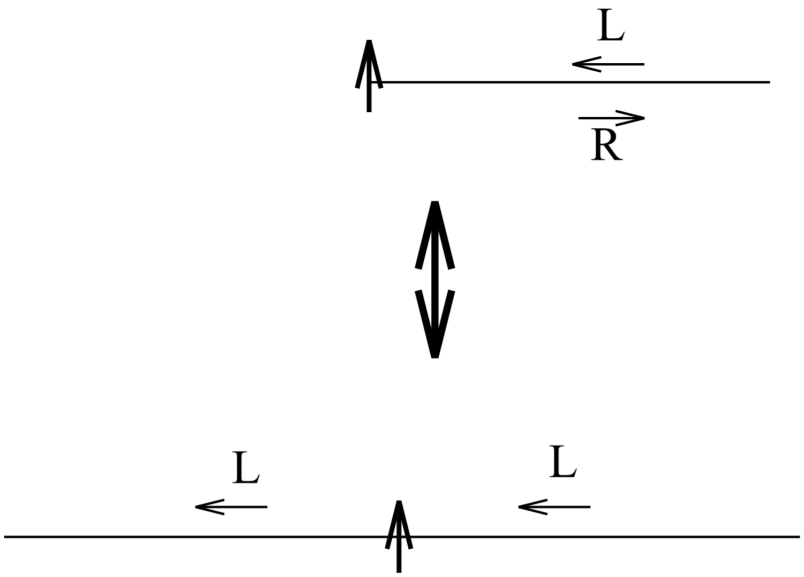

FIG. 4. Reflecting the left-movers to the negative axis.

Figure 5.3: The figure is taken from [92].

product $\mathcal{O}^\dagger\mathcal{O}$ of scalar operator $\mathcal{O}$ and the screening corresponds to the condensation of $\mathcal{O}$. The large N limit of the Kondo model is $N \to \infty$, $\lambda \to 0$ with λN fixed. [34] considers an impurity in a totally anti-symmetric representation of $SU(N)$, so the associated Young tableau has a single column with $q < N$ boxes. The spin is then written in terms of Abrikosov pseudo-fermions χ:

$$S^a = \chi^{\dagger i} T^a{}_i{}^j \chi_j, \qquad a = 1, 2, \ldots N^2 - 1, \tag{5.8}$$

where χ is in the fundamental representation of $SU(N)$. Physical states have q units of χ's $U(1)$ charge, which means the constraint should be imposed as

$$\chi^\dagger \chi = q. \tag{5.9}$$

In essence, the charge density of the Abrikosov fermions is given by the size of the totally antisymmetric representation. One then has the singlet operator

$$\mathscr{O} \equiv \psi_L^\dagger \chi. \tag{5.10}$$

By using the $SU(N)$ algebra identity, the Kondo coupling is now:

$$J^a S^a = (\psi_L^\dagger T^a \psi_L)(\chi^\dagger T^a \chi) = \frac{1}{2}[\mathscr{O}\mathscr{O}^\dagger - \frac{q}{N}(\psi_L^\dagger T \psi_L)] \tag{5.11}$$

The condensate $\langle \mathscr{O} \rangle$ corresponds to screened phase.

5.1.1.3 Holographic Kondo Model

[34] combines the CFT and large N descriptions, which is a Chern-Simons gauge field in (2+1)-dimensional AdS_3 space, dual to the Kac-Moody current, coupled to a holographic superconductor along an AdS_2 subspace. The action of the bottom-up gravity dual for Kondo model is:

$$S = S_{Einstein-Hilbert} + S_{CS} + S_{AdS_2}, \tag{5.12}$$

where

$$S_{CS} = -\frac{N}{4\pi}\int_{AdS_3} Tr(A \wedge dA + \frac{2}{3}A \wedge A \wedge A), \tag{5.13}$$

$$S_{AdS_2} = -N\int d^3x\delta(x)\sqrt{-g}[\frac{1}{4}f^2 + g^{mn}(D_m\Phi)^\dagger(D_m\Phi) + M^2\Phi^\dagger\Phi]. \tag{5.14}$$

The corresponding metric is then

$$ds^2 = \frac{1}{z^2}(\frac{dz^2}{f(z)} - f(z)dt^2 + dx^2), \tag{5.15}$$

where $f(z) = 1 - \frac{z^2}{z_H^2}$, $T = \frac{1}{2\pi z_H}$. The following calculation exhibits several characteristic features of the Kondo effect, including a dynamically generated scale, Entanglement entropy for magnetic impurity, and so on. The Chern-Simons terms in the action means the ambient electrons do not propagate.

5.1.1.4 Propagation of the Ambient Electrons

A new paper [99] says that they get the logarithmic rise of the resistivity in a holographic Kondo model. The action they use consists of a bulk Maxwell term instead of Chern-Simons term:

$$S_{Kondo} = -N\int\sqrt{-g_{(3)}}d^3x(\mathscr{L}_{AdS_3} - \delta(x)\mathscr{L}_{AdS_2}), \tag{5.16}$$

$$\mathscr{L}_{AdS_3} = \frac{1}{2\kappa_3^2}(R + \frac{2}{L^2}) - \frac{1}{4e_3^2}F^2, \tag{5.17}$$

$$\mathscr{L}_{AdS_2} = \frac{1}{4e_2^2}f^2 + (D^m\Phi)^\dagger(D_m\Phi) + M^2\Phi^\dagger\Phi$$

where $D_m \equiv \partial_m + iq_3A_m - iq_2a_m$. The metric is btz:

$$ds^2 = \frac{1}{z^2}(\frac{dz^2}{h(z)} - h(z)dt^2 + dx^2), \tag{5.18}$$

where $h(z)$ is the *blackening factor* given by $h(z) = 1 - \frac{z^2}{z_H^2}$, $T = \frac{1}{2\pi z_H}$. They use two assumptions to simplify the EOM : $q_3 \ll q_2 = 1$ and $q_2e_2^2 \ll q_3e_3^2 = 1$. These

two limits allow them to work under two kinds of probe limits. The first limit treats A_μ as a probe field for the AdS_2 fields. So one can look for the solutions of $\phi(z)$ and $a_t(z)$, independent of A_μ . The second limit allows one to solve for a_t by setting its source to zero. Based on these simplifications, without numerical calculation, they finally get

$$\rho_{dc}(T) = -\frac{R_0}{N}\lambda_K \ln\frac{T}{T_K}. \tag{5.19}$$

Unfortunately, the results of this paper contains a calculational mistake. To be specific, after doing Fourier transformation on one of the key equations of motion, they missed the $\delta(\omega)$ term

$$E_x'' + \left(\frac{\omega^2 f'(z)}{p^2(z)f(z)} + \frac{1}{z}\right)E_x' + \frac{p^2(z)}{f^2(z)}E_x = \frac{kj_0(z)}{izf(z)}\delta(\omega), \tag{5.20}$$

where $E_x = E_x(z)$ is the electric field, $h(z) = 1 - z^2/z_h^2$, $p^2(z) = \omega^2 - f(z)k^2$,$j_0(z) = -2a_t\phi^2$. In the following we will try to investigate the conductivity of this model in our way, and explain our calculation and results.

5.2 Probe Limit

5.2.1 Setup and Equation of Motion

We consider the same metric as before in the BTZ black hole (5.18). with z_H denoting the horizon position. Now let Σ denote the hypersurface defined by

$$\Sigma = \{(t, z, x = 0) \mid t \in \mathbb{R}, z \in [0, z_H]\}\,. \tag{5.21}$$

This surface separates the spacetime into two regions, which we denote by U^+ and U^- for $x > 0$ and $x < 0$ respectively, and the induced metric on the hypersurface is given by

$$ds^2_{\mathrm{AdS}_2} = \gamma_{mn}dx^m dx^n = \frac{1}{z^2}\left(-h(z)dt^2 + \frac{1}{h(z)}dz^2\right). \tag{5.22}$$

In this section, Greek indices are taken to range over the coordinates of the BTZ metric, and Latin indices are taken to range over those of the induced AdS_2 metric.

We rewrite the action (5.16) in a more explicit way

$$\begin{aligned} S = \int_V dx^3 \Bigg[&\sqrt{-g}\left(\frac{1}{2\kappa_3^2}(R+2) - \frac{1}{4e_3^2}F_{\mu\nu}F^{\mu\nu}\right) \\ &- \delta(x)\sqrt{-\gamma}\left(\frac{1}{4e_2^2}f_{mn}f^{mn} + (D^m\Phi)^\dagger(D_m\Phi) + M^2\Phi^\dagger\Phi\right)\Bigg]. \end{aligned} \tag{5.23}$$

where $F = \mathrm{d}A$ and $f = \mathrm{d}a$, and D_m is the gauge-covariant derivative operator defined on the AdS_2 subspace

$$D_m : \Phi \mapsto (\partial_m + iq_3 A_m|_\Sigma - iq_2 a_m)\,\Phi, \tag{5.24}$$

on a complex-valued scalar field Φ, where $A_m|_\Sigma$ is the restriction of A_m to the hypersurface Σ. Additionally, we work in a gauge[1] in which

$$A_z = 0, \quad a_z = 0. \tag{5.25}$$

We take $\Phi = \phi \mathrm{e}^{\mathrm{i}\psi}$ for real-valued fields $\phi \geq 0$ and $0 \leq \psi < 2\pi$. By varying the action with respect to corresponding fields, we then obtain the following equations of motion:

$$\begin{aligned}
z\partial_t\partial_z A_t - hz\partial_x\partial_z A_x &= k_3\phi^2 h(\partial_z\psi)\delta(x) && (5.26\text{: } A_z)\\
h\partial_z\left(z\partial_z A_t\right) + z\partial_x F_{xt} &= k_3\phi^2\chi_t\delta(x) && (5.26\text{: } A_t)\\
z\partial_t F_{xt} + h\partial_z\left(hz\partial_z A_x\right) &= 0 && (5.26\text{: } A_x)\\
\partial_t^2\phi - h\partial_z\left(h\partial_z\phi\right) &= \left(\chi_t^2 - h^2(\partial_z\psi)^2 - M^2h/z^2\right)\phi && (5.26\text{: } \phi)\\
\partial_t\left(\phi^2\chi_t\right) - h\partial_z\left(\phi^2 h\partial_z\psi\right) &= 0 && (5.26\text{: } \psi)\\
z^2\partial_t\partial_z a_t &= -k_2\phi^2 h\partial_z\psi && (5.26\text{: } a_z)\\
h\partial_z\left(z^2\partial_z a_t\right) &= -k_2\phi^2\chi_t && (5.26\text{: } a_t)
\end{aligned}$$

where we have defined $k_i := 2q_i e_i^2$ for $i = 2, 3$ and

$$\chi_m := \left(\partial_m\psi + q_3 A_m|_\Sigma - q_2 a_m\right). \tag{5.27}$$

5.2.2 Junction conditions

The equations of motions derived are couplings between bulk and surface fields. The Maxwell field directly connects the background and the defect. It is not immediately clear how the bulk Maxwell field should be affected by the surface Σ and its localized fields. In this part, we will attempt to elucidate the proper treatment of these fields.

5.2.2.1 First junction condition

We only have one spacial direction x. Due to the presence of the defect at $x = 0$, the gauge field is separated into two parts. In deriving the first junction condition on the fields A_μ at the surface Σ, we follow the general procedure outlined in reference [100]

[1] The general equations of motion before gauge fixing are presented in section 7.1

— only we do so for the gauge field A_μ as opposed to the metric. The procedure is as follows. We begin by writing A_μ as a distribution-valued field

$$A_\mu = A_\mu^+ \Theta(x) + A_\mu^- \Theta(-x), \tag{5.28}$$

where Θ is the unit step function. Then we express the terms of the action in terms of this field. The field F depends on derivatives of A_μ:

$$\partial_\nu A_\mu = \left(\partial_\nu A_\mu^+\right) \Theta(x) + \left(\partial_\nu A_\mu^-\right) \Theta(-x) + \left(A_\mu^+ - A_\mu^-\right) \delta(x) \delta^x{}_\nu, \tag{5.29}$$

where we have identified the distribution $\delta(x)$ as the derivative in x of $\Theta(x)$. The Maxwell tensor $F_{\mu\nu}$ is then

$$F_{\mu\nu} = 2\partial_{[\mu} A_{\nu]} = F_{\mu\nu}^+ \Theta(x) + F_{\mu\nu}^- \Theta(-x) + \delta(x) \left[\delta^x{}_\mu \left(A_\nu^+ - A_\nu^-\right) - \delta^x{}_\nu \left(A_\mu^+ - A_\mu^-\right)\right], \tag{5.30}$$

and so

$$F_{\mu\nu} F^{\mu\nu} = F_{\mu\nu}^+ F^{\mu\nu} \Theta(x) + F_{\mu\nu}^- F^{\mu\nu} \Theta(-x) + 2\delta(x) \left(A_\nu^+ - A_\nu^-\right) F^{x\nu}. \tag{5.31}$$

The key insight of reference [100] is that all terms proportional to $\Theta(x)\delta(x)$ or $\Theta(-x)\delta(x)$ must be identically zero. The intuitive interpretation of this requirement is that any term in the action must be well-defined as a distribution, and $\Theta(x)\delta(x)$ is not well-defined as a distribution.

Admittedly, this argument for removing terms of the type $\delta(x)\Theta(x)$ seems somewhat unmotivated. It would be useful to think of $\delta(x)$ and $\Theta(x)$ as the limiting cases of differentiable real-valued functions; that is, let $\delta(x) = \lim_{a\to 0} f_a(x)$ and $\Theta(x) = \lim_{a\to 0} F_a(x)$, where

$$f_a(x) = \frac{1}{\sqrt{\pi} a} e^{-x^2/a^2}, \quad F_a(x) = \frac{1}{2}\left(1 + \mathrm{erf}(x/a)\right), \tag{5.32}$$

and $erf(x/a)$ is the error function defined by

$$\mathrm{erf}(x) = \frac{1}{\sqrt{\pi}} \int_{-x}^{x} e^{-t^2} dt \tag{5.33}$$

Then the issue becomes more clear: we obtain different limits depending on which of x or a we take to 0 first.

$$\lim_{a\to 0} \lim_{x\to 0} f_a(x) F_a(x) = \infty, \quad \lim_{x\to 0} \lim_{a\to 0} f_a(x) F_a(x) = 0. \tag{5.34}$$

It should be clear that such a quantity cannot represent a physical observable.

Examining (5.31), we see that since F^{xx} is identically 0, we need only worry about the terms $(A_\nu^+ - A_\nu^-)$ for $\nu = z, t$. According to the above requirement, these must be zero. Hence we arrive at our first junction condition.

Proposition 5.2.1 (First junction condition)**.** *In order for F^2 to be a well-defined quantity as a distribution across and on the surface Σ, we must have that*

$$0 = [A_m]_\Sigma := \lim_{x\to 0^+} A_m - \lim_{x\to 0^-} A_m \tag{5.35}$$

for $m \in \{z, t\}$.

We then have the corresponding corollary:

Corollary 5.2.1.1. *F_{tz} and F_{zt} have a well-defined limit as $x \to 0$.*

$$[F_{tz}]_\Sigma = 0 = [F_{zt}]_\Sigma \,. \tag{5.36}$$

5.2.2.2 Second junction condition

By requiring that the Maxwell term in the action should be well-defined, we get the the first junction condition. The first two equations of motion also contain a term with $\delta(x)$, which means there are other junction conditions need to be satisfied. To derive the second junction condition, we examine (7.1: A_t) and (7.1: A_z), the general forms of (5.26: A_t) and (5.26: A_z). We expect that all of the fields in this equation will satisfy the homogeneous equation for all $x \neq 0$, and the delta distribution will provide a junction condition on the fields at $x = 0$. We obtain

$$\partial_t (zF_{tz}) + hz\partial_x F_{zx} = 0 \quad \forall x \neq 0, \tag{5.37a}$$

$$h^2\partial_z (zF_{tz}) + hz\partial_x F_{tx} = 0 \quad \forall x \neq 0, \tag{5.37b}$$

$$z\,[F_{mx}]_\Sigma = -k_3 \left(\partial_m \psi + q_3 A_m|_\Sigma - q_2 a_m\right)\phi^2, \quad \forall m \in \{t, z\} \tag{5.37c}$$

where (5.37c) was obtained by integrating the equations in x over an interval $(-\epsilon, \epsilon)$, taking the limit $\epsilon \to 0$, and applying (5.36) to remove the term containing ${F_{tz}}^2$.

Now we obtain the second junction condition from (5.37c):

Proposition 5.2.2 (Second junction condition)**.** *It follows from* (5.36)*,* (7.1: A_t) *and* (7.1: A_z) *that F_{tx} must have the discontinuity across Σ given by* (5.37c)*.*

In the gauge given by (5.25), (5.37c) reduces to

$$z\,[F_{tx}]_\Sigma = -k_3\phi^2\chi_t, \tag{5.38a}$$

$$z\partial_z\,[A_x]_\Sigma = -k_3\phi^2\partial_z\psi. \tag{5.38b}$$

[2]There is in fact a case in which this term does not go to zero: when A_t or A_z contains a term proportional to $\delta(x)$. Perhaps this should be further explored since it is distinct from the considerations in section (5.2.4); however, we find it reasonable to assume the contrary since terms proportional to $\delta(x)$ would make the terms $A_m|_\Sigma$ as well as the x derivatives (5.37) ill-defined.

5.2.3 Static background solution

We now seek the static background solutions of the equations of motion, particularly in the asymptotic limit $z \to 0$. Removing the t-dependent terms from the equations of motion (5.26), we obtain the static background equations of motion:

$$\begin{aligned}
\partial_x \partial_z A_x &= 0 && (5.39\colon A_z)\\
h\partial_z \left(z\partial_z A_t\right) + z\partial_x^2 A_t &= 0 \quad \forall x \neq 0 && (5.39\colon A_t)\\
\partial_z \left(hz\partial_z A_x\right) &= 0 && (5.39\colon A_x)\\
h\left(h\phi'\right)' &= \left(M^2 h/z^2 - \chi^2\right)\phi && (5.39\colon \phi)\\
0 &= \psi' && (5.39\colon a_z)\\
h\left(z^2 a_t'\right)' &= -k_2\phi^2\chi && (5.39\colon a_t)\\
z\left[\partial_x A_t\right]_\Sigma &= k_3\phi^2\chi && (5.39\colon A_t|_\Sigma)
\end{aligned}$$

where

$$\chi := q_3\, A_t|_\Sigma - q_2 a_t, \tag{5.40}$$

and we have used ϕ',ψ', and a_t' as the derivatives in z of these fields since there is no ambiguity in the static system. Note that in its general form, $(5.39\colon a_z)$ would require either $\psi' \equiv 0$ or $\phi \equiv 0$ in the static case, but setting $\phi \equiv 0$ would mean that ϕ is identically zero in every gauge; moreover, given that ψ only appears in $\Phi = \phi \mathrm{e}^{\psi}$, a trivial value of ϕ would make ψ irrelevant. Hence we conclude that $\psi' \equiv 0$.

Now, following references [101, 102], we switch to the r coordinate, defined by

$$r = \log\left(\frac{1+\sqrt{h}}{2z}\right), \tag{5.41}$$

which is ostensibly preferable to z since z is not a proper Fefferman-Graham (FG) coordinates [102].[3] In the asymptotic limit as $z \to 0$ ($r \to \infty$), we have

$$\partial_z \to -e^r \partial_r, \quad z \to e^{-r}. \tag{5.42}$$

Hence the asymptotic equations of motion in terms of the r coordinate are

[3] It is not clear whether this coordinate change is necessary or helpful for the asymptotic expansion: perhaps it only becomes necessary once one wishes to write down the Hamilton-Jacobi equation; nevertheless we will use the r coordinate here for consistency with the aforementioned works.

$$\partial_r \partial_x A_x = 0 \qquad (5.43\text{: } A_z)$$

$$\left(\partial_r^2 + \mathrm{e}^{-2r}\partial_x^2\right) A_t = 0 \quad \forall x \neq 0 \qquad (5.43\text{: } A_t)$$

$$\partial_r^2 A_x = 0 \qquad (5.43\text{: } A_x)$$

$$\ddot{\phi} + \dot{\phi} = \left(M^2 - \mathrm{e}^{-2r}\chi^2\right)\phi \qquad (5.43\text{: } \phi)$$

$$\ddot{a}_t - \dot{a}_t = -k_2 \chi \phi^2 \qquad (5.43\text{: } a_t)$$

$$\mathrm{e}^{-r}\left[\partial_x A_t\right]_\Sigma = k_3 \chi \phi^2 \qquad (5.43\text{: } \Sigma, t)$$

where we have use the notation $\dot{\phi} = \partial_r \phi$ and $\dot{a}_t = \partial_r a_t$.

It should be clear at this point what makes this model importantly different from that considered in reference [34]: in the latter, the asymptotic equations for ϕ and a_t completely decouple from the bulk gauge fields A_μ, whereas here the Maxwell fields remain coupled. Nevertheless, we shall see that to low orders in the expansion (under seemingly reasonable assumptions), these terms do not contribute.

Consider first $(5.43\text{: } a_t)$. Assuming that $\phi \to 0$ in the asymptotic limit, this reduces to

$$0 \approx \ddot{a}_t - \dot{a}_t, \tag{5.44}$$

which is readily solved by

$$a_t^{(0)} = Q\mathrm{e}^r. \tag{5.45}$$

Following reference [101], we identify Q as the charge. (Of course one could also add a constant term, which is usually denoted μ and identified as the chemical potential; however, to first order this will not contribute).

In order to obtain the first order contribution to ϕ using $(5.43\text{: } \phi)$, we must first determine A_t. Now although $(5.43\text{: } A_t)$ applies only for $x \neq 0$, we have already established in the first junction condition (5.35) that A_t should be continuous across Σ. Hence the asymptotic expansion of $A_t|_\Sigma$ should be equal to that of A_t, when its coefficients are evaluated at $x = 0$.[4]

Noting that e^{-2r} asymptotes to 0 very rapidly, we expect that to lowest order,

$$A_t^{(0)} = a(x) + b(x)r. \tag{5.46}$$

Evidently this term is relatively small, and its contribution in $(5.43\text{: } \phi)$ is negligible to lowest order. Therefore, we find for ϕ the constant-coefficient differential equation

$$\ddot{\phi} + \dot{\phi} = \left(M^2 - q_2^2 Q^2\right)\phi, \tag{5.47}$$

whose characteristic equation for the ansatz $\mathrm{e}^{\zeta r}$ is

$$\zeta^2 + \zeta - \left(M^2 - q_2^2 Q^2\right) = 0. \tag{5.48}$$

[4] Actually, this statement is not exactly trivial. We consider in (5.2.4) the case in which $\lim_{x\to 0} A_t$ is not necessarily equal to $A_t|_\Sigma$.

The roots are

$$\zeta_\pm = -\frac{1}{2} \pm \sqrt{\frac{1}{4} + M^2 - q_2^2 Q^2}. \tag{5.49}$$

Note that two very different general solutions for ϕ are obtained depending on whether the expression under the radical is zero or not. Now in references [34, 101], a similar point is reached (the expression is the same if $q_2^2 = 1$); the authors proceed by choosing to work at the Breitenlohner-Freedman (BF) bound, $M^2 + 1/4 = Q^2$. For us, we need to investigate all the possibilities.

5.2.3.1 Case: Degenerate roots

Assume that $M^2+1/4 = q_2^2 Q^2$. In this case the roots are degenerate, and the general lowest order solution for ϕ is

$$\phi^{(0)} = (-\alpha r + \beta)\mathrm{e}^{-r/2}. \tag{5.50}$$

Putting this back into (5.43: a_t) gives the next order contribution

$$a_t^{(1)} = \frac{2}{3} Q q_2^2 e_2^2 \alpha^2 \left[(r - \beta/\alpha)^3 + 3(r - \beta/\alpha)^2 + 6(r - \beta/\alpha) + 6\right], \tag{5.51}$$

and we conclude that to the lowest order

$$a_t = Q\mathrm{e}^r + \frac{2}{3} Q q_2^2 e_2^2 \alpha^2 \left[(r - \beta/\alpha)^3 + 3(r - \beta/\alpha)^2 + 6(r - \beta/\alpha) + 6\right] + \dots \tag{5.52}$$

Returning to z coordinates, we have

$$a_t = \frac{Q}{z} - \frac{2}{3} Q q_2^2 e_2^2 \alpha^2 \left[(\log(z) + \beta/\alpha)^3 - 3(\log(z) + \beta/\alpha)^2 + 6(\log(z) + \beta/\alpha) - 6\right] + \dots \tag{5.53a}$$

$$\phi = \sqrt{z}\,(\alpha \log(z) + \beta) + \dots, \tag{5.53b}$$

which agrees with the expansion seen in reference [34].

5.2.3.2 Case: Distinct roots

Let us now consider the other case, in which $M^2 + 1/4 > q_2^2 Q^2$ and so the roots ζ_+ and ζ_- are distinct. Then

$$\phi^{(0)} = \left(c_+ \mathrm{e}^{\Omega r} + c_- \mathrm{e}^{-\Omega r}\right) \mathrm{e}^{-r/2}, \tag{5.54}$$

where

$$\Omega := \sqrt{1/4 + M^2 - q_2^2 Q^2}. \tag{5.55}$$

Putting this into (5.43: a_t), we obtain that

$$\ddot{a}_t^{(1)} - \dot{a}_t^{(1)} \approx -2q_2^2e_2^2\left(Q + a_t^{(1)}\mathrm{e}^{-r}\right)\left(c_+^2\mathrm{e}^{2\Omega r} + 2c_+c_- + c_-^2\mathrm{e}^{-2\Omega r}\right). \tag{5.56}$$

At this point, in order to simplify calculations, we make another assumption: that $2\Omega \ll 1$. This is to say that $M^2 + 1/4 - q_2^2Q^2$ is only slightly larger than zero — a small deviation from the previous case. Following this assumption, we can be sure that the $a_t^{(1)}$ term on the right is negligible. We also can reasonably assume the same for the c_-^2 term. Following these assumptions, we obtain

$$a_t^{(1)} = 2Qq_2^2e_2^2\left[\frac{c_+^2}{2\Omega(1-2\Omega)}\mathrm{e}^{2\Omega r} + 2c_+c_-(r+1)\right], \tag{5.57}$$

and we conclude that to lowest order

$$a_t = Q\mathrm{e}^r + 2Qq_2^2e_2^2\left[\frac{c_+^2}{2\Omega(1-2\Omega)}\mathrm{e}^{2\Omega r} + 2c_+c_-(r+1)\right] + \dots \tag{5.58}$$

Returning to z coordinates, we have

$$a_t = \frac{Q}{z} + 2Qq_2^2e_2^2\left[\frac{c_+^2}{2\Omega(1-2\Omega)}z^{-2\Omega} + 2c_+c_-(1-\log(z))\right] + \dots \tag{5.59a}$$

$$\phi = \sqrt{z}\left(c_+z^{-\Omega} + c_-z^{\Omega}\right) + \dots \tag{5.59b}$$

This quite notably differs from the previous case in that ϕ does not have a $\log(z)$ contribution to leading order.

5.2.3.3 Asymptotic consistency check

Let us now check whether our equations are consistent in the boundary limit $z \to 0$. In particular, we would like to examine the second junction condition (5.37c), which, in the case of a static configuration, takes the form

$$k_3\left(q_3\,A_t|_\Sigma - q_2a_t\right)\phi^2 = z\left[\partial_xA_t\right]_\Sigma. \tag{5.60}$$

If we insert the asymptotic expansion (5.53) of the first case, we obtain

$$k_3\left(q_3\left(a(0) - b(0)\log(z)\right) - q_2\frac{Q}{z}\right)z\left(\alpha\log(z) + \beta\right)^2 = z\left[\left(a'(x) - b'(x)\log(z)\right)\right]_\Sigma. \tag{5.61}$$

The left side of this expression is inevitably divergent, owing to the presence of the Q/z term, which will provide for the presence of a term proportional to $\log(z)$, so long as q_2, Q, and α are all nonzero. This divergence seems to be incompatible with the right side of the equation, which appears to go to zero in the asymptotic limit.

For the second case, let us now insert the asymptotic expansion (5.59) into 5.60.

$$k_3\left(q_3\left(a(0)-b(0)\log(z)\right)-q_2\frac{Q}{z}\right)z\left(c_+z^{-\Omega}+c_-z^{\Omega}\right)^2=z\left[\left(a'(x)-b'(x)\log(z)\right)\right]_\Sigma. \tag{5.62}$$

Alas, again we find that the left side is divergent in general. This time the issue would be resolved if $c_+ = 0$.

5.2.4 Static background solution

In the previous section, there was an implicit assumption made that the asymptotic expansion of A_t in the limit $x \to 0$ is equal to the asymptotic expansion of $A_t|_\Sigma$. This was used when (5.46) was substituted into (5.43: ϕ) in order to obtain the asymptotic form of ϕ. Since the previous method arrived at contradictory results, let us now do away with this assumption and re-examine (5.43) more carefully, treating A_t and $A_t|_\Sigma$ separately.

We start by combining (5.43: Σ, t) and (5.43: a_t)[5] to obtain –

$$k_2\mathrm{e}^{-r}\left[\partial_x A_t\right]_\Sigma=-k_3\left(\ddot{a}_t-\dot{a}_t\right). \tag{5.63}$$

Now, the solution for A_t with $x \neq 0$ will be the same as the above in (5.46). Putting this into the left side of (5.63), we find

$$k_2\mathrm{e}^{-r}\left(\left[a'(x)\right]_\Sigma+\left[b'(x)\right]_\Sigma r\right)=-k_3\left(\ddot{a}_t-\dot{a}_t\right). \tag{5.64}$$

Since a and b depend only on x for the static background case under consideration and since $[f(x)]_\Sigma$ removes x-dependence, the resulting terms are simply real-valued constants. (We assume neither a' nor b' has an infinite discontinuity, as this would immediately make (5.64) inconsistent). Thus we can safely replace these with the more aesthetically-pleasing c_0 and c_1, into which we also absorb the other prefactors. Therefore, we finally arrive at

$$\mathrm{e}^{-r}\left(c_0+c_1 r\right)=\ddot{a}_t-\dot{a}_t, \tag{5.65}$$

whose general solution is

$$a_t=Q\mathrm{e}^{r}+\mu+\mathrm{e}^{-r}\left(\frac{c_0}{2}+\frac{3c_1}{4}+\frac{c_1}{2}r\right). \tag{5.66}$$

Returning now to (5.43: a_t), we obtain

$$\chi\phi^2=\frac{1}{k_2}\mathrm{e}^{-r}\left(c_0+c_1 r\right). \tag{5.67}$$

[5] One consequence of this alternative approach is that we can no longer do a "consistency check" on the junction condition (5.43: Σ, t) since we are now taking it as an a priori assumption in deriving the asymptotics. Thus its consistency is obviously ensured by construction.

At this point, the idea is to insert this result into (5.43: ϕ) to eliminate χ and thereby get an ordinary differential equation for ϕ:

$$M^2\phi^4 - \mathrm{e}^{-4r}\left(d_0 + d_1 r\right)^2 = \phi^3\left(\dot{\phi} + \ddot{\phi}\right). \tag{5.68}$$

Setting $\phi = \xi \mathrm{e}^{-r}$, we get

$$M^2\xi^4 - \left(d_0 + d_1 r\right)^2 = \xi^3\left(\ddot{\xi} - \dot{\xi}\right). \tag{5.69}$$

Unfortunately this does little to ease our pain. (5.69) is still highly non-linear in general.

If we can assume that $\mathrm{e}^{-r} \ll \phi$, then (5.68) reduces to the much more friendly looking

$$M^2\phi \approx \dot{\phi} + \ddot{\phi}, \tag{5.70}$$

whose general solution is

$$\phi \approx \mathrm{e}^{-r/2}\left(c_+ \mathrm{e}^{\Omega_0 r} + c_- \mathrm{e}^{-\Omega_0 r}\right), \tag{5.71}$$

where

$$\Omega_0 := \sqrt{M^2 + 1/4}. \tag{5.72}$$

In this case, if we now return to (5.43: a_t) and insert our first order expansions (5.66) and (5.71) for a_t and ϕ respectively, we can solve for χ and hence $A_t|_\Sigma$, for which we obtain

$$A_t|_\Sigma = \frac{q_2}{q_3} a_t + \ldots \tag{5.73}$$

There is no obvious inconsistency here, but we do obtain that A_t and $A_t|_\Sigma$ have starkly different asymptotic expansions in the $r \to \infty$ limit.

5.3 Including the Backreaction

An issue with all of the preceding work is that we begin with a static background BTZ metric (5.18), which involves no consideration of backreaction. But if we indeed place non-trivial matter fields along a sharp defect in the bulk spacetime, Einstein's equations guarantee that the bulk spacetime will be deformed by the matter fields. Backreaction will take place. In the related literature, such backreaction is ignored on the grounds that the matter fields can be treated as probe fields; this is the justification presented in reference [99], for example. The difficulties in dealing with the model thus far have suggested that perhaps neglecting this backreaction is not possible, due to the singular nature of the defect.

5.3.1 Embedding

How exactly do we go about backreacting our system? In this section we will follow references [103, 104] and do the following. Let us continue with the original metric ansatz of (5.18), but instead of considering Σ to by a hypersurface embedded by a single projection map onto $x = 0$, we allow two separate embedding maps

$$X^+ : \psi(\Sigma) \ni (t, z) \mapsto (t, z, \lambda(z)) \,, \tag{5.74a}$$
$$X^- : \psi(\Sigma) \ni (t, z) \mapsto (t, z, -\lambda(z)) \,, \tag{5.74b}$$

where $\psi : \Sigma \to \mathbb{R}\times[0, z_H]$ is a global coordinate chart of Σ, and $\lambda(z)$ is a smooth, non-negative function on $[0, z_H]$. We identify points on the two embeddings, effectively cutting out the region between them. That is, if $\mathcal{M}_{\text{BTZ}}$ is the original BTZ manifold, and $\Psi : \mathcal{M}_{\text{BTZ}} \to \mathbb{R} \times [0, z_H] \times \mathbb{R}$ is its smooth coordinate chart into (t, z, x) coordinates; then we are forming a new manifold $\mathcal{M}$ from the quotient $\mathcal{M} = \mathcal{M}_{\text{BTZ}}/\!\sim$ where $\sim$ is the equivalence relation given by the following definition. Let $p, q \in \mathcal{M}_{\text{BTZ}}$. Assume $\Psi(p) = (t_p, z_p, x_p)$ and $\Psi(q) = (t_q, z_q, x_q)$. Then we write $p \sim q$ if $t_p = t_q$, $z_p = z_q$, and $x_p, x_q \in [-\lambda(z_p), \lambda(z_p)]$. Then we can write

$$\mathcal{M} = V^- \cup \Sigma \cup V^+, \tag{5.75}$$

where we define V^+ and V^- by

$$\Psi(V^+) := \{(t, z, x) \in \mathbb{R} \times [0, z_H] \times \mathbb{R} \mid x > \lambda(z)\} \,, \tag{5.76a}$$
$$\Psi(V^-) := \{(t, z, x) \in \mathbb{R} \times [0, z_H] \times \mathbb{R} \mid x < -\lambda(z)\} \,, \tag{5.76b}$$

which differ technically from our previous definitions but are in keeping with the notion that Σ should divide our bulk manifold into two halves. It is clear then that we have effectively removed the volume of space between the embeddings X^+ and X^- of the hypersurface Σ.

We will have an induced metric on each embedded surface. It follows from (5.74) that in (t, z) coordinates, we will have

$$\gamma_{tt} = g_{tt}, \quad \gamma_{tz} = \gamma_{zt} = 0, \quad \gamma_{zz} = g_{zz} + g_{xx}\lambda'^2. \tag{5.77}$$

5.3.2 Action and equations of motion in backreacted geometry

We consider the same action as in (5.23), but we must be slightly more careful here due to the non-trivial embedding of Σ. The actions of (5.17) and (5.1.1.4) become

$$S_{\text{EM}} = \int_{V^+\cup V^-} \sqrt{-g}\, \mathrm{d}^3x \left(\frac{1}{2\kappa_3^2}(R + 2) - \frac{1}{4e_3^2}F^{\mu\nu}F_{\mu\nu}\right), \tag{5.78}$$

$$S_{\text{AdS}_2} = \int_\Sigma \sqrt{-\gamma}\, \mathrm{d}^2x \left(\frac{1}{4e_2^2}f^{mn}f_{mn} + (D^m\Phi)^\dagger(D_m\Phi) + M^2\Phi^\dagger\Phi\right), \tag{5.79}$$

where the label under the integral symbol is there to remind us of the manifold we are integrating over; that the actual coordinates integrated over are the (t, z, x) coordinates of the embeddings is to be understood.

Now our challenge is to derive the equations of motion in this modified geometry. To do this, let us start by making a coordinate change from x to y, defined by

$$y = \begin{cases} x + \lambda(z), & x < -\lambda(z) \\ 0, & -\lambda(z) \leq x \leq \lambda(z) \\ x - \lambda(z), & x > \lambda(z) \end{cases} \tag{5.80}$$

in which case we have

$$S_{\text{EM}} = \int_{-\infty}^{\infty} dt \int_0^{z_H} dz \int_{-\infty}^{\infty} dy \sqrt{-\tilde{g}} \left(\frac{1}{2\kappa_3^2}(R+2) - \frac{1}{4e_3^2} F^{\mu\nu} F_{\mu\nu} \right), \tag{5.81}$$

$$S_{\text{AdS}_2} = \int_{-\infty}^{\infty} dt \int_0^{z_H} dz \sqrt{-\gamma} \left(\frac{1}{4e_2^2} f^{mn} f_{mn} + (D^m \Phi)^\dagger (D_m \Phi) + M^2 \Phi^\dagger \Phi \right), \tag{5.82}$$

and so we can combine them into

$$\begin{aligned} S = \int_{-\infty}^{\infty} dt \int_0^{z_H} dz \int_{-\infty}^{\infty} dy \Bigg[& \sqrt{-\tilde{g}} \left(\frac{1}{2\kappa_3^2}(R+2) - \frac{1}{4e_3^2} F^{\mu\nu} F_{\mu\nu} \right) \\ & - \delta(y) \sqrt{-\gamma} \left(\frac{1}{4e_2^2} f^{mn} f_{mn} + (D^m \Phi)^\dagger (D_m \Phi) + M^2 \Phi^\dagger \Phi \right) \Bigg]. \end{aligned} \tag{5.83}$$

In these new coordinates, the metric of (5.18) becomes

$$ds^2_{\text{BTZ}} = \tilde{g}_{\alpha\beta} \, \mathrm{d}y^\alpha \otimes \mathrm{d}y^\beta = \frac{1}{z^2} \left(-h \mathrm{d}t^2 + \left(1/h + \xi'^2 \right) \mathrm{d}z^2 + \mathrm{d}y^2 + 2\xi' \mathrm{d}z \, \mathrm{d}y \right), \tag{5.84}$$

which satisfies $\sqrt{-\tilde{g}} = \sqrt{-g}$ for all nonzero y, since the Jacobian determinant is 1. Here we have defined for convenience

$$\xi(z, y) := \begin{cases} -\lambda(z), & y < 0 \\ \lambda(z), & y > 0 \end{cases} \tag{5.85}$$

and identified $\xi' := \partial_z \xi$.

The new general equations of motion are[6]

[6] It may be somewhat alarming that equations (5.86) all contain the term ξ', which is not defined at $y = 0$. The resolution is to realize that (5.86: A_z) and (5.86: A_t) both contain a delta distribution, which is only defined when integrated over y, in which case ξ' ceases to be a problem. For (5.86: A_y), we simply must take it to be undefined at $y = 0$. Its validity when taking differences over Σ remains intact.

$$zw\Big(\partial_t\left(F_{tz}-\xi' F_{ty}\right)+h\partial_y F_{zy}\Big)=-k_3\delta(y)h\phi^2\chi_z \qquad (5.86\colon A_z)$$

$$h\partial_z\left(zF_{tz}-z\xi' F_{ty}\right)-z\partial_y\left(h\xi' F_{tz}-w^2F_{ty}\right)=-k_3\delta(y)w\phi^2\chi_t \qquad (5.86\colon A_t)$$

$$z\partial_t\left(h\xi' F_{tz}-w^2F_{ty}\right)+h\partial_z\left(hzF_{zy}\right)=0\quad\forall y\neq 0 \qquad (5.86\colon A_y)$$

where

$$w(z):=\sqrt{1+h\lambda'^2}, \qquad (5.87)$$

The equations for the remaining fields are the same as given in (7.1: ϕ), (7.1: ψ), (7.1: a_t) and (7.1: a_z).

5.3.3 Junction conditions: Induced metric

Our induced metric has dependence on the embedding of Σ through $\lambda(z)$. This new "filed" $\lambda(z)$ must be determined by appropriate conditions. In this case, we use the *Israel junction conditions*, first introduced in reference [105]. We cite the form presented in reference [100]:

$$[\gamma_{ij}]_\Sigma=0, \qquad (5.88a)$$

$$[K_{ij}]_\Sigma-\gamma_{ij}[K]_\Sigma=-\kappa S_{ij}, \qquad (5.88b)$$

where K_{ij} are the components of the second fundamental form

$$K_{ij}=(\nabla_\beta n_\alpha)\,\partial_i X^\alpha\,\partial_j X^\beta, \qquad (5.89)$$

n is the unit normal vector field to the embedding of Σ pointing from V^- to V^+, K is the contraction $K=\gamma^{ij}K_{ij}$, and S_{ij} is the canonical energy-momentum tensor associated with the defect given by

$$S_{ij}:=-\frac{2}{\sqrt{-\gamma}}\frac{\delta S_{\mathrm{AdS}_2}}{\delta\gamma^{ij}}. \qquad (5.90)$$

(5.88a) is trivially satisfied, due to the square in (5.77), so we need only consider (5.88b). To do this, we must find the forms of both K_{ij} and S_{ij}; then these will be used to place constraints on the yet undetermined $\lambda(z)$. The explicit form of the unit normal vector n^α in (t,z,x) coordinates is

$$n^\alpha=\frac{z}{w}\left(0,-h\xi',1\right). \qquad (5.91)$$

It follows that only the diagonal components of K_{ij} are non-trivial. These are

$$K_{tt} = \frac{(h'z - 2h)h^2\xi'}{2hwz^2}, \tag{5.92a}$$

$$K_{zz} = \frac{(2hw^2 - h'z)\xi' - 2hz\xi''}{2hwz^2}. \tag{5.92b}$$

Since $[\xi]_\Sigma = 2\lambda$, the differences across Σ are given by

$$[K_{tt}]_\Sigma = \frac{(h'z - 2h)h^2\lambda'}{hwz^2}, \tag{5.93a}$$

$$[K_{zz}]_\Sigma = \frac{(2hw^2 - h'z)\lambda' - 2hz\lambda''}{hwz^2}. \tag{5.93b}$$

The curvature scalar is

$$K = \frac{\left(4hw^2 - zh'w^2 - zh'\right)\xi' - 2zh\xi''}{2w^3}. \tag{5.94}$$

and its difference across Σ is

$$[K]_\Sigma = \frac{\left(4hw^2 - zh'w^2 - zh'\right)\lambda' - 2zh\lambda''}{w^3}. \tag{5.95}$$

Finally, the stress-energy tensor is

$$S_{ij} = -\gamma_{ij}\left(\frac{1}{4e_2^2}f^{mn}f_{mn} + (D^m\Phi)^\dagger(D_m\Phi) + M^2\Phi^\dagger\Phi\right) + \left(\frac{1}{e_2^2}\gamma^{mn}f_{im}f_{jn} + (D_i\Phi)^\dagger(D_j\Phi) + (D_j\Phi)^\dagger(D_i\Phi)\right). \tag{5.96}$$

Given the fact that both the metric and extrinsic curvature are diagonal, we can obtain the independent pieces of (5.88b) from the following by (respectively) contracting with γ^{ij}, subtracting the diagonal parts, and taking the off-diagonal parts.

$$[K]_\Sigma = \kappa\gamma^{ij}S_{ij}, \tag{5.97a}$$

$$\tag{5.97b}$$

These give respectively

$$\left(4hw^2 - zh'w^2 - zh'\right)\lambda' - 2zh\lambda'' = 2\kappa w^3\left(\frac{1}{4e_2^2}f^{mn}f_{mn} - M^2\phi^2\right) \tag{5.98}$$

$$-\frac{h^2}{2\kappa zw}\left(h'\lambda'^3 - 2\lambda''\right) = w^2\left((\partial_t\phi)^2 + \chi_t^2\phi^2\right) + h^2\left((\partial_z\phi)^2 + \chi_z^2\phi^2\right) \tag{5.99}$$

$$(\partial_t\phi)(\partial_z\phi) + \chi_t\chi_z\phi^2 = 0 \tag{5.100}$$

The terms χ_t and χ_z are defined by (5.27). These equations — along with the ordinary equations of motions for ϕ, f_{mn}, and χ_m — must be solved to obtain the embedding function $\lambda(z)$.

5.3.4 Junction conditions: Gauge field

While the first junction condition of (5.2.1) will remain the same[7], the second junction condition of (5.2.2) will not, as it depended on the forms of (7.1: A_z) and (7.1: A_t), which are now to be replaced by (5.86: A_z) and (5.86: A_t) respectively. In this case, we obtain the homogeneous equations

$$\partial_t \left(F_{tz} - \xi' F_{ty}\right) + h\partial_y F_{zy} = 0 \quad \forall y \neq 0 \tag{5.101a}$$

$$h\partial_z\Big(z\left(F_{tz} - \xi' F_{ty}\right)\Big) - z\partial_y\left(h\xi' F_{tz} - w^2 F_{ty}\right) = 0 \quad \forall y \neq 0 \tag{5.101b}$$

and the matching conditions

$$zw^2 \left[F_{zy}\right]_\Sigma = k_3 w \chi_z \phi^2 \tag{5.102a}$$

$$-2zh\lambda' F_{tz} + zw^2 \left[F_{ty}\right]_\Sigma = k_3 w \chi_t \phi^2 \tag{5.102b}$$

An immediate consequence of (5.102b) is that F_{tz} is independent of y,

$$\partial_y F_{tz} = 0. \tag{5.103}$$

Taking the difference of (5.86: A_y) over Σ gives another condition, namely

$$0 = 2hz\lambda'\partial_t F_{tz} - zw^2\partial_t \left[F_{ty}\right]_\Sigma + h\partial_z\left(hz\left[F_{zy}\right]_\Sigma\right), \tag{5.104}$$

which we should ensure is consistent with equations (5.102). We can readily solves equations (5.102a) and (5.102b) for $[F_{zy}]_\Sigma$ and $[F_{ty}]_\Sigma$ respectively. Upon inserting the results into (5.104), we obtain

$$0 = \phi\Big(hw\phi\chi_z h' + h^2\Big(2w\chi_z\partial_z\phi + \phi\left(w\partial_z\chi_z - \chi_z w'\right)\Big) - w^3\left(2\chi_t\partial_t\phi + \phi\partial_t\chi_t\right)\Big), \tag{5.105}$$

a condition entirely independent of F.

5.3.5 The static system

Thus far, for the general backreacted system we have established the equations of motion ((5.3.2)), the junction conditions on the metric ((5.3.3)), and the junction conditions on the gauge fields ((5.3.4)). Let us now summarize these results in the static case (no time-derivatives or time dependence) with the gauge fixed to that given by (5.25).

[7] We need only change the x in (5.35) to a y.

The equations of motion and gauge field matching conditions are

$$h\partial_z(z\xi'\partial_y A_t - z\partial_z A_t) = \partial_y(w^2 z\partial_y A_t - z\xi'\partial_z A_t), \quad \forall y \neq 0 \qquad (5.106\colon A_t)$$
$$2h\lambda'(A_t + 2z\partial_z A_t) = k_3\chi w\phi^2 + zw^2\left[\partial_y A_t\right]_\Sigma \qquad (5.106\colon \Sigma, t)$$
$$\partial_z\partial_y A_y = 0 \qquad (5.106\colon A_z)$$
$$\partial_z\left(zh\partial_z A_y\right) = 0 \qquad (5.106\colon A_y)$$
$$h\phi M^2 - z^2\chi^2\phi = \frac{hz^2}{w}\partial_z\left(\frac{h\phi'}{w}\right) \qquad (5.106\colon \phi)$$
$$k_2 w\phi^2\chi + h\partial_z(z^2 a_t'/w) = 0 \qquad (5.106\colon a_t)$$
$$\psi' = 0 \qquad (5.106\colon a_z)$$

And the metric junction conditions are

$$h^3\lambda' = \kappa\left(\chi^2 w^2\phi^2 + h^2\phi'^2\right) \qquad (5.107)$$
$$z^2h^2\lambda' = \kappa\left(M^2 w^2\phi^2 + z^4 a_t'^2\right) \qquad (5.108)$$

We use ϕ' to denote the z derivative of this fields in this section; there is no ambiguity due to the lack of t-dependence. As before,

$$\chi := q_3\, A_t|_\Sigma - q_2 a_t, \quad w := \sqrt{1 + h\lambda'^2}.$$

We have also simplified the equations above under the assumption that ϕ is non-trivial, which is what gives rise to $(5.106\colon a_z)$. There are two apparently independent conditions on the embedding field λ. This apparently extraneous conditions makes the system over-determined.

5.3.6 Further generalization

5.3.6.1 Charging the black hole

So far we have been considering a spacetime with a black hole that has a mass but no charge. Let us now consider a more general system. According to reference [106], a general rotationally symmetric, time-invariant black hole in asymptotically AdS spacetime in $2+1$ dimensions can be described by the metric

$$ds^2 = -N(r)^2 f(r)^2 \mathrm{d}t^2 + f(r)^{-2}\mathrm{d}r^2 + r^2\left(\mathrm{d}\theta + N^\theta(r)\mathrm{d}t^2\right), \qquad (5.109)$$

where $(t, r, \theta) \in \mathbb{R} \times (r_H, +\infty) \times [0, 2\pi)$ is a set of coordinates for some global chart Ψ on the spacetime manifold. r_H is the outer horizon position, given by the first

positive solution of $f(r)^2 = 0$, which we assume exists. This metric can be related to our usual BTZ metric ansatz (5.18) by taking the coordinate transformation

$$r = 1/z, \quad x = \theta, \tag{5.110}$$

and making the identifications

$$N(r)^2 = 1, \quad f(r)^2 = r^2 - 1/z_H^2, \quad N^\theta(r) = 0. \tag{5.111}$$

The x coordinate is allowed to range over all $\mathbb{R}$, and is identified as the half-space.

If we want to allow our black hole to have charge, however, reference [106] gives that $f(r)^2$ should be extended to

$$f(r)^2 = 1 - M_{\text{bh}} - \frac{1}{4}Q_{\text{bh}}^2 \log(r^2). \tag{5.112}$$

In this case, the metric in (t, z, x) coordinates takes the form

$$ds^2 = \frac{1}{z^2}\left(-H\mathrm{d}t^2 + \frac{1}{H}\mathrm{d}z^2 + \mathrm{d}x^2\right), \tag{5.113}$$

where

$$H(z) := 1 - M_{\text{bh}} z^2 - \frac{1}{4}Q_{\text{bh}}^2 z^2 \log(z^2). \tag{5.114}$$

We can see immediately that this reduces to the previous case when we set $Q_{\text{bh}} = 0$ and $M_{\text{bh}} = 1/z_H^2$.

5.3.6.2 Extending the metric ansatz

In (5.3.1) we explained how might try to perform backreaction in a way that is motivated by a "double embedding"' of the defect, through a function λ. In hindsight, we can see that this is merely an interpretation of the metric given by (5.84). We could generalize this by replacing ξ' by some general undetermined function $G_{zy}(z, y)$.

$$ds^2 = \frac{1}{z^2}\left(-h\mathrm{d}t^2 + \left(\frac{1}{h} + G_{zy}^2\right)\mathrm{d}z^2 + \mathrm{d}y^2 + 2G_{zy}\mathrm{d}z\,\mathrm{d}y\right). \tag{5.115}$$

Doing so would allow for a more rich y dependence in the metric tensor, so perhaps we would expect this to give consistent static solutions. And we can reduce this to the previous case if we set $G_{zy}(z, y) = \xi'(z, y)$.

Let us combine the generalizations and work through them together to see if a consistent solution can be obtained. We shall consider the metric tensor to be

$$ds^2 = g_{\mu\nu}\,\mathrm{d}y^\mu \otimes \mathrm{d}y^\nu := \frac{1}{z^2}\left(-H\mathrm{d}t^2 + \left(\frac{1}{H} + G_{zz}\right)\mathrm{d}z^2 + \mathrm{d}y^2 + 2G_{zy}\mathrm{d}z\,\mathrm{d}y\right). \tag{5.116}$$

We have added G_{zz} just to be even more general. This and other background metrics have been tried, but thus far all have either yielded an inconsistency or have implied $\phi \equiv 0$.

5.4 Discussion

Our aim was to include dynamical background fields involving a Yang-Mills term in the supergravity action in order to describe the propagation of strongly correlated electrons in the presence of impurities. However, In the probe limit case, the ansatz presented leads to an inconsistency in the AdS boundary behavior of the gauge field A_μ dual to the electron current. The second junction condition is also inconsistent near the boundary after substituting the solutions back to it. In the backreaction case, the defect field $\lambda(z)$ is over determined by the Israel junction condition. Thus the AdS dual model considered here was found to be too simple to yield the desired structures. In the next setp, including the backreaction on the full geometry is necessary and the AdS_2 subspace will be smeared out instead of $\delta(x)$.

6 Conclusion and Outlook

Chapters 3, 4 and 5 present the theme of this thesis–applying and generalizing AdS/CFT correspondence to models relevant for condensed matter physics. In chapter 3, by constructing dark solitons in holographic superfluids system with backreaction, the BCS and BEC limits of the BEC/BCS crossover are studied. Stress-energy tensor and grand potential are calculated in order to discuss the instability of the dark soliton. Chapter 4 dealt with metal-insulator phase transition induced by disorder. In chapter 5, we investigated the holographic Kondo model with a Maxwell term in both probe limit and considering backreaction.

6.1 Dark Solitons in Holographic Superfluids

Solitons in holographic superfluid systems in probe limit [14, 19, 20] were found very useful for studying BEC/BCS crossover. In particular, the standard quantization 3.2 for the scalar field corresponds to the BCS limit of the BEC/BCS crossover, while the alternative quantization corresponds to the BEC limit. The correspondences are obtained by comparing the charge depletion in the two quantization with the result from condensed matter physics [16]. In probe limit, the physical results are unreliable as temperature decreases, because the condensate grows stronger and the backreaction to the background becomes non-negligible. As such, we predicted that the quantity of depletion of the charge density would be closer to the result in [16]. But the final results are opposite which is unexpected. One of the reason may be the temperature we reach is still not low enough. As lowering the temperature, it gets more and more difficult to find the solution or needs more time for the relaxation to reach the given precision. Backreaction provides a new insight for studying BEC/BCS crossover. Currently, we only studied the two limits of BEC/BCS crossover. One of the following work is to study the crossover region with considering the backreaction.

The dark soliton in superfluid is unstable when it is subjected to transverse perturbation (the perturbation moves in the perpendicular direction of the soliton), and will be ended with vortex-anti-vortex pairs. There are two arguments for this phenomenon according to the signs of the effective mass and the surface tension of the soliton. Our holographic model shows that the effective mass is negative and the surface tension is positive for the holographic soliton.

6.2 Gravity Dual Phase Transitions

The original Hawking-Page phase transition [29] happens between the thermal AdS spacetime and AdS black hole spacetime. The name then is generalized to the case that a phase transition occurs between AdS balck hole and AdS soliton geometry. At a critical value of the black hole temperature, the free energies of them are the same which indicates a phase transition. Adding disorder to the system change their free energies, because kinetic energy brought by disorder will dissipate in spacetime with a black hole. Before going to the numerical calculation, we analytically constructed the AdS_{d+1} soliton geometry coupled with a scalar field. The geometry was perturbed on the boundary with marginally relevant quenched disorder. We then resorted to numerical calculation to obtain the precise geometry solutions of AdS soliton and AdS black hole, and obtained solutions with different strength of disorder. We write down the free energy by calculating the on-shell Euclidean action, and the next step is to calculate it numerically for the solutions we obtained.

6.3 Holographic Kondo Model

The resistivity has a $log\,(T)$ term in the original Kondo model, which contributes to forming the minimum in resistivity at very low temperature. How to obtain the same term in holographic Kondo model is an interesting topic. We added a dynamical background fields involving a Yang-Mills term in the supergravity action to the previous holographic model [34], which describes the propagation of strongly correlated electrons in the presence of impurities. With different ansatz, we calculated the solutions of the equations of motion in both probe limit and backreacted case. However, there is an inconsistency on the AdS boundary in the gauge field A_μ which is dual to the electron current. To address this issue, in the future we will improve this model by including the full backreaction of the matter fields considered here to the geometry and the metric.

7 Appendices

7.1 General Equations of Motion of the Combined Action in the Holographic Kondo model

In this section, we simply present the general equations of motion following from the action in 5.23, without fixing a particular gauge. These are

$$z\partial_t F_{tz} + hz\partial_x F_{zx} = -k_3\delta(x)\phi^2 h\chi_z \qquad (7.1\colon A_z)$$
$$h\partial_z(zF_{tz}) + z\partial_x F_{tx} = -k_3\delta(x)\phi^2\chi_t \qquad (7.1\colon A_t)$$
$$h\partial_z(hzF_{zx}) - z\partial_t F_{tx} = 0 \qquad (7.1\colon A_x)$$
$$h\partial_z(h\partial_z\phi) - \partial_t^2\phi = \left(M^2h/z^2 + h^2\chi_z^2 - \chi_t^2\right)\phi \qquad (7.1\colon \phi)$$
$$\partial_t\left(\chi_t\phi^2\right) - h\partial_z\left(h\chi_z\phi^2\right) = 0 \qquad (7.1\colon \psi)$$
$$h\partial_z\left(z^2 f_{tz}\right) = k_2\chi_t\phi^2 \qquad (7.1\colon a_t)$$
$$z^2\partial_t f_{tz} = k_2 h\chi_z\phi^2 \qquad (7.1\colon a_z)$$

where χ_m is given by (5.27).

7.2 Boundary Term, Gauss Theorem and Volume Element

Volume element:

$$\varepsilon_{a_1\cdots a} = \pm\sqrt{|g|}(e^1)_{a_1}\wedge\cdots(e^n)_{a_n}$$

where the $\pm$ corresponds to right hand and left hand coordinates respectfully.

Gauss theorem:

$$\int_{i(N)}(\nabla_a v^a)\varepsilon = \pm\int_{\partial N} v^a n_a\hat{\varepsilon} \quad \text{(take } +1 \text{ when } n^a n_a = +1\text{, take } -1 \text{ when } n^a n_a = -1\text{)}$$

$$\hat{\varepsilon}_{a_1\cdots a_{n-1}} = n^b \varepsilon_{ba_1\cdots a_{n-1}}, \tag{7.2}$$

here $n^b = (e_1)^b$ is the right hand unit vector[1].

Take $P_{21}$of [107] for example:

$$S = -\frac{1}{2}\int d^{d+1}x\sqrt{-g}(g^{mn}\partial_m\varphi\partial_n\varphi + m^2\varphi^2)$$

$$ds^2 = \frac{1}{r^2}(dr^2 + dx^\mu dx_\mu), \qquad \text{so that } g^{rr} = r^2,\ g^{\mu\nu} = r^2\eta^{\mu\nu}\ .$$

EOM:

$$\begin{aligned} 0 = \nabla_m\nabla^m\varphi - m^2\varphi &= \frac{1}{\sqrt{-g}}\partial_m(\sqrt{-g}g^{mn}\partial_n\varphi) - m^2\varphi \\ &= r^{d+1}\partial_r(r^{-d+1}\partial_r\varphi) + r^2\,\Box\,\varphi - m^2\varphi, \qquad \text{where } \Box = \partial_\mu\partial^\mu. \end{aligned}$$

The EOM puts the action on shell:

$$\begin{aligned} S = &-\frac{1}{2}\int d^{d+1}x[\partial_r(r^{-d+1}\varphi\partial_r\varphi) + \partial_\mu(r^{-d+1}\varphi\eta^{\mu\nu}\partial_\nu\varphi) \\ &- \varphi\partial_r(r^{-d+1}\partial_r\varphi) - r^{-d+1}\varphi\,\Box\,\varphi + r^{-d-1}m^2\varphi^2] \qquad (7.3) \\ = &-\frac{1}{2}\int d^{d+1}x[\partial_r(r^{-d+1}\varphi\partial_r\varphi) + \partial_\mu(r^{-d+1}\varphi\eta^{\mu\nu}\partial_\nu\varphi)] \qquad (7.4) \\ = &-\frac{1}{2}\int d^{d+1}x\partial_m(r^{-d-1}\varphi\partial^m\varphi). \qquad (7.5) \end{aligned}$$

The blue part has no boundary (only holographic direction has boundary), so the result is *zero*. We have the following left:

$$S = -\frac{1}{2}\int dr\partial_r(\int d^dx r^{-d+1}\varphi\partial_r\varphi). \tag{7.6}$$

So,

$$S = -\frac{1}{2}\int d^dx r^{-d+1}\varphi\partial_r\varphi\ |_{r=\epsilon}^{r=\infty} = \frac{1}{2}\int_{r=\epsilon} d^dx r^{-d}\varphi r\partial_r\varphi \tag{7.7}$$

Let us use the Gauss theorem to do this again. The integrand should be a divergence, so we keep the blue part first,

$$S = -\frac{1}{2}\int d^{d+1}x\partial_m(r^{-d-1}\varphi\partial^m\varphi). \tag{7.8}$$

The integrand is not the form $\partial_\mu v^\mu$ (in Euclidean space, $\nabla\cdot\vec{A} = \partial_\mu A^\mu$), but it is $\partial_\mu(fv^\mu)$ instead. The reason is that now we are working on curved spacetime, the integrand in Gauss theorem now is $\nabla_\mu A^\mu = \frac{1}{\sqrt{-g}}\partial_\mu(\sqrt{-g}A^\mu)$.

[1]Front Latin letters a, b etc. for the abstract indices, middle Latin letters m, n etc. for the whole spacetime indices, Greek letters μ, ν etc. for boundary indices.

Using the Gauss theorem in differential form, the measure in (7.8) should first be written in volume element:

$$\begin{aligned} S &= -\frac{1}{2}\int d^{d+1}x\partial_m(r^{-d-1}\varphi\partial^m\varphi) = -\frac{1}{2}\int d^{d+1}x\sqrt{-g}\frac{1}{\sqrt{-g}}\partial_m(\sqrt{-g}\varphi\partial^m\varphi) \\ &= -\frac{1}{2}\int d^{d+1}x\sqrt{-g}\nabla_m\nabla^m\varphi \\ &= -\frac{1}{2}\int \varepsilon\nabla_m\nabla^m\varphi \end{aligned} \tag{7.9}$$

$$\varepsilon = +\sqrt{|g|}dr\wedge d\vec{x} = d^{d+1}x\sqrt{-g}$$

"+" means we take the right hand basis.

$r = const$ defines the slice or boundary we are interested in. The boundary co-vector (without normalizing) is

$$\tilde{n}_\mu = \nabla_\mu(r - const) = (1, 0, \cdots 0),$$

which points inwards ($r \to \infty$ direction) on the conformal boundary $r = 0$. The corresponding outward unit co-vector is

$$n_a = (-\frac{1}{\sqrt{g^{rr}}}, 0, \cdots 0)\mid_{r=\epsilon}, n_a = (\frac{1}{\sqrt{g^{rr}}}, 0, \cdots 0)\mid_{r=\infty}.$$

and the "-" sign in the first co-vector is because we always take the unit vector n^m pointing outwards ($r \to 0$ is the integration outward direction near the conformal boundary in the case we are considering).

If $\{(e_\mu)^a\}$ is the right-hand orthonormalized basis, we take $(e_1)^a = -n^a \equiv N^a$(pointing to $r \to \infty$), because N^a is the right hand basis. Then,

$$\varepsilon_{a_1\cdots a_n} = (e^1\wedge\cdots\wedge e^n)_{a_1\cdots a_n} = \pm(-n_{a_1})\wedge(e^2\wedge\cdots\wedge e^n)_{a_2\cdots a_n},$$

which takes + when $n^a n_a = +1$, take− when $n^a n_a = -1$.

So we have

$$\varepsilon_{a_1\cdots a_n} = (e^1\wedge\cdots\wedge e^n)_{a_1\cdots a_n} = -n_{a_1}\wedge(e^2\wedge\cdots\wedge e^n)_{a_2\cdots a_n}$$

in our case.

The reduced volume element on the boundary is

$$\begin{aligned} \hat{\varepsilon}_{a_1\cdots a_{n-1}} &= (e^2\wedge\cdots\wedge e^n)_{a_1\cdots a_{n-1}} = N^b\varepsilon_{ba_1\cdots a_{n-1}} = (-n^b)\varepsilon_{ba_1\cdots a_{n-1}} \\ &= [-(g^{rr}n_r)(\partial_r)^b][\varepsilon_{ra_1\cdots a_{n-1}}(dr)_b] = r^2\frac{1}{r}d^dx\sqrt{-g} = \frac{1}{r^d}d^dx = d^dx\sqrt{|\gamma|} \end{aligned}$$

we use N^a other than n^a to contract ε, for $\varepsilon_{a_1\cdots a_n}$ is defined by the right hand basis.

So (7.9) becomes

$$S = -\frac{1}{2}\int_{r=\infty,\epsilon} \hat{\varepsilon} n_a \nabla^a \varphi = -\frac{1}{2}\int_{r=\infty,\epsilon} \hat{\varepsilon} n_r \partial^r \varphi = -\frac{1}{2}\int_{r=\infty,\epsilon} \hat{\varepsilon} n_r g^{rr} \partial_r \varphi$$
$$= -\frac{1}{2}[\int_{r=\epsilon} \frac{1}{r^d}\hat{d^d x}(-\frac{1}{\sqrt{g^{rr}}}) g^{rr}\partial_r\varphi + \int_{r=\infty} \frac{1}{r^d}\hat{d^d x}(+\frac{1}{\sqrt{g^{rr}}}) g^{rr}\partial_r\varphi] = \frac{1}{2}\int_{r=\epsilon} d^d x r^{-d}\varphi r \partial_r \varphi,$$

which coincides with (7.7).

7.3 Black Hole Temperature and Surface Gravity

Eq. (12.5.5) in $P_{331}$of [108]

$$\chi^b \nabla_b \chi_a = \kappa \chi_a \tag{7.10}$$

which is the geodesic equation in non-affine parameterization. The equation is evaluated on Killing horizon. If $\chi^a = (\partial_u)^a$ is affine with u the affine parameter, we can not use (7.10) to calculate surface gravity.

We now change to eq. (12.5.14)

$$\kappa^2 = -\frac{1}{2}(\nabla^a \chi^b)(\nabla_a \chi_b). \tag{7.11}$$

We are going to show that changing to affine parameter will still get the surface gravity by (7.11).

Assuming v is the non-affine parameter for Killing vector χ^a

$$\chi^a = (\partial_v)^a = \frac{\partial u}{\partial v}(\partial_u)^a = f(v)(\partial_u)^a \equiv f k^a,$$

where $k^a = (\partial_u)^a$ is the Killing vector with affine parameter u. Then,

$$\chi_a = (dv)_a = \frac{\partial v}{\partial u}(du)_a = \frac{1}{f}k_a.$$

So,

$$\kappa^2 = -\frac{1}{2}(\nabla^a \chi^b)(\nabla_a \chi_b)$$
$$= -\frac{1}{2}[f\cdot\frac{1}{f}(\nabla^a k^b)(\nabla_a k_b) + (\partial^a f)(\partial_a \frac{1}{f})k^b k_b + \frac{1}{f}(\partial^a f)k^b(\nabla_a k_b) + f(\nabla^a k^b)(\partial_a \frac{1}{f})k_b]$$
$$= -\frac{1}{2}(\nabla^a k^b)(\nabla_a k_b),$$

The blue part is *zereo*, for $k^a k_a = 0$ on horizon; the red part is obviously *zero*.

7.4 Conductivity

Consider a field theory containing an operator $\mathcal{O}$ with an external classical source ϕ_0. At the level of linear response theory the one-point function of $\mathcal{O}$ is linear in ϕ_0, and when expressed in Fourier space the proportionality constant is simply the thermal retarded correlator G^R of $\mathcal{O}$

$$\left\langle \mathscr{O}(\omega,\vec{k})\right\rangle_{QFT} = -G^R(\omega,\vec{k})\phi_0(\omega,\vec{k}), \tag{7.12}$$

where ω and $\vec{k}$ denote the frequency and spatial momentum respectively.

The low frequency limit defines a transport coefficient χ:

$$\chi = -\lim_{\omega\to 0}\lim_{\vec{k}\to 0}\frac{1}{\omega}\mathrm{Im}G^R(\omega,\vec{k}). \tag{7.13}$$

For the shear viscosity η, one takes $\mathcal{O} = T_{xy}$, the off-diagonal component of the stress tensor. For (DC) conductivity σ one takes $\mathcal{O} = J_z$, where J_z is a component of the electric current. According to AdS/CFT, in Euclidean signature, we have the relation between the dual theory generating function and the on-shell supergravity action:

$$\left\langle exp[-\int d^dx\phi_0\mathscr{O}]\right\rangle_{QFT} = e^{-S_{grav}[\phi(r\to\infty)=\phi_0]}. \tag{7.14}$$

Derivatives of the on-shell gravity action with respect to this boundary value ϕ_0 will give us correlators for $\mathcal{O}$. The one point function in the presence of source ϕ_0 can be written as:

$$\langle\mathscr{O}(x^\mu)\rangle_\phi = \lim_{r\to\infty} r^{\Delta-d}\Pi(r,x^\mu). \tag{7.15}$$

We have taken the fact that the derivative of an on-shell action with respect to the boundary value of a field is simply equal to the canonical momentum conjugate to the field, evaluated at the boundary. Taking a Fourier transform of (7.15) and comparing with (7.12), we obtain a simple formula for the thermal retarded correlator G_R:

$$G_R = -\lim_{r\to\infty} r^{\Delta-d}\frac{\Pi(r,k_\mu)}{\phi(r,k_\mu)}. \tag{7.16}$$

A bulk gauge field A_M with action

$$S = -\frac{1}{4g_{d+1}^2}\int d^{d+1}x\sqrt{-g}F_{MN}F^{MN}\int_{r\to\infty} d^dx\sqrt{-\gamma}A_\mu j^\mu \tag{7.17}$$

is now dual to a conserved current $\mathscr{J}^\mu$ in the boundary theory. j^μ is the conjugate momentum and the conductivity can be written as

$$\langle\mathscr{J}(k_\mu)\rangle_{QFT} = j^i(r\to\infty)(k_\mu) \equiv \sigma^{ij}(k_\mu)F_{jt}(r\to\infty). \tag{7.18}$$

so we get the AC conductivity (Kubo formula)

$$\sigma^{ij}(k_\mu) = -\frac{G_R^{ij}(k_\mu)}{i\omega}. \tag{7.19}$$

The DC conductivity is obtained by the zero momentum limit of above equations. Due to the rotational symmetry at zero momentum, we have

$$\sigma_{ij} = \sigma\delta_{ij} \tag{7.20}$$

Let us take a toy model for the above calculation. Considering the bulk gauge fields with action 7.17 propagating on the following dimensional background,

$$ds^2 = \frac{L^2}{z^2}(-f(z)dt^2 + \frac{dz^2}{f(z)} + d\boldsymbol{x}^2) \tag{7.21}$$

where $f(z) = 1 - (z/z_0)^d$ and the temperature of the CFT is $T = d/(4\pi z_0)$. Take the bulk gauge field proportional to $e^{-i\omega t + i\boldsymbol{q}\cdot\boldsymbol{x}}$, and $\boldsymbol{q} = 0$ is sufficient to get the conductivity from the Kubo formula. Gauge field component A_i satisfies the EOM

$$u^{d-3}[\frac{f(u)}{u^{d-3}}A_i'(u)]' + \frac{w^2}{f(u)}A_i(u) = 0,$$

Asymptotic analysis:

$$u \to 0 : A_i(u) = A_0 + A_1 u^{d-2}, \tag{7.22}$$

$$u \to 1 : A_i(u) = (1-u)^{-iw/d}a(u), \tag{7.23}$$

which is ingoing boundary condition for causality reason, and $a(u)$ is regular at $u = 1$. The current-current retarded correlation function is evaluated from the on-shell boundary action:

$$S = \lim_{u\to 0}\frac{(L/z_0)^{d-3}}{2g_{d+1}^2}\int\frac{d\omega}{2\pi}\frac{d^{d-1}}{(2\pi)^{d-1}}\frac{A_i'(\omega,u)A_i(-\omega,u)}{z_0 u^{d-3}} \tag{7.24}$$

Read off $C_{ij}^{ret}(\omega, \boldsymbol{q} = 0)$ from above, then the Kubo formula gives the DC conductivity,

$$\sigma = \frac{1}{g_{d+1}^2}(\frac{L}{z^0})^{d-3} \sim T^{d-3} \sim \omega^{d-3}. \tag{7.25}$$

Recall that $[g_{d+1}^2] = [Length]^{d-3}$ and $[\omega] = [T] =$ mass.

7.5 De Turck Method in Holography

The paper [109] investigates optical conductivity by adding a gravitational background lattice to the simplest holographic model. The de Turck method is used to get the backreacted static solution. The action and ansatz they take are

$$S = \frac{1}{16\pi G_N}\int d^4x\sqrt{-g}[R + \frac{6}{L^2} - \frac{1}{2}F^2 - 2\nabla_a\Phi\nabla^a\Phi - 4V(\Phi)], \tag{7.26}$$

$$ds^2 = \frac{L^2}{z^2}[-(1-z)P(z)Q_{tt}dt^2 + \frac{Q_{zz}dz^2}{P(z)(1-z)} + Q_{xx}(dx + z^2Q_{xz}dz)^2 + Q_{yy}dy^2]. \tag{7.27}$$

The key point is, for the Einstein equation $G_{ab} = 0$ where the Ricci scalar R has been replace from taking the trace of the equation, one should add the following new term

$$G^H_{ab} \equiv G_{ab} - \nabla_{(a}\xi_{b)} = 0, \tag{7.28}$$

where $\xi^a = g^{cd}[\Gamma^a_{cd}(g) - \bar{\Gamma}^a_{cd}(\bar{g})]$ and $\bar{\Gamma}^a_{cd}(\bar{g})$ is the Levi-Civita connection associated with a reference metric $\bar{g}$. The reference metric should be chose to have the same asymptotics and horizon structure as g.

Any solution to $G_{ab} = 0$ with $\xi = 0$ is the solution to $G^H_{ab} = 0$. However, the converse is not necessarily true. $\xi = 0$ should be checked. The repeated result we get are showed in Fig. 7.1.

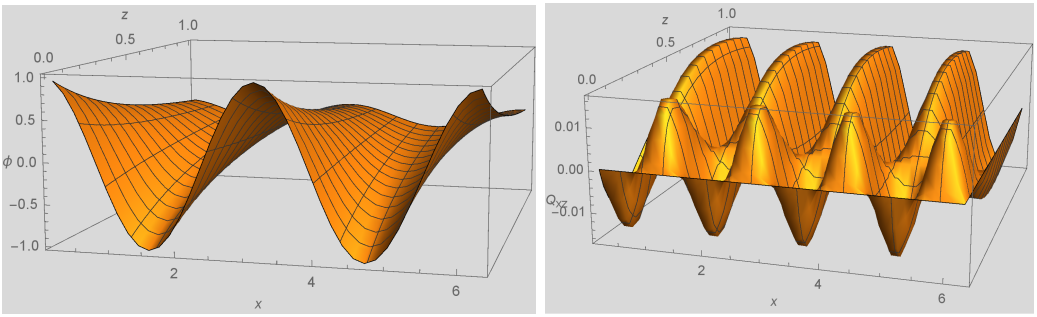

Figure 7.1: $z = 0$ is the conformal boundary. The left one is for Qxz, and the right one for ϕ.

7.6 Mathematica Codes for Chapter 3

In this section, we present our Mathematica code used for chapter 3. This work is mainly performed in collaboration with Zhongshan Xu. There are two parts of the

codes. The first part is to derive the equations of motion of the system. We then write down the Einstein-de Turck equations. By expanding the equations near the horizon, and requiring that the functions are regular here, we obtained the boundary conditions of the equations on the horizon side. Finally we linearize the Einstein-de Turck equations and the boundary conditions by the Newton-Kantorovich method (see [110] for the detail).

The second part starts from the "Preparation" in the code, where we first import the linearized equations. We then apply pseudo-spectral method for discretization. We add the boundary conditions on the conformal boundary side to the Einstein-de Turck equations, and give a constant function as the seed for iteration. The Newton relaxation method are used for finding solutions. At last we plot the results..

```
ClearAll["Global`*"];
SetDirectory[NotebookDirectory[]];
$Assumptions = 0 ≤ r ≤ 1;
L = 1;
Λ = -3;
m^2 = -2;
```

equations

metric、connection、curvature

```
vars = {t, r, x, y}; dim = Length[vars]; xa[μ_] := vars⟦μ⟧;
ds^2 = zh^2/(1 - r^2)^2 (-f[r] Q1[r, x] Dt[t]^2 + 4 r^2 Q2[r, x] Dt[r]^2/(zh^2 f[r]) +
      Q4[r, x] (Dt[x] - 2 r/zh Q3[r, x] Dt[r])^2 + Q5[r, x] Dt[y]^2);
coematrix = Coefficient[ds^2, Dt[vars] ⊗ Dt[vars]];
metric = Simplify[1/2 (coematrix + DiagonalMatrix[Diagonal[coematrix]])];
gbb[μ_, ν_] := metric⟦μ, ν⟧;
invmetric = Simplify[Inverse[metric]];
gaa[μ_, ν_] := invmetric⟦μ, ν⟧;
g = Simplify[Det[metric]];
Γabb[λ_, μ_, ν_] :=
  Simplify[Sum[1/2 gaa[λ, σ] (-∂_xa[σ] gbb[μ, ν] + ∂_xa[μ] gbb[ν, σ] + ∂_xa[ν] gbb[σ, μ]), {σ, 1, dim}]];
refΓabb[λ_, μ_, ν_] := With[{rule = {Q1[r, x] → 1, Q2[r, x] → 1, Q3[r, x] → 0,
      Q4[r, x] → 1, Q5[r, x] → 1, _(-,-)[r, x] → 0}}, Γabb[λ, μ, ν] /. rule];
Rabbb[ρ_, σ_, μ_, ν_] := Simplify[∂_xa[μ] Γabb[ρ, ν, σ] - ∂_xa[ν] Γabb[ρ, μ, σ] +
    Sum[(Γabb[ρ, μ, λ] Γabb[λ, ν, σ] - Γabb[ρ, ν, λ] Γabb[λ, μ, σ]), {λ, 1, dim}]];
Rbb[σ_, ν_] := Simplify[Sum[Rabbb[ρ, σ, ρ, ν], {ρ, 1, dim}]];
Array[refΓabb, {dim, dim, dim}] // MatrixForm
```

equations of scalar field and maxwell field

```
(*ansatz for scalar field*)
Φ = Φstar = (1 - r^2)/zh Q6[r, x]; V = m^2 (Φ Φstar);
(*ansatz for maxwell field*)
A = {mu r^2 Q7[r, x], 0, 0, 0};
Ab[μ_] := A[[μ]]; Aa[ν_] := Sum[gaa[σ, ν] Ab[σ], {σ, 1, dim}];
DΦb[μ_] := ∂_xa[μ] Φ - i Ab[μ] Φ;
DΦstarb[μ_] := ∂_xa[μ] Φstar + i Ab[μ] Φstar;

Fbb[μ_, ν_] := ∂_xa[μ] Ab[ν] - ∂_xa[ν] Ab[μ];
Fba[μ_, ν_] := Sum[gaa[ν, σ] Fbb[μ, σ], {σ, 1, dim}];
Faa[μ_, ν_] := Sum[gaa[μ, σ] Fba[σ, ν], {σ, 1, dim}];
Maxwella[ν_] :=
  1/Sqrt[-g] Sum[∂_xa[μ] (Sqrt[-g] Faa[μ, ν]), {μ, 1, dim}] - i Sum[gaa[ν, σ] (Φstar DΦb[σ] - Φ DΦstarb[σ]), {σ, 1, dim}];
Scalar = Simplify[1/Sqrt[-g] Sum[(∂_xa[μ] # - i Ab[μ] # &)[Sqrt[-g] Sum[gaa[μ, ν] DΦb[ν], {ν, 1, dim}]], {μ, 1, dim}] - m^2 Φ];
eq1 = Simplify[Scalar];
eq2 = DeleteDuplicates[DeleteCases[0][Simplify[Array[Maxwella, {dim}]]]];
```

equations of Einstein and DeTurck

```
(*DeTurck Vector*)
ξa[λ_] := Simplify[Sum[Sum[gaa[μ, ν] (Γabb[λ, μ, ν] - refΓabb[λ, μ, ν]), {ν, 1, dim}], {μ, 1, dim}]];
ξb[ν_] := Simplify[Sum[gbb[μ, ν] ξa[μ], {μ, 1, dim}]];
Dξbb[μ_, ν_] := ∂_xa[μ] ξb[ν] - Sum[Γabb[σ, μ, ν] ξb[σ], {σ, 1, dim}];
Einsteinbb[μ_, ν_] := Rbb[μ, ν] - Λ gbb[μ, ν] -
  e (1/2 (DΦb[μ] DΦstarb[ν] + DΦb[ν] DΦstarb[μ]) + 1/2 gbb[μ, ν] V
    + 1/2 Sum[Fbb[μ, σ] Fba[ν, σ], {σ, 1, dim}] - gbb[μ, ν]/8 Sum[Sum[Fbb[ρ, σ] Faa[ρ, σ], {σ, 1, dim}], {ρ, 1, dim}]);
DeTurckbb[μ_, ν_] := Einsteinbb[μ, ν] - 1/2 (Dξbb[μ, ν] + Dξbb[ν, μ]);
eq3 = DeleteDuplicates[
   DeleteCases[0][Flatten[Simplify[Array[DeTurckbb, {dim, dim}]]]]];
```

reduction of DeTurck equations

```
Table[{Coefficient[eq3[[i]], {Q1^(2,0)[r, x], Q2^(2,0)[r, x],
      Q3^(2,0)[r, x], Q4^(2,0)[r, x], Q5^(2,0)[r, x]}] // Simplify,
   Coefficient[eq3[[i]], {Q1^(0,2)[r, x], Q2^(0,2)[r, x], Q3^(0,2)[r, x],
      Q4^(0,2)[r, x], Q5^(0,2)[r, x]}] // Simplify}, {i, 5}] // MatrixForm
```

```
eq3[[3]] = eq3[[3]] + (2 r)/zh Q3[r, x] eq3[[4]];
eq3[[2]] = eq3[[2]] - (4 r^2)/zh^2 Q3[r, x]^2 eq3[[4]] + (4 r)/zh Q3[r, x] eq3[[3]];
Table[{Coefficient[eq3[[i]], {Q1^(2,0)[r, x], Q2^(2,0)[r, x],
      Q3^(2,0)[r, x], Q4^(2,0)[r, x], Q5^(2,0)[r, x]}] // Simplify,
   Coefficient[eq3[[i]], {Q1^(0,2)[r, x], Q2^(0,2)[r, x], Q3^(0,2)[r, x],
      Q4^(0,2)[r, x], Q5^(0,2)[r, x]}] // Simplify}, {i, 5}] // MatrixForm
```

final equations

```
f[r_] := 1 - (1 + (e mu^2)/(4 zh^2)) (1 - r^2)^3 + (e mu^2)/(4 zh^2) (1 - r^2)^4;
nonfactor[eqs_] := Block[{First, Last, FactorList},
   SetAttributes[{First, Last, FactorList}, Listable];
   Simplify[First[Last[FactorList[eqs]]]]];
check = Simplify[Sum[ξa[σ] ξb[σ], {σ, 1, dim}]];
eom = Simplify[Flatten[{eq3, eq1, eq2}]];
(*extract the nontrivial factor of eqs for solving*)
eqs = Simplify[nonfactor[eom]];
```

conditions

regular conditions

```
subeqs = eqs /. {h_^(i_,j_)[r, x] :> ∂_{r,i},{x,j} (Series[h[r, x], {r, 0, 3}]),
    h_[r, x] :> Series[h[r, x], {r, 0, 3}]};
```

```
SeriesCoefficient[subeqs[[1]], {r, 0, 0}] // Simplify
rcs[1] = Q1[0, x] - Q2[0, x];
rule =
  {Q2[0, x] → Q1[0, x], Q2^(0,1)[0, x] → Q1^(0,1)[0, x] , Q2^(0,2)[0, x] → Q1^(0,2)[0, x]};
```

```
SeriesCoefficient[subeqs[[2]], {r, 0, 0}] /. rule // Simplify
rcs[2] = SeriesCoefficient[subeqs[[2]], {r, 0, 1}] /. rule // Simplify
AppendTo[rule, Q2^(1,0)[0, x] → 2 Q1^(1,0)[0, x]]
```

```
SeriesCoefficient[subeqs[[3]], {r, 0, 0}] /. rule // Simplify
rcs[3] = SeriesCoefficient[subeqs[[3]], {r, 0, 1}] /. rule // Simplify
```

```
rcs[4] = SeriesCoefficient[subeqs[[4]], {r, 0, 0}] /. rule // Simplify
AppendTo[rule, Q4^(1,0)[0, x] → 0]
```

```
rcs[5] = SeriesCoefficient[subeqs[[5]], {r, 0, 0}] /. rule // Simplify
AppendTo[rule, Q5^(1,0)[0, x] → 0]
```

```
rcs[6] = SeriesCoefficient[subeqs[[6]], {r, 0, 0}] /. rule // Simplify
AppendTo[rule, Q6^(1,0)[0, x] → 0]
```

```
rcs[7] = SeriesCoefficient[subeqs[[7]], {r, 0, 0}] /. rule // Simplify
```

final conditions

```
bcsr1 = {Q1[r, x] - 1, Q2[r, x] - 1, Q3[r, x],
    Q4[r, x] - 1, Q5[r, x] - 1, Q6^(1,0)[r, x], Q7[r, x] - 1};
bcsr0 = {Q1[r, x] - Q2[r, x], Q2^(1,0)[r, x], Q3^(1,0)[r, x],
    Q4^(1,0)[r, x], Q5^(1,0)[r, x], Q6^(1,0)[r, x], Q7^(1,0)[r, x]};
```

linearization

```
{δ[Q1], δ[Q2], δ[Q3], δ[Q4], δ[Q5], δ[Q6], δ[Q7]} =
  {δQ1, δQ2, δQ3, δQ4, δQ5, δQ6, δQ7};
δQ = {δQ1[r, x], δQ2[r, x], δQ3[r, x], δQ4[r, x],
    δQ5[r, x], δQ6[r, x], δQ7[r, x]};
linearize[eqs_, {x_, y_}] := Module[
    {rule1 = {h_^(i_,j_)[x, y] → h^(i,j)[x, y] + ϵ δ[h]^(i,j)[x, y],
        h_[x, y] → h[x, y] + ϵ δ[h][x, y]},
     rule2 = {h_^(i_,j_)[x, y] /; StringPart[ToString[h], 1] == "δ" → d_(i,j) h[x, y],
        h_[x, y] /; StringPart[ToString[h], 1] == "δ" → eye h[x, y]}, δeqs},
    δeqs = Simplify[∂_ϵ (eqs /. rule1) /. ϵ → 0] ;
    Simplify[δeqs /. rule2]];
δeqs = Simplify[linearize[eqs, {r, x}]];
δbcsr1 = Simplify[linearize[bcsr1, {r, x}]];
δbcsr0 = Simplify[linearize[bcsr0, {r, x}]];
jacobi = Simplify[Collect[Normal[CoefficientArrays[δeqs, δQ][[2]]], eye]];
jacobir1 = Simplify[Collect[Normal[CoefficientArrays[δbcsr1, δQ][[2]]], eye]];
jacobir0 = Simplify[Collect[Normal[CoefficientArrays[δbcsr0, δQ][[2]]], eye]];
```

export

```
jacobi = Replace[jacobi, 0 → zero, 2];
jacobir1 = Replace[jacobir1, 0 → zero, 2];
jacobir0 = Replace[jacobir0, 0 → zero, 2];
eqs >> eqs.m;
bcsr1 >> bcsr1.m;
bcsr0 >> bcsr0.m;
jacobi >> jacobi.m;
jacobir1 >> jacobir1.m;
jacobir0 >> jacobir0.m;
check >> check.m;
```

Preparation

```
ClearAll["Global`*"]
SetDirectory[NotebookDirectory[]];
eqs = << eqs.m;
bcsr1 = << bcsr1.m;
bcsr0 = << bcsr0.m;
jacobi = << jacobi.m;
jacobir1 = << jacobir1.m;
jacobir0 = << jacobir0.m;
check = << check.m;
(*Parameters*)
L = 1; Lr = 1.0; Lx = 20.0; mu = 5.6;
e = 0.25; tc = 0.2099; tau = 0.5; t = tau tc; T = t mu;
zh = 1/6 (4 π T + Sqrt[16 π^2 T^2 + 3 e mu^2]);
Nr = 30; Nx = 100; Nrx = Nr * Nx;
Eye = IdentityMatrix[Nrx]; Zero = ConstantArray[0, {Nrx, Nrx}];
(*Chebshev*)
chebp[n_] := Table[Cos[i π/(n - 1.0)], {i, 0, n - 1}];
cheb[n_, l_] := Module[{x, c, sdm}, x = chebp[n];
   c = Table[If[i == 1 || i == n, 2.0, 1.0], {i, 1, n}];
   sdm = 2/l Table[If[i ≠ j, c[[i]]/c[[j]] (-1)^(i+j)/(x[[i]] - x[[j]]), 0], {i, 1, n}, {j, 1, n}];
   sdm -= DiagonalMatrix[Total[sdm, {2}]]];
dr = cheb[Nr, Lr];
drs[0] = IdentityMatrix[Nr]; drs[1] = dr; drs[2] = dr.dr;
gridr = 0.5 (chebp[Nr] + 1);
rr = gridr⊗ConstantArray[1, Nx];
R = Flatten[rr];
(*boundary index of holographic coordinate*)
r1 = Flatten[Position[R, n_ /; n == gridr[[1]]]];
r0 = Flatten[Position[R, n_ /; n == gridr[[-1]]]];
rb = Join[r0, r1];
(*Fourier*)
fourier[n_, l_] := π/l Table[
    If[i == j, 0, (-1)^(i-j) If[Mod[n, 2] == 0, Cot[π * (i - j)/n], Csc[π * (i - j)/n]]],
    {i, 1, n}, {j, 1, n}];
dx = fourier[Nx, Lx];
dxs[0] = IdentityMatrix[Nx]; dxs[1] = dx; dxs[2] = dx.dx;
gridx = Lx/Nx Range[-Nx/2, Nx/2 - 1];
xx = ConstantArray[1, Nr]⊗gridx;
```

```
X = Flatten[xx];
(*derivative matrix after vectorization*)
Do[If[i + j ≤ 2, ds[i, j] = KroneckerProduct[drs[i], dxs[j]]],
  {i, 0, 2}, {j, 0, 2}];
```

Solution

initialization

```
SetDirectory["data"];
last = 1;
If[last == 1,
 (*last outcome*)
 q[1] = s[Q1] = << Q1.m;
 q[2] = s[Q2] = << Q2.m;
 q[3] = s[Q3] = << Q3.m;
 q[4] = s[Q4] = << Q4.m;
 q[5] = s[Q5] = << Q5.m;
 q[6] = s[Q6] = << Q6.m;
 q[7] = s[Q7] = << Q7.m;,
 (*seed*)
 q[1] = s[Q1] = ConstantArray[1, Nrx];
 q[2] = s[Q2] = ConstantArray[1, Nrx];
 q[3] = s[Q3] = ConstantArray[0, Nrx];
 q[4] = s[Q4] = ConstantArray[1, Nrx];
 q[5] = s[Q5] = ConstantArray[1, Nrx];
 q[6] = s[Q6] = 4 Tanh[X - Lx/4] Tanh[-X - Lx/4];
 q[7] = s[Q7] = ConstantArray[0.5, Nrx];]

(*reshape*)
Do[req[i] = ArrayReshape[q[i], {Nr, Nx}], {i, 7}];
(*interpolate function*)
Do[interfunq[i] = ListInterpolation[
    Append[req[i]^T, req[i][[;; , 1]]]^T, {gridr, Append[gridx, 0.5 Lx]}], {i, 7}];
```

interpolation

```
(*resample*)
Do[q[k] = Flatten[Table[interfunq[k][gridr[[i]], gridx[[j]]], {i, Nr}, {j, Nx}]],
  {k, 7}];
{s[Q1], s[Q2], s[Q3], s[Q4], s[Q5], s[Q6], s[Q7]} =
  {q[1], q[2], q[3], q[4], q[5], q[6], q[7]};
```

iteration

```
seed = Join[q[1], q[2], q[3], q[4], q[5], q[6], q[7]];
length = Length[seed];
eps = 10^-10; k = 0; kmax = 9; done = 1; rmssollist = {};
Monitor[While[done == 1 && k < kmax,
  diseqs = eqs /. {h_^(i_,j_)[r, x] → ds[i, j].s[h], h_[r, x] → s[h], r → R};
  disbcsr1 =
   bcsr1 /. {h_^(i_,j_)[r, x] :→ (ds[i, j][[r1]]).s[h], h_[r, x] :→ s[h][[r1]]};
  disbcsr0 = bcsr0 /. {h_^(i_,j_)[r, x] :→ (ds[i, j][[r0]]).s[h],
     h_[r, x] :→ s[h][[r0]]};
  diseqs[[ ;; , r1]] = disbcsr1;
  diseqs[[ ;; , r0]] = disbcsr0;
  b = -Flatten[diseqs];

  J = jacobi /. {h_^(i_,j_)[r, x] → ds[i, j].s[h],
     h_[r, x] → s[h], d_i_,j_ → ds[i, j], eye → Eye, zero → Zero, r → R};
  Jr1 = jacobir1 /. {h_^(i_,j_)[r, x] :→ (ds[i, j][[r1]]).s[h], h_[r, x] :→ s[h][[r1]],
     d_i_,j_ :→ ds[i, j][[r1]], eye :→ Eye[[r1]], zero :→ Zero[[r1]]};
  Jr0 = jacobir0 /. {h_^(i_,j_)[r, x] :→ (ds[i, j][[r0]]).s[h], h_[r, x] :→ s[h][[r0]],
     d_i_,j_ :→ ds[i, j][[r0]], eye :→ Eye[[r0]], zero :→ Zero[[r0]]};
  J[[ ;; ,  ;; , r1]] = Jr1;
  J[[ ;; ,  ;; , r0]] = Jr0;
  J = ArrayFlatten[J];
  sol = LinearSolve[J, b];
  seed += sol; k++;
  reseed = ArrayReshape[seed, {7, Nrx}];
  q[1] = s[Q1] = reseed[[1]];
  q[2] = s[Q2] = reseed[[2]];
  q[3] = s[Q3] = reseed[[3]];
  q[4] = s[Q4] = reseed[[4]];
  q[5] = s[Q5] = reseed[[5]];
  q[6] = s[Q6] = reseed[[6]];
  q[7] = s[Q7] = reseed[[7]];
  rmssol = Sqrt[Total[sol^2]/length];
  AppendTo[rmssollist, rmssol];
  If[rmssol ≤ eps, done = 0];
 ], rmssollist]
Print[rmssollist];
```

data and visualization

```
gridr = Reverse[gridr];
Do[solq[i] = ArrayReshape[q[i], {Nr, Nx}], {i, 7}];
```

```
orderp = (solq[6][[1]]);
density = mu zh (1 + 1/2 (dr[[1]].solq[7]));
ListPlot3D[
 Flatten[Table[{gridr[[i]], gridx[[j]], solq[6][[i, j]]}, {i, Nr}, {j, Nx}], 1],
 PlotRange → All, LabelStyle →
  Directive[Black, FontFamily → "Times New Roman", Black, 12], AxesLabel →
  {Style["r", Italic, 14], Style["x", Italic, 14], Style["Q6", Italic, 14]}]
ListPlot3D[Flatten[Table[{gridr[[i]], gridx[[j]], solq[7][[i, j]]},
   {i, Nr}, {j, Nx}], 1], PlotRange → All, LabelStyle →
  Directive[Black, FontFamily → "Times New Roman", Black, 12], AxesLabel →
  {Style["r", Italic, 14], Style["x", Italic, 14], Style["Q7", Italic, 14]}]
ListPlot3D[Flatten[Table[{gridr[[i]], gridx[[j]], solq[1][[i, j]]},
   {i, Nr}, {j, Nx}], 1], PlotRange → All, LabelStyle →
  Directive[Black, FontFamily → "Times New Roman", Black, 12], AxesLabel →
  {Style["r", Italic, 14], Style["x", Italic, 14], Style["Q1", Italic, 14]}]
ListPlot3D[Flatten[Table[{gridr[[i]], gridx[[j]], solq[2][[i, j]]},
   {i, Nr}, {j, Nx}], 1], PlotRange → All, LabelStyle →
  Directive[Black, FontFamily → "Times New Roman", Black, 12], AxesLabel →
  {Style["r", Italic, 14], Style["x", Italic, 14], Style["Q2", Italic, 14]}]
ListPlot3D[Flatten[Table[{gridr[[i]], gridx[[j]], solq[3][[i, j]]},
   {i, Nr}, {j, Nx}], 1], PlotRange → All, LabelStyle →
  Directive[Black, FontFamily → "Times New Roman", Black, 12], AxesLabel →
  {Style["r", Italic, 14], Style["x", Italic, 14], Style["Q3", Italic, 14]}]
ListPlot3D[Flatten[Table[{gridr[[i]], gridx[[j]], solq[4][[i, j]]},
   {i, Nr}, {j, Nx}], 1], PlotRange → All, LabelStyle →
  Directive[Black, FontFamily → "Times New Roman", Black, 12], AxesLabel →
  {Style["r", Italic, 14], Style["x", Italic, 14], Style["Q4", Italic, 14]}]
ListPlot3D[Flatten[Table[{gridr[[i]], gridx[[j]], solq[5][[i, j]]},
   {i, Nr}, {j, Nx}], 1], PlotRange → All, LabelStyle →
  Directive[Black, FontFamily → "Times New Roman", Black, 12], AxesLabel →
  {Style["r", Italic, 14], Style["x", Italic, 14], Style["Q5", Italic, 14]}]
ListPlot[Table[{gridx[[i]], orderp[[i]]}, {i, 1, Nx}], PlotRange → All]
ListPlot[Table[{gridx[[i]], density[[i]]}, {i, 1, Nx}], PlotRange → All]
fitorderp =
 FindFit[Table[{gridx[[i]] + Lx/4, orderp[[i]]}, {i, Nx/2}], a Tanh[x/ξ], {a, ξ}, x]
fitdensity = FindFit[Table[{gridx[[i]] + Lx/4, density[[i]]}, {i, Nx/2}],
  -a Sech[x/ξ]^2 + c, {a, ξ, c}, x]
ListPlot[Table[{gridx[[i]] + Lx/4, 1/a orderp[[i]] /. fitorderp}, {i, Nx/2}]]
ListPlot[Table[{gridx[[i]] + Lx/4, 1/c density[[i]] /. fitdensity}, {i, Nx/2}]]
Show[ListPlot[Table[{gridx[[i]] + Lx/4, orderp[[i]]}, {i, Nx/2}]],
```

```
Plot[a Tanh[x/ξ] /. fitorderp, {x, -Lx/4, Lx/4}]]
Show[ListPlot[Table[{gridx[[i]] + Lx/4, density[[i]]}, {i, Nx/2}], PlotRange → All],
 Plot[(-a Sech[x/ξ]^2 + c) /. fitdensity, {x, -Lx/4, Lx/4}], PlotRange → All]
```

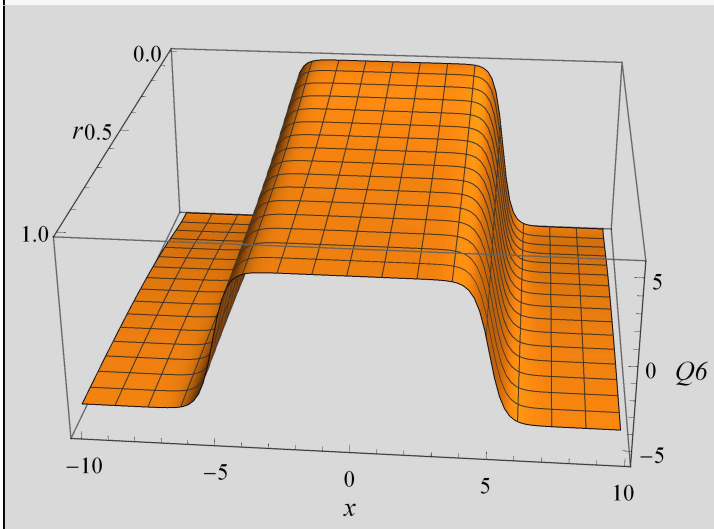

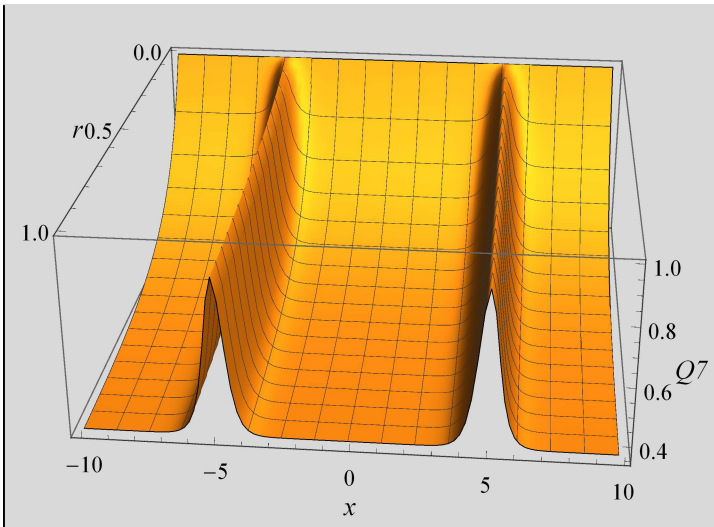

7.7 C Codes for Chapter 4

In chapter 4, we restrict the disorder to the x spatial direction, which is periodic. In order to mimic a chaotic disorder, we need at least (around) 50 modes in (4.42) in x direction. The lowest frequency of these modes is then $k_1 = 1/50$, so the largest period for all $\cos(k_n x)$ is 100π. We then need (around) 500 points to discretize x direction in order to have a good fit for the highest frequency mode $\cos(x)$. Even though each function only has two variables, the size of the Jacobi matrix for the linearized Einstein-de Turck equations is huge. So we only use Mathematica to derive the Einstein-de Turck equations as we did in section (7.6). We then resort to C language for the numerical calculation, which reduces the memory usage and running time dramatically. The C codes for chapter 4 include two parts. The fist part is the main code, which includes a file called "eqsandjacobi.h" at line 36. The second part is the file "eqsandjacobi.h" which contains the equations and Jacobi matrix. These codes are performed in collaboration with Florian Goth.

```cpp
/*For this project, we have 6 equations with 6 functions. Each function has two arguments 'r' and 'x'. 1-r^2=z, so the boundary place is r=1*/

#include <iostream>
#include <cstdlib>
#include <cstdio>
#include <netcdf.h>
#include <cstring>
#include <string>
#include <time.h>
#include <fstream>
#define MAXBUFSIZE  ((int) 1e6)// This will be used in readdata function
//#include <cblas.
#include <random>
#include <cmath>
//#define EIGEN_USE_BLAS
#include <eigen3/Eigen/QR>
#include <eigen3/Eigen/Dense>
#include <eigen3/unsupported/Eigen/KroneckerProduct>
using namespace std;
using namespace Eigen;


//global variables, are automatically set to zero if no specified initialization, while arbitrary value for local variables.
constexpr double plusy = 0.1*4*M_PI/3; // yplus will be used in "eqsandjacobi.h"
constexpr double plusysq = pow(plusy, 2);
constexpr double plusy4 = pow(plusy, 4);
constexpr double plusy6 = pow(plusy, 6);

//template <typename DerivedA>
//inline ArrayXXd arraypdt(const ArrayBase<DerivedA> & , const MatrixXd & ); //n dimensional array multiplied by nxn dimensional array
template <typename DerivedA, typename DerivedB>
inline ArrayXXd arraypdt(const ArrayBase<DerivedA> & , const ArrayBase<DerivedB> & );

template <typename Derived>
inline ArrayXXd arraypdt_idty(const ArrayBase<Derived> & ); //change n dimensional array to n by n dimensonal diagonal array

#include "eqsandjacobi.h"
MatrixXd fourier(int, double);//Fourier derivative matrix

ArrayXd chebp(int);//cheb grids

MatrixXd cheb(int, double);//chebsev derivative matrix

//Export the position of specified value
template <typename Derived>
ArrayXd position(const ArrayBase<Derived> & , double );

//netcdf: write data
template <typename Derived>
void writenetcdf(string, const DenseBase<Derived> &, double *);

//netcdf: read data from file and write it to a matrix
void readwrite(string , double* );

int main(int argc, char *argv[])
{
    clock_t t1,t2;
    t1=clock();

    int nr=atoi(argv[1]);//grid number in 'r' direction
    int nx=atoi(argv[2]);//grid number in 'x' direction
    int n=nr*nx;
    int nnx=n-nx;
    int le=20; //largest iteration steps
    double lr=1.0; //length of 'r' direction
    double lx=2*M_PI;//length of 'x' direction
    double epsilon=1.e-6;//solution precision

    ArrayXd* grid;
```

```
70        grid = new ArrayXd [2];
71
72        grid[0]=(lx/nx)*(ArrayXd::LinSpaced(nx,-nx/2.,(nx/2.)-1));//x grids
73        grid[1]=(chebp(nr)+1.)/2;//r grids
74
75        double k0=1., v=0.5;
76
77        int nm=25;
78        random_device rd;  //Will be used to obtain a seed for the random number engine
79        mt19937 gen(rd()); //Standard mersenne_twister_engine seeded with rd()
80        uniform_real_distribution<> rand(0., 2.0*M_PI);
81
82        ArrayXd phi1(nx);
83        for (int i=1; i<nx; ++i)
84            phi1+=cos(i*k0/nm*grid[0] + rand(gen));
85        phi1 = (4*v*k0/nm)*phi1;
86
87        ArrayXd vr=kroneckerProduct(grid[1].matrix(),
          MatrixXd::Constant(nx,1,1));//Flattening r. Kronecker product of two arrays
          yields array of one dimensions.
88
89        ArrayXd* vx;
90        vx = new ArrayXd [1];
91        vx[0]
          =kroneckerProduct(MatrixXd::Constant(nr,1,1),grid[0].matrix());//Flattening x.
92
93        delete[] grid;
94
95        MatrixXd* dxs;
96        dxs = new MatrixXd [2];
97        dxs[0] = fourier(nx, lx);
98        dxs[1] = (dxs[0])*(dxs[0]);
99
100       MatrixXd* drs;
101       drs = new MatrixXd [2];
102       drs[0] = cheb(nr,lr);
103       drs[1] = (drs[0])*(drs[0]);
104       //donot need to change right side to .array(), for do1 has been declared as
          array, assign matrix to array is valid and vice verse.
105       Matrix<double,Dynamic,Dynamic,RowMajor>
          d01=kroneckerProduct(MatrixXd::Identity(nr,nr), dxs[0]);
106       Matrix<double,Dynamic,Dynamic,RowMajor>
          d02=kroneckerProduct(MatrixXd::Identity(nr,nr), dxs[1]);
107       Matrix<double,Dynamic,Dynamic,RowMajor> d10=kroneckerProduct(drs[0],
          MatrixXd::Identity(nx,nx));//derivative in r direction
108       Matrix<double,Dynamic,Dynamic,RowMajor> d11=kroneckerProduct(drs[0], dxs[0]);
109       Matrix<double,Dynamic,Dynamic,RowMajor> d20=kroneckerProduct(drs[1],
          MatrixXd::Identity(nx,nx));
110
111
112
113       delete[] dxs;
114       delete[] drs;
115       ArrayXd Q1 = ArrayXd::Constant(n,1);
116       ArrayXd Q2 = ArrayXd::Constant(n,1);
117       ArrayXd Q3 = ArrayXd::Zero(n,1);
118       ArrayXd Q4 = ArrayXd::Constant(n,1);
119       ArrayXd Q5 = ArrayXd::Constant(n,1);
120       ArrayXd phi = 0.1*cos(k0*vx[0]);
121       delete[] vx;
122
123
124       int k=0; ArrayXd nor;
125
126       do
127       {
128           VectorXd b=eqs(Q1,Q2,Q3,Q4,Q5,phi,d01,d02,d10,d11,d20,vr);
129
130           b.segment(0,nx)=Q1.segment(0,nx)-1;
              b.segment(nnx,nx)=Q1.segment(nnx,nx)-Q2.segment(nnx,nx);
131           b.segment(n,nx)=Q2.segment(0,nx)-1;
              b.segment(2*n-nx,nx)=d10.block(nnx,0,nx,n)*Q2.matrix();
132           b.segment(2*n,nx)=Q3.segment(0,nx);
```

```
            b.segment(3*n-nx,nx)=d10.block(nnx,0,nx,n)*Q3.matrix();
133         b.segment(3*n,nx)=Q4.segment(0,nx)-1;
            b.segment(4*n-nx,nx)=d10.block(nnx,0,nx,n)*Q4.matrix();
134         b.segment(4*n,nx)=Q5.segment(0,nx)-1;
            b.segment(5*n-nx,nx)=d10.block(nnx,0,nx,n)*Q5.matrix();
135         b.segment(5*n,nx)=phi.segment(0,nx)-phi1.segment(0,nx);
            b.segment(6*n-nx,nx)=d10.block(nnx,0,nx,n)*phi.matrix();
136
137         //The locally dynamic eigen variables will be released out of this scope
138         {
139             MatrixXd Jr(3 * (nnx), 3 * (nnx)); // Jr: reduced Jacobi
140             MatrixXd Jt(3 * (nnx), 3 * (nnx)); // Jt: temporary data of reduced Jacobi
141
142             VectorXd temp(3 * (nnx));
143
144             {
145 #pragma omp sections
146                 {
147 #pragma omp section
148                     {
149                 //The Jacobi matrix is divided into 4 by 4 blocks here. From left to
                    right and top to bottom there are A, B, C and D blocks.
150                 //Jr is the J11 or A block of REDUCED Jacobi Matrix
151                 MatrixXd J = jacobi(Q1, Q2, Q3, Q4, Q5, phi, d01, d02, d10, d11,
                    d20, vr, 11);
152                 J.block(nnx, 0, nx, n) = MatrixXd::Identity(n, n).block(nnx, 0, nx,
                    n);
153                 Jr.block(0, 0, nnx, nnx) = J.block(nx, nx, nnx, nnx);
154                 temp.segment(0, nnx) = b.segment(nx, nnx) - J.block(nx, 0, nnx, nx)
                    * b.segment(0, nx);
155
156                 J = jacobi(Q1, Q2, Q3, Q4, Q5, phi, d01, d02, d10, d11, d20, vr, 12);
157                 J.block(nnx, 0, nx, n) = MatrixXd::Zero(nx, n);
158                 Jr.block(0, nnx, nnx, nnx) = J.block(nx, nx, nnx, nnx);
159                 temp.segment(0, nnx) = temp.segment(0, nnx) - J.block(nx, 0, nnx,
                    nx) * b.segment(n, nx);
160
161                 J = jacobi(Q1, Q2, Q3, Q4, Q5, phi, d01, d02, d10, d11, d20, vr, 13);
162                 J.block(nnx, 0, nx, n) = MatrixXd::Zero(nx, n);
163                 Jr.block(0, 2 * nnx, nnx, nnx) = J.block(nx, nx, nnx, nnx);
164                 temp.segment(0, nnx) = temp.segment(0, nnx) - J.block(nx, 0, nnx,
                    nx) * b.segment(2 * n, nx);
165                     }
166
167 #pragma omp section
168 {
169                 MatrixXd J = jacobi(Q1, Q2, Q3, Q4, Q5, phi, d01, d02, d10, d11,
                    d20, vr, 21);
170                 J.block(nnx, 0, nx, n) = MatrixXd::Zero(nx, n);
171                 Jr.block(nnx, 0, nnx, nnx) = J.block(nx, nx, nnx, nnx);
172                 temp.segment(nnx, nnx) = b.segment(n + nx, nnx) - J.block(nx, 0,
                    nnx, nx) * b.segment(0, nx);
173
174                 J = jacobi(Q1, Q2, Q3, Q4, Q5, phi, d01, d02, d10, d11, d20, vr, 22);
175                 J.block(nnx, 0, nx, n) = d10.block(nnx, 0, nx, n);
176                 Jr.block(nnx, nnx, nnx, nnx) = J.block(nx, nx, nnx, nnx);
177                 temp.segment(nnx, nnx) = temp.segment(nnx, nnx) - J.block(nx, 0,
                    nnx, nx) * b.segment(n, nx);
178
179                 J = jacobi(Q1, Q2, Q3, Q4, Q5, phi, d01, d02, d10, d11, d20, vr, 23);
180                 J.block(nnx, 0, nx, n) = MatrixXd::Zero(nx, n);
181                 Jr.block(nnx, 2 * nnx, nnx, nnx) = J.block(nx, nx, nnx, nnx);
182                 temp.segment(nnx, nnx) = temp.segment(nnx, nnx) - J.block(nx, 0,
                    nnx, nx) * b.segment(2 * n, nx);
183 }
184
185 #pragma omp section
186 {
187                 MatrixXd J = jacobi(Q1, Q2, Q3, Q4, Q5, phi, d01, d02, d10, d11,
                    d20, vr, 31);
188                 J.block(nnx, 0, nx, n) = MatrixXd::Zero(nx, n);
189                 Jr.block(2 * nnx, 0, nnx, nnx) = J.block(nx, nx, nnx, nnx);
190                 temp.segment(2 * nnx, nnx) = b.segment(2 * n + nx, nnx) -
```

```
                    J.block(nx, 0, nnx, nx) * b.segment(0, nx);

                    J = jacobi(Q1, Q2, Q3, Q4, Q5, phi, d01, d02, d10, d11, d20, vr, 32);
                    J.block(nnx, 0, nx, n) = MatrixXd::Zero(nx, n);
                    Jr.block(2 * nnx, nnx, nnx, nnx) = J.block(nx, nx, nnx, nnx);
                    temp.segment(2 * nnx, nnx) = temp.segment(2 * nnx, nnx) -
                    J.block(nx, 0, nnx, nx) * b.segment(n, nx);

                    J = jacobi(Q1, Q2, Q3, Q4, Q5, phi, d01, d02, d10, d11, d20, vr, 33);
                    J.block(nnx, 0, nx, n) = d10.block(nnx, 0, nx, n);
                    Jr.block(2 * nnx, 2 * nnx, nnx, nnx) = J.block(nx, nx, nnx, nnx);
                    temp.segment(2 * nnx, nnx) = temp.segment(2 * nnx, nnx) -
                    J.block(nx, 0, nnx, nx) * b.segment(2 * n, nx);
    }
    }
    #pragma omp sections
                    {
    #pragma omp section
                        {

                    //Jt is J12 or B block of REDUCED Jacobi Matrix
                    MatrixXd J = jacobi(Q1, Q2, Q3, Q4, Q5, phi, d01, d02, d10, d11,
                    d20, vr, 14);
                    J.block(nnx, 0, nx, n) = MatrixXd::Zero(nx, n);
                    Jt.block(0, 0, nnx, nnx) = J.block(nx, nx, nnx, nnx);
                    temp.segment(0, nnx) = temp.segment(0, nnx) - J.block(nx, 0, nnx,
                    nx) * b.segment(3 * n, nx);

                    J = jacobi(Q1, Q2, Q3, Q4, Q5, phi, d01, d02, d10, d11, d20, vr, 15);
                    J.block(nnx, 0, nx, n) = MatrixXd::Zero(nx, n);
                    Jt.block(0, nnx, nnx, nnx) = J.block(nx, nx, nnx, nnx);
                    temp.segment(0, nnx) = temp.segment(0, nnx) - J.block(nx, 0, nnx,
                    nx) * b.segment(4 * n, nx);

                    J = jacobi(Q1, Q2, Q3, Q4, Q5, phi, d01, d02, d10, d11, d20, vr, 16);
                    J.block(nnx, 0, nx, n) = MatrixXd::Zero(nx, n);
                    Jt.block(0, 2 * nnx, nnx, nnx) = J.block(nx, nx, nnx, nnx);
                    temp.segment(0, nnx) = temp.segment(0, nnx) - J.block(nx, 0, nnx,
                    nx) * b.segment(5 * n, nx);
                        }

    #pragma omp section
    {

                    MatrixXd J = jacobi(Q1, Q2, Q3, Q4, Q5, phi, d01, d02, d10, d11,
                    d20, vr, 24);
                    J.block(nnx, 0, nx, n) = MatrixXd::Zero(nx, n);
                    Jt.block(nnx, 0, nnx, nnx) = J.block(nx, nx, nnx, nnx);
                    temp.segment(nnx, nnx) = temp.segment(nnx, nnx) - J.block(nx, 0,
                    nnx, nx) * b.segment(3 * n, nx);

                    J = jacobi(Q1, Q2, Q3, Q4, Q5, phi, d01, d02, d10, d11, d20, vr, 25);
                    J.block(nnx, 0, nx, n) = MatrixXd::Zero(nx, n);
                    Jt.block(nnx, nnx, nnx, nnx) = J.block(nx, nx, nnx, nnx);
                    temp.segment(nnx, nnx) = temp.segment(nnx, nnx) - J.block(nx, 0,
                    nnx, nx) * b.segment(4 * n, nx);

                    J = jacobi(Q1, Q2, Q3, Q4, Q5, phi, d01, d02, d10, d11, d20, vr, 26);
                    J.block(nnx, 0, nx, n) = MatrixXd::Zero(nx, n);
                    Jt.block(nnx, 2 * nnx, nnx, nnx) = J.block(nx, nx, nnx, nnx);
                    temp.segment(nnx, nnx) = temp.segment(nnx, nnx) - J.block(nx, 0,
                    nnx, nx) * b.segment(5 * n, nx);
    }

    #pragma omp section
    {
                    MatrixXd J = jacobi(Q1, Q2, Q3, Q4, Q5, phi, d01, d02, d10, d11,
                    d20, vr, 34);
                    J.block(nnx, 0, nx, n) = MatrixXd::Zero(nx, n);
                    Jt.block(2 * nnx, 0, nnx, nnx) = J.block(nx, nx, nnx, nnx);
                    temp.segment(2 * nnx, nnx) =
                            temp.segment(2 * nnx, nnx) - J.block(nx, 0, nnx, nx) *
                            b.segment(3 * n, nx);
```

```
251
252                 J = jacobi(Q1, Q2, Q3, Q4, Q5, phi, d01, d02, d10, d11, d20, vr, 35);
253                 J.block(nnx, 0, nx, n) = MatrixXd::Zero(nx, n);
254                 Jt.block(2 * nnx, nnx, nnx, nnx) = J.block(nx, nx, nnx, nnx);
255                 temp.segment(2 * nnx, nnx) =
256                         temp.segment(2 * nnx, nnx) - J.block(nx, 0, nnx, nx) *
                            b.segment(4 * n, nx);
257
258                 J = jacobi(Q1, Q2, Q3, Q4, Q5, phi, d01, d02, d10, d11, d20, vr, 36);
259                 J.block(nnx, 0, nx, n) = MatrixXd::Zero(nx, n);
260                 Jt.block(2 * nnx, 2 * nnx, nnx, nnx) = J.block(nx, nx, nnx, nnx);
261                 temp.segment(2 * nnx, nnx) =
262                         temp.segment(2 * nnx, nnx) - J.block(nx, 0, nnx, nx) *
                            b.segment(5 * n, nx);
263 }
264                 }
265             };
266
267             HouseholderQR<Ref<MatrixXd> > qr(Jr);
268             VectorXd Aib1;
269 #pragma omp sections
270             {
271 #pragma omp section
272                 {
273             Aib1 = qr.solve(-temp);
274             writenetcdf("Aib1.nc", Aib1, Aib1.data());
275                 }
276 #pragma omp section
277             {
278                 MatrixXd JJ = qr.solve(Jt);//qr still stores the decomposition of A,
                    and share the memory with Jr. JJ is AiB, and peak memory may appear
                    here
279                 Jr = JJ;
280                 writenetcdf("AiB.nc", JJ, JJ.data());
281
282             }
283             }
284
285 #pragma omp sections
286             {
287 #pragma omp section
288                 {
289                 //Jt is J21 or C block of REDUCED Jacobi Matrix
290                 MatrixXd J = jacobi(Q1, Q2, Q3, Q4, Q5, phi, d01, d02, d10, d11,
                    d20, vr, 41);
291                 J.block(nnx, 0, nx, n) = MatrixXd::Zero(nx, n);
292                 Jt.block(0, 0, nnx, nnx) = J.block(nx, nx, nnx, nnx);
293                 temp.segment(0, nnx) = b.segment(3 * n + nx, nnx) - J.block(nx, 0,
                    nnx, nx) * b.segment(0, nx);
294
295                 J = jacobi(Q1, Q2, Q3, Q4, Q5, phi, d01, d02, d10, d11, d20, vr, 42);
296                 J.block(nnx, 0, nx, n) = MatrixXd::Zero(nx, n);
297                 Jt.block(0, nnx, nnx, nnx) = J.block(nx, nx, nnx, nnx);
298                 temp.segment(0, nnx) = temp.segment(0, nnx) - J.block(nx, 0, nnx,
                    nx) * b.segment(n, nx);
299
300                 J = jacobi(Q1, Q2, Q3, Q4, Q5, phi, d01, d02, d10, d11, d20, vr, 43);
301                 J.block(nnx, 0, nx, n) = MatrixXd::Zero(nx, n);
302                 Jt.block(0, 2 * nnx, nnx, nnx) = J.block(nx, nx, nnx, nnx);
303                 temp.segment(0, nnx) = temp.segment(0, nnx) - J.block(nx, 0, nnx,
                    nx) * b.segment(2 * n, nx);
304                 }
305
306 #pragma omp section
307 {
308                 MatrixXd J = jacobi(Q1, Q2, Q3, Q4, Q5, phi, d01, d02, d10, d11,
                    d20, vr, 51);
309                 J.block(nnx, 0, nx, n) = MatrixXd::Zero(nx, n);
310                 Jt.block(nnx, 0, nnx, nnx) = J.block(nx, nx, nnx, nnx);
311                 temp.segment(nnx, nnx) = b.segment(4 * n + nx, nnx) - J.block(nx, 0,
                    nnx, nx) * b.segment(0, nx);
312
313                 J = jacobi(Q1, Q2, Q3, Q4, Q5, phi, d01, d02, d10, d11, d20, vr, 52);
```

```
314                 J.block(nnx, 0, nx, n) = MatrixXd::Zero(nx, n);
315                 Jt.block(nnx, nnx, nnx, nnx) = J.block(nx, nx, nnx, nnx);
316                 temp.segment(nnx, nnx) = temp.segment(nnx, nnx) - J.block(nx, 0,
                    nnx, nx) * b.segment(n, nx);
317
318                 J = jacobi(Q1, Q2, Q3, Q4, Q5, phi, d01, d02, d10, d11, d20, vr, 53);
319                 J.block(nnx, 0, nx, n) = MatrixXd::Zero(nx, n);
320                 Jt.block(nnx, 2 * nnx, nnx, nnx) = J.block(nx, nx, nnx, nnx);
321                 temp.segment(nnx, nnx) = temp.segment(nnx, nnx) - J.block(nx, 0,
                    nnx, nx) * b.segment(2 * n, nx);
322 }
323
324 #pragma omp section
325 {
326                 MatrixXd J = jacobi(Q1, Q2, Q3, Q4, Q5, phi, d01, d02, d10, d11,
                    d20, vr, 61);
327                 J.block(nnx, 0, nx, n) = MatrixXd::Zero(nx, n);
328                 Jt.block(2 * nnx, 0, nnx, nnx) = J.block(nx, nx, nnx, nnx);
329                 temp.segment(2 * nnx, nnx) = b.segment(5 * n + nx, nnx) -
                    J.block(nx, 0, nnx, nx) * b.segment(0, nx);
330
331                 J = jacobi(Q1, Q2, Q3, Q4, Q5, phi, d01, d02, d10, d11, d20, vr, 62);
332                 J.block(nnx, 0, nx, n) = MatrixXd::Zero(nx, n);
333                 Jt.block(2 * nnx, nnx, nnx, nnx) = J.block(nx, nx, nnx, nnx);
334                 temp.segment(2 * nnx, nnx) = temp.segment(2 * nnx, nnx) -
                    J.block(nx, 0, nnx, nx) * b.segment(n, nx);
335
336                 J = jacobi(Q1, Q2, Q3, Q4, Q5, phi, d01, d02, d10, d11, d20, vr, 63);
337                 J.block(nnx, 0, nx, n) = MatrixXd::Zero(nx, n);
338                 Jt.block(2 * nnx, 2 * nnx, nnx, nnx) = J.block(nx, nx, nnx, nnx);
339                 temp.segment(2 * nnx, nnx) = temp.segment(2 * nnx, nnx) -
                    J.block(nx, 0, nnx, nx) * b.segment(2 * n, nx);
340 }
341             };
342
343 #pragma omp sections
344             {
345 #pragma omp section
346                 {
347             Aib1 = (Jt * Aib1).eval();//Now Aib1 is CAib1
348                 }
349 #pragma omp section
350 {
351             Jr = Jt*Jr;
352 }
353             }
354
355 #pragma omp sections
356             {
357 #pragma omp section
358                 {
359                 //Jt is J22 or D block of REDUCED Jacobi Matrix
360                 MatrixXd J = jacobi(Q1, Q2, Q3, Q4, Q5, phi, d01, d02, d10, d11,
                    d20, vr, 44);
361                 J.block(nnx, 0, nx, n) = d10.block(nnx, 0, nx, n);
362                 Jt.block(0, 0, nnx, nnx) = J.block(nx, nx, nnx, nnx);
363                 temp.segment(0, nnx) = temp.segment(0, nnx) - J.block(nx, 0, nnx,
                    nx) * b.segment(3 * n, nx);
364
365                 J = jacobi(Q1, Q2, Q3, Q4, Q5, phi, d01, d02, d10, d11, d20, vr, 45);
366                 J.block(nnx, 0, nx, n) = MatrixXd::Zero(nx, n);
367                 Jt.block(0, nnx, nnx, nnx) = J.block(nx, nx, nnx, nnx);
368                 temp.segment(0, nnx) = temp.segment(0, nnx) - J.block(nx, 0, nnx,
                    nx) * b.segment(4 * n, nx);
369
370                 J = jacobi(Q1, Q2, Q3, Q4, Q5, phi, d01, d02, d10, d11, d20, vr, 46);
371                 J.block(nnx, 0, nx, n) = MatrixXd::Zero(nx, n);
372                 Jt.block(0, 2 * nnx, nnx, nnx) = J.block(nx, nx, nnx, nnx);
373                 temp.segment(0, nnx) = temp.segment(0, nnx) - J.block(nx, 0, nnx,
                    nx) * b.segment(5 * n, nx);
374                 }
375
376 #pragma omp section
```

```
377                 {
378                 MatrixXd J = jacobi(Q1, Q2, Q3, Q4, Q5, phi, d01, d02, d10, d11,
                    d20, vr, 54);
379                 J.block(nnx, 0, nx, n) = MatrixXd::Zero(nx, n);
380                 Jt.block(nnx, 0, nnx, nnx) = J.block(nx, nx, nnx, nnx);
381                 temp.segment(nnx, nnx) = temp.segment(nnx, nnx) - J.block(nx, 0,
                    nnx, nx) * b.segment(3 * n, nx);
382
383                 J = jacobi(Q1, Q2, Q3, Q4, Q5, phi, d01, d02, d10, d11, d20, vr, 55);
384                 J.block(nnx, 0, nx, n) = d10.block(nnx, 0, nx, n);
385                 Jt.block(nnx, nnx, nnx, nnx) = J.block(nx, nx, nnx, nnx);
386                 temp.segment(nnx, nnx) = temp.segment(nnx, nnx) - J.block(nx, 0,
                    nnx, nx) * b.segment(4 * n, nx);
387
388                 J = jacobi(Q1, Q2, Q3, Q4, Q5, phi, d01, d02, d10, d11, d20, vr, 56);
389                 J.block(nnx, 0, nx, n) = MatrixXd::Zero(nx, n);
390                 Jt.block(nnx, 2 * nnx, nnx, nnx) = J.block(nx, nx, nnx, nnx);
391                 temp.segment(nnx, nnx) = temp.segment(nnx, nnx) - J.block(nx, 0,
                    nnx, nx) * b.segment(5 * n, nx);
392                 }
393
394   #pragma omp section
395                 {
396                 MatrixXd J = jacobi(Q1, Q2, Q3, Q4, Q5, phi, d01, d02, d10, d11,
                    d20, vr, 64);
397                 J.block(nnx, 0, nx, n) = MatrixXd::Zero(nx, n);
398                 Jt.block(2 * nnx, 0, nnx, nnx) = J.block(nx, nx, nnx, nnx);
399                 temp.segment(2 * nnx, nnx) =
400                         temp.segment(2 * nnx, nnx) - J.block(nx, 0, nnx, nx) *
                            b.segment(3 * n, nx);
401
402                 J = jacobi(Q1, Q2, Q3, Q4, Q5, phi, d01, d02, d10, d11, d20, vr, 65);
403                 J.block(nnx, 0, nx, n) = MatrixXd::Zero(nx, n);
404                 Jt.block(2 * nnx, nnx, nnx, nnx) = J.block(nx, nx, nnx, nnx);
405                 temp.segment(2 * nnx, nnx) =
406                         temp.segment(2 * nnx, nnx) - J.block(nx, 0, nnx, nx) *
                            b.segment(4 * n, nx);
407
408                 J = jacobi(Q1, Q2, Q3, Q4, Q5, phi, d01, d02, d10, d11, d20, vr, 66);
409                 J.block(nnx, 0, nx, n) = d10.block(nnx, 0, nx, n);
410                 Jt.block(2 * nnx, 2 * nnx, nnx, nnx) = J.block(nx, nx, nnx, nnx);
411                 temp.segment(2 * nnx, nnx) =
412                         temp.segment(2 * nnx, nnx) - J.block(nx, 0, nnx, nx) *
                            b.segment(5 * n, nx);
413                 }
414
415               };
416
417               Aib1 = -temp - Aib1;//Now Aib1 is b2-CAib1
418
419               Jt -= Jr;//Jt is D-CAiB
420
421               HouseholderQR<Ref<MatrixXd> > qr1(Jt);
422               temp = qr1.solve(Aib1);//temp is y2 =(x4,x5,x6)= (D-CAiB)i(b2-CAib1)
423
424               Q4.segment(0,nx) = Q4.segment(0,nx).matrix() - b.segment(3*n,nx);
425               Q4.segment(nx,nnx) = Q4.segment(nx,nnx).matrix() + temp.segment(0, nnx);
426               Q5.segment(0,nx) = Q5.segment(0,nx).matrix() - b.segment(4*n,nx);
427               Q5.segment(nx,nnx) = Q5.segment(nx,nnx).matrix() + temp.segment(nnx, nnx);
428               phi.segment(0,nx) = phi.segment(0,nx).matrix() - b.segment(5*n,nx);
429               phi.segment(nx,nnx) = phi.segment(nx,nnx).matrix() +
                  temp.segment(2*(nnx), nnx);
430
431               readwrite("Aib1.nc", Aib1.data());
432               readwrite("AiB.nc", Jt.data());
433               temp = Aib1 - Jt * temp;// Now temp is y1 = (x1,x2,x3) =Aib1-AiB*y2
434
435
436               Q1.segment(0,nx) = Q1.segment(0,nx).matrix() - b.segment(0,nx);
437               Q1.segment(nx,nnx) = Q1.segment(nx,nnx).matrix() + temp.segment(0, nnx);
438               Q2.segment(0,nx) = Q2.segment(0,nx).matrix() - b.segment(n,nx);
439               Q2.segment(nx,nnx) = Q2.segment(nx,nnx).matrix() + temp.segment(nnx, nnx);
440               Q3.segment(0,nx) = Q3.segment(0,nx).matrix() - b.segment(2*n,nx);
```

```
441             Q3.segment(nx,nnx) = Q3.segment(nx,nnx).matrix() + temp.segment(2*(nnx),
                nnx);
442
443
444             nor.conservativeResize(k+1);
445             nor(k)=temp.lpNorm<Infinity>();
446
447
448         };
449
450         cout << "Current iteration step is " << k <<endl;
451         cout << "Infinity norm of solutions is " << '\n' << nor <<endl;
452
453         k++;
454
455     }while(k<le && nor(k-1) > epsilon);
456
457     writenetcdf("Q3.nc", Q3, Q3.data());
458
459     t2=clock();
460     float diff ((float)t2-(float)t1);
461     cout << "Running time is "<< diff / CLOCKS_PER_SEC<< 's' << endl;
462     return 0;
463 }
464
465 //Fourier derivative matrix
466 MatrixXd fourier(int nx, double lx)
467 {
468     MatrixXd dx(nx,nx);
469     for (int j=1;j<nx+1;++j)
470     {
471         for (int i=1;i<nx+1;++i)
472         {
473             i==j ? dx(i-1,j-1)=0.:(fmod(nx,2)==0?
                dx(i-1,j-1)=(M_PI/lx)*pow(-1.,i-j)/(tan(M_PI*(i-j)/nx)):dx(i-1,j-1)=(M_PI/
                lx)*pow(-1.,i-j)/(sin(M_PI*(i-j)/nx) ));
474         }
475     }
476     return dx;
477 }
478
479 //chebsev grids
480 ArrayXd chebp(int nr)
481 {
482     ArrayXd gridr2(nr);
483     for (int i=0; i<nr; ++i)
484     {
485         *(gridr2.data()+i)=cos(i*M_PI/(nr-1));
486     }
487     return gridr2;
488 }
489
490 //chebsev derivative matrix
491 MatrixXd cheb(int nr, double lr)
492 {
493     ArrayXd x=chebp(nr), c(nr);
494     MatrixXd sdm(nr,nr);
495     for (int i=1;i<nr+1;++i)
496     {
497         i==1||i==nr ? c(i-1)=2.0 : c(i-1)=1.0;
498     }
499
500     for (int j=1; j<nr+1; ++j)
501     {
502         for (int i=1; i<nr+1; ++i)
503         {
504             i!=j ? sdm(i-1,j-1)=(2/lr)*(c(i-1)/c(j-1))*(pow(-1,i+j)/(x(i-1)-x(j-1)))
                : sdm(i-1,j-1)=0;
505         }
506     }
507
508     sdm-=sdm.rowwise().sum().asDiagonal();
509     return sdm;
```

```
510 }
511
512 // Present the positon of specified value
513 template <typename Derived>
514 ArrayXd position(const ArrayBase<Derived> & v, double x)//expression template can
    avoid copy to temperary if v is an (pseudo-)expression, like v.asDiagnal()
515 {   ArrayXd pos;//pos is 0 by 0 size by default if no specified initialization, so
    pos(_number) is invalid before resize, but pos=Knownmatrix/array is allowed
516     int k=0;
517     for (int i=0, size = static_cast<int>(v.size()); i < size; ++i)
518     {
519         if (v(i)==x)
520         {
521             pos.conservativeResize(k+1);// pos.resize() will lose the previous value.
522             pos(k)=i;
523             ++k;
524         }
525     }
526     return pos;
527 }
528
529
530 //netcdf: write data
531 //Based on
    https://git.physik.uni-wuerzburg.de/itpa-computers/admin_meeting_protocols/blob/master
    /NetCDF4/netcdf_c_write.cpp
532 template <typename Derived>
533 void writenetcdf(string name, const DenseBase<Derived>& eigendata, double*
    eigenpointer)
534 {
535     char filename[name.length()+1];
536     strcpy(filename,name.c_str());
537     int row = static_cast<int>((eigendata).rows());
538     int col = static_cast<int>((eigendata).cols());
539     int siz = row*col;
540
541     if (row==1 || col==1)
542     {
543         int rank = 1;
544         int dim[1] = {siz};
545         int dimid[1] = {0};
546         int ncid;
547         // open the file in NetCDF4 -> HDF5 format but still enforce the old classic
            model.
548         int retval = nc_create(filename, NC_CLOBBER | NC_NETCDF4 | NC_CLASSIC_MODEL,
            &ncid);
549         //netcdf is now by default in define mode, s let's define our data
550         // first the dimensionality
551         retval = nc_def_dim(ncid, "temperature", dim[0], dimid);
552         //retval = nc_def_dim(ncid, "energy", dim[1], &(dimid[1]));
553         //next comes the data type
554         int varid;
555         retval = nc_def_var(ncid, "vector", NC_DOUBLE, rank, dimid, &varid);
556
557         //enable deflate compression
558         nc_def_var_deflate(ncid, varid, 1/*enable shuffle filter*/, 1/*enable
            deflate*/, 9/*compression strength*/);
559         //end define mode
560         retval = nc_enddef(ncid);
561         // last index of the dimension array varies fastest
562         retval = nc_put_var_double(ncid, varid, eigenpointer);
563         nc_close(ncid);
564     }
565     else
566     {
567         int rank = 2;
568         int dim[2] = {row, col};
569         int dimid[2] = {0};
570         int ncid;
571
572         // open the file in NetCDF4 -> HDF5 format but still enforce the old classic
            model.
573         int retval = nc_create(filename, NC_CLOBBER | NC_NETCDF4 | NC_CLASSIC_MODEL,
```

```
            &ncid);
574         //netcdf is now by default in define mode, s let's define our data
575         // first the dimensionality
576         retval = nc_def_dim(ncid, "temperature", dim[0], dimid);
577         retval = nc_def_dim(ncid, "energy", dim[1], &(dimid[1]));
578         //next comes the data type
579         int varid;
580         retval = nc_def_var(ncid, "matrix", NC_DOUBLE, rank, dimid, &varid);
581
582         //enable deflate compression
583         nc_def_var_deflate(ncid, varid, 1/*enable shuffle filter*/, 1/*enable
            deflate*/, 9/*compression strength*/);
584         //end define mode
585         retval = nc_enddef(ncid);
586         // last index of the dimension array varies fastest
587         retval = nc_put_var_double(ncid, varid, eigenpointer);
588         nc_close(ncid);
589     };
590
591 }
592
593 //netcdf: read data from file and write it to a matrix
594 //Based on
    https://git.physik.uni-wuerzburg.de/itpa-computers/admin_meeting_protocols/blob/master
    /NetCDF4/netcdf_c_read.cpp
595 void readwrite(string name, double* eigenpointer)
596 {
597     char filename[name.length()+1];
598     strcpy(filename,name.c_str());
599     int ncid;
600     // open the file. NC_NOWRITE tells netcdf that we want read-oly
601     int retval = nc_open(filename, NC_NOWRITE, &ncid);
602     // we know there is a dataset called "matrix" so let's retrieve that
603     int varid;
604     retval = nc_inq_varid(ncid, "vector", &varid);
605     //now we have the id -> query dimensionality
606     int rank;
607     retval = nc_inq_varndims(ncid, varid, &rank);
608     if (rank==1)
609     {
610         //read the entire vector
611         retval = nc_get_var_double(ncid, varid, eigenpointer);
612         nc_close(ncid);
613     }
614     else
615     {
616         retval = nc_inq_varid(ncid, "matrix", &varid);
617         //read the entire matrix
618         retval = nc_get_var_double(ncid, varid, eigenpointer);
619         nc_close(ncid);
620     };
621
622 }
623
624
```

```cpp
//This is the file "eqsandjacobi.h" that included in the line 38 of previous main code.
//We present equations of motion and the Jacobi matrix in this file.

#include <eigen3/Eigen/Dense>
using namespace Eigen;

//n dimensional array multiplied by nxn dimensional array
template <typename DerivedA, typename DerivedB>
inline ArrayXXd arraypdt(const ArrayBase<DerivedA> & v, const ArrayBase<DerivedB> & w)
{
    int siz = static_cast<int>(v.size());
    ArrayXXd resh(siz, siz);

    for (int i = 0; i < siz; ++i)
        resh.row(i) = v(i) * w.row(i);
    return resh;
}

//change n dimensional array to n by n dimensonal diagonal array
template <typename Derived>
inline ArrayXXd arraypdt_idty(const ArrayBase<Derived> & v)
{
    int siz = static_cast<int>(v.size());
    MatrixXd resh =v.matrix().asDiagonal();

    return resh.array();
}

//Equations of motion
ArrayXd eqs(const ArrayXd& Q1, const ArrayXd& Q2, const ArrayXd& Q3, const ArrayXd& Q4, const ArrayXd& Q5, const ArrayXd& phi,\
const MatrixXd& z01, const  MatrixXd& z02, const  MatrixXd& z10, const  MatrixXd& z11, const  MatrixXd& z20, const ArrayXd& r)
{
    //First, we define some expressions to make the equations of motion look more compact.
   int siz= static_cast<int>(Q1.size());
    ArrayXd eq(6*siz);
    ArrayXd r2 = pow(r,2);
    ArrayXd r3 = pow(r,3);
    ArrayXd r4 = pow(r,4);
    ArrayXd r5 = pow(r,5);
    ArrayXd r6 = pow(r,6);
    ArrayXd r7 = pow(r,7);
    ArrayXd r8 = pow(r,8);
    ArrayXd r9 = pow(r,9);
    ArrayXd r10 = pow(r,10);
    ArrayXd r11 = pow(r,11);
    ArrayXd r12 = pow(r,12);
    ArrayXd r13 = pow(r,13);
    ArrayXd r14 = pow(r,14);

    ArrayXd Q12 = pow(Q1, 2);
    ArrayXd Q22 = pow(Q2, 2);
    ArrayXd Q32 = pow(Q3, 2);
    ArrayXd Q42 = pow(Q4, 2);
    ArrayXd Q52 = pow(Q5, 2);

    ArrayXd Q452 = Q42 * Q52;

    ArrayXd q1z01 = z01*Q1.matrix();
    ArrayXd q1z02 = z02*Q1.matrix();
    ArrayXd q1z10 = z10*Q1.matrix();
    ArrayXd q1z11 = z11*Q1.matrix();
    ArrayXd q1z20 = z20*Q1.matrix();
    ArrayXd q2z01 = z01*Q2.matrix();
    ArrayXd q2z02 = z02*Q2.matrix();
    ArrayXd q2z10 = z10*Q2.matrix();
    ArrayXd q2z11 = z11*Q2.matrix();
    ArrayXd q2z20 = z20*Q2.matrix();
    ArrayXd q3z01 = z01*Q3.matrix();
```

```
      ArrayXd q3z02 = z02*Q3.matrix();
      ArrayXd q3z10 = z10*Q3.matrix();
      ArrayXd q3z11 = z11*Q3.matrix();
      ArrayXd q3z20 = z20*Q3.matrix();
      ArrayXd q4z01 = z01*Q4.matrix();
      ArrayXd q4z02 = z02*Q4.matrix();
      ArrayXd q4z10 = z10*Q4.matrix();
      ArrayXd q4z11 = z11*Q4.matrix();
      ArrayXd q4z20 = z20*Q4.matrix();
      ArrayXd q5z01 = z01*Q5.matrix();
      ArrayXd q5z02 = z02*Q5.matrix();
      ArrayXd q5z10 = z10*Q5.matrix();
      ArrayXd q5z11 = z11*Q5.matrix();
      ArrayXd q5z20 = z20*Q5.matrix();
      ArrayXd phiz01 = z01*phi.matrix();
      ArrayXd phiz02 = z02*phi.matrix();
      ArrayXd phiz10 = z10*phi.matrix();
      ArrayXd phiz11 = z11*phi.matrix();
      ArrayXd phiz20 = z20*phi.matrix();

      ArrayXd omr2 = -1 + r2;
      ArrayXd exp21 = -3 + r2;
      ArrayXd omr22 = pow(omr2, 2);
      ArrayXd exp2 = exp21*r2 + 3;
      ArrayXd exp8 = (-7*r2 + 12)*r2 - 3;
      ArrayXd exp19 = (8*r2 - 21)*r2 + 15;
      ArrayXd exp1 = ((r2 - 4)*r2 + 6)*r2 - 3;
      ArrayXd exp3 = exp2*r2 - 3;
      ArrayXd exp5 = ((4*r2 - 15)*r2 + 20)*r2 - 9;
      ArrayXd exp6  = exp2*r2 + 3;
      ArrayXd exp20 = ((7*r2 - 20)*r2 + 18)*r2 - 3;
      ArrayXd exp22 = ((11*r2 - 30)*r2 + 24)*r2 - 3;
      ArrayXd exp7 =  ((((r2 - 6)*r2 + 15)*r2 - 21)*r2 + 18)*r2 - 9;
      ArrayXd exp9 = (((((-7*r2 + 41)*r2 - 99)*r2 + 120)*r2 - 69)*r2 + 9)*r2 + 9;
      ArrayXd exp10 = phiz01*((5*r2 - 9)*r2 + 3 + 4*q3z01*r*exp2);
      ArrayXd exp11 = r*((-4*r2 + 11)*r2 - 9);
      ArrayXd exp18 = (((r2 - 4)*r2 + 6)*r2 - 6)*r2 + 3;
      ArrayXd exp23 = (5*r2 - 12)*r2 + 3 + 4*q3z11*omr22*exp2;


//Equations of motion. There are six equations here, separated by a comma.
   eq << Q5*r*exp1*((q1z10 + 2*q1z01*Q3)*(q1z10 + \
2*q1z01*Q3)*Q4*r*exp1*plusysq + Q2*(4*q1z01*q1z01*r*omr2 - \
q1z10*Q4*exp3*plusysq)) + \
Q1*(Q4*Q5*r2*exp1*plusysq*(q1z10*exp11 - q1z20*exp1 - \
4*Q3*exp2*(2*q1z01*r + q1z11*omr2) + \
2*Q32*exp2*(-2*q1z02*omr2 + q1z10*r*exp2*plusysq)) - \
2*Q2*(Q4*(-(q1z10*r3*omr2*exp2*exp2) + Q5*exp3*exp3)*plusysq - \
Q5*r2*exp1*(-2*q1z02*omr2 + q1z10*r*exp2*plusysq))) + \
2*Q12*(Q4*Q5*plusysq*(-3*omr2*omr2*omr2*exp6 + \
2*Q32*r2*exp2*exp2*exp3*plusysq) + \
2*Q2*r2*exp2*(Q5*exp3*plusysq + Q4*(exp3*plusysq + \
Q5*(4*phi*phi*omr22 + 6*plusysq)))),Q22*(q1z10 + \        // The first equation
2*q1z01*Q3)*Q452*r*exp1*((q1z10 + 2*q1z01*Q3)*r*exp1 - \
4*Q2*exp3)*plusysq + 2*Q1*Q22*Q452*omr2*(6*Q2*omr22*exp6 + \
(2*q1z10 + q2z10 + 4*q1z01*Q3)*r*exp7)*plusysq + Q12*(-3*(q2z10 + \
2*q2z01*Q3)*(q2z10 + 2*q2z01*Q3)*Q452*r2*exp1*exp1*plusysq + \
2*Q2*Q4*Q52*r2*exp1*(4*q2z01*q2z01 - 4*q2z01*q2z01*r2 - \
3*q2z20*Q4*plusysq + 9*q2z10*Q4*r*plusysq + 6*q2z20*Q4*r2*plusysq - \
11*q2z10*Q4*r3*plusysq - 4*q2z20*Q4*r4*plusysq + \
4*q2z10*Q4*r5*plusysq + q2z20*Q4*r6*plusysq + \
4*Q3*Q4*exp2*(2*q2z01*r + q2z11*omr2)*plusysq + \
8*q2z01*Q3*Q3*Q3*Q4*r*exp2*exp2*plusy4 + \
2*Q32*Q4*exp2*plusysq*(2*q2z02*omr2 + q2z10*r*exp2*plusysq)) + \
8*Q2*Q2*Q2*r2*exp2*(-3*Q4*Q52*omr2*omr2*omr2*plusysq + (2*Q3*q4z01 \
+ q4z10)*Q52*r*exp1*plusysq + Q42*(-3*Q5*omr2*omr2*omr2*plusysq + \
(2*Q3*q5z01 + q5z10)*r*exp1*plusysq - 2*Q52*(2*phi*phi*omr22 + \
3*plusysq))) + Q22*((2*Q3*q4z01 + q4z10)*(2*Q3*q4z01 + \
q4z10)*Q52*r2*exp1*exp1*plusysq + 4*Q4*Q52*r2*exp1*(2*q2z02*omr2 \
+ 4*Q3*q4z01*exp2*(-r + q3z01*omr2)*plusysq + exp2*(-(q2z10*r) \
+ 2*q4z10*(-r + q3z01*omr2))*plusysq) + Q42*(-4*Q5*(q2z10 + \
4*Q3*q5z01 + 2*q5z10)*r3*omr2*exp2*exp2*plusysq + (2*Q3*q5z01 + \
q5z10)*(2*Q3*q5z01 + q5z10)*r2*exp1*exp1*plusysq - \
```

```
4*Q52*((((((((((-2*r2 + 20)*r2 - 90)*r2 + 236)*r2 - 392)*r2 + 420)*r2 - 282)*r2 +
108)*r2 - 18)*phiz10*phiz10*r2
- 8*phi*phiz10*r3*omr2*omr2*omr2*exp2*exp2 - \
8*phi*phi*r4*exp1*exp1 - 9*plusysq + 18*r2*plusysq - \
36*q3z01*q3z01*r2*plusysq - 72*q3z01*r3*plusysq - 99*r4*plusysq + \
144*q3z01*q3z01*r4*plusysq + 216*q3z01*r5*plusysq + 168*r6*plusysq - \
240*q3z01*q3z01*r6*plusysq - 264*q3z01*r7*plusysq - 135*r8*plusysq + \
216*q3z01*q3z01*r8*plusysq + 168*q3z01*r9*plusysq + 54*r10*plusysq - \
112*q3z01*q3z01*r10*plusysq - 56*q3z01*r11*plusysq - 9*r12*plusysq + \
32*q3z01*q3z01*r12*plusysq + 8*q3z01*r13*plusysq - \
4*q3z01*q3z01*r14*plusysq - \
2*Q32*r2*omr2*exp2*exp2*(4*phiz01*phiz01*omr2*omr2*omr2 + \
exp8*plusy4 - 4*q3z01*r*exp2*plusy4) - \
4*Q3*r2*omr2*exp2*exp2*(4*phi*phiz01*r*omr22 + \
2*phiz01*phiz10*omr2*omr2*omr2 - \
q3z10*r*exp2*plusy4))))),Q1*Q22*Q452*plusysq*(Q3*Q4*(exp9)*plusysq \  // The second
equation
- r*(exp18)*(-2*q1z01 + q3z10*Q4*exp2*plusysq)) + \
Q22*Q452*r*omr2*plusysq*(-2*q1z01*Q2*exp3 + (q1z10 + \
2*q1z01*Q3)*exp2*(q1z01*r*omr2 + Q3*Q4*exp3*plusysq)) + \
Q12*r2*exp2*(4*Q2*Q2*Q2*(q4z01*Q52 + Q42*q5z01)*r*omr2*plusysq - \
(q2z10 + 2*q2z01*Q3)*Q452*omr2*plusysq*(-(Q3*Q4*(r*(exp21) + \
2*q3z01*exp1)*plusysq) + 2*Q3*Q3*Q3*Q4*r*exp2*exp2*plusy4 + \
omr2*(q2z01 - q3z10*Q4*exp2*plusysq)) + \
Q2*Q4*Q52*plusysq*(2*Q3*Q3*Q3*Q42*exp2*(exp22 + \
4*q3z01*r*exp1)*plusy4 - omr2*(-2*q2z01*q4z10*omr2 + \
8*q2z01*Q4*(r - q3z01*omr2) + Q42*(q3z10*r*(exp19) + \
q3z20*exp1)*plusysq) + Q3*(4*q2z01*q4z01*omr22 - Q42*(exp23 + \
4*q3z01*r*(exp5))*plusysq) + 2*Q32*Q4*exp1*plusysq*(2*q2z01*r + \
Q4*(-2*q3z02*omr2 + 3*q3z10*r*exp2*plusysq))) + \
Q22*(-4*Q32*Q4*(q4z01*Q52 + Q42*q5z01)*r*exp1*plusy4 + \
omr2*(-(q4z01*q4z10*Q52*omr2*plusysq) + 4*Q4*q4z01*Q52*(r - \
q3z01*omr2)*plusysq + 2*q3z10*Q4*Q4*Q4*Q5*r*exp2*plusy4 + \
Q42*(-4*Q5*q5z01*r*plusysq + q5z01*q5z10*omr2*plusysq + \
2*Q52*(-4*phiz01*phiz10 + 12*phiz01*phiz10*r2 - 12*phiz01*phiz10*r4 + \
4*phiz01*phiz10*r6 + 8*phi*phiz01*r*omr22 - 2*q3z02*omr2*plusysq + \
3*q3z10*r*plusy4 - 3*q3z10*r3*plusy4 + q3z10*r5*plusy4))) + \
2*Q3*(-(q4z01*q4z01*Q52*omr22*plusysq) - Q4*q4z10*Q52*r*exp1*plusy4 \
+ Q4*Q4*Q4*(-(q5z10*r*exp1) + Q5*(exp20))*plusy4 + \
Q42*(q5z01*q5z01*omr22*plusysq + \
Q52*(8*phiz01*phiz01*omr2*omr2*omr2*omr2 - 4*q3z01*r*exp1*plusy4 + \
(exp20)*plusy4))))),Q1*Q22*Q452*exp3*(-4*Q4*r + \                    // The third
equation
q4z10*omr2)*plusy4 + \
2*q1z01*Q22*Q452*omr2*plusysq*(q1z01*r*omr2 + \
2*Q3*Q4*exp3*plusysq) + \
Q12*r*(-2*q2z01*Q452*omr2*plusysq*(-2*Q3*Q4*(r*(exp21) + \
2*q3z01*exp1)*plusysq + 4*Q3*Q3*Q3*Q4*r*exp2*exp2*plusy4 - \
omr2*(q2z01 + 2*q3z10*Q4*exp2*plusysq)) + \
Q2*Q4*Q52*plusy4*(-((2*Q3*q4z01 + q4z10)*(2*Q3*q4z01 + \
q4z10)*omr22*exp2) + 4*Q42*(-omr2*(3*omr22 - 4*q3z01*r*exp2 + \
2*q3z01*q3z01*exp1) + 2*Q32*r*exp2*exp2*(r + \
2*q3z01*omr2)*plusysq) - Q4*omr2*(q4z10*exp11 - q4z20*exp1 - \
4*Q3*exp2*(2*q4z01*r + q4z11*omr2) + \
2*Q32*exp2*(-2*q4z02*omr2 + q4z10*r*exp2*plusysq))) + \
2*Q22*(-3*q4z01*q4z01*Q52*omr22*plusysq - \
Q4*Q52*omr2*plusysq*(-2*q4z02*omr2 + 4*Q3*q4z01*r*exp2*plusysq \
+ q4z10*r*exp2*plusysq) - \
4*Q4*Q4*Q4*plusysq*(-(Q5*r2*exp2*plusysq) + \
Q3*q5z01*r*exp1*plusysq + Q52*(2*phi*phi*omr22 + 3*plusysq)) + \
Q42*(q5z01*q5z01*omr22*plusysq - q4z10*Q5*r*exp1*plusy4 + \
4*Q52*(2*phiz01*phiz01*omr2*omr2*omr2*omr2 + \
r2*exp2*plusy4))),-(Q2*Q4*Q5*exp3*(-4*Q5*r + \                       // The fourth
equation
q5z10*omr2)*plusysq) + Q1*r*(2*Q2*(2*q5z01*q5z01*omr22 - \
4*Q52*r2*exp2*plusysq + Q5*omr2*(-2*q5z02*omr2 + \
q5z10*r*exp2*plusysq) + Q4*(-4*Q5*r2*exp2*plusysq + \
q5z10*r*exp1*plusysq + 4*Q52*(2*phi*phi*omr22 + 3*plusysq))) + \
Q4*plusysq*((2*Q3*q5z01 + q5z10)*(2*Q3*q5z01 + q5z10)*omr22*exp2 - \
4*Q52*(-3*omr2*omr2*omr2 + 2*Q32*r2*exp2*exp2*plusysq) + \
Q5*omr2*(q5z10*exp11 - q5z20*exp1 - 4*Q3*exp2*(2*q5z01*r + \
q5z11*omr2) + 2*Q32*exp2*(-2*q5z02*omr2 + \
q5z10*r*exp2*plusysq)))),Q2*Q4*Q5*r*omr2*(4*phiz01*q1z01*Q2*omr2\   // The fifth
```

```
    equaiton
211  + 4*phiz01*q1z01*Q32*Q4*exp1*plusysq + q1z10*Q4*exp2*(2*phi*r + \
212 phiz10*omr2)*plusysq + 2*Q3*Q4*exp2*(2*phi*q1z01*r + \
213 (phiz10*q1z01 + phiz01*q1z10)*omr2)*plusysq) + Q1*((-q2z10 - \
214 2*q2z01*Q3)*Q42*Q5*r*exp1*(2*phi*r + (phiz10 + \
215 2*phiz01*Q3)*omr2)*plusysq + 4*Q22*r*(-(phiz01*q4z01*Q5*omr22) + \
216 Q4*(2*phiz02*Q5 + phiz01*q5z01)*omr22 + 4*phi*Q42*Q5*plusysq) + \
217 Q2*Q4*(Q4*((2*Q3*q5z01 + q5z10)*r*exp1*(2*phi*r + (phiz10 + \
218 2*phiz01*Q3)*omr2) + 2*Q5*(4*phi*r*(exp3 + q3z01*r*exp1) + \
219 omr22*(3*phiz10 + 3*phiz20*r + 6*phiz10*q3z01*r - 9*phiz10*r2 - \
220 3*phiz20*r3 - 6*phiz10*q3z01*r3 + 5*phiz10*r4 + phiz20*r5 + \
221 2*phiz10*q3z01*r5 + 4*phiz02*Q32*r*exp2 + 2*phiz01*q3z10*r*exp2 + \
222 2*Q3*(2*phiz11*r*exp2 + phiz01*(exp10))))))*plusysq + \
223 Q5*r*omr2*(4*phiz01*q2z01*omr2 + \
224 4*phiz01*Q32*q4z01*exp1*plusysq + q4z10*exp2*(2*phi*r + \
225 phiz10*omr2)*plusysq + 2*Q3*exp2*(2*phi*q4z01*r + (phiz10*q4z01 + \
226 phiz01*q4z10)*omr2)*plusysq)));                                          // The sixth
    equtionn
227     return eq;
228 }
229
230
231 // Jacobi matrix
232 MatrixXd jacobi(const ArrayXd& Q1, const ArrayXd& Q2, const ArrayXd& Q3, const
    ArrayXd& Q4, const ArrayXd& Q5, const ArrayXd& phi,\
233 const MatrixXd& z01, const MatrixXd& z02, const MatrixXd& z10, const MatrixXd& z11,
    const MatrixXd& z20, const ArrayXd& r, int label)
234 {
235     //We define some expressions to make the Jacobi matrix look more compact.
236     int siz= static_cast<int>(Q1.rows());
237     ArrayXd r2 = pow(r,2);
238     ArrayXd r3 = pow(r,3);
239     ArrayXd r4 = pow(r,4);
240     ArrayXd r5 = pow(r,5);
241     ArrayXd r6 = pow(r,6);
242     ArrayXd r7 = pow(r,7);
243     ArrayXd r8 = pow(r,8);
244     ArrayXd r9 = pow(r,9);
245     ArrayXd r10 = pow(r,10);
246     ArrayXd r11 = pow(r,11);
247     ArrayXd r12 = pow(r,12);
248     ArrayXd r13 = pow(r,13);
249     ArrayXd r14 = pow(r,14);
250
251     ArrayXd Q12 = pow(Q1, 2);
252     ArrayXd Q22 = pow(Q2, 2);
253     ArrayXd Q32 = pow(Q3, 2);
254     ArrayXd Q42 = pow(Q4, 2);
255     ArrayXd Q52 = pow(Q5, 2);
256
257     ArrayXd Q452 = Q42 * Q52;
258
259     ArrayXd q1z01 = z01*Q1.matrix();
260     ArrayXd q1z02 = z02*Q1.matrix();
261     ArrayXd q1z10 = z10*Q1.matrix();
262     ArrayXd q1z11 = z11*Q1.matrix();
263     ArrayXd q1z20 = z20*Q1.matrix();
264     ArrayXd q2z01 = z01*Q2.matrix();
265     ArrayXd q2z02 = z02*Q2.matrix();
266     ArrayXd q2z10 = z10*Q2.matrix();
267     ArrayXd q2z11 = z11*Q2.matrix();
268     ArrayXd q2z20 = z20*Q2.matrix();
269     ArrayXd q3z01 = z01*Q3.matrix();
270     ArrayXd q3z02 = z02*Q3.matrix();
271     ArrayXd q3z10 = z10*Q3.matrix();
272     ArrayXd q3z11 = z11*Q3.matrix();
273     ArrayXd q3z20 = z20*Q3.matrix();
274     ArrayXd q4z01 = z01*Q4.matrix();
275     ArrayXd q4z02 = z02*Q4.matrix();
276     ArrayXd q4z10 = z10*Q4.matrix();
277     ArrayXd q4z11 = z11*Q4.matrix();
278     ArrayXd q4z20 = z20*Q4.matrix();
279     ArrayXd q5z01 = z01*Q5.matrix();
```

```
        ArrayXd q5z02 = z02*Q5.matrix();
        ArrayXd q5z10 = z10*Q5.matrix();
        ArrayXd q5z11 = z11*Q5.matrix();
        ArrayXd q5z20 = z20*Q5.matrix();
        ArrayXd phiz01 = z01*phi.matrix();
        ArrayXd phiz02 = z02*phi.matrix();
        ArrayXd phiz10 = z10*phi.matrix();
        ArrayXd phiz11 = z11*phi.matrix();
        ArrayXd phiz20 = z20*phi.matrix();

        ArrayXd omr2 = -1 + r2;
        ArrayXd exp21 = -3 + r2;
        ArrayXd omr22 = pow(omr2, 2);
        ArrayXd exp2 = exp21*r2 + 3;
        ArrayXd exp8 = (-7*r2 + 12)*r2 - 3;
        ArrayXd exp19 = (8*r2 - 21)*r2 + 15;
        ArrayXd exp1 = ((r2 - 4)*r2 + 6)*r2 - 3;
        ArrayXd exp3 = exp2*r2 - 3;
        ArrayXd exp4 = 6*Q5 + exp3;
        ArrayXd exp5 = ((4*r2 - 15)*r2 + 20)*r2 - 9;
        ArrayXd exp6  = exp2*r2 + 3;
        ArrayXd exp7 =  ((((r2 - 6)*r2 + 15)*r2 - 21)*r2 + 18)*r2 - 9;
        ArrayXd exp9 = (((((-7*r2 + 41)*r2 - 99)*r2 + 120)*r2 - 69)*r2 + 9)*r2 + 9;
        ArrayXd exp10 = phiz01*((5*r2 - 9)*r2 + 3 + 4*q3z01*r*exp2);
        ArrayXd exp11 = r*((-4*r2 + 11)*r2 - 9);
        ArrayXd exp26 = Q12*Q22;
        ArrayXd exp12 = exp26*q3z01*Q42*Q52;
        ArrayXd exp13 = phiz10*exp26*Q42*Q52;
        ArrayXd exp24 = Q1*Q2;
        ArrayXd exp14 = exp24*Q42*Q5;
        ArrayXd exp15 = exp26*Q42*Q5;
        ArrayXd exp16 = exp26*Q3;
        ArrayXd exp17 = Q2*Q4*Q5;
        ArrayXd exp18 = (((r2 - 4)*r2 + 6)*r2 - 6)*r2 + 3;
        ArrayXd exp20 = ((7*r2 - 20)*r2 + 18)*r2 - 3;
        ArrayXd exp22 = ((11*r2 - 30)*r2 + 24)*r2 - 3;
        ArrayXd exp23 = (5*r2 - 12)*r2 + 3 + 4*q3z11*omr22*exp2;
        ArrayXd exp25 = Q12*Q2;
        ArrayXd exp27 = Q3*Q4;
        ArrayXd exp28 = Q4*Q52;
        ArrayXd exp29 = Q1*Q22;
//We devide the Jacobi matrix into 6 by 6 blocks in order to read it separately in the main code. This will reduce the memory usage.
if (label==11) // The block of the Jacobi matrix J11
{
    return arraypdt_idty(Q4*Q5*r2*exp1*plusysq*(q1z10*exp11 - q1z20*exp1 - \
4*Q3*exp2*(2*q1z01*r + q1z11*omr2) + \
2*Q32*exp2*(-2*q1z02*omr2 + q1z10*r*exp2*plusysq)) - \
2*Q2*(Q4*(-(q1z10*r3*omr2*pow(exp2,2)) + Q5*pow(exp3,2))*plusysq - \
Q5*r2*exp1*(-2*q1z02*omr2 + q1z10*r*exp2*plusysq)) + \
4*Q1*(Q4*Q5*plusysq*(-3*pow(omr2,3)*exp6 + \
2*Q32*r2*pow(exp2,2)*exp3*plusysq) + \
2*Q2*r2*exp2*(Q5*exp3*plusysq + Q4*(4*pow(phi,2)*Q5*omr22 + \
exp4*plusysq)))) + arraypdt((8*q1z01*Q2*Q5*r2*omr2*exp1 - \
8*Q1*exp27*Q5*r3*exp2*exp1*plusysq + 4*Q3*(q1z10 + \
2*q1z01*Q3)*Q4*Q5*r2*pow(exp1,2)*plusysq),z01.array()) + \
arraypdt((-4*exp24*Q5*r2*omr2*exp1 - \
4*Q1*Q32*Q4*Q5*r2*omr2*exp2*exp1*plusysq),z02.array()) + \
arraypdt((2*exp24*Q4*r3*omr2*pow(exp2,2)*plusysq + \
2*exp24*Q5*r3*exp2*exp1*plusysq + \
Q1*Q4*Q5*r2*exp11*exp1*plusysq + 2*(q1z10 + \
2*q1z01*Q3)*Q4*Q5*r2*pow(exp1,2)*plusysq - \
exp17*r*exp1*exp3*plusysq + \
2*Q1*Q32*Q4*Q5*r3*pow(exp2,2)*exp1*plusy4),z10.array()) - \
arraypdt(4*Q1*exp27*Q5*r2*omr2*exp2*exp1*plusysq,z11.array()) - \
arraypdt(Q1*Q4*Q5*r2*pow(exp1,2)*plusysq,z20.array());
}
else if (label==12) // The block of the Jacobi matrix J12
{
        return arraypdt_idty(Q5*r*exp1*(4*pow(q1z01,2)*r*omr2 -
        q1z10*Q4*exp3*plusysq) - \
2*Q1*(Q4*(-(q1z10*r3*omr2*pow(exp2,2)) + Q5*pow(exp3,2))*plusysq - \
Q5*r2*exp1*(-2*q1z02*omr2 + q1z10*r*exp2*plusysq)) + \
```

```
4*Q12*r2*exp2*(Q5*exp3*plusysq + Q4*(4*pow(phi,2)*Q5*omr22 + \
exp4*plusysq)));
}
else if (label==13) // The block of the Jacobi matrix J13
{
    return arraypdt_idty(4*q1z01*(q1z10 + \
2*q1z01*Q3)*Q4*Q5*r2*pow(exp1,2)*plusysq - \
4*Q1*Q4*Q5*r2*exp2*exp1*(2*q1z01*r + q1z11*omr2)*plusysq + \
8*Q12*exp27*Q5*r2*pow(exp2,2)*exp3*plusy4 + \
4*Q1*exp27*Q5*r2*exp2*exp1*plusysq*(-2*q1z02*omr2 + \
q1z10*r*exp2*plusysq));
}
else if (label==21) // The block of the Jacobi matrix J21
{
    return arraypdt_idty(2*\
Q22*Q452*omr2*(6*Q2*omr22*exp6 + (2*q1z10 + q2z10 + \
4*q1z01*Q3)*r*exp7)*plusysq + 2*Q1*(-3*pow(q2z10 + \
2*q2z01*Q3,2)*Q452*r2*pow(exp1,2)*plusysq + \
2*Q2*exp28*r2*exp1*(4*pow(q2z01,2) - 4*pow(q2z01,2)*r2 - \
3*q2z20*Q4*plusysq + 9*q2z10*Q4*r*plusysq + 6*q2z20*Q4*r2*plusysq - \
11*q2z10*Q4*r3*plusysq - 4*q2z20*Q4*r4*plusysq + \
4*q2z10*Q4*r5*plusysq + q2z20*Q4*r6*plusysq + \
4*exp27*exp2*(2*q2z01*r + q2z11*omr2)*plusysq + \
8*q2z01*pow(Q3,3)*Q4*r*pow(exp2,2)*plusy4 + \
2*Q32*Q4*exp2*plusysq*(2*q2z02*omr2 + q2z10*r*exp2*plusysq)) + \
8*pow(Q2,3)*r2*exp2*(-3*exp28*pow(omr2,3)*plusysq + (2*Q3*q4z01 + \
q4z10)*Q52*r*exp1*plusysq + Q42*(-3*Q5*pow(omr2,3)*plusysq + \
(2*Q3*q5z01 + q5z10)*r*exp1*plusysq - 2*Q52*(2*pow(phi,2)*omr22 + \
3*plusysq))) + Q22*(pow(2*Q3*q4z01 + \
q4z10,2)*Q52*r2*pow(exp1,2)*plusysq + \
4*exp28*r2*exp1*(2*q2z02*omr2 + 4*Q3*q4z01*exp2*(-r + \
q3z01*omr2)*plusysq + exp2*(-(q2z10*r) + 2*q4z10*(-r + \
q3z01*omr2))*plusysq) + Q42*(-4*Q5*(q2z10 + 4*Q3*q5z01 + \
2*q5z10)*r3*omr2*pow(exp2,2)*plusysq + pow(2*Q3*q5z01 + \
q5z10,2)*r2*pow(exp1,2)*plusysq - 4*Q52*(
(((((((((-2*r2 + 20)*r2 - 90)*r2 + 236)*r2 - 392)*r2 + 420)*r2 - 282)*r2 + 108)*r2 -
18)
*pow(phiz10,2)*r2
-8*phi*phiz10*r3*pow(omr2,3)*pow(exp2,2) - 8*pow(phi,2)*r4*pow(exp1,2) \
- 9*plusysq + 18*r2*plusysq - 36*pow(q3z01,2)*r2*plusysq - \
72*q3z01*r3*plusysq - 99*r4*plusysq + 144*pow(q3z01,2)*r4*plusysq + \
216*q3z01*r5*plusysq + 168*r6*plusysq - 240*pow(q3z01,2)*r6*plusysq - \
264*q3z01*r7*plusysq - 135*r8*plusysq + 216*pow(q3z01,2)*r8*plusysq + \
168*q3z01*r9*plusysq + 54*r10*plusysq - 112*pow(q3z01,2)*r10*plusysq \
- 56*q3z01*r11*plusysq - 9*r12*plusysq + 32*pow(q3z01,2)*r12*plusysq \
+ 8*q3z01*r13*plusysq - 4*pow(q3z01,2)*r14*plusysq - \
2*Q32*r2*omr2*pow(exp2,2)*(4*pow(phiz01,2)*pow(omr2,3) + \
(exp8)*plusy4 - 4*q3z01*r*exp2*plusy4) - \
4*Q3*r2*omr2*pow(exp2,2)*(4*phi*phiz01*r*omr22 + \
2*phiz01*phiz10*pow(omr2,3) - q3z10*r*exp2*plusy4)))))) + \
arraypdt((2*Q22*Q3*(q1z10 + 2*q1z01*Q3)*Q452*r2*pow(exp1,2)*plusysq + \
8*exp29*Q3*Q452*r*omr2*exp7*plusysq + \
2*Q22*Q3*Q452*r*exp1*((q1z10 + 2*q1z01*Q3)*r*exp1 - \
4*Q2*exp3)*plusysq),z01.array()) + arraypdt((Q22*(q1z10 + \
2*q1z01*Q3)*Q452*r2*pow(exp1,2)*plusysq + \
4*exp29*Q452*r*omr2*exp7*plusysq + Q22*Q452*r*exp1*((q1z10 + \
2*q1z01*Q3)*r*exp1 - 4*Q2*exp3)*plusysq),z10.array());
}
else if (label==22) // The block of the Jacobi matrix J22
{
    return arraypdt_idty(-4*Q22*(q1z10 + \
2*q1z01*Q3)*Q452*r*exp1*exp3*plusysq + \
12*exp29*Q452*pow(omr2,3)*exp6*plusysq + 2*Q2*(q1z10 + \
2*q1z01*Q3)*Q452*r*exp1*((q1z10 + 2*q1z01*Q3)*r*exp1 - \
4*Q2*exp3)*plusysq + 4*exp24*Q452*omr2*(6*Q2*omr22*exp6 + \
(2*q1z10 + q2z10 + 4*q1z01*Q3)*r*exp7)*plusysq + \
2*Q12*exp28*r2*exp1*(4*pow(q2z01,2) - 4*pow(q2z01,2)*r2 - \
3*q2z20*Q4*plusysq + 9*q2z10*Q4*r*plusysq + 6*q2z20*Q4*r2*plusysq - \
11*q2z10*Q4*r3*plusysq - 4*q2z20*Q4*r4*plusysq + \
4*q2z10*Q4*r5*plusysq + q2z20*Q4*r6*plusysq + \
4*exp27*exp2*(2*q2z01*r + q2z11*omr2)*plusysq + \
8*q2z01*pow(Q3,3)*Q4*r*pow(exp2,2)*plusy4 + \
2*Q32*Q4*exp2*plusysq*(2*q2z02*omr2 + q2z10*r*exp2*plusysq)) + \
```

```
24*exp26*r2*exp2*(-3*exp28*pow(omr2,3)*plusysq + (2*Q3*q4z01 + \
q4z10)*Q52*r*exp1*plusysq + Q42*(-3*Q5*pow(omr2,3)*plusysq + \
(2*Q3*q5z01 + q5z10)*r*exp1*plusysq - 2*Q52*(2*pow(phi,2)*omr22 + \
3*plusysq))) + 2*exp25*(pow(2*Q3*q4z01 + \
q4z10,2)*Q52*r2*pow(exp1,2)*plusysq + \
4*exp28*r2*exp1*(2*q2z02*omr2 + 4*Q3*q4z01*exp2*(-r + \
q3z01*omr2)*plusysq + exp2*(-(q2z10*r) + 2*q4z10*(-r + \
q3z01*omr2))*plusysq) + Q42*(-4*Q5*(q2z10 + 4*Q3*q5z01 + \
2*q5z10)*r3*omr2*pow(exp2,2)*plusysq + pow(2*Q3*q5z01 + \
q5z10,2)*r2*pow(exp1,2)*plusysq - 4*Q52*(
(((((((((-2*r2 + 20)*r2 - 90)*r2 + 236)*r2 - 392)*r2 + 420)*r2 - 282)*r2 + 108)*r2 -
18)
*pow(phiz10,2)*r2
- 8*phi*phiz10*r3*pow(omr2,3)*pow(exp2,2) - 8*pow(phi,2)*r4*pow(exp1,2) \
- 9*plusysq + 18*r2*plusysq - 36*pow(q3z01,2)*r2*plusysq - \
72*q3z01*r3*plusysq - 99*r4*plusysq + 144*pow(q3z01,2)*r4*plusysq + \
216*q3z01*r5*plusysq + 168*r6*plusysq - 240*pow(q3z01,2)*r6*plusysq - \
264*q3z01*r7*plusysq - 135*r8*plusysq + 216*pow(q3z01,2)*r8*plusysq + \
168*q3z01*r9*plusysq + 54*r10*plusysq - 112*pow(q3z01,2)*r10*plusysq \
- 56*q3z01*r11*plusysq - 9*r12*plusysq + 32*pow(q3z01,2)*r12*plusysq \
+ 8*q3z01*r13*plusysq - 4*pow(q3z01,2)*r14*plusysq - \
2*Q32*r2*omr2*pow(exp2,2)*(4*pow(phiz01,2)*pow(omr2,3) + \
(exp8)*plusy4 - 4*q3z01*r*exp2*plusy4) - \
4*Q3*r2*omr2*pow(exp2,2)*(4*phi*phiz01*r*omr22 + \
2*phiz01*phiz10*pow(omr2,3) - q3z10*r*exp2*plusy4))))) + \
arraypdt((16*exp25*q2z01*exp28*r2*exp1 - 16*exp25*q2z01*exp28*r4*exp1 \
+ 16*exp25*Q3*Q452*r3*exp2*exp1*plusysq - 12*Q12*Q3*(q2z10 + \
2*q2z01*Q3)*Q452*r2*pow(exp1,2)*plusysq + \
16*exp25*pow(Q3,3)*Q452*r3*pow(exp2,2)*exp1*plusy4),z01.array()) + \
arraypdt((8*exp26*exp28*r2*omr2*exp1 + \
8*exp25*Q32*Q452*r2*omr2*exp2*exp1*plusysq),z02.array()) + \
arraypdt((-4*exp15*r3*omr2*pow(exp2,2)*plusysq + \
18*exp25*Q452*r3*exp1*plusysq - 22*exp25*Q452*r5*exp1*plusysq + \
8*exp25*Q452*r7*exp1*plusysq - \
4*exp26*exp28*r3*exp2*exp1*plusysq - 6*Q12*(q2z10 + \
2*q2z01*Q3)*Q452*r2*pow(exp1,2)*plusysq + \
2*exp29*Q452*r*omr2*exp7*plusysq + \
4*exp25*Q32*Q452*r3*pow(exp2,2)*exp1*plusy4),z10.array()) + \
arraypdt(8*exp25*Q3*Q452*r2*omr2*exp2*exp1*plusysq,z11.array()) + \
arraypdt((-6*exp25*Q452*r2*exp1*plusysq + 12*exp25*Q452*r4*exp1*plusysq \
- 8*exp25*Q452*r6*exp1*plusysq + \
2*exp25*Q452*r8*exp1*plusysq),z20.array());
}
else if (label==23) // The block of the Jacobi matrix J23
{
    return arraypdt_idty(-16*exp15*q5z01*r3*(\
omr2)*pow(exp2,2)*plusysq + \
16*Q12*pow(Q2,3)*q4z01*Q52*r3*exp2*exp1*plusysq + \
16*Q12*pow(Q2,3)*Q42*q5z01*r3*exp2*exp1*plusysq + \
2*q1z01*Q22*(q1z10 + 2*q1z01*Q3)*Q452*r2*pow(exp1,2)*plusysq - \
12*Q12*q2z01*(q2z10 + 2*q2z01*Q3)*Q452*r2*pow(exp1,2)*plusysq + \
4*exp26*q4z01*(2*Q3*q4z01 + q4z10)*Q52*r2*pow(exp1,2)*plusysq + \
4*exp26*Q42*q5z01*(2*Q3*q5z01 + q5z10)*r2*pow(exp1,2)*plusysq + \
8*Q1*q1z01*Q22*Q452*r*omr2*exp7*plusysq + \
8*exp25*Q452*r2*exp2*exp1*(2*q2z01*r + q2z11*omr2)*plusysq + \
16*exp26*Q4*q4z01*Q52*r2*exp2*exp1*(-r + q3z01*omr2)*plusysq \
+ 2*q1z01*Q22*Q452*r*exp1*((q1z10 + 2*q1z01*Q3)*r*exp1 - \
4*Q2*exp3)*plusysq + \
48*exp25*q2z01*Q32*Q452*r3*pow(exp2,2)*exp1*plusy4 + \
8*exp25*Q3*Q452*r2*exp2*exp1*plusysq*(2*q2z02*omr2 + \
q2z10*r*exp2*plusysq) + \
16*exp16*Q452*r2*omr2*pow(exp2,2)*(4*pow(phiz01,2)*pow(omr2,3) \
+ (exp8)*plusy4 - 4*q3z01*r*exp2*plusy4) + \
16*exp26*Q452*r2*omr2*pow(exp2,2)*(4*phi*phiz01*r*omr22 + \
2*phiz01*phiz10*pow(omr2,3) - q3z10*r*exp2*plusy4)) + \
arraypdt((288*exp12*r2*plusysq + 288*exp26*Q452*r3*plusysq - \
1152*exp12*r4*plusysq - 864*exp26*Q452*r5*plusysq + \
1920*exp12*r6*plusysq + 1056*exp26*Q452*r7*plusysq - \
1728*exp12*r8*plusysq - 672*exp26*Q452*r9*plusysq + \
896*exp12*r10*plusysq + 224*exp26*Q452*r11*plusysq - \
256*exp12*r12*plusysq - 32*exp26*Q452*r13*plusysq + \
32*exp12*r14*plusysq + \
16*exp16*Q4*q4z01*Q52*r2*omr2*exp2*exp1*plusysq + \
```

```
8*exp26*Q4*q4z10*Q52*r2*omr2*exp2*exp1*plusysq - \
32*exp26*Q32*Q452*r3*omr2*pow(exp2,3)*plusy4),z01.array()) - \
arraypdt(16*exp16*Q452*r3*omr2*pow(exp2,3)*plusy4,z10.array());
}
else if (label==31) // The block of the Jacobi matrix J31
{
    return arraypdt_idty(Q22*\
Q452*plusysq*(exp27*(exp9)*plusysq - r*(exp18)*(-2*q1z01 + \
q3z10*Q4*exp2*plusysq)) + 2*Q1*r2*exp2*(4*pow(Q2,3)*(q4z01*Q52 + \
Q42*q5z01)*r*omr2*plusysq - (q2z10 + \
2*q2z01*Q3)*Q452*omr2*plusysq*(-(exp27*(r*(exp21) + \
2*q3z01*exp1)*plusysq) + 2*pow(Q3,3)*Q4*r*pow(exp2,2)*plusy4 + \
omr2*(q2z01 - q3z10*Q4*exp2*plusysq)) + \
Q2*exp28*plusysq*(2*pow(Q3,3)*Q42*exp2*(exp22 + \
4*q3z01*r*exp1)*plusy4 - omr2*(2*q2z01*(4*Q4*r - \
4*q3z01*Q4*omr2 - q4z10*omr2) + Q42*(q3z10*r*(exp19) + \
q3z20*exp1)*plusysq) + Q3*(4*q2z01*q4z01*omr22 - Q42*(exp23 + \
4*q3z01*r*(exp5))*plusysq) + 2*Q32*Q4*exp1*plusysq*(2*q2z01*r + \
Q4*(-2*q3z02*omr2 + 3*q3z10*r*exp2*plusysq))) + \
Q22*(-4*Q32*Q4*(q4z01*Q52 + Q42*q5z01)*r*exp1*plusy4 + \
2*Q3*(-(pow(q4z01,2)*Q52*omr22*plusysq) - \
Q4*q4z10*Q52*r*exp1*plusy4 + pow(Q4,3)*(-(q5z10*r*exp1) + \
Q5*(exp20))*plusy4 + Q42*(pow(q5z01,2)*omr22*plusysq + \
Q52*(8*pow(phiz01,2)*pow(omr2,4) - 4*q3z01*r*exp1*plusy4 + \
(exp20)*plusy4))) + omr2*(-(q4z01*q4z10*Q52*omr2*plusysq) + \
4*Q4*q4z01*Q52*(r - q3z01*omr2)*plusysq + \
2*q3z10*pow(Q4,3)*Q5*r*exp2*plusy4 + Q42*(-4*Q5*q5z01*r*plusysq + \
q5z01*q5z10*omr2*plusysq + 2*Q52*(4*phiz01*omr22*(2*phi*r + \
phiz10*omr2) + plusysq*(-2*q3z02*omr2 + \
q3z10*r*exp2*plusysq)))))) + arraypdt((Q22*(q1z10 + \
2*q1z01*Q3)*Q452*r2*omr22*exp2*plusysq - \
2*pow(Q2,3)*Q452*r*omr2*exp3*plusysq + \
2*exp29*Q452*r*(exp18)*plusysq + \
2*Q22*Q3*Q452*r*omr2*exp2*plusysq*(q1z01*r*omr2 + \
exp27*exp3*plusysq)),z01.array()) + \
arraypdt(Q22*Q452*r*omr2*exp2*plusysq*(q1z01*r*omr2 + \
exp27*exp3*plusysq),z10.array());
}
else if (label==32) // The block of the Jacobi matrix J32
{
    return arraypdt_idty(12*exp26*(q4z01*Q52 + \
Q42*q5z01)*r3*omr2*exp2*plusysq - \
2*q1z01*Q22*Q452*r*omr2*exp3*plusysq + \
2*exp24*Q452*plusysq*(exp27*(exp9)*plusysq - r*(exp18)*(-2*q1z01 + \
q3z10*Q4*exp2*plusysq)) + \
2*Q2*Q452*r*omr2*plusysq*(-2*q1z01*Q2*exp3 + (q1z10 + \
2*q1z01*Q3)*exp2*(q1z01*r*omr2 + exp27*exp3*plusysq)) + \
Q12*exp28*r2*exp2*plusysq*(2*pow(Q3,3)*Q42*exp2*(exp22 + \
4*q3z01*r*exp1)*plusy4 - omr2*(2*q2z01*(4*Q4*r - \
4*q3z01*Q4*omr2 - q4z10*omr2) + Q42*(q3z10*r*(exp19) + \
q3z20*exp1)*plusysq) + Q3*(4*q2z01*q4z01*omr22 - Q42*(exp23 + \
4*q3z01*r*(exp5))*plusysq) + 2*Q32*Q4*exp1*plusysq*(2*q2z01*r + \
Q4*(-2*q3z02*omr2 + 3*q3z10*r*exp2*plusysq))) + \
2*exp25*r2*exp2*(-4*Q32*Q4*(q4z01*Q52 + Q42*q5z01)*r*exp1*plusy4 \
+ 2*Q3*(-(pow(q4z01,2)*Q52*omr22*plusysq) - \
Q4*q4z10*Q52*r*exp1*plusy4 + pow(Q4,3)*(-(q5z10*r*exp1) + \
Q5*(exp20))*plusy4 + Q42*(pow(q5z01,2)*omr22*plusysq + \
Q52*(8*pow(phiz01,2)*pow(omr2,4) - 4*q3z01*r*exp1*plusy4 + \
(exp20)*plusy4))) + omr2*(-(q4z01*q4z10*Q52*omr2*plusysq) + \
4*Q4*q4z01*Q52*(r - q3z01*omr2)*plusysq + \
2*q3z10*pow(Q4,3)*Q5*r*exp2*plusy4 + Q42*(-4*Q5*q5z01*r*plusysq + \
q5z01*q5z10*omr2*plusysq + 2*Q52*(4*phiz01*omr22*(2*phi*r + \
phiz10*omr2) + plusysq*(-2*q3z02*omr2 + \
q3z10*r*exp2*plusysq)))))) + arraypdt((-(Q12*(q2z10 + \
2*q2z01*Q3)*Q452*r2*omr22*exp2*plusysq) + \
4*exp25*exp27*q4z01*Q52*r2*omr22*exp2*plusysq + \
2*exp25*Q4*q4z10*Q52*r2*omr22*exp2*plusysq - \
8*exp25*Q452*r2*omr2*exp2*(r - q3z01*omr2)*plusysq + \
4*exp25*Q32*Q452*r3*exp2*exp1*plusy4 - \
2*Q12*Q3*Q452*r2*omr2*exp2*plusysq*(-(exp27*(r*(exp21) + \
2*q3z01*exp1)*plusysq) + 2*pow(Q3,3)*Q4*r*pow(exp2,2)*plusy4 + \
omr2*(q2z01 - q3z10*Q4*exp2*plusysq))),z01.array()) - \
arraypdt(Q12*Q452*r2*omr2*exp2*plusysq*(-(exp27*(r*(exp21) + \
```

```
2*q3z01*exp1)*plusysq) + 2*pow(Q3,3)*Q4*r*pow(exp2,2)*plusy4 + \
omr2*(q2z01 - \
q3z10*Q4*exp2*plusysq)),z10.array());
}
else if (label==33) // The block of the Jacobi matrix J33
{
    return arraypdt_idty(-8*exp16*Q4*(q4z01*Q52 + \
Q42*q5z01)*r3*exp2*exp1*plusy4 + Q22*(q1z10 + \
2*q1z01*Q3)*pow(Q4,3)*Q52*r*omr2*exp2*exp3*plusy4 + \
exp29*pow(Q4,3)*Q52*(exp9)*plusy4 + Q12*(q2z10 + \
2*q2z01*Q3)*pow(Q4,3)*Q52*r2*omr2*exp2*(r*(exp21) + \
2*q3z01*exp1)*plusy4 - 6*Q12*Q32*(q2z10 + \
2*q2z01*Q3)*pow(Q4,3)*Q52*r3*omr2*pow(exp2,3)*plusy6 + \
6*exp25*Q32*pow(Q4,3)*Q52*r2*pow(exp2,2)*(exp22 + \
4*q3z01*r*exp1)*plusy6 + \
2*q1z01*Q22*Q452*r*omr2*exp2*plusysq*(q1z01*r*omr2 + \
exp27*exp3*plusysq) + \
exp25*exp28*r2*exp2*plusysq*(4*q2z01*q4z01*omr22 - Q42*(exp23 + \
4*q3z01*r*(exp5))*plusysq) - \
2*Q12*q2z01*Q452*r2*omr2*exp2*plusysq*(-(exp27*(r*(exp21) + \
2*q3z01*exp1)*plusysq) + 2*pow(Q3,3)*Q4*r*pow(exp2,2)*plusy4 + \
omr2*(q2z01 - q3z10*Q4*exp2*plusysq)) + \
4*exp25*Q3*Q452*r2*exp2*exp1*plusy4*(2*q2z01*r + \
Q4*(-2*q3z02*omr2 + 3*q3z10*r*exp2*plusysq)) + \
2*exp26*r2*exp2*(-(pow(q4z01,2)*Q52*omr22*plusysq) - \
Q4*q4z10*Q52*r*exp1*plusy4 + pow(Q4,3)*(-(q5z10*r*exp1) + \
Q5*(exp20))*plusy4 + Q42*(pow(q5z01,2)*omr22*plusysq + \
Q52*(8*pow(phiz01,2)*pow(omr2,4) - 4*q3z01*r*exp1*plusy4 + \
(exp20)*plusy4)))) + arraypdt((8*exp25*q2z01*Q452*r2*omr22*exp2*plusysq - \
4*exp26*Q4*q4z01*Q52*r2*omr22*exp2*plusysq - \
8*exp16*Q452*r3*exp2*exp1*plusy4 + 2*Q12*Q3*(q2z10 + \
2*q2z01*Q3)*pow(Q4,3)*Q52*r2*omr2*exp2*exp1*plusy4 - \
4*exp25*Q3*pow(Q4,3)*Q52*r3*exp2*(exp5)*plusy4 + \
8*exp25*pow(Q3,3)*pow(Q4,3)*Q52*r3*pow(exp2,2)*exp1*plusy6),z01.array()) + \
arraypdt((4*exp26*Q452*r2*omr2*exp2*plusysq - \
4*exp26*Q452*r4*omr2*exp2*plusysq - \
4*exp25*Q32*pow(Q4,3)*Q52*r2*omr2*exp2*exp1*plusy4),z02.array()) + \
arraypdt((6*exp26*Q452*r3*omr2*exp2*plusy4 - \
6*exp26*Q452*r5*omr2*exp2*plusy4 + \
2*exp26*Q452*r7*omr2*exp2*plusy4 + \
2*exp26*pow(Q4,3)*Q5*r3*omr2*pow(exp2,2)*plusy4 + Q12*(q2z10 + \
2*q2z01*Q3)*pow(Q4,3)*Q52*r2*omr22*pow(exp2,2)*plusy4 - \
exp25*pow(Q4,3)*Q52*r3*omr2*exp2*(exp19)*plusy4 - \
exp29*pow(Q4,3)*Q52*r*exp2*(exp18)*plusy4 + \
6*exp25*Q32*pow(Q4,3)*Q52*r3*pow(exp2,2)*exp1*plusy6),z10.array()) - \
arraypdt(4*exp25*Q3*pow(Q4,3)*Q52*r2*omr22*pow(exp2,2)*plusy4,z11.array()) - \
arraypdt(exp25*pow(Q4,3)*Q52*r2*omr2*exp2*exp1*plusy4,z20.array());
}
else if (label==14) // The block of the Jacobi matrix J14
{
    return arraypdt_idty(pow(q1z10 + \
2*q1z01*Q3,2)*Q5*r2*pow(exp1,2)*plusysq - \
q1z10*Q2*Q5*r*exp1*exp3*plusysq - \
2*exp24*(-(q1z10*r3*omr2*pow(exp2,2)) + Q5*pow(exp3,2))*plusysq + \
2*Q12*Q5*plusysq*(-3*pow(omr2,3)*exp6 + \
2*Q32*r2*pow(exp2,2)*exp3*plusysq) + \
4*exp25*r2*exp2*(4*pow(phi,2)*Q5*omr22 + exp4*plusysq) + \
Q1*Q5*r2*exp1*plusysq*(q1z10*exp11 - q1z20*exp1 - \
4*Q3*exp2*(2*q1z01*r + q1z11*omr2) + \
2*Q32*exp2*(-2*q1z02*omr2 + \
q1z10*r*exp2*plusysq)));
}
else if (label==15) // The block of the Jacobi matrix J15
{
    return arraypdt_idty(4*exp25*r2*exp2*exp3*plusysq - \
2*exp24*Q4*pow(exp3,2)*plusysq + \
4*exp25*Q4*r2*exp2*(4*pow(phi,2)*omr22 + 6*plusysq) + \
2*exp24*r2*exp1*(-2*q1z02*omr2 + q1z10*r*exp2*plusysq) + \
2*Q12*Q4*plusysq*(-3*pow(omr2,3)*exp6 + \
2*Q32*r2*pow(exp2,2)*exp3*plusysq) + \
Q1*Q4*r2*exp1*plusysq*(q1z10*exp11 - q1z20*exp1 - \
4*Q3*exp2*(2*q1z01*r + q1z11*omr2) + \
2*Q32*exp2*(-2*q1z02*omr2 + q1z10*r*exp2*plusysq)) + \
```

```
r*exp1*(pow(q1z10 + 2*q1z01*Q3,2)*Q4*r*exp1*plusysq + \
Q2*(4*pow(q1z01,2)*r*omr2 - \
q1z10*Q4*exp3*plusysq)));
}
else if (label==16) // The block of the Jacobi matrix J16
{
    return arraypdt_idty(32*phi*Q12*exp17*r2*omr22*exp2);
}
else if (label==24) // The block of the Jacobi matrix J24
{
    return arraypdt_idty(-24*Q12*pow(Q2,3)*\
Q52*r2*pow(omr2,3)*exp2*plusysq - \
6*exp25*q2z20*exp28*r2*exp1*plusysq + \
18*exp25*q2z10*exp28*r3*exp1*plusysq + \
12*exp25*q2z20*exp28*r4*exp1*plusysq - \
22*exp25*q2z10*exp28*r5*exp1*plusysq - \
8*exp25*q2z20*exp28*r6*exp1*plusysq + \
8*exp25*q2z10*exp28*r7*exp1*plusysq + \
2*exp25*q2z20*exp28*r8*exp1*plusysq - 6*Q12*pow(q2z10 + \
2*q2z01*Q3,2)*exp28*r2*pow(exp1,2)*plusysq + \
8*exp25*exp27*Q52*r2*exp2*exp1*(2*q2z01*r + \
q2z11*omr2)*plusysq + 2*Q22*(q1z10 + \
2*q1z01*Q3)*exp28*r*exp1*((q1z10 + 2*q1z01*Q3)*r*exp1 - \
4*Q2*exp3)*plusysq + 4*exp29*exp28*omr2*(6*Q2*omr22*exp6 + \
(2*q1z10 + q2z10 + 4*q1z01*Q3)*r*exp7)*plusysq + \
16*exp25*q2z01*pow(Q3,3)*exp28*r3*pow(exp2,2)*exp1*plusy4 + \
4*exp25*Q32*exp28*r2*exp2*exp1*plusysq*(2*q2z02*omr2 + \
q2z10*r*exp2*plusysq) + 4*exp26*Q52*r2*exp1*(2*q2z02*omr2 + \
4*Q3*q4z01*exp2*(-r + q3z01*omr2)*plusysq + exp2*(-(q2z10*r) + \
2*q4z10*(-r + q3z01*omr2))*plusysq) + \
16*Q12*pow(Q2,3)*Q4*r2*exp2*(-3*Q5*pow(omr2,3)*plusysq + \
(2*Q3*q5z01 + q5z10)*r*exp1*plusysq - 2*Q52*(2*pow(phi,2)*omr22 + \
3*plusysq)) + 2*exp25*Q52*r2*exp1*(4*pow(q2z01,2) - \
4*pow(q2z01,2)*r2 - 3*q2z20*Q4*plusysq + 9*q2z10*Q4*r*plusysq + \
6*q2z20*Q4*r2*plusysq - 11*q2z10*Q4*r3*plusysq - \
4*q2z20*Q4*r4*plusysq + 4*q2z10*Q4*r5*plusysq + q2z20*Q4*r6*plusysq + \
4*exp27*exp2*(2*q2z01*r + q2z11*omr2)*plusysq + \
8*q2z01*pow(Q3,3)*Q4*r*pow(exp2,2)*plusy4 + \
2*Q32*Q4*exp2*plusysq*(2*q2z02*omr2 + q2z10*r*exp2*plusysq)) + \
2*exp26*Q4*(-4*Q5*(q2z10 + 4*Q3*q5z01 + \
2*q5z10)*r3*omr2*pow(exp2,2)*plusysq + pow(2*Q3*q5z01 + \
q5z10,2)*r2*pow(exp1,2)*plusysq - 4*Q52*(
(((((((-2*r2 + 20)*r2 - 90)*r2 + 236)*r2 - 392)*r2 + 420)*r2 - 282)*r2 + 108)*r2 -
18)
*pow(phiz10,2)*r2
- 8*phi*phiz10*r3*pow(omr2,3)*pow(exp2,2) - 8*pow(phi,2)*r4*pow(exp1,2) \
- 9*plusysq + 18*r2*plusysq - 36*pow(q3z01,2)*r2*plusysq - \
72*q3z01*r3*plusysq - 99*r4*plusysq + 144*pow(q3z01,2)*r4*plusysq + \
216*q3z01*r5*plusysq + 168*r6*plusysq - 240*pow(q3z01,2)*r6*plusysq - \
264*q3z01*r7*plusysq - 135*r8*plusysq + 216*pow(q3z01,2)*r8*plusysq + \
168*q3z01*r9*plusysq + 54*r10*plusysq - 112*pow(q3z01,2)*r10*plusysq \
- 56*q3z01*r11*plusysq - 9*r12*plusysq + 32*pow(q3z01,2)*r12*plusysq \
+ 8*q3z01*r13*plusysq - 4*pow(q3z01,2)*r14*plusysq - \
2*Q32*r2*omr2*pow(exp2,2)*(4*pow(phiz01,2)*pow(omr2,3) + \
(exp8)*plusy4 - 4*q3z01*r*exp2*plusy4) - \
4*Q3*r2*omr2*pow(exp2,2)*(4*phi*phiz01*r*omr22 + \
2*phiz01*phiz10*pow(omr2,3) - q3z10*r*exp2*plusy4)))) + \
arraypdt((16*Q12*pow(Q2,3)*Q3*Q52*r3*exp2*exp1*plusysq + \
4*exp16*(2*Q3*q4z01 + q4z10)*Q52*r2*pow(exp1,2)*plusysq + \
16*exp16*exp28*r2*exp2*exp1*(-r + \
q3z01*omr2)*plusysq),z01.array()) + \
arraypdt((8*Q12*pow(Q2,3)*Q52*r3*exp2*exp1*plusysq - \
8*exp26*exp28*r3*exp2*exp1*plusysq + \
8*exp26*q3z01*exp28*r2*omr2*exp2*exp1*plusysq + \
2*exp26*(2*Q3*q4z01 + \
q4z10)*Q52*r2*pow(exp1,2)*plusysq),z10.array());
}
else if (label==25) // The block of the Jacobi matrix J25
{
    return arraypdt_idty(-24*Q12*pow(Q2,3)*Q42*r2*pow(\
omr2,3)*exp2*plusysq - \
48*Q12*pow(Q2,3)*Q4*Q5*r2*pow(omr2,3)*exp2*plusysq - \
4*exp26*Q42*(q2z10 + 4*Q3*q5z01 + \
```

```
2*q5z10)*r3*omr2*pow(exp2,2)*plusysq + 16*Q12*pow(Q2,3)*(2*Q3*q4z01 \
+ q4z10)*Q5*r3*exp2*exp1*plusysq - 6*Q12*pow(q2z10 + \
2*q2z01*Q3,2)*Q42*Q5*r2*pow(exp1,2)*plusysq + \
2*exp26*pow(2*Q3*q4z01 + q4z10,2)*Q5*r2*pow(exp1,2)*plusysq + \
2*Q22*(q1z10 + 2*q1z01*Q3)*Q42*Q5*r*exp1*((q1z10 + \
2*q1z01*Q3)*r*exp1 - 4*Q2*exp3)*plusysq + \
4*exp29*Q42*Q5*omr2*(6*Q2*omr22*exp6 + (2*q1z10 + q2z10 + \
4*q1z01*Q3)*r*exp7)*plusysq - \
32*Q12*pow(Q2,3)*Q42*Q5*r2*exp2*(2*pow(phi,2)*omr22 + 3*plusysq) + \
8*exp26*Q4*Q5*r2*exp1*(2*q2z02*omr2 + 4*Q3*q4z01*exp2*(-r + \
q3z01*omr2)*plusysq + exp2*(-(q2z10*r) + 2*q4z10*(-r + \
q3z01*omr2))*plusysq) + 4*Q12*exp17*r2*exp1*(4*pow(q2z01,2) - \
4*pow(q2z01,2)*r2 - 3*q2z20*Q4*plusysq + 9*q2z10*Q4*r*plusysq + \
6*q2z20*Q4*r2*plusysq - 11*q2z10*Q4*r3*plusysq - \
4*q2z20*Q4*r4*plusysq + 4*q2z10*Q4*r5*plusysq + q2z20*Q4*r6*plusysq + \
4*exp27*exp2*(2*q2z01*r + q2z11*omr2)*plusysq + \
8*q2z01*pow(Q3,3)*Q4*r*pow(exp2,2)*plusy4 + \
2*Q32*Q4*exp2*plusysq*(2*q2z02*omr2 + q2z10*r*exp2*plusysq)) - \
8*exp15*(
(((((((((-2*r2 + 20)*r2 - 90)*r2 + 236)*r2 - 392)*r2 + 420)*r2 - 282)*r2 + 108)*r2 -
18)
*pow(phiz10,2)*r2
- 8*phi*phiz10*r3*pow(omr2,3)*pow(exp2,2) - \
8*pow(phi,2)*r4*pow(exp1,2) - 9*plusysq + 18*r2*plusysq - \
36*pow(q3z01,2)*r2*plusysq - 72*q3z01*r3*plusysq - 99*r4*plusysq + \
144*pow(q3z01,2)*r4*plusysq + 216*q3z01*r5*plusysq + 168*r6*plusysq - \
240*pow(q3z01,2)*r6*plusysq - 264*q3z01*r7*plusysq - 135*r8*plusysq + \
216*pow(q3z01,2)*r8*plusysq + 168*q3z01*r9*plusysq + 54*r10*plusysq - \
112*pow(q3z01,2)*r10*plusysq - 56*q3z01*r11*plusysq - 9*r12*plusysq + \
32*pow(q3z01,2)*r12*plusysq + 8*q3z01*r13*plusysq - \
4*pow(q3z01,2)*r14*plusysq - \
2*Q32*r2*omr2*pow(exp2,2)*(4*pow(phiz01,2)*pow(omr2,3) + \
(exp8)*plusy4 - 4*q3z01*r*exp2*plusy4) - \
4*Q3*r2*omr2*pow(exp2,2)*(4*phi*phiz01*r*omr22 + \
2*phiz01*phiz10*pow(omr2,3) - q3z10*r*exp2*plusy4))) + \
arraypdt((-16*exp16*Q42*Q5*r3*omr2*pow(exp2,2)*plusysq + \
16*Q12*pow(Q2,3)*Q3*Q42*r3*exp2*exp1*plusysq + \
4*exp16*Q42*(2*Q3*q5z01 + q5z10)*r2*pow(exp1,2)*plusysq),z01.array()) + \
arraypdt((-8*exp15*r3*omr2*pow(exp2,2)*plusysq + \
8*Q12*pow(Q2,3)*Q42*r3*exp2*exp1*plusysq + \
2*exp26*Q42*(2*Q3*q5z01 + \
q5z10)*r2*pow(exp1,2)*plusysq),z10.array());
}
else if (label==26) // The block of the Jacobi matrix J26
{
    return arraypdt_idty(-64*phi*Q12*pow(Q2,3)*Q452*r2*\
omr22*exp2 + 32*exp13*r3*pow(omr2,3)*pow(exp2,2) + \
64*phiz01*exp16*Q452*r3*pow(omr2,3)*pow(exp2,2) + \
64*phi*exp26*Q452*r4*pow(exp1,2)) + \
arraypdt((64*phi*exp16*Q452*r3*pow(omr2,3)*pow(exp2,2) + \
32*phiz10*exp16*Q452*r2*pow(omr2,4)*pow(exp2,2)+ \
64*phiz01*exp26*Q32*Q452*r2*pow(omr2,4)*pow(exp2,2)),z01.array()) + \
arraypdt((
(((((((((-2*r2 + 20)*r2 - 90)*r2 + 236)*r2 - 392)*r2 + 420)*r2 - 282)*r2 + 108)*r2 -
18)
*exp13*r2*(-8)
+ 32*phi*exp26*Q452*r3*pow(omr2,3)*pow(exp2,2) + \
32*phiz01*exp16*Q452*r2*pow(omr2,4)*pow(exp2,2)),z10.array());
}
else if (label==34) // The block of the Jacobi matrix J34
{
    return arraypdt_idty(8*Q12*pow(Q2,\
3)*Q4*q5z01*r3*omr2*exp2*plusysq - \
8*exp25*q2z01*exp28*r2*omr2*exp2*(r - q3z01*omr2)*plusysq + \
4*exp26*q4z01*Q52*r2*omr2*exp2*(r - q3z01*omr2)*plusysq + \
6*exp26*q3z10*Q42*Q5*r3*omr2*pow(exp2,2)*plusy4 + Q12*(q2z10 + \
2*q2z01*Q3)*q3z10*Q452*r2*omr22*pow(exp2,2)*plusy4 - \
2*exp16*q4z10*Q52*r3*exp2*exp1*plusy4 - \
8*exp26*Q32*Q42*q5z01*r3*exp2*exp1*plusy4 - \
4*exp26*Q32*(q4z01*Q52 + Q42*q5z01)*r3*exp2*exp1*plusy4 + \
Q22*Q3*(q1z10 + 2*q1z01*Q3)*Q452*r*omr2*exp2*exp3*plusy4 - \
exp29*q3z10*Q452*r*exp2*(exp18)*plusy4 + \
exp29*Q3*Q452*(exp9)*plusy4 + Q12*Q3*(q2z10 + \
```

```
2*q2z01*Q3)*Q452*r2*omr2*exp2*(r*(exp21) + 2*q3z01*exp1)*plusy4 \
- 2*exp25*Q452*r2*omr2*exp2*(q3z10*r*(exp19) + \
q3z20*exp1)*plusy4 - 2*exp25*Q3*Q452*r2*exp2*(exp23 + \
4*q3z01*r*(exp5))*plusy4 + \
6*exp16*Q42*r2*exp2*(-(q5z10*r*exp1) + Q5*(exp20))*plusy4 - \
2*Q12*pow(Q3,3)*(q2z10 + \
2*q2z01*Q3)*Q452*r3*omr2*pow(exp2,3)*plusy6 + \
4*exp25*pow(Q3,3)*Q452*r2*pow(exp2,2)*(exp22 + \
4*q3z01*r*exp1)*plusy6 + \
2*exp25*Q32*Q452*r2*exp2*exp1*plusy4*(-2*q3z02*omr2 + \
3*q3z10*r*exp2*plusysq) - 2*Q12*(q2z10 + \
2*q2z01*Q3)*exp28*r2*omr2*exp2*plusysq*(-(exp27*(r*(exp21) + \
2*q3z01*exp1)*plusysq) + 2*pow(Q3,3)*Q4*r*pow(exp2,2)*plusy4 + \
omr2*(q2z01 - q3z10*Q4*exp2*plusysq)) + \
2*exp29*exp28*plusysq*(exp27*(exp9)*plusysq - r*(exp18)*(-2*q1z01 + \
q3z10*Q4*exp2*plusysq)) + \
2*exp25*Q32*exp28*r2*exp2*exp1*plusy4*(2*q2z01*r + \
Q4*(-2*q3z02*omr2 + 3*q3z10*r*exp2*plusysq)) + \
2*Q22*exp28*r*omr2*plusysq*(-2*q1z01*Q2*exp3 + (q1z10 + \
2*q1z01*Q3)*exp2*(q1z01*r*omr2 + exp27*exp3*plusysq)) + \
4*exp16*Q4*r2*exp2*(pow(q5z01,2)*omr22*plusysq + \
Q52*(8*pow(phiz01,2)*pow(omr2,4) - 4*q3z01*r*exp1*plusy4 + \
(exp20)*plusy4)) + \
2*exp26*Q4*r2*omr2*exp2*(-4*Q5*q5z01*r*plusysq + \
q5z01*q5z10*omr2*plusysq + 2*Q52*(4*phiz01*omr22*(2*phi*r + \
phiz10*omr2) + plusysq*(-2*q3z02*omr2 + q3z10*r*exp2*plusysq))) \
+ exp25*Q52*r2*exp2*plusysq*(2*pow(Q3,3)*Q42*exp2*(exp22 + \
4*q3z01*r*exp1)*plusy4 - omr2*(2*q2z01*(4*Q4*r - \
4*q3z01*Q4*omr2 - q4z10*omr2) + Q42*(q3z10*r*(exp19) + \
q3z20*exp1)*plusysq) + Q3*(4*q2z01*q4z01*omr22 - Q42*(exp23 + \
4*q3z01*r*(exp5))*plusysq) + 2*Q32*Q4*exp1*plusysq*(2*q2z01*r + \
Q4*(-2*q3z02*omr2 + 3*q3z10*r*exp2*plusysq)))) + \
arraypdt((4*Q12*pow(Q2,3)*Q52*r3*omr2*exp2*plusysq + \
4*exp25*q2z01*exp27*Q52*r2*omr22*exp2*plusysq - \
4*exp16*q4z01*Q52*r2*omr22*exp2*plusysq - \
exp26*q4z10*Q52*r2*omr22*exp2*plusysq + \
4*exp26*exp28*r2*omr2*exp2*(r - q3z01*omr2)*plusysq - \
4*exp26*Q32*exp28*r3*exp2*exp1*plusy4),z01.array()) + \
arraypdt((2*exp25*q2z01*exp28*r2*omr22*exp2*plusysq - \
exp26*q4z01*Q52*r2*omr22*exp2*plusysq - \
2*exp16*exp28*r3*exp2*exp1*plusy4),z10.array());
}
else if (label==35) // The block of the Jacobi matrix J35
{
    return arraypdt_idty(8*Q12*pow(Q2,3)*\
q4z01*Q5*r3*omr2*exp2*plusysq - \
4*exp26*Q42*q5z01*r3*omr2*exp2*plusysq - \
4*exp16*pow(q4z01,2)*Q5*r2*omr22*exp2*plusysq - \
2*exp26*q4z01*q4z10*Q5*r2*omr22*exp2*plusysq + \
8*exp26*Q4*q4z01*Q5*r2*omr2*exp2*(r - q3z01*omr2)*plusysq + \
2*exp26*q3z10*pow(Q4,3)*r3*omr2*pow(exp2,2)*plusy4 - \
8*exp26*Q32*Q4*q4z01*Q5*r3*exp2*exp1*plusy4 - \
4*exp16*Q4*q4z10*Q5*r3*exp2*exp1*plusy4 + \
2*exp16*pow(Q4,3)*r2*exp2*(exp20)*plusy4 + \
4*exp16*Q42*Q5*r2*exp2*(8*pow(phiz01,2)*pow(omr2,4) - \
4*q3z01*r*exp1*plusy4 + (exp20)*plusy4) - 2*Q12*(q2z10 + \
2*q2z01*Q3)*Q42*Q5*r2*omr2*exp2*plusysq*(-(exp27*(r*(exp21) + \
2*q3z01*exp1)*plusysq) + 2*pow(Q3,3)*Q4*r*pow(exp2,2)*plusy4 + \
omr2*(q2z01 - q3z10*Q4*exp2*plusysq)) + \
2*exp29*Q42*Q5*plusysq*(exp27*(exp9)*plusysq - r*(exp18)*(-2*q1z01 + \
q3z10*Q4*exp2*plusysq)) + \
4*exp15*r2*omr2*exp2*(4*phiz01*omr22*(2*phi*r + \
phiz10*omr2) + plusysq*(-2*q3z02*omr2 + q3z10*r*exp2*plusysq)) \
+ 2*Q22*Q42*Q5*r*omr2*plusysq*(-2*q1z01*Q2*exp3 + (q1z10 + \
2*q1z01*Q3)*exp2*(q1z01*r*omr2 + exp27*exp3*plusysq)) + \
2*Q12*exp17*r2*exp2*plusysq*(2*pow(Q3,3)*Q42*exp2*(exp22 + \
4*q3z01*r*exp1)*plusy4 - omr2*(2*q2z01*(4*Q4*r - \
4*q3z01*Q4*omr2 - q4z10*omr2) + Q42*(q3z10*r*(exp19) + \
q3z20*exp1)*plusysq) + Q3*(4*q2z01*q4z01*omr22 - Q42*(exp23 + \
4*q3z01*r*(exp5))*plusysq) + 2*Q32*Q4*exp1*plusysq*(2*q2z01*r + \
Q4*(-2*q3z02*omr2 + 3*q3z10*r*exp2*plusysq)))) + \
arraypdt((4*Q12*pow(Q2,3)*Q42*r3*omr2*exp2*plusysq - \
4*exp15*r3*omr2*exp2*plusysq + \
```

```
4*exp16*Q42*q5z01*r2*omr22*exp2*plusysq + \
exp26*Q42*q5z10*r2*omr22*exp2*plusysq - \
4*exp26*Q32*pow(Q4,3)*r3*exp2*exp1*plusy4),z01.array()) + \
arraypdt((exp26*Q42*q5z01*r2*omr22*exp2*plusysq - \
2*exp16*pow(Q4,3)*r3*exp2*exp1*plusy4),z10.array());
}
else if (label==36) // The block of the Jacobi matrix J36
{
    return arraypdt_idty(16*phiz01*exp26*\
Q452*r3*pow(omr2,3)*exp2) + arraypdt((16*phi*exp26*Q452*r3*omr2*exp2 - \
32*phi*exp26*Q452*r5*omr2*exp2 + \
16*phi*exp26*Q452*r7*omr2*exp2 + 8*exp13*r2*pow(omr2,4)*exp2 \
+ 32*phiz01*exp16*Q452*r2*pow(omr2,4)*exp2),z01.array()) + \
arraypdt(8*phiz01*exp26*Q452*r2*pow(omr2,4)*exp2,z10.array());
}
else if (label==41) // The block of the Jacobi matrix J41
{
    return arraypdt_idty(Q22*Q452*exp3*\
(-4*Q4*r + q4z10*omr2)*plusy4 + \
2*Q1*r*(-2*q2z01*Q452*omr2*plusysq*(-2*exp27*(r*(exp21) + \
2*q3z01*exp1)*plusysq + 4*pow(Q3,3)*Q4*r*pow(exp2,2)*plusy4 - \
omr2*(q2z01 + 2*q3z10*Q4*exp2*plusysq)) + \
Q2*exp28*plusy4*(-(pow(2*Q3*q4z01 + q4z10,2)*omr22*exp2) + \
4*Q42*(-omr2*(3*omr22 - 4*q3z01*r*exp2 + 2*pow(q3z01,2)*exp1) + \
2*Q32*r*pow(exp2,2)*(r + 2*q3z01*omr2)*plusysq) - \
Q4*omr2*(q4z10*exp11 - q4z20*exp1 - 4*Q3*exp2*(2*q4z01*r + \
q4z11*omr2) + 2*Q32*exp2*(-2*q4z02*omr2 + \
q4z10*r*exp2*plusysq))) + 2*Q22*(-3*pow(q4z01,2)*Q52*omr22*plusysq \
- exp28*omr2*plusysq*(-2*q4z02*omr2 + \
4*Q3*q4z01*r*exp2*plusysq + q4z10*r*exp2*plusysq) + \
Q42*(pow(q5z01,2)*omr22*plusysq - q4z10*Q5*r*exp1*plusy4 + \
4*Q52*(2*pow(phiz01,2)*pow(omr2,4) + r2*exp2*plusy4)) - \
4*pow(Q4,3)*plusysq*(Q3*q5z01*r*exp1*plusysq + \
Q5*(-(r2*exp2*plusysq) + Q5*(2*pow(phi,2)*omr22 + 3*plusysq)))))) + \
arraypdt((2*q1z01*Q22*Q452*r*omr22*plusysq + \
2*Q22*Q452*omr2*plusysq*(q1z01*r*omr2 + \
2*exp27*exp3*plusysq)),z01.array());
}
else if (label==42) // The block of the Jacobi matrix J42
{
    return arraypdt_idty(2*exp24*Q452*exp3*(-4*Q4*r + \
q4z10*omr2)*plusy4 + 4*q1z01*Q2*Q452*omr2*plusysq*(q1z01*r*omr2 \
+ 2*exp27*exp3*plusysq) + Q12*exp28*r*plusy4*(-(pow(2*Q3*q4z01 + \
q4z10,2)*omr22*exp2) + 4*Q42*(-omr2*(3*omr22 - 4*q3z01*r*exp2 + \
2*pow(q3z01,2)*exp1) + 2*Q32*r*pow(exp2,2)*(r + \
2*q3z01*omr2)*plusysq) - Q4*omr2*(q4z10*exp11 - q4z20*exp1 - \
4*Q3*exp2*(2*q4z01*r + q4z11*omr2) + \
2*Q32*exp2*(-2*q4z02*omr2 + q4z10*r*exp2*plusysq))) + \
4*exp25*r*(-3*pow(q4z01,2)*Q52*omr22*plusysq - \
exp28*omr2*plusysq*(-2*q4z02*omr2 + 4*Q3*q4z01*r*exp2*plusysq \
+ q4z10*r*exp2*plusysq) + Q42*(pow(q5z01,2)*omr22*plusysq - \
q4z10*Q5*r*exp1*plusy4 + 4*Q52*(2*pow(phiz01,2)*pow(omr2,4) + \
r2*exp2*plusy4)) - 4*pow(Q4,3)*plusysq*(Q3*q5z01*r*exp1*plusysq + \
Q5*(-(r2*exp2*plusysq) + Q5*(2*pow(phi,2)*omr22 + 3*plusysq))))) + \
arraypdt((2*Q12*q2z01*Q452*r*omr22*plusysq - \
2*Q12*Q452*r*omr2*plusysq*(-2*exp27*(r*(exp21) + \
2*q3z01*exp1)*plusysq + 4*pow(Q3,3)*Q4*r*pow(exp2,2)*plusy4 - \
omr2*(q2z01 + \
2*q3z10*Q4*exp2*plusysq))),z01.array());
}
else if (label==43) // The block of the Jacobi matrix J43
{
    return arraypdt_idty(-8*exp26*Q4*q4z01*Q52*r2*omr2*(\
exp2)*plusy4 - 4*exp25*Q4*q4z01*(2*Q3*q4z01 + \
q4z10)*Q52*r*omr22*exp2*plusy4 - \
8*exp26*pow(Q4,3)*q5z01*r2*exp1*plusy4 + \
4*q1z01*Q22*pow(Q4,3)*Q52*omr2*exp3*plusy4 + \
4*exp25*Q452*r*omr2*exp2*(2*q4z01*r + q4z11*omr2)*plusy4 + \
4*Q12*q2z01*pow(Q4,3)*Q52*r*omr2*(r*(exp21) + \
2*q3z01*exp1)*plusy4 - \
24*Q12*q2z01*Q32*pow(Q4,3)*Q52*r2*omr2*pow(exp2,2)*plusy6 + \
16*exp25*Q3*pow(Q4,3)*Q52*r2*pow(exp2,2)*(r + 2*q3z01*omr2)*plusy6 \
- 4*exp25*Q3*Q452*r*omr2*exp2*plusy4*(-2*q4z02*omr2 + \
```

```
q4z10*r*exp2*plusysq)) + \
arraypdt((8*Q12*q2z01*Q3*pow(Q4,3)*Q52*r*omr2*exp1*plusy4 - \
16*exp25*pow(Q4,3)*Q52*r*omr2*exp2*(-r + q3z01*omr2)*plusy4 + \
16*exp25*Q32*pow(Q4,3)*Q52*r2*omr2*pow(exp2,2)*plusy6),z01.array()) + \
arraypdt(4*Q12*q2z01*pow(Q4,3)*Q52*r*omr22*exp2*plusy4,z10.array());
}
else if (label==51) // The block of the Jacobi matrix J51
{
    return arraypdt_idty(r*(Q4*plusysq*(pow(2*\
Q3*q5z01 + q5z10,2)*omr22*exp2 - 4*Q52*(-3*pow(omr2,3) + \
2*Q32*r2*pow(exp2,2)*plusysq) + Q5*omr2*(q5z10*exp11 - \
q5z20*exp1 - 4*Q3*exp2*(2*q5z01*r + q5z11*omr2) + \
2*Q32*exp2*(-2*q5z02*omr2 + q5z10*r*exp2*plusysq))) + \
2*Q2*(2*pow(q5z01,2)*omr22 - 4*Q52*r2*exp2*plusysq + \
Q5*omr2*(-2*q5z02*omr2 + q5z10*r*exp2*plusysq) + \
Q4*(q5z10*r*exp1*plusysq + 4*Q5*(-(r2*exp2*plusysq) + \
Q5*(2*pow(phi,2)*omr22 + 3*plusysq))))));
}
else if (label==52) // The block of the Jacobi matrix J52
{
    return arraypdt_idty(-(Q4*Q5*exp3*(-4*Q5*r + \
q5z10*omr2)*plusysq) + 2*Q1*r*(2*pow(q5z01,2)*omr22 - \
4*Q52*r2*exp2*plusysq + Q5*omr2*(-2*q5z02*omr2 + \
q5z10*r*exp2*plusysq) + Q4*(q5z10*r*exp1*plusysq + \
4*Q5*(-(r2*exp2*plusysq) + Q5*(2*pow(phi,2)*omr22 + \
3*plusysq)))));
}
else if (label==53) // The block of the Jacobi matrix J53
{
    return arraypdt_idty(4*Q1*Q4*q5z01*(2*Q3*q5z01 + \
q5z10)*r*omr22*exp2*plusysq - 4*Q1*Q4*Q5*r*omr2*exp2*(2*q5z01*r \
+ q5z11*omr2)*plusysq - 16*Q1*exp27*Q52*r3*pow(exp2,2)*plusy4 + \
4*Q1*exp27*Q5*r*omr2*exp2*plusysq*(-2*q5z02*omr2 + \
q5z10*r*exp2*plusysq));
}
else if (label==61) // The block of the Jacobi matrix J61
{
    return arraypdt_idty((-q2z10 - 2*q2z01*Q3)*Q42*Q5*r*exp1*(2*phi*r + (phiz10 + \
2*phiz01*Q3)*omr2)*plusysq + 4*Q22*r*(-(phiz01*q4z01*Q5*omr22) + \
Q4*(2*phiz02*Q5 + phiz01*q5z01)*omr22 + 4*phi*Q42*Q5*plusysq) + \
Q2*Q4*(Q4*((2*Q3*q5z01 + q5z10)*r*exp1*(2*phi*r + (phiz10 + \
2*phiz01*Q3)*omr2) + 2*Q5*(4*phi*r*(exp3 + q3z01*r*exp1) + \
omr22*(3*phiz10 + 3*phiz20*r + 6*phiz10*q3z01*r - 9*phiz10*r2 - \
3*phiz20*r3 - 6*phiz10*q3z01*r3 + 5*phiz10*r4 + phiz20*r5 + \
2*phiz10*q3z01*r5 + 4*phiz02*Q32*r*exp2 + 2*phiz01*q3z10*r*exp2 + \
2*Q3*(2*phiz11*r*exp2 + phiz01*(exp10))))))*plusysq + \
Q5*r*omr2*(4*phiz01*q2z01*omr2 + \
4*phiz01*Q32*q4z01*exp1*plusysq + q4z10*exp2*(2*phi*r + \
phiz10*omr2)*plusysq + 2*Q3*exp2*(2*phi*q4z01*r + (phiz10*q4z01 + \
phiz01*q4z10)*omr2)*plusysq))) + arraypdt((4*phiz01*Q22*Q4*Q5*r*omr22 + \
4*phi*Q2*Q3*Q42*Q5*r2*omr2*exp2*plusysq + \
2*phiz10*Q2*Q3*Q42*Q5*r*omr22*exp2*plusysq + \
4*phiz01*Q2*Q32*Q42*Q5*r*omr2*exp1*plusysq),z01.array()) + \
arraypdt((2*phiz01*Q2*Q3*Q42*Q5*r*omr22*exp2*plusysq + \
Q2*Q42*Q5*r*omr2*exp2*(2*phi*r + \
phiz10*omr2)*plusysq),z10.array());
}
else if (label==62) // The block of the Jacobi matrix J62
{
    return arraypdt_idty(4*phiz01*q1z01*exp17*r*omr22 + \
8*exp24*r*(-(phiz01*q4z01*Q5*omr22) + Q4*(2*phiz02*Q5 + \
phiz01*q5z01)*omr22 + 4*phi*Q42*Q5*plusysq) + \
Q4*Q5*r*omr2*(4*phiz01*q1z01*Q2*omr2 + \
4*phiz01*q1z01*Q32*Q4*exp1*plusysq + q1z10*Q4*exp2*(2*phi*r + \
phiz10*omr2)*plusysq + 2*exp27*exp2*(2*phi*q1z01*r + \
(phiz10*q1z01 + phiz01*q1z10)*omr2)*plusysq) + \
Q1*Q4*(Q4*((2*Q3*q5z01 + q5z10)*r*exp1*(2*phi*r + (phiz10 + \
2*phiz01*Q3)*omr2) + 2*Q5*(4*phi*r*(exp3 + q3z01*r*exp1) + \
omr22*(3*phiz10 + 3*phiz20*r + 6*phiz10*q3z01*r - 9*phiz10*r2 - \
3*phiz20*r3 - 6*phiz10*q3z01*r3 + 5*phiz10*r4 + phiz20*r5 + \
2*phiz10*q3z01*r5 + 4*phiz02*Q32*r*exp2 + 2*phiz01*q3z10*r*exp2 + \
2*Q3*(2*phiz11*r*exp2 + phiz01*(exp10))))))*plusysq + \
Q5*r*omr2*(4*phiz01*q2z01*omr2 + \
```

```
4*phiz01*Q32*q4z01*exp1*plusysq + q4z10*exp2*(2*phi*r + \
phiz10*omr2)*plusysq + 2*Q3*exp2*(2*phi*q4z01*r + (phiz10*q4z01 + \
phiz01*q4z10)*omr2)*plusysq))) + arraypdt((4*phiz01*Q1*exp17*r*omr22 - \
2*Q1*Q3*Q42*Q5*r*exp1*(2*phi*r + (phiz10 + \
2*phiz01*Q3)*omr2)*plusysq),z01.array()) - arraypdt(Q1*Q42*Q5*r*exp1*(2*phi*r + \
(phiz10 + \
2*phiz01*Q3)*omr2)*plusysq,z10.array());
}
else if (label==63) // The block of the Jacobi matrix J63
{
    return arraypdt_idty(16*phiz02*exp24*Q3*Q42*Q5*r*omr22*(\
exp2)*plusysq + 8*phiz01*q1z01*Q2*Q3*Q42*Q5*r*omr2*exp1*plusysq - \
2*phiz01*Q1*(q2z10 + 2*q2z01*Q3)*Q42*Q5*r*omr2*exp1*plusysq + \
8*phiz01*exp24*exp27*q4z01*Q5*r*omr2*exp1*plusysq + \
2*phiz01*exp24*Q42*(2*Q3*q5z01 + q5z10)*r*omr2*exp1*plusysq + \
2*Q2*Q42*Q5*r*omr2*exp2*(2*phi*q1z01*r + (phiz10*q1z01 + \
phiz01*q1z10)*omr2)*plusysq - 2*Q1*q2z01*Q42*Q5*r*exp1*(2*phi*r + \
(phiz10 + 2*phiz01*Q3)*omr2)*plusysq + \
2*exp24*Q42*q5z01*r*exp1*(2*phi*r + (phiz10 + \
2*phiz01*Q3)*omr2)*plusysq + \
2*Q1*exp17*r*omr2*exp2*(2*phi*q4z01*r + (phiz10*q4z01 + \
phiz01*q4z10)*omr2)*plusysq + \
4*exp14*omr22*(2*phiz11*r*exp2 + phiz01*(exp10))*plusysq) + \
arraypdt((12*phiz10*exp14*r*omr22*plusysq - \
12*phiz10*exp14*r3*omr22*plusysq + \
4*phiz10*exp14*r5*omr22*plusysq + \
16*phiz01*exp24*Q3*Q42*Q5*r*omr22*exp2*plusysq + \
8*phi*exp14*r2*exp1*plusysq),z01.array()) + \
arraypdt(4*phiz01*exp14*r*omr22*exp2*plusysq,z10.array());
}
else if (label==44) // The block of the Jacobi matrix J44
{
    return arraypdt_idty(4*Q12*q2z01*q3z10*\
Q452*r*omr22*exp2*plusy4 - 4*exp29*Q452*r*exp3*plusy4 + \
4*q1z01*Q22*Q3*Q452*omr2*exp3*plusy4 + \
2*exp29*exp28*exp3*(-4*Q4*r + q4z10*omr2)*plusy4 + \
4*Q12*q2z01*Q3*Q452*r*omr2*(r*(exp21) + 2*q3z01*exp1)*plusy4 - \
8*Q12*q2z01*pow(Q3,3)*Q452*r2*omr2*pow(exp2,2)*plusy6 - \
2*exp26*Q52*r*omr2*plusysq*(-2*q4z02*omr2 + \
4*Q3*q4z01*r*exp2*plusysq + q4z10*r*exp2*plusysq) + \
4*q1z01*Q22*exp28*omr2*plusysq*(q1z01*r*omr2 + \
2*exp27*exp3*plusysq) + 8*exp25*Q452*r*plusy4*(-omr2*(3*omr22 - \
4*q3z01*r*exp2 + 2*pow(q3z01,2)*exp1) + 2*Q32*r*pow(exp2,2)*(r + \
2*q3z01*omr2)*plusysq) - \
4*Q12*q2z01*exp28*r*omr2*plusysq*(-2*exp27*(r*(exp21) + \
2*q3z01*exp1)*plusysq + 4*pow(Q3,3)*Q4*r*pow(exp2,2)*plusy4 - \
omr2*(q2z01 + 2*q3z10*Q4*exp2*plusysq)) - \
exp25*exp28*r*omr2*plusy4*(q4z10*exp11 - q4z20*exp1 - \
4*Q3*exp2*(2*q4z01*r + q4z11*omr2) + \
2*Q32*exp2*(-2*q4z02*omr2 + q4z10*r*exp2*plusysq)) + \
4*exp26*Q4*r*(pow(q5z01,2)*omr22*plusysq - q4z10*Q5*r*exp1*plusy4 \
+ 4*Q52*(2*pow(phiz01,2)*pow(omr2,4) + r2*exp2*plusy4)) - \
24*exp26*Q42*r*plusysq*(Q3*q5z01*r*exp1*plusysq + \
Q5*(-(r2*exp2*plusysq) + Q5*(2*pow(phi,2)*omr22 + 3*plusysq))) + \
exp25*Q52*r*plusy4*(-(pow(2*Q3*q4z01 + q4z10,2)*omr22*exp2) + \
4*Q42*(-omr2*(3*omr22 - 4*q3z01*r*exp2 + 2*pow(q3z01,2)*exp1) + \
2*Q32*r*pow(exp2,2)*(r + 2*q3z01*omr2)*plusysq) - \
Q4*omr2*(q4z10*exp11 - q4z20*exp1 - 4*Q3*exp2*(2*q4z01*r + \
q4z11*omr2) + 2*Q32*exp2*(-2*q4z02*omr2 + \
q4z10*r*exp2*plusysq)))) + arraypdt((-12*exp26*q4z01*Q52*r*omr22*plusysq - \
8*exp16*exp28*r2*omr2*exp2*plusy4 + \
8*exp25*Q3*Q452*r2*omr2*exp2*plusy4 - 4*exp25*exp27*(2*Q3*q4z01 \
+ q4z10)*Q52*r*omr22*exp2*plusy4),z01.array()) + \
arraypdt((4*exp26*exp28*r*omr22*plusysq + \
4*exp25*Q32*Q452*r*omr22*exp2*plusy4),z02.array()) + \
arraypdt((-2*exp26*exp28*r2*omr2*exp2*plusy4 - 2*exp25*Q4*(2*Q3*q4z01 \
+ q4z10)*Q52*r*omr22*exp2*plusy4 - \
exp25*Q452*r*omr2*exp11*plusy4 - \
2*exp15*r2*exp1*plusy4 + exp29*Q452*omr2*exp3*plusy4 \
- 2*exp25*Q32*Q452*r2*omr2*pow(exp2,2)*plusy6),z10.array()) + \
arraypdt(4*exp25*Q3*Q452*r*omr22*exp2*plusy4,z11.array()) + \
arraypdt(exp25*Q452*r*omr2*exp1*plusy4,z20.array());
}
```

```
  else if (label==45) // The block of the Jacobi matrix J45
  {
      return arraypdt_idty(-12*exp26*pow(q4z01,2)*Q5*r*\
  omr22*plusysq + 8*exp26*pow(Q4,3)*r3*exp2*plusy4 - \
  2*exp26*Q42*q4z10*r2*exp1*plusy4 + \
  2*exp29*Q42*Q5*exp3*(-4*Q4*r + q4z10*omr2)*plusy4 - \
  16*exp26*pow(Q4,3)*Q5*r*plusysq*(2*pow(phi,2)*omr22 + 3*plusysq) - \
  4*exp26*Q4*Q5*r*omr2*plusysq*(-2*q4z02*omr2 + \
  4*Q3*q4z01*r*exp2*plusysq + q4z10*r*exp2*plusysq) + \
  4*q1z01*Q22*Q42*Q5*omr2*plusysq*(q1z01*r*omr2 + \
  2*exp27*exp3*plusysq) + \
  16*exp15*r*(2*pow(phiz01,2)*pow(omr2,4) + r2*exp2*plusy4) \
  - 4*Q12*q2z01*Q42*Q5*r*omr2*plusysq*(-2*exp27*(r*(exp21) + \
  2*q3z01*exp1)*plusysq + 4*pow(Q3,3)*Q4*r*pow(exp2,2)*plusy4 - \
  omr2*(q2z01 + 2*q3z10*Q4*exp2*plusysq)) + \
  2*Q12*exp17*r*plusy4*(-(pow(2*Q3*q4z01 + q4z10,2)*omr22*exp2) + \
  4*Q42*(-omr2*(3*omr22 - 4*q3z01*r*exp2 + 2*pow(q3z01,2)*exp1) + \
  2*Q32*r*pow(exp2,2)*(r + 2*q3z01*omr2)*plusysq) - \
  Q4*omr2*(q4z10*exp11 - q4z20*exp1 - 4*Q3*exp2*(2*q4z01*r + \
  q4z11*omr2) + 2*Q32*exp2*(-2*q4z02*omr2 + \
  q4z10*r*exp2*plusysq)))) + arraypdt((4*exp26*Q42*q5z01*r*omr22*plusysq - \
  8*exp16*pow(Q4,3)*r2*exp1*plusy4),z01.array());
  }
  else if (label==46) // The block of the Jacobi matrix J46
  {
      return arraypdt_idty(-32*phi*exp26*pow(Q4,3)\
  *Q52*r*omr22*plusysq) + \
  arraypdt(32*phiz01*exp26*Q452*r*pow(omr2,4),z01.array());
  }
  else if (label==54) // The block of the Jacobi matrix J54
  {
      return arraypdt_idty(-(Q2*Q5*exp3*(-4*Q5*r + \
  q5z10*omr2)*plusysq) + 2*exp24*r*(q5z10*r*exp1*plusysq + \
  4*Q5*(-(r2*exp2*plusysq) + Q5*(2*pow(phi,2)*omr22 + 3*plusysq))) + \
  Q1*r*plusysq*(pow(2*Q3*q5z01 + q5z10,2)*omr22*exp2 - \
  4*Q52*(-3*pow(omr2,3) + 2*Q32*r2*pow(exp2,2)*plusysq) + \
  Q5*omr2*(q5z10*exp11 - q5z20*exp1 - 4*Q3*exp2*(2*q5z01*r + \
  q5z11*omr2) + 2*Q32*exp2*(-2*q5z02*omr2 + \
  q5z10*r*exp2*plusysq))));
  }
  else if (label==55) // The block of the Jacobi matrix J55
  {
      return arraypdt_idty(-8*exp24*Q4*r3*exp2*plusysq - \
  16*exp24*Q5*r3*exp2*plusysq + 4*exp17*r*exp3*plusysq - \
  Q2*Q4*exp3*(-4*Q5*r + q5z10*omr2)*plusysq + \
  16*Q1*exp17*r*(2*pow(phi,2)*omr22 + 3*plusysq) + \
  2*exp24*r*omr2*(-2*q5z02*omr2 + q5z10*r*exp2*plusysq) - \
  8*Q1*Q4*Q5*r*plusysq*(-3*pow(omr2,3) + 2*Q32*r2*pow(exp2,2)*plusysq) \
  + Q1*Q4*r*omr2*plusysq*(q5z10*exp11 - q5z20*exp1 - \
  4*Q3*exp2*(2*q5z01*r + q5z11*omr2) + \
  2*Q32*exp2*(-2*q5z02*omr2 + q5z10*r*exp2*plusysq))) + \
  arraypdt((8*exp24*q5z01*r*omr22 - 8*Q1*exp27*Q5*r2*omr2*exp2*plusysq + \
  4*Q1*exp27*(2*Q3*q5z01 + q5z10)*r*omr22*exp2*plusysq),z01.array()) + \
  arraypdt((-4*exp24*Q5*r*omr22 - 4*Q1*Q32*Q4*Q5*r*omr22*exp2*plusysq),z02.array()) + \
  arraypdt((2*exp24*Q5*r2*omr2*exp2*plusysq + 2*Q1*Q4*(2*Q3*q5z01 + \
  q5z10)*r*omr22*exp2*plusysq + Q1*Q4*Q5*r*omr2*exp11*plusysq + \
  2*exp24*Q4*r2*exp1*plusysq - exp17*omr2*exp3*plusysq + \
  2*Q1*Q32*Q4*Q5*r2*omr2*pow(exp2,2)*plusy4),z10.array()) - \
  arraypdt(4*Q1*exp27*Q5*r*omr22*exp2*plusysq,z11.array()) - \
  arraypdt(Q1*Q4*Q5*r*omr2*exp1*plusysq,z20.array());
  }
  else if (label==56) // The block of the Jacobi matrix J56
  {
      return arraypdt_idty(32*phi*exp24*exp28*r*omr22);
  }
  else if (label==64) // The block of the Jacobi matrix J64
  {
      return arraypdt_idty(4*exp29*(2*phiz02*\
  Q5 + phiz01*q5z01)*r*omr22 + 32*phi*exp29*Q4*Q5*r*plusysq + \
  4*phiz01*q1z01*Q2*Q32*Q4*Q5*r*omr2*exp1*plusysq + \
  q1z10*exp17*r*omr2*exp2*(2*phi*r + phiz10*omr2)*plusysq + \
  2*Q2*exp27*Q5*r*omr2*exp2*(2*phi*q1z01*r + (phiz10*q1z01 + \
  phiz01*q1z10)*omr2)*plusysq - 2*Q1*(q2z10 + \
```

```
2*q2z01*Q3)*Q4*Q5*r*exp1*(2*phi*r + (phiz10 + \
2*phiz01*Q3)*omr2)*plusysq + exp24*Q4*((2*Q3*q5z01 + \
q5z10)*r*exp1*(2*phi*r + (phiz10 + 2*phiz01*Q3)*omr2) + \
2*Q5*(4*phi*r*(exp3 + q3z01*r*exp1) + omr22*(3*phiz10 + 3*phiz20*r \
+ 6*phiz10*q3z01*r - 9*phiz10*r2 - 3*phiz20*r3 - 6*phiz10*q3z01*r3 + \
5*phiz10*r4 + phiz20*r5 + 2*phiz10*q3z01*r5 + 4*phiz02*Q32*r*exp2 + \
2*phiz01*q3z10*r*exp2 + 2*Q3*(2*phiz11*r*exp2 + \
phiz01*(exp10)))))*plusysq + Q2*Q5*r*omr2*(4*phiz01*q1z01*Q2*omr2 \
+ 4*phiz01*q1z01*Q32*Q4*exp1*plusysq + q1z10*Q4*exp2*(2*phi*r + \
phiz10*omr2)*plusysq + 2*exp27*exp2*(2*phi*q1z01*r + \
(phiz10*q1z01 + phiz01*q1z10)*omr2)*plusysq) + \
exp24*(Q4*((2*Q3*q5z01 + q5z10)*r*exp1*(2*phi*r + (phiz10 + \
2*phiz01*Q3)*omr2) + 2*Q5*(4*phi*r*(exp3 + q3z01*r*exp1) + \
omr22*(3*phiz10 + 3*phiz20*r + 6*phiz10*q3z01*r - 9*phiz10*r2 - \
3*phiz20*r3 - 6*phiz10*q3z01*r3 + 5*phiz10*r4 + phiz20*r5 + \
2*phiz10*q3z01*r5 + 4*phiz02*Q32*r*exp2 + 2*phiz01*q3z10*r*exp2 + \
2*Q3*(2*phiz11*r*exp2 + phiz01*(exp10)))))*plusysq + \
Q5*r*omr2*(4*phiz01*q2z01*omr2 + \
4*phiz01*Q32*q4z01*exp1*plusysq + q4z10*exp2*(2*phi*r + \
phiz10*omr2)*plusysq + 2*Q3*exp2*(2*phi*q4z01*r + (phiz10*q4z01 + \
phiz01*q4z10)*omr2)*plusysq))) + arraypdt((-4*phiz01*exp29*Q5*r*omr22 + \
4*phi*exp24*exp27*Q5*r2*omr2*exp2*plusysq + \
2*phiz10*exp24*exp27*Q5*r*omr22*exp2*plusysq + \
4*phiz01*exp24*Q32*Q4*Q5*r*omr2*exp1*plusysq),z01.array()) + \
arraypdt((2*phiz01*exp24*exp27*Q5*r*omr22*exp2*plusysq + \
Q1*exp17*r*omr2*exp2*(2*phi*r + \
phiz10*omr2)*plusysq),z10.array());
}
else if (label==65) // The block of the Jacobi matrix J65
{
    return arraypdt_idty(8*phiz02*exp29*Q4*r*omr22 - \
4*phiz01*exp29*q4z01*r*omr22 + 16*phi*exp29*Q42*r*plusysq - \
Q1*(q2z10 + 2*q2z01*Q3)*Q42*r*exp1*(2*phi*r + (phiz10 + \
2*phiz01*Q3)*omr2)*plusysq + 2*exp24*Q42*(4*phi*r*(exp3 + \
q3z01*r*exp1) + omr22*(3*phiz10 + 3*phiz20*r + 6*phiz10*q3z01*r - \
9*phiz10*r2 - 3*phiz20*r3 - 6*phiz10*q3z01*r3 + 5*phiz10*r4 + \
phiz20*r5 + 2*phiz10*q3z01*r5 + 4*phiz02*Q32*r*exp2 + \
2*phiz01*q3z10*r*exp2 + 2*Q3*(2*phiz11*r*exp2 + \
phiz01*(exp10))))*plusysq + Q2*Q4*r*omr2*(4*phiz01*q1z01*Q2*omr2 \
+ 4*phiz01*q1z01*Q32*Q4*exp1*plusysq + q1z10*Q4*exp2*(2*phi*r + \
phiz10*omr2)*plusysq + 2*exp27*exp2*(2*phi*q1z01*r + \
(phiz10*q1z01 + phiz01*q1z01*omr2)*plusysq) + \
exp24*Q4*r*omr2*(4*phiz01*q2z01*omr2 + \
4*phiz01*Q32*q4z01*exp1*plusysq + q4z10*exp2*(2*phi*r + \
phiz10*omr2)*plusysq + 2*Q3*exp2*(2*phi*q4z01*r + (phiz10*q4z01 + \
phiz01*q4z10)*omr2)*plusysq)) + arraypdt((4*phiz01*exp29*Q4*r*omr22 + \
2*exp24*Q3*Q42*r*exp1*(2*phi*r + (phiz10 + \
2*phiz01*Q3)*omr2)*plusysq),z01.array()) + arraypdt(exp24*Q42*r*exp1*(2*phi*r + \
(phiz10 + 2*phiz01*Q3)*omr2)*plusysq,z10.array());
}
else if (label==66) // The block of the Jacobi matrix J66
{
    return arraypdt_idty(16*exp29*Q42*Q5*r*plusysq \
+ 2*q1z10*Q2*Q42*Q5*r2*omr2*exp2*plusysq + \
4*q1z01*Q2*Q3*Q42*Q5*r2*omr2*exp2*plusysq + \
4*exp24*exp27*q4z01*Q5*r2*omr2*exp2*plusysq + \
2*exp24*Q4*q4z10*Q5*r2*omr2*exp2*plusysq - 2*Q1*(q2z10 + \
2*q2z01*Q3)*Q42*Q5*r2*exp1*plusysq + 2*exp24*Q42*(2*Q3*q5z01 + \
q5z10)*r2*exp1*plusysq + 8*exp14*r*(exp3 + \
q3z01*r*exp1)*plusysq) + arraypdt((4*q1z01*Q22*Q4*Q5*r*omr22 + \
4*exp24*q2z01*Q4*Q5*r*omr22 - 4*exp29*q4z01*Q5*r*omr22 + \
4*exp29*Q4*q5z01*r*omr22 + \
2*q1z10*Q2*Q3*Q42*Q5*r*omr22*exp2*plusysq + \
4*exp24*q3z10*Q42*Q5*r*omr22*exp2*plusysq + \
2*exp24*exp27*q4z10*Q5*r*omr22*exp2*plusysq + \
4*q1z01*Q2*Q32*Q42*Q5*r*omr2*exp1*plusysq - 2*Q1*Q3*(q2z10 + \
2*q2z01*Q3)*Q42*Q5*r*omr2*exp1*plusysq + \
4*exp24*Q32*Q4*q4z01*Q5*r*omr2*exp1*plusysq + \
2*exp24*Q3*Q42*(2*Q3*q5z01 + q5z10)*r*omr2*exp1*plusysq + \
4*exp24*Q3*Q42*Q5*omr22*(exp10)*plusysq),z01.array()) + \
arraypdt((8*exp29*Q4*Q5*r*omr22 + \
8*exp24*Q32*Q42*Q5*r*omr22*exp2*plusysq),z02.array()) + \
arraypdt((6*exp14*omr22*plusysq + 12*exp24*q3z01*Q42*Q5*r*omr22*plusysq \
```

```
- 18*exp14*r2*omr22*plusysq - \
12*exp24*q3z01*Q42*Q5*r3*omr22*plusysq + \
10*exp14*r4*omr22*plusysq + \
4*exp24*q3z01*Q42*Q5*r5*omr22*plusysq + \
q1z10*Q2*Q42*Q5*r*omr22*exp2*plusysq + \
2*q1z01*Q2*Q3*Q42*Q5*r*omr22*exp2*plusysq + \
2*exp24*exp27*q4z01*Q5*r*omr22*exp2*plusysq + \
exp24*Q4*q4z10*Q5*r*omr22*exp2*plusysq - Q1*(q2z10 + \
2*q2z01*Q3)*Q42*Q5*r*omr2*exp1*plusysq + exp24*Q42*(2*Q3*q5z01 + \
q5z10)*r*omr2*exp1*plusysq),z10.array()) + \
arraypdt(8*exp24*Q3*Q42*Q5*r*omr22*exp2*plusysq,z11.array()) + \
arraypdt((6*exp14*r*omr22*plusysq - 6*exp14*r3*omr22*plusysq + \
2*exp14*r5*omr22*plusysq),z20.array());
};


}

```

Bibliography

[1] Leonard Susskind. The World as a hologram. *J. Math. Phys.*, 36:6377–6396, 1995. [arXiv:9409089].

[2] S. Carlip. Black Hole Thermodynamics. *Int. J. Mod. Phys.*, D23:1430023, 2014. [arXiv:1410.1486].

[3] Juan Martin Maldacena. The Large N limit of superconformal field theories and supergravity. *Int. J. Theor. Phys.*, 38:1113–1133, 1999. [Adv. Theor. Math. Phys.2,231(1998)][arXiv:9711200].

[4] W. Zwerger. *The BCS-BEC crossover and the Unitary Fermi Gas*. Lecture Notes in Physics. Springer, Chicago, USA, 2011.

[5] Eagles D. M. Possible pairing without superconductivity at low carrier concentrations in bulk and thin-film superconducting semiconductors. *Phys. Rev.*, 186:454, 1969.

[6] C. A. Regal, M. Greiner, and D. S. Jin. Observation of resonance condensation of fermionic atom pairs. *Phys. Rev. Lett.*, 92:040403, 2004.

[7] M.W. Zwierlein, C.A. Stan, C.H. Schunck, S.M.F. Raupach, A.J. Kerman, and W. Ketterle. Condensation of pairs of fermionic atoms near a Feshbach resonance. *Phys. Rev. Lett.*, 92:120403, 2004.

[8] J. Kinast, S.L. Hemmer, M.E. Gehm, A. Turlapov, and J. E. Thomas. Evidence for superfluidity in a resonantly interacting Fermi gas. *Phys. Rev. Lett.*, 92:150402, 2004.

[9] T. Bourdel, L. Khaykovich, J. Cubizolles, J. Zhang, M. Teichmann F. Chevy, L. Tarruell, S.J.J.M.F. Kokkelmans, and C. Salomon. Experimental study of the BEC-BCS crossover region in lithium-6. *Phys. Rev. Lett.*, 93:050401, 2004.

[10] C. Chin, M. Bartenstein, A. Altmeyer, S. Riedl, S. Jochim, J. Hecker-Denschlag, and R. Grimm. Observation of the pairing gap in a strongly interacting Fermi gas. *Science*, 305:1128, 2004.

[11] R. I. Kamar M. W. Jack G. B. Partridge, K. E. Strecker and R. G. Hulet. Molecular probe of pairing in the BEC-BCS crossover. *Phys. Rev. Lett.*, 95:020404, 2005.

[12] A. Schirotzek C. H. Schunck M. W. Zwierlein, J. R. Abo-Shaeer and W. Ketterle. Vortices and superfluidity in a strongly interacting Fermi gas. *Nature*, 435:1047–1051, 2005.

[13] Mohit Randeria and Edward Taylor. BCS-BEC Crossover and the Unitary Fermi Gas. *Ann. Rev. Condensed Matter Phys.*, 5:209–232, 2014. [arXiv:1306.5785].

[14] Ville Keranen, Esko Keski-Vakkuri, Sean Nowling, and K. P. Yogendran. Solitons as Probes of the Structure of Holographic Superfluids. *New J. Phys.*, 13:065003, 2011. [arXiv:1012.0190].

[15] T. L. Ho R. Sensarma, M. Randeria. Vortices in Superfluid Fermi Gases through the BEC to BCS Crossover. *Phys. Rev. Lett.*, 96:090403, 2006. [arXiv:0510761].

[16] Mauro Antezza, Franco Dalfovo, Lev P. Pitaevskii, and Sandro Stringari. Dark solitons in a superfluid Fermi gas. *Phys. Rev. A*, 76:043610, 2007. [arXiv:0706.0601].

[17] Lincoln D Carr and Joachim Brand. *Emergent Nonlinear Phenomena in Bose-Einstein Condensates*. Springer-Verlag, 2008.

[18] Yuri Kivshar and Barry Luther-Davies. Dark optical solitons: Physics and applications. *Phys. Rept.*, 81:298, 1998.

[19] Ville Keranen, Esko Keski-Vakkuri, Sean Nowling, and K. P. Yogendran. Dark Solitons in Holographic Superfluids. *Phys. Rev.*, D80:121901, 2009. [arXiv:0906.5217].

[20] Ville Keranen, Esko Keski-Vakkuri, Sean Nowling, and K. P. Yogendran. Inhomogeneous Structures in Holographic Superfluids: I. Dark Solitons. *Phys. Rev.*, D81:126011, 2010. [arXiv:0911.1866].

[21] Yusuke Nishida and Hiroaki Abuki. BCS-BEC crossover in a relativistic superfluid and its significance to quark matter. *Phys. Rev.*, D72:096004, 2005. [arXiv:0504083].

[22] Matthew Headrick, Sam Kitchen, and Toby Wiseman. A New approach to static numerical relativity, and its application to Kaluza-Klein black holes. *Class. Quant. Grav.*, 27:035002, 2010. [arXiv:0905.1822].

[23] Pau Figueras, James Lucietti, and Toby Wiseman. Ricci solitons, Ricci flow, and strongly coupled CFT in the Schwarzschild Unruh or Boulware vacua. *Class. Quant. Grav.*, 28:215018, 2011. [arXiv:1104.4489].

[24] Alexander Adam, Sam Kitchen, and Toby Wiseman. A numerical approach to finding general stationary vacuum black holes. *Class. Quant. Grav.*, 29:165002, 2012. [arXiv:1105.6347].

[25] Pau Figueras and Toby Wiseman. Stationary holographic plasma quenches and numerical methods for non-Killing horizons. *Phys. Rev. Lett.*, 110:171602, 2013. [arXiv:1212.4498].

[26] Sebastian Fischetti, Donald Marolf, and Jorge E. Santos. AdS flowing black funnels: Stationary AdS black holes with non-Killing horizons and heat transport in the dual CFT. *Class. Quant. Grav.*, 30:075001, 2013. [arXiv:1212.4820].

[27] Zhongshan Xu, Yiqiang Du, Johanna Erdmenger, Yu Tian, Jie Ren, and Zhuoyu Xian. Holographic Superfluid Solitons with Backreaction. To appear.

[28] Yiqiang Du, Johanna Erdmenger, Florian Goth, René Meyer, Jackson Wu, and Zhongshan Xu. Phase Transition Induced by Disorder between AdS Soltion and AdS Black Hole Geometries. To appear.

[29] S.W. Hawking and D.N. Page. Thermodynamics of black holes in anti-de Sitter space. *Commun. Math. Phys.*, 87:577, 1983.

[30] Edward Witten. Anti-de Sitter space, thermal phase transition, and confinement in gauge theories. *Adv. Theor. Math. Phys.*, 2:505–532, 1998. [,89(1998)].

[31] Sean A. Hartnoll and Jorge E. Santos. Disordered horizons: Holography of randomly disordered fixed points. *Phys. Rev. Lett.*, 112:231601, 2014. [arXiv:1402.0872].

[32] Yiqiang Du, Johanna Erdmenger, Dilyn Fullerton, and René Meyer. Defect Embeddings in Holographic Background with Propagating Mater Fields. To appear.

[33] J. Kondo. Resistance Minimum in Dilute Magnetic Alloys. *Prog. Theo. Phys.*, 32:no. 1 37–49, 1964.

[34] Johanna Erdmenger, Carlos Hoyos, Andy O'Bannon, and Jackson Wu. A Holographic Model of the Kondo Effect. *JHEP*, 12:086, 2013. [arXiv:1310.3271].

[35] S. S. Gubser, Igor R. Klebanov, and Alexander M. Polyakov. Gauge theory correlators from noncritical string theory. *Phys. Lett.*, B428:105–114, 1998. [arXiv:9802109].

[36] Edward Witten. Anti-de Sitter space and holography. *Adv. Theor. Math. Phys.*, 2:253–291, 1998. [arXiv:9802150].

[37] Gary T. Horowitz and Andrew Strominger. Black strings and P-branes. *Nucl. Phys.*, B360:197–209, 1991.

[38] Charles Fefferman and C. Robin Graham. Conformal invariants. In *Élie Cartan et les mathématiques d'aujourd'hui - Lyon, 25-29 juin 1984*, number S131 in Astérisque, pages 95–116. Société mathématique de France, 1985.

[39] Sebastian de Haro, Sergey N. Solodukhin, and Kostas Skenderis. Holographic reconstruction of space-time and renormalization in the AdS / CFT correspondence. *Commun. Math. Phys.*, 217:595–622, 2001. [arXiv:0002230].

[40] Kostas Skenderis. Lecture notes on holographic renormalization. *Class. Quant. Grav.*, 19:5849–5876, 2002. [arXiv:0209067].

[41] Carlos Alfonso Bayona and Nelson R. F. Braga. Anti-de Sitter boundary in Poincare coordinates. *Gen. Rel. Grav.*, 39:1367–1379, 2007. [arXiv:0512182].

[42] Martin Ammon and Johanna Erdmenger. *Gauge/gravity duality.* Cambridge University Press, Cambridge, 2015. [Inspire].

[43] Gleb Arutyunov. *Lectures on String Theory*. Utrecht University, 2009.

[44] B. Zwiebach. *A first course in string theory*. Cambridge University Press, 2006.

[45] Makoto Natsuume. AdS/CFT Duality User Guide. *Lect. Notes Phys.*, 903:pp.1–294, 2015. [Inspire].

[46] David Tong. String Theory. 2009.

[47] Elias Kiritsis. *Introduction to superstring theory*, volume B9 of *Leuven notes in mathematical and theoretical physics*. Leuven U. Press, Leuven, 1998. [arXiv:9709062].

[48] John H. Schwarz. Introduction to superstring theory. *NATO Sci. Ser. C*, 566:143–187, 2001. [Inspire].

[49] Gerard 't Hooft. Dimensional reduction in quantum gravity. *Conf. Proc.*, C930308:284–296, 1993. [arXiv:9310026].

[50] Leonard Susskind. The World as a hologram. *J. Math. Phys.*, 36:6377–6396, 1995. [arXiv:9409089].

[51] Jacob D Bekenstein. Black holes and the second law. *Lettere Al Nuovo Cimento (1971–1985)*, 4(15):737–740, 1972.

[52] Jacob D Bekenstein. Black holes and entropy. *Physical Review D*, 7(8):2333, 1973.

[53] Stephen W Hawking. Black holes and thermodynamics. *Physical Review D*, 13(2):191, 1976.

[54] G. 't Hooft. *Nucl. Phys. B*, 72:461, 1974.

[55] Shinsei Ryu and Tadashi Takayanagi. Topological Insulators and Superconductors from String Theory. *Phys. Rev.*, D82:086014, 2010. [arXiv:1007.4234].

[56] Carlos Hoyos-Badajoz, Kristan Jensen, and Andreas Karch. A Holographic Fractional Topological Insulator. *Phys. Rev.*, D82:086001, 2010. [arXiv:1007.3253].

[57] Mukund Rangamani. Gravity and Hydrodynamics: Lectures on the fluid-gravity correspondence. *Class. Quant. Grav.*, 26:224003, 2009. [arXiv:0905.4352].

[58] Sayantani Bhattacharyya, Veronika E Hubeny, Shiraz Minwalla, and Mukund Rangamani. Nonlinear Fluid Dynamics from Gravity. *JHEP*, 02:045, 2008. [arXiv:0712.2456].

[59] Marc Montull, Alex Pomarol, and Pedro J. Silva. The Holographic Superconductor Vortex. *Phys. Rev. Lett.*, 103:091601, 2009. [arXiv:0906.2396].

[60] Tameem Albash and Clifford V. Johnson. Vortex and Droplet Engineering in Holographic Superconductors. *Phys. Rev.*, D80:126009, 2009. [arXiv:0906.1795].

[61] Sean A. Hartnoll, Christopher P. Herzog, and Gary T. Horowitz. Building a Holographic Superconductor. *Phys. Rev. Lett.*, 101:031601, 2008. [arXiv:0803.3295].

[62] G.C. Strinatii P. Pieri. From the Bogoliubov-de Gennes equations for superfluid fermions to the Gross-Pitaevskii equation for condensed bosons. *Phys.Rev.Lett.*, 91:030401, 2003. [arXiv:0301023].

[63] Sean A. Hartnoll, Christopher P. Herzog, and Gary T. Horowitz. Holographic Superconductors. *JHEP*, 12:015, 2008. [arXiv:0810.1563].

[64] Oliver DeWolfe, Oscar Henriksson, and Chaolun Wu. A holographic model for pseudogap in BCSâBEC crossover (I): Pairing fluctuations, double-trace deformation and dynamics of bulk bosonic fluid. *Annals Phys.*, 387:75–120, 2017. [arXiv:1611.07023].

[65] Edward Witten. Multitrace operators, boundary conditions, and AdS / CFT correspondence. 2001. [arXiv:0112258].

[66] Thomas Hartman and Leonardo Rastelli. Double-trace deformations, mixed boundary conditions and functional determinants in AdS/CFT. *JHEP*, 01:019, 2008. [arXiv:0602106].

[67] Luca Vecchi. Multitrace deformations, Gamow states, and Stability of AdS/CFT. *JHEP*, 04:056, 2011. [arXiv:1005.4921].

[68] C. P. Herzog, P. K. Kovtun, and D. T. Son. Holographic model of superfluidity. *Phys. Rev.*, D79:066002, 2009. [arXiv:0809.4870].

[69] Sean A. Hartnoll. Lectures on holographic methods for condensed matter physics. *Class. Quant. Grav.*, 26:224002, 2009. [arXiv:0903.3246].

[70] Sean A. Hartnoll, Andrew Lucas, and Subir Sachdev. Holographic quantum matter. 2016. [arXiv:1612.07324].

[71] Vijay Balasubramanian and Per Kraus. A Stress tensor for Anti-de Sitter gravity. *Commun. Math. Phys.*, 208:413–428, 1999. [arXiv:hep-th/9902121].

[72] Kostas Skenderis. Asymptotically Anti-de Sitter space-times and their stress energy tensor. *Int. J. Mod. Phys.*, A16:740–749, 2001. [arXiv:hep-th/0010138].

[73] Minyong Guo, Shanquan Lan, Chao Niu, Yu Tian, and Hongbao Zhang. Note on Zero Temperature Holographic Superfluids. *Class. Quant. Grav.*, 33(12):127001, 2016. [arXiv:1602.03824].

[74] Ãscar J. C. Dias, Jorge E. Santos, and Benson Way. Numerical Methods for Finding Stationary Gravitational Solutions. *Class. Quant. Grav.*, 33(13):133001, 2016. [arXiv:1510.02804].

[75] Oscar J.C. Dias, Gary T. Horowitz, Nabil Iqbal, and Jorge E. Santos. Vortices in holographic superfluids and superconductors as conformal defects. *JHEP*, 04:096, 2014. [arXiv:1311.3673].

[76] Shanquan Lan, Wenbiao Liu, and Yu Tian. Static structures of the BCS-like holographic superfluid in AdS4 spacetime. *Phys. Rev.*, D95(6):066013, 2017. [arXiv:1701.02921].

[77] Gary T. Horowitz and Jorge E. Santos. General Relativity and the Cuprates. *JHEP*, 06:087, 2013. [arXiv:1302.6586].

[78] G.V. Shlyapnikov P.O. Fedichev, A.E. Muryshev. Dissipative dynamics of a kink state in a Bose-condensed gas. *Phys. Rev. A*, 60:3220, 1999. [arXiv:9905062].

[79] A. Cetoli, J. Brand, R.G. Scott, F. Dalfovo, and L.P. Pitaevskii. Snake instability of dark solitons in fermionic superfluids. *Phys. Rev. A*, 88:043639, 2013. [arXiv:1307.3717].

[80] Minyong Guo, Esko Keski-Vakkuri, Hong Liu, Yu Tian, and Hongbao Zhang. Decay of dark solitons and a non-equilibrium dynamical phase transition. 2018. [arXiv:1810.11424].

[81] P. W. Anderson. Absence of Diffusion in Certain Random Lattices. *Phys. Rev.*, 109:(5): 1492–1505, 1958.

[82] Sean A. Hartnoll, David M. Ramirez, and Jorge E. Santos. Emergent scale invariance of disordered horizons. *JHEP*, 09:160, 2015. [arXiv:1504.03324].

[83] P. Noziéres. A âFermi-liquidâ Description of the Kondo Problem at Low Temperatures. *Jour. Low Temp. Phys.*, 17:31–42, 1974.

[84] N. Andrei. Diagonalization of the Kondo Hamiltonian. *Phys. Rev. Lett.*, 45:379–382, 1980.

[85] P. Wiegmann. Towards an exact solution of the Anderson model. *Physics Letters A*, 80:163–167, 1980.

[86] K. G. Wilson. The Renormalization Group: Critical Phenomena and the Kondo Problem. *Rev. Mod. Phys.*, 47:773, 1975.

[87] I. Affleck. A Current Algebra Approach To The Kondo Effect. *Nucl. Phys.*, B336:517, 1990.

[88] I. Affleck and A. Ludwig. Critical Theory of Overscreened Kondo Fixed Points. *Nucl. Phys.*, B360:641–696, 1991.

[89] I. Affleck and A. Ludwig. The Kondo Effect, Conformal Field Theory and Fusion Rules. *Nucl. Phys.*, B352:849–862, 1991.

[90] I. Affleck and A. Ludwig. Universal Non-integer âGround State Degeneracyâ in Critical Quantum Systems. *Phys.Rev.Lett.*, 67:161–164, 1991.

[91] I. Affleck and A. Ludwig. Exact Conformal-field-theory Results on the Multichannel Kondo Effect: Single-fermion Greenâs function, Self-energy, and Resistivity. *Phys.Rev.*, B48:7297–7321, 1993.

[92] Ian Affleck. Conformal field theory approach to the Kondo effect. *Acta Phys. Polon.*, B26:1869–1932, 1995. [arXiv:9512099].

[93] N. E. Bickers. Review of techniques in the large-N expansion for dilute magnetic alloys. *Rev. Mod. Phys.*, 59:845–939, 1987.

[94] Alexander Cyril Hewson. *The Kondo Problem to Heavy Fermions*. Cambridge University Press, 1993.

[95] D.L. Cox and A. Zawadowski. Exotic Kondo Effects in Metals: Magnetic Ions in a Crystalline Electric Field and Tunneling Centers. *Advances in Physics*, 47:599, 1998. [arXiv:9704103].

[96] Dilyn Fullerton. Einstein-Maxwell holographic Kondo model. [Exchange student report, University of British Columbia, unpublished].

[97] N. Read and D. M. Newns. On the solution of the Coqblin-Schriffer Hamiltonian by the large-N expansion technique. *Journal of Physics C: Solid State Physics*, 16 no. 17:3273, 1983.

[98] P. Coleman and N. Andrei. Diagonalisation of the generalised Anderson model. *Journal of Physics C: Solid State Physics*, 19 no. 17:3211, 1986.

[99] Bikash Padhi, Apoorv Tiwari, Chandan Setty, and Philip W. Phillips. Log-rise of the Resistivity in the Holographic Kondo Model. *Phys. Rev.*, D97(6):066012, 2018. [arXiv:1709.06086].

[100] Eric Poisson. *A relativist's toolkit: the mathematics of black-hole mechanics*. Cambridge University Press, 2004.

[101] Johanna Erdmenger, Carlos Hoyos, Andy OâBannon, Ioannis Papadimitriou, Jonas Probst, and Jackson MS Wu. Two-point functions in a holographic Kondo model. *Journal of High Energy Physics*, 2017(3):39, 2017.

[102] Andy O'Bannon, Ioannis Papadimitriou, and Jonas Probst. A Holographic Two-Impurity Kondo Model. *JHEP*, 01:103, 2016. [arXiv:1510.08123].

[103] Johanna Erdmenger, Mario Flory, Carlos Hoyos, Max-Niklas Newrzella, and Jackson Wu. Entanglement entropy in a holographic Kondo model. *Fortschritte der Physik*, 64(1):109–130, 2016.

[104] Johanna Erdmenger, Mario Flory, and Max-Niklas Newrzella. Bending branes for dcft in two dimensions. *Journal of High Energy Physics*, 2015(1):58, 2015.

[105] Werner Israel. Singular hypersurfaces and thin shells in general relativity. *Il Nuovo Cimento B (1965-1970)*, 44(1):1–14, 1966.

[106] Cristian Martinez, Claudio Teitelboim, and Jorge Zanelli. Charged rotating black hole in three spacetime dimensions. *Physical Review D*, 61(10):104013, 2000.

[107] Andrea Marzolla. *The Ward identity of Symmetry Breaking from Holographic Renormalization*. PhD thesis, Brussels U., PTM, 2017. [arXiv:1712.09251].

[108] Robert M. Wald. *General Relativity*. Chicago Univ. Pr., Chicago, USA, 1984.

[109] Gary T. Horowitz, Jorge E. Santos, and David Tong. Optical Conductivity with Holographic Lattices. *JHEP*, 07:168, 2012. [arXiv:1204.0519].

[110] John P. Boyd. *Chebyshev and Fourier Spectral Methods*. Dover Books on Mathematics. Dover Publications, Mineola, NY, second edition, 2001.

Acknowledgments

I get a lot of help and supports during my PhD study, and I would like to express my gratitude towards them here.

In the first place, I would like to express my deep gratitude to my supervisor Professor Johanna Erdmenger. She gives me continuous support during my study. She also generously gives her time to me on valuable and constructive suggestions during my research work, which I appreciate very much.

Next, I would like to thank René Meyer not only for the help and support on my research, but also for the warm-hearted concern for my life. He is not only a friend, but also like a second advisor for me.

I would like to thank the China Scholarship Council for providing me with the funding, and thank Professor Yi Ling, Yu Tian, Xiaoning Wu and Hongbao Zhang for supporting the application of the scholarship.

I would like to thank Raimond Abt, Pascal Fries, Dilyn Fullerton, Marius Gerbershagen, Florian Goth, Kevin Grosvenor, Haye Hinrichsen, Shanquan Lan, Li Li, Nina Miekley, Chao Niu, Christian Northe, Jie Ren, Ignacio Reyes, Manuel Schrauth, Zhenjiu Wang, Jackson Wu, Xianxin Wu, Zhuoyu Xian, Zhongshan Xu, Yuan Yan, Songbo Zhang and Suting Zhao for helpful discussions and pleasant time together.

I also thank Peter Quigley for helping me with the English check of this thesis.

Finally, I wish to thank my wife Xiaotong An for her love, support, encouragement and enjoyable company, and also thank my parents, brother and my friends for their support and encouragement throughout my study.